Effects of Bolt Position Within Long Slots on Extended Single Plate Connections

by

Cassidy N. Jackson

A Report Submitted to the Faculty of the

Milwaukee School of Engineering

In Partial Fulfillment of the

Requirements for the Degree of

Master of Science in Architectural Engineering

Milwaukee, Wisconsin

August 2022

Abstract

A common connection for steel members framing into concrete walls consists of a single plate with long-slotted holes welded to an embed plate. This connection accounts for the different construction tolerances allowed by the two materials, providing space for the structural members during erection. While these connections are frequently used in practice, the amount of information available to understand how the long slots affect the behavior of the single plate is limited. The purpose of this experimental research initiative is to contribute information on the connection's behavior to aid in the development of a design procedure.

The experimental program consisted of twenty test specimens which incorporated two variables: slot spacing and bolt group position. This project focuses on effects of the five different bolt group positions within the slotted holes. These specimens were loaded in shear while qualitative and quantitative data were gathered on plate displacement, plate capacity, and flexural and bearing behavior.

The results from the analysis show a correlation between the bolt group position and connection capacity: as the bolt group was positioned closer to the weld, the connection capacity increased; as the bolts were positioned farthest from the weld, the capacity decreased. A correlation between the bolt group position and the flexural and bearing behavior of the plate was observed as well; greater flexural behavior was observed at bolt group positions farthest from the weld, while greater bearing behavior was observed at bolt group positions closest to the weld. However, the information gathered in this project was limited, and further experimentation should be pursued to further contribute to the understanding of this connection's behavior.

Acknowledgments

This capstone project report would not have been completed without the support of many people and organizations. First and foremost, I would like to thank Zalk Josephs Fabricators LLC for their generous donation of testing materials and specimens that contributed toward this project initiative.

I would like to extend a special thank you to my project advisor, Dr. Christopher Raebel, for his consistent guidance, extensive knowledge, and relentless support. He expressed a profound belief in my abilities and was very encouraging through the entire process. I am also grateful to Dr. Pouria Bahmani and Adam Friedman for their constructive advice and insightful suggestions. I appreciate Casey Peterson and Steve Herlache for their fruitful discussion during the development of this project.

This project would not have been possible without the help and support of Drake Taxon as he worked on his project in conjunction with my own. I want to extend my appreciation for the significant amount of time and effort he contributed to the research and experimental program for our respective projects.

Finally, I would like to express my immense appreciation for my family and friends who have encouraged me through this process. In particular, I would like to thank my parents for their unwavering belief in my abilities and their continued support in all that I do.

Table of Contents

List of Figures

List of Tables

Nomenclature

Symbols

E	modulus of elasticity, psi (MPa)
F_u	ultimate tensile strength of material, psi (MPa)
F_y	yield strength of material, psi (MPa)
P, P_b	bolt position within the slot, %
S	spacing between slots, in. (mm)
σ	stress
ϵ	strain

Abbreviations

ACI	American Concrete Institute
AISC	American Institute of Steel Construction
ANSI	American National Standards Institute
ASTM	American Society of Testing Materials
ft	feet
in.	inches
kip	kilopound
kN	kilonewton
ksi	kips per square inch
LVDT	linear variable differential transformer
m	meters
mm	millimeters
MPa	megapascals
PL	plate section
psi	pounds per square inch
W	wide flange beam section

Glossary

Butterworth Filter	"a type of signal processing filter designed to have a frequency response as flat as possible in the passband." (Electrical4U, 2021)
Median Filter	a filtering process that uses the median of the filtered data to create a filtered image, taking out noise in data (Ohki et al., 2021)

Chapter 1: Introduction

1.1 Background

The use of single-plate shear connections, also referred to as shear tabs, are common for various structural applications. This connection is composed of a single plate welded to a supporting member on both sides, and then bolted to the supported member. They are used to connect steel members to other steel members, as well as steel members to concrete members. These connections offer several advantages, including simpler shop fabrication and erection, and increased safety during erection.

Per Part 10 of the AISC *Manual* (AISC, 2016a), there are two different configurations for these connections: the conventional configuration and the extended configuration. The conventional configuration specifies certain dimensional limitations, allowing for a simplified design procedure for the connection. For example, the connection permits a single vertical row of standard or short-slotted bolt holes, with as few as two bolts and as many as twelve bolts in that row. These connections also limit the dimension from the bolt row to the welded connection to the supporting member to be less than or equal to 3½ in. (88.9 mm). The second configuration, the extended configuration, does not specify any limitations, except for meeting the requirements for bolt holes found in J3.2 in the AISC *Specification* (AISC, 2016b).

When determining which configuration to use, the material of the connecting members could greatly influence that decision. The connection between a steel beam and a concrete wall could be used for this example. The fabrication tolerance for steel members is ±1⁄16 in. (2 mm) for those that are less than 30 ft., and ±⅛ in. (3 mm) for those

that are greater than 30 ft. There is also a tolerance permitted for members with adjustable items of ±⅜ in. (10 mm) to established finish lines and ±3⁄16 in. (5 mm) to abutting ends. This tolerance is permitted for members with connection pieces that allow for lateral movement, such as connecting plates or angles with slotted holes (AISC, 2016a). On the other side of the connection, concrete has a permitted tolerance of ±1 in. (25.4 mm) in any direction (ACI, 2010).

To address the great differences between the two materials' tolerances used in this connection, the extended configuration for the single-plate shear connection could be utilized. A typical detail for the connection between a steel beam and concrete wall is shown in Figure 1-1, which can consist of an extended plate with slotted holes that is welded to a concrete embed plate. The slotted holes in the single plate meet the criteria to classify the member as an adjustable item, while also providing the tolerances needed during erection.

However, as aforementioned, the extended single plate must meet the requirements of J3.2. The AISC *Specification* recommends the use of standard or short-slotted holes for these connections, unless otherwise approved by the engineer of record (AISC, 2016b). The use of standard or short-slotted holes do not meet the requirements from the increased tolerance in the steel-to-concrete connection. Long-slotted holes meet that requirement but lack the specifications and recommendations that would be useful for a typical design.

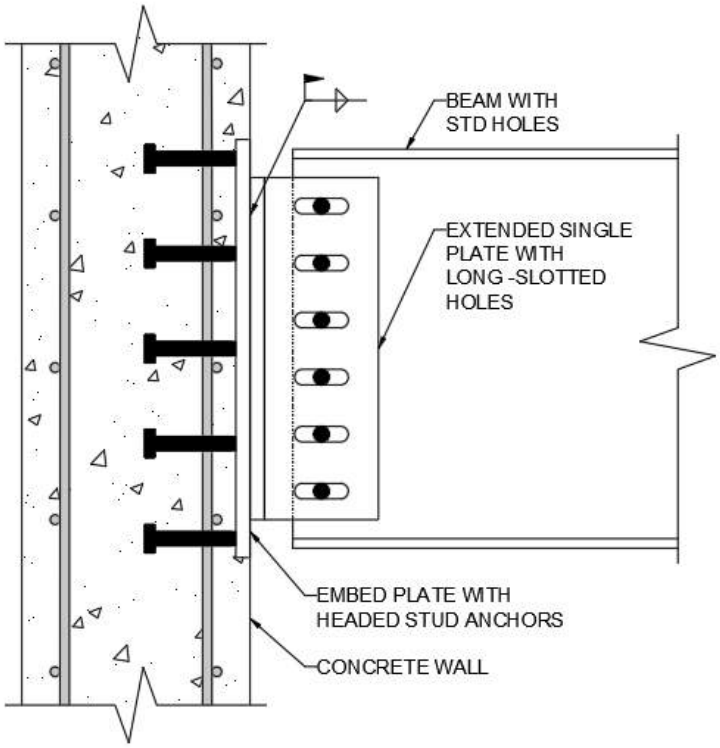

Figure 1-1: Typical Detail for Single Plate Connection with Long Slots.

1.2 Purpose

As seen throughout the AISC *Manual* from the different specifications and design recommendations, there has been significant research and experimental work done for connections with standard and short-slotted holes. However, that is not the case for connections with long-slotted holes. For that reason, the purpose of this experimental research initiative was to gain a better understanding of the behavior of a single plate with long-slotted holes. There are several factors that could influence the behavior of this connection; this report focuses on the effect the bolt group position within the slots has on this connection.

Chapter 2: Literature Review

Throughout the years, there has been significant research done to understand the behaviors of single plate shear connections. These connections have been divided into two categories: conventional configuration, and extended configuration. Even though both configurations have a suggested design procedure, the extended configuration does not provide clear guidance on certain aspects of design, such as the use of long-slotted holes. The following chapter will discuss design procedures for the different connection configurations, the work that has been done to better understand the connection behavior, and the unanswered questions that remain.

2.1 Shear Plate Design

The AISC *Specification* provides well-outlined design procedures for single-plate shear connections. The most detailed procedure provided is for the conventional configuration, which is defined by its dimensional limitations. Some of the limitations include: a single row of bolts; between two and twelve bolts in the row; eccentricity between the weld line and bolt line must be equal to or less than 3½ in. (88.9 mm); only standard holes or short-slotted holes transverse to the load can be used (AISC, 2016a, p. 10-88). The purpose of these limitations is to reduce the number of limit states that will control while designing the connection. The few design checks for this configuration include bolt shear, plate bearing, and plate tearout; due to the dimensional limitations, plate buckling will not control.

The design procedure found in the AISC *Specification*, 14th edition, was based on the research and testing performed by Muir and Thornton. Their work, summarized in an article in *Engineering Journal*, posed the reasons for needing a revised procedure in

reference to the one in the 13th edition. The article, “The Development of a New Design Procedure for Conventional Single-Plate Shear Connections” compared the dimensional limitations and limit states used in the previous design procedure to that of the new one, highlighting the changes due to advances in research and materials (Muir & Thornton, 2011).

In the 13th edition, the design procedure for single-plate shear connections relied on reduction factors that allowed engineers to neglect the eccentricity from the weld line to the bolt line. After reanalysis of data, Muir and Thornton determined that the eccentricity should be considered during design since it directly affects the strength of the bolt group, which is a limit state that is likely to govern in these connections. Other limit states they found could govern include shear yielding, shear rupture, flexural yielding, and block shear. However, they state that block shear will not govern as long as the horizontal edge distance is greater than the vertical edge distance (Muir & Thornton, 2011).

In the article, “Design of Single Plate Shear Connections,” Astaneh, Call, and McMullin describe their experimental initiative to apply direct shear and rotation to a single plate shear connection to verify the proposed design procedures and identify additional limit states. Up to that point, there were experiments performed that studied the effects of rotation on single plates, and the effects of direct shear on single plates. They wanted to take a more realistic approach and study the effects of both rotation and direct shear applied to a single plate connecting a steel beam to a steel column (Astaneh, Call & McMullin, 1989).

There were five full-scale tests performed that were divided into two groups: group one used A325 bolts, A36 grade beams, and 1½ in. (38.1 mm) edge distance; and group two used A490 bolts, grade 50 beams, and 1⅛ in. (28.6 mm) edge distance. Group one contained three tests, one with seven bolt rows, one with five bolt rows, and one with three bolt rows; group two contained two tests, one with five bolt rows, and the other with three bolt rows. Both groups used A36 plate material and ¾ in. (19.1 mm) diameter bolts at 3-in. (76.2 mm) spacing (Astaneh et al., 1989).

Each specimen in group one showed similar behaviors, the most important of which was significant inelastic shear deformations. The specimens in group two showed similar behaviors as those in group one; however, shear yielding in the plate was more apparent in these specimens. After discussing the observations during testing, they determined that "shear tabs go through three distinctive phases of behavior" (Astaneh et al., 1989, p. 24). In phase one, the moment applied to the shear tab makes it act like a short cantilever beam. During the second phase, as the load continuously increases, the shear yielding effect also increases, making the shear tab act like a deep beam. If the connection reaches phase three before failure, the shear tab starts to act like the diagonal member of a truss due to the great deformations it has endured up to that point (Astaneh et al., 1989).

After further evaluation of the data and observations from the experimental initiative, they outlined a design procedure for single plate shear tabs. This design procedure included general requirements that put dimensional limitations on the design of shear tabs and included two design examples. They also listed the different limit states that should be considered while designing these types of connections: plate yielding, bolt

fracture, weld fracture, fracture of the net section of the plate, and bearing failure of bolt holes (Astaneh et al., 1989).

2.2 Extended Shear Plate Design

The AISC *Specification* also provides an outline for the extended configuration for single-plate shear connections. There are fewer dimensional limitations for this configuration, allowing for single-plate shear connections to be used in various situations. However, with less restrictions on the plate configuration, there are more limit states to consider. Those limit states include weld strength, shear strength of bolts, bearing and tearout strength of bolts, shear yield and shear rupture of plate, block shear strength, and strength of the connecting elements in flexure (AISC, 2016b).

In the report, *Design of Extended Shear Tabs*, Sherman and Ghorbanpoor describe their three-phase initiative to develop a design procedure for extended single plate shear connections. They pointed out a few of the many applications associated with the extended configuration of a single plate shear connection, and the obstacles that would arise when the conventional configuration would be used. Therefore, rather than the bolt line extending 3 in. (76.2 mm) from the web of the supporting member in the conventional configuration, it should extend 3 in. (76.2 mm) beyond the flanges of the supporting member. The objectives for this project were to evaluate the capacity of extended shear plates, to determine the critical limit states, to identify additional limit states, to determine the location of the shear reaction eccentricity, and to recommend a design procedure (Sherman & Ghorbanpoor, 2002).

There were seventeen tests conducted in the first phase of this experiment, which consisted of a single column of three- and five-bolt extended shear plates connected to

column webs and girder webs. Other variables that changed between the different specimens within those four groups included the supporting member size and stiffness, weld configuration, and either the use of standard holes with snug tight bolts or short-slotted holes with fully tightened bolts. After the first phase, there were a few unanswered questions about the use of snug tight bolts in short-slotted holes, the criteria for sizing stiffener plates, and the behavior of extended shear plates connected to a column web with only one stiffener at the top of the connection. The four tests in phase two were conducted to answer those questions. Then, the project extended into a third phase, consisting of ten tests of six- and eight-bolt extended shear plate connections studied like those in phase one (Sherman & Ghorbanpoor, 2002).

The data from each subsequent phase added to the understanding of the behavior of extended shear plate connections, providing Sherman and Ghorbanpoor the information needed to outline a design procedure and list the many conclusions resulting from this project. Two additional limit states were found that should be considered in certain situations: web mechanism failure for columns with high slenderness ratios, and plate twisting for unstiffened connections. Based on the experimental eccentricity, they found that there were three different limit states that could govern during design, depending on the configuration: bolt shear, shear yielding, and web mechanism failure. Also, they determined that there was no significant effect on the connection capacity based on the tightening type used in standard or short-slotted holes (Sherman & Ghorbanpoor, 2002).

With a similar purpose, Muir and Hewitt published their article, “Design of Unstiffened Single-Plate Shear Connections,” in *Engineering Journal* which describes

their work in developing a design procedure for extended single-plate shear connections for the AISC *Steel Construction Manual*, 13th edition. They start off by acknowledging that these types of connections have been used for several decades, but have lacked "a well-defined, simple and rational design procedure" (Muir & Hewitt, 2009, p. 67). They decided to model the connection after a fixed-end beam to account for the moment that will be applied due to the increased eccentricity, rather than after a pinned-end beam that only transfers shear reactions (Muir & Hewitt, 2009).

Based on this model, they walk through the steps for designing an extended plate. The procedure includes determining the plate thickness, the required bolt group, checking the different limit states, sizing the weld, checking supported beam brace points, and checking serviceability requirements. Those limit states include plate shear yielding, plate shear rupture, plate block shear rupture, plate flexure with the von Mises shear reduction, and plate buckling. This generalized design procedure allows for the design of extended shear plates to be designed with several columns of bolts using standard and short-slotted holes (Muir & Hewitt, 2009).

2.3 Extended Shear Plate with Long Slots

While there is some AISC guidance when designing extended plates, there is little when it comes to long-slotted holes in those plates. In section J3.2, part (b) states that long-slotted holes may be used in single-plate design as long as it is approved by the engineer of record. Part (f) of that section also states that long-slotted holes may be used in one of the connecting parts for slip-critical and bearing-type connections (AISC, 2016b, p. 16.1-128). This verbiage allows different engineers to design connections for

conditions with large tolerances without the research and testing to fully understand how the connection will behave in the field (AISC, 2016b).

In an attempt to understand the behavior of this type of connection, Peterson (2014) constructed several finite analysis models in SAP2000 to observe the two-dimensional behavior of the single plates loaded in shear for different bolt diameters, bolt spacings, and slot widths. The original model outlined a ½ in. (12.7 mm) thick and 6 in. (152.4 mm) wide shear plate with two 13⁄16 in. (2.06 mm) tall and 3 in. (76.2 mm) wide slotted holes. The left side of the plate was modeled to be rigid, imitating the connection to a concrete wall. The bolts were modeled to be located at the right end of the slotted holes, farthest from the rigid support, showing the worst-case scenario. To accurately model the force applied by ¾ in. (19.1 mm) diameter bolts onto the plate, Peterson applied 23.8 kips (106 kN) to each slotted hole by modeling in compression only springs and linking them to the nodes associated with where the bolt was to be located (Peterson, 2014).

The results from the original test showed very small plate deformations, but very high stress concentrations. Due to the pattern seen between the slotted holes, as well as above and below the slotted holes, Peterson concluded that those sections of the plate were acting like small cantilever beams. After analyzing models with an increased number of bolt rows, Peterson observed that as the number of bolts increase, the stresses experienced by the plate decreases. Further comparison between the different models shows that the stress pattern is consistent regardless of the number of bolt rows the plate has; the upper left corner of the lowest slotted hole and the lower left corner of the plate

were observed to have the highest stress concentrations on all of the models (Peterson, 2014).

In Peterson's concluding remarks and recommendations, he acknowledges the limitations of the models created for his project. The yielding of the material was not considered, which hindered the stresses from redistributing through the plate. Also, due to the models being two-dimensional, any plate buckling and twisting that could occur was not able to be observed. However, Peterson provided recommendations that could achieve more accurate results and a better understanding for how this connection behaves. One suggestion was to create a nonlinear model; an advanced model could provide different failure modes that the plate would experience, show the three-dimensional deformed shape, and provide a better representation of the plate's behavior after yielding. The other suggestion was to set up a full-scale experiment to study the actual behavior of this type of connection (Peterson, 2014).

Man, Grondin, and Driver (2006) conducted an experiment for a similar connection: slotted holes in clip angle shear connections. Their report describes the experimental program and the observations from their experimental program, which included different configurations of single and double angle shear connections. The main variables for the different specimen include end distance, edge distance, cope dimensions, and the use of plate washers (Man, Grondin & Driver, 2006).

After analyzing the data and observations made, there were several findings that provided a better understanding for the behavior of these connections. Comparing the specimens with short-slotted holes and those with long-slotted holes, it was observed that the angles with shorter slots had a greater capacity; the angles with long slots typically

failed by angle end tearing. They also observed that using plate washers while testing showed an increase in capacity when compared to tests without plate washers, which was attributed to the change in governing failure modes. While this experimental initiative was focused on angles, the findings from this report are useful in understanding the behavior of slotted holes (Man, Grondin & Driver, 2006).

Another experimental initiative was conducted by Wollenslegel (2020), and the purpose of this project was to investigate the behavior of extra-long slots in reference to slip critical loads. This experiment consisted of thirty-three unique bolted joint configurations, with two of each configuration tested, split into nine different series of joints. The different variables used in these configurations include slot length, slot orientation, plate thickness, plate surface conditions, slot spacing, and bolt location within the slots (Wollenslegel, 2020).

After testing each specimen in direct shear, several observations were made regarding the different variables studied. One observation was that the average initial slip load was lower than the calculated slip load. It was also observed that the specimens that were blast-cleaned had higher slip loads than those that had cleaned mill scale surfaces. Another observation pointed out that the capacity increased as the spacing between the slots increased. There was also an inverse correlation between the length of the slots; as the length of the slot increased, the capacity decreased. While the trends that were observed were slight, they were still noticeable and worth stating. Unfortunately, the conclusions made in this report are not final; Wollenslegel noted that the final report will contain further analysis with revised conclusions, but has not been published (Wollenslegel, 2020).

Chapter 3: Experimental Program

Experimental testing was conducted at the Milwaukee School of Engineering's (MSOE) Construction Science and Engineering Center (CSEC). This experimental program aimed to gather behavioral data for extended single plate connections with long-slotted holes when subjected to a force perpendicular to the slots. As this research and experimental initiative was unprecedented, it is expected that the results from this project will provide an initial understanding of the plate behavior for this type of connection.

A series of twenty experiments were conducted to observe the behavior of the extended single plate connection with respect to two different variables: bolt group position within the long slots, and slot spacing. This project focused on the effects of the long slots due to the bolt group position within the slots. The data collected was also used for a parallel project, which the reader is also encouraged to read (Taxon, 2021).

3.1 Hypotheses

Before the experimental program was conducted, hypotheses were conceived based on previous research of an elastic finite element analysis (Peterson, 2014). As the connection is subjected to the transverse force, the plate behavior is thought to change when the bolt group position changes. When the bolt group is located closest to the welded edge of the connection, the plate is thought to behave similar to one with standard holes and engage in bearing. As the bolt group is positioned farther from the welded edge, the plate is thought to respond by a combination of shear and flexure. The plate sections between the slots are thought to act as cantilever beams when resisting the load, resulting in the plate bending.

3.2 Test Specimen Overview

This experimental program utilized a test specimen assembly design that consisted of two plates: a ¼ in. (6.35 mm) thick extended single plate welded to a PL 1 in. x 10 in. x 1 ft-10 in. (25.4 mm x 254 mm x 559 mm) base plate, as shown in Figure 3-1. The extended single plate included a set of three long slots that were 13⁄16 in. x 2 13⁄16 in. (20.6 mm x 7.8 mm). The slot length is longer than that specified in AISC by 15⁄16 in. (23.8 mm). The base plate was used to simulate the fixity a concrete embed plate would provide in the real-world application of this connection, while also eliminating the need to use concrete in the experimental setup.

As aforementioned, the test specimen assembly had to accommodate two variables: varying bolt group positions and varying slot spacings. The test specimen assembly had four different slot spacing configurations "S" of 3 in. (76.2 mm), 3½ in. (88.9 mm), 4 in. (102 mm), and 4½ in. (114 mm), as shown in Figure 3-2. As the spacing between the slots increases, the length of the extended single plate increases as well, ranging from 10 in. (254 mm) to 13 in. (330 mm). The five different bolt group positions vary within the slots, with a range of the bolt group positioned closest and farthest to the welded edge. At the 0% position, the bolt group location is closest to the welded edge; at the 100% position, the bolt group location is farthest from the welded edge. The remaining bolt group positions are at the quarter points within the slots: 25%, 50%, and 75%, where the ascending positions are located farther from the welded edge. The bolt group positions can be seen in Figure 3-3.

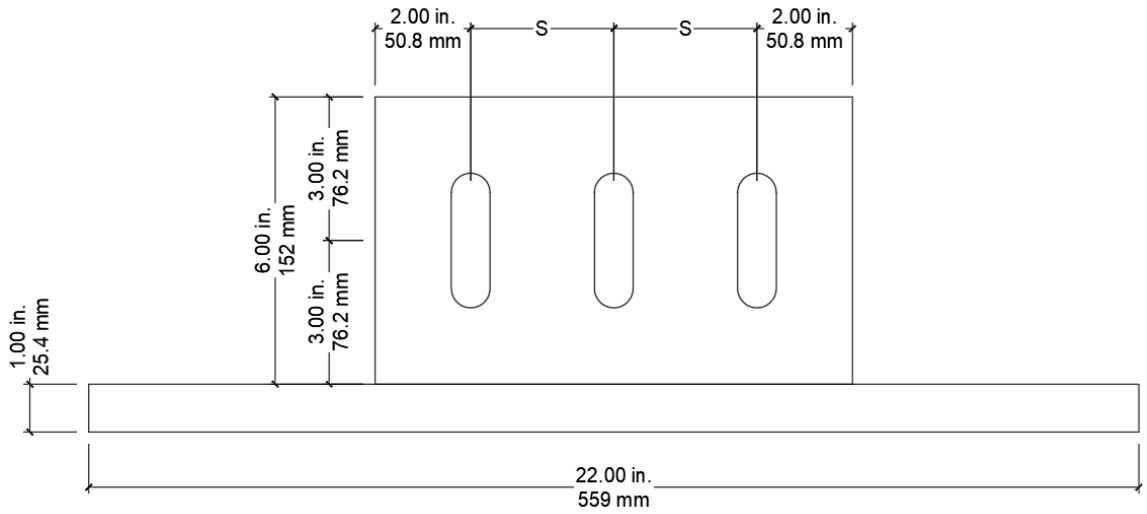

Figure 3-1: Test Specimen Configuration.

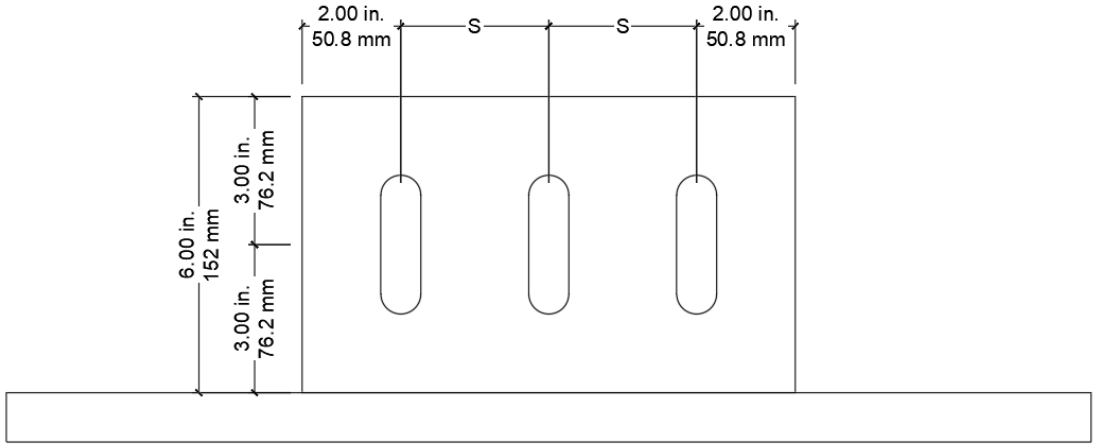

BOLT SPACINGS, S	
in.	mm
3.00	76.2
3.50	88.9
4.00	102
4.50	114

Figure 3-2: Test Specimen Bolt Spacings.

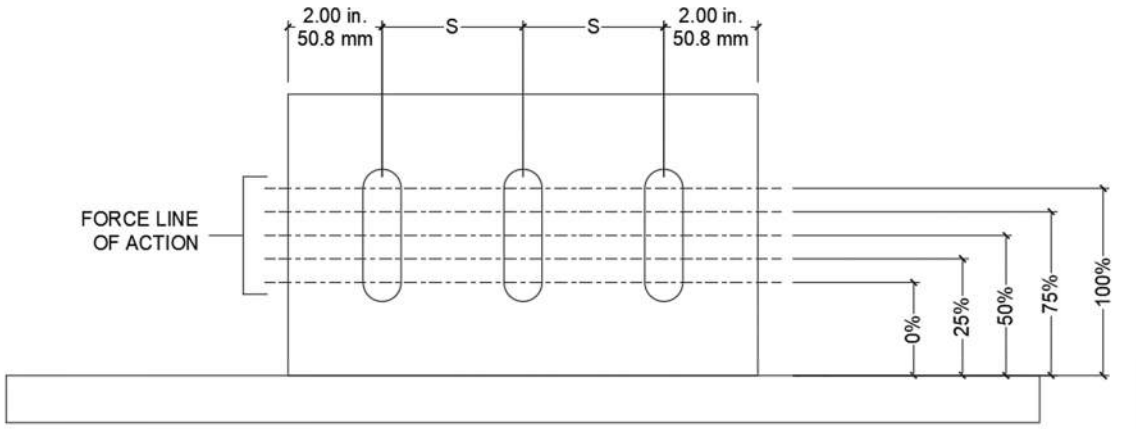

BOLT POSITIONS, P		
%	in.	mm
0	2.00	50.8
25	2.50	63.5
50	3.00	76.2
75	3.50	88.9
100	4.00	102

Figure 3-3: Test Specimen Bolt Position.

To differentiate and identify the test specimen, a naming convention was established and utilized throughout the experimental program; the structure of the specimen naming convention is shown in Figure 3-4. Each test specimen was accompanied by an identification card with their respective identifier through the testing process, which can be seen in all the photos and videos for this experimental program.

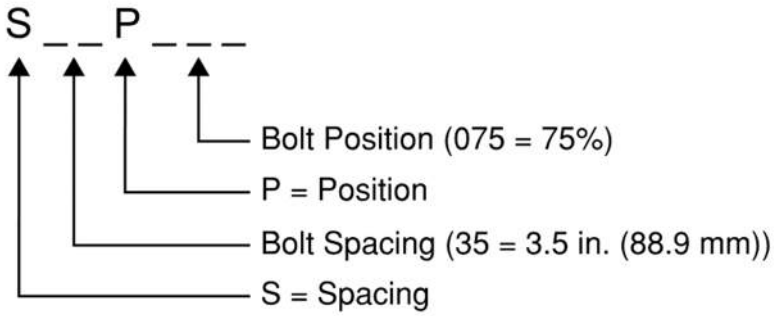

Figure 3-4: Test Naming Convention.

3.2.1 Expected Capacities

The plates used for the test specimen and other fabricated components in the experimental program were specified as ASTM A572 Grade 50. Material samples with dimensions of ¼ in. x 1½ in. x 12 in. (6.35 mm x 38.1 mm x 305 mm) were sent to Metallurgical Associates, Inc. (MAI) in Waukesha, Wisconsin to be tested. The material tests were performed to determine the true yield stress and ultimate stress, providing a better understanding of the plate properties and more precise information to include in calculations. The material testing results concluded that the average yield stress, F_y, was 62.7 ksi (432 MPa), and the average ultimate stress, F_u, was 72.9 ksi (502 MPa). The results from the material testing can be found in Appendix A.

Since this experimental program aimed to determine plate behavior, there was a desire to see how the bolts interacted with the plate when under shear loading. For that reason, the bolts were specified to be type N bolts bearing, including threads in the shear plane and not have slip resistance. This would allow for the bolts to bear into the long slots of the plate, illustrating the behavior of the plate without resistance from the bolts. Further, the point of failure for the slip-critical condition would be based on the bolts, rather than the plate.

The test specimens were designed per the provisions in the AISC *Specification*, along with additional limit state checks that could govern for this experimental program, determined through engineering judgement. In these designs there were six limit states that were considered, including weld strength from Section J2 of the AISC *Specification*, bolt shear from J3.6, bolt bearing from J3.10, plate shear yield and plate shear rupture from J4.2, block shear strength from J4.3, and flexural strength of the connecting

elements from J4.5. Table 3-1 shows the expected capacities from these calculations.

As the bolt group position increased, the expected capacity decreased; the trend from the expected capacities aligns with the hypotheses for this experimental program. A visual of this trend can be seen in Figure 3-5. From the calculations, there were different limit states that would govern depending on the test. It should be noted that from the initial calculations, most of the tests with higher bolt group positions were expected to fail in bolt plate flexure, with some expected to also fail in bolt bearing. The tests at the lowest bolt group position were expected to fail in bolt bearing or plate shear rupture.

Table 3-1: Expected Capacities and Failure Modes for Each Test Specimen.

TEST ID	EXPECTED CAPACITY kip (kN)	EXPECTED FAILURE MODE
S30P100	22.1 (98.1)	Bolt Plate Flexure
S30P075	29.4 (131)	Bolt Plate Flexure
S30P050	44.1 (196)	Bolt Plate Flexure
S30P025	60.8 (270)	Plate Shear Rupture
S30P000	60.8 (270)	Plate Shear Rupture
S35P100	31.6 (141)	Bolt Plate Flexure
S35P075	42.1 (187)	Bolt Plate Flexure
S35P050	61.3 (273)	Bolt Bearing/Bolt Plate Flexure
S35P025	67.9 (302)	Bolt Bearing/Bolt Plate Flexure
S35P000	71.7 (319)	Plate Shear Rupture
S40P100	43.1 (192)	Bolt Plate Flexure
S40P075	57.5 (256)	Bolt Plate Flexure
S40P050	61.3 (273)	Bolt Bearing/Bolt Plate Flexure
S40P025	67.9 (302)	Bolt Bearing/Bolt Plate Flexure
S40P000	82.0 (365)	Bolt Bearing
S45P100	56.6 (252)	Bolt Plate Flexure
S45P075	59.1 (263)	Bolt Bearing/Bolt Plate Flexure
S45P050	61.3 (273)	Bolt Bearing/Bolt Plate Flexure
S45P025	67.9 (302)	Bolt Bearing/Bolt Plate Flexure
S45P000	82.0 (365)	Bolt Bearing

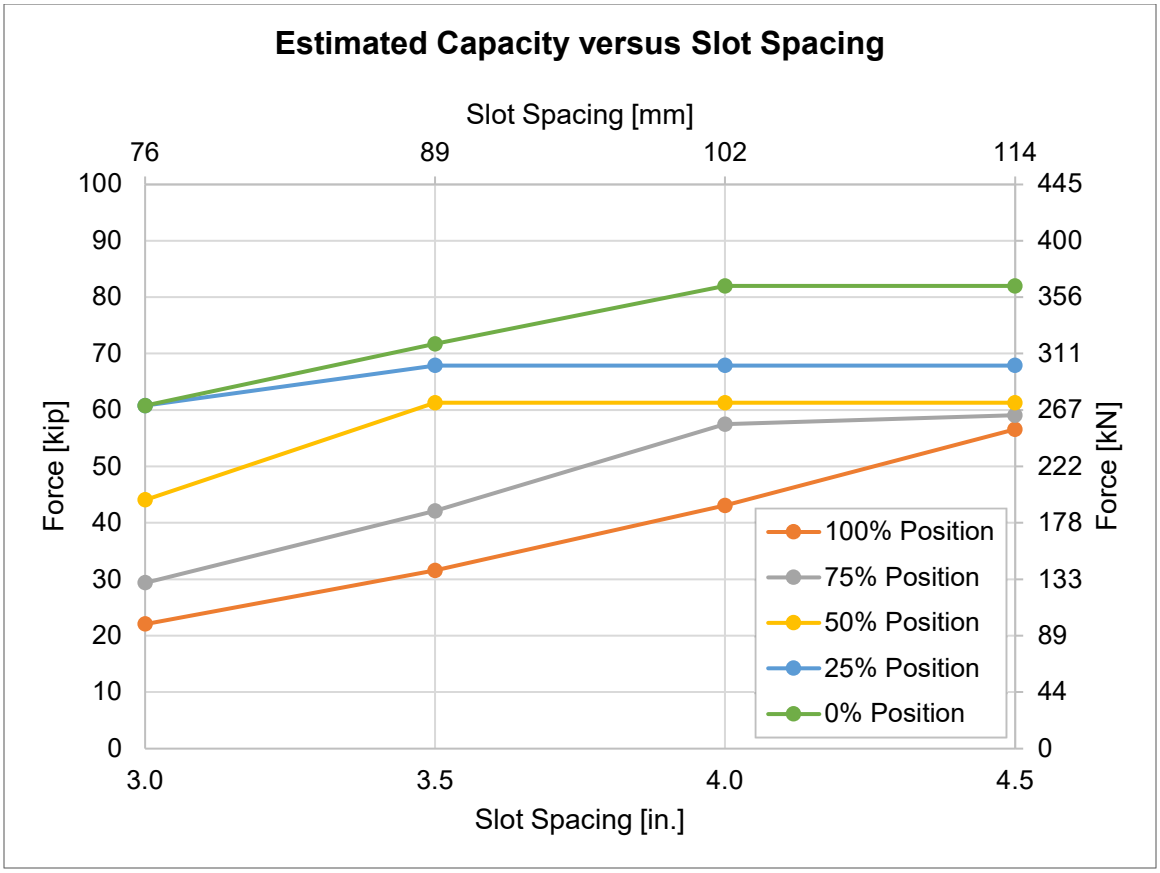

Figure 3-5: Estimated Capacity versus Slot Spacing Graph.

A sample set of calculations for the test specimens, as well as the other fabricated items such as the yoke assembly and sandwich plates, can be found in Appendix B.

3.3 Test Assembly Overview

3.3.1 Test Assembly

Utilizing the resources provided through MSOE, the test setup was composed of various elements from past graduate research projects, donated fabricated items, and purchased items. A schematic of the test setup is shown in

Figure 3-6. A W18x76 support beam served as the base for the entire assembly, providing stiffness to the experiment and attachment locations for the test specimen and data acquisition elements.

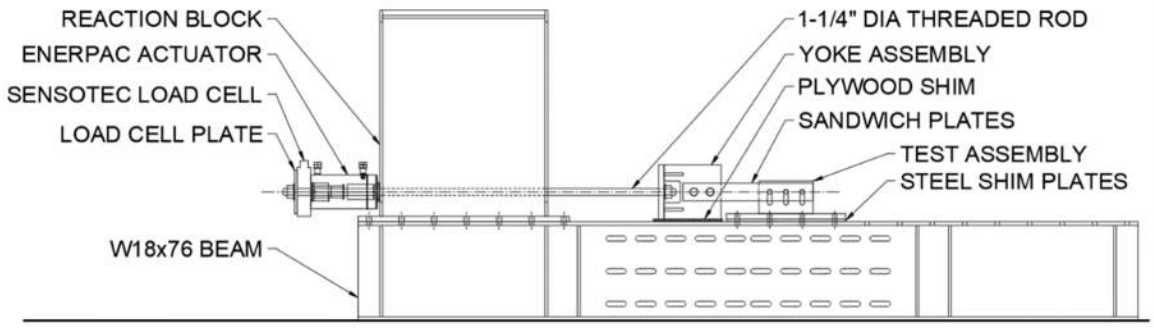

Figure 3-6: Test Assembly Schematic.

A series of welded plates formed the reaction block which was bolted to the top flange of the support beam. The reaction block served as an attachment location for the Enerpac RRH-606 “Holl-O-Cylinder” hydraulic actuator. The support beam, reaction block, and the actuator used are pictured in Figure 3-7. The actuator, with a maximum stroke of 6½ in. (166 mm) and maximum capacity of 120 kips (534 kN), was used to apply the load. A Sensotec 41-A530-01-03 load cell, with a maximum capacity of 100 kips (445 kN), was used to measure the load from the actuator. A 1 in. (25.4 mm) thick plate was placed behind the load cell to stabilize it for the load to be accurately measured. Figure 3-8 shows the two pieces of equipment that were used for the experiments.

Figure 3-7: Support Beam, Reaction Block, and Hydraulic Actuator.

Figure 3-8: Enerpac Hydraulic Actuator (left) and Sensotec Load Cell (right).

A 1¼ in. (31.8 mm) diameter Grade B7 threaded rod was used to connect the test specimen to the load cell and actuator, providing a means for tensile load transfer through the threaded rod. The threaded rod length was initially 12 ft (3.66 m) but was cut down to 8 ft (2.44 m). The threaded rod was attached to a fabricated yoke assembly, which was supported by a plywood shim. The shim provided a raised platform for the yoke assembly, allowing it to be level with the threaded rod and the specimen assembly.

The yoke assembly was a fabricated item meant to be part of the connection between the test specimen assembly and the threaded rod. This assembly, as seen in Figure 3-9, consisted of two ½ in. (12.7 mm) plates welded to a 1 in. (25.4 mm) base plate. The threaded rod was placed through the opening in the vertical plate and secured to the assembly with a nut and washer. To connect the yoke assembly to the test specimen assembly, two thick "sandwich" plates were bolted to the yoke and the test specimen. There were four sets of these PL 1 in. x 3½ in. (25.4 mm x 88.9 mm) plates, each pair increased 1 in. (25.4 mm) in length, from 2 ft-0 in. (610 mm) to 2 ft-3 in. (686 mm), to accommodate for the different slot spacings of the specimen. These plates had

two different diameter bolt holes along the length: two 1⅜ in. (34.9 mm) diameter bolt holes for the yoke assembly side, and three ¹³⁄₁₆ in. (20.6 mm) diameter bolt holes for the test specimen assembly side. Each set of the sandwich plates can be seen in Figure 3-9.

To avoid moving the actuator to achieve the different bolt positions, the test specimen assembly was placed on top of a specific number of shim plates to achieve the bolt group position during the test. One of the shim plates can be seen in Figure 3-10. For the bolt group position closest to the welded edge, the specimen was sitting on five shim plates; for the bolt group position farthest from the welded edge, the specimen was sitting on one shim plate. The specimen assembly and shim plates were bolted to the top flange of the support beam using ¾ in. (19.1 mm) diameter tension control bolts. The length of the tension control bolts for each position increased as the number of shims increased. The length of the tension control bolts ranged from 3½ in. (88.9 mm) to 5¼ in. (133 mm). The shop drawings for each fabricated item can be found in Appendix C.

Figure 3-9: Yoke Assembly (left) and Sandwich Plates (right).

Figure 3-10: Steel Shim Plate.

3.3.2 Instrumentation

There were three measurements that were taken as part of these experiments: load, displacement, and strain. As aforementioned, a Sensotec load cell was used to measure applied load on the specimen. Strain rosettes were used on some specimens to understand the strain that the specimen undergoes at the base of the slotted hole. Linear variable displacement transducers (LVDTs) were used to measure displacement at two locations on the specimens. A rosette can be seen in Figure 3-11, and the LVDTs set up on the test specimen are shown in Figure 3-12.

The rosette strain gauges were applied to fourteen of the twenty test specimens: the 0%, 50%, and 100% bolt group positions for each spacing, and the 3-in. (76.2 mm) spacing at 25% and 75%. This rosette collected strain data in three different directions – 45 degrees towards the load, perpendicular to the load, and 45 degrees away from the load – enabling the calculation of principal stresses at the point of the gauge. These data provide information on the shear and flexure within the plate that cannot be observed otherwise.

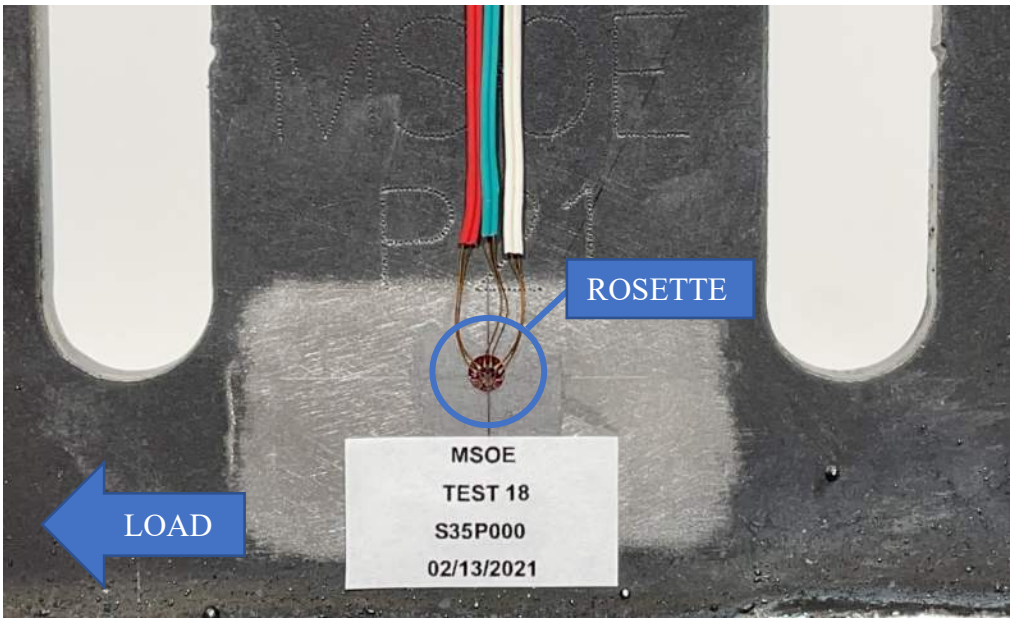

Figure 3-11: Rosette on Test Specimen.

The LVDTs gathered displacement data for two distinct aspects of the test setup: lateral displacement of the single plate and vertical displacement of the base plate. There was an LVDT with a 2-in. (50.8 mm) stroke placed near the top of the single plate on the non-loaded edge. This LVDT measured the lateral displacement and deformation of the single plate when subjected to the transverse force. Due to the size of the shear tab, a rare earth magnet and a small nut were positioned on the top edge of the plate to hold the tip of the LVDT in place during the test. A second LVDT with a 1-in. (25.4 mm) stroke was placed on the non-loaded edge of the base plate in the test specimen assembly, measuring vertical displacement. The purpose of this LVDT was to monitor the rotational displacement of the test specimen assembly, providing information on whether the assumed fixity was correct.

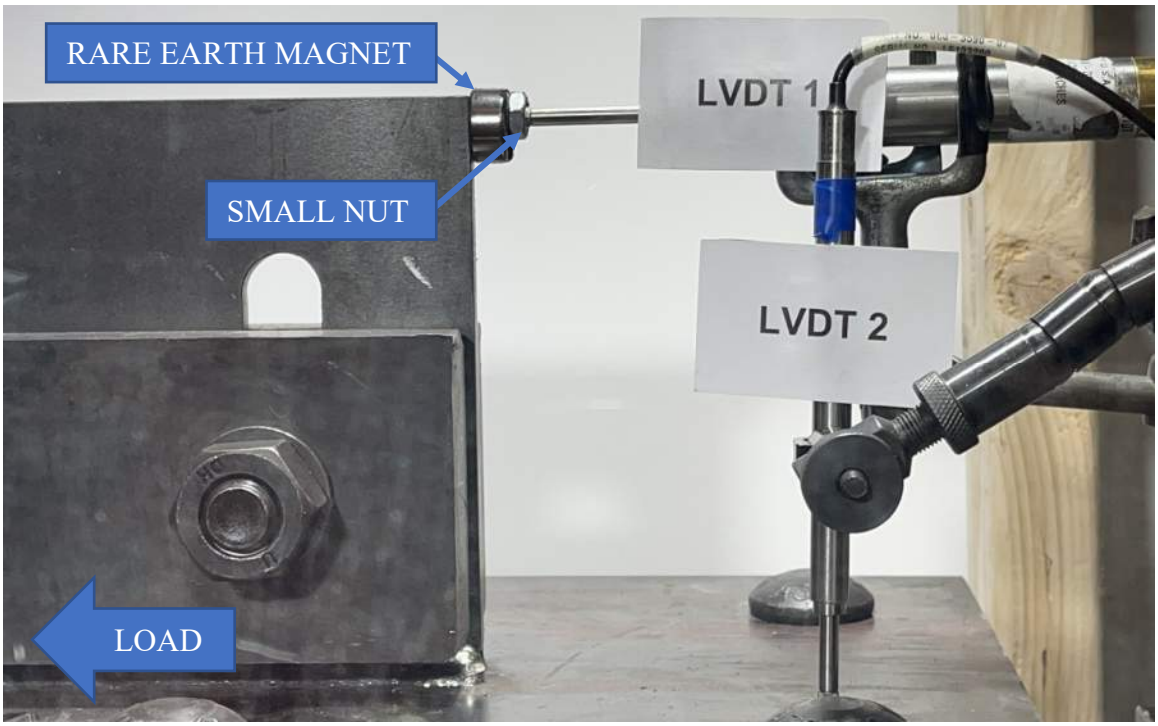

Figure 3-12: LVDTs on Test Specimen.

3.4 Test Procedure

Consistency between the different tests in the experimental program is important when considering certain variables during the analysis of the data gathered. Therefore, a test procedure was created and followed for each test that was performed. This was done in an effort to minimize outside factors and variabilities that could affect the results of the experiment. As different challenges arose for the different tests, certain steps were added or modified in an effort to remedy the complication.

3.4.1 Pre-Test Procedure

Before any testing setup began, each specimen was thoroughly documented. The specimens were sorted and labeled with their respective name per the naming convention. Once identified, measurements of the extended single plates were taken to ensure the

dimensions of the specimens matched those specified in the shop drawings, and that they were consistent among all the specimens.

For the tests that had rosettes attached, a procedure was followed to ensure the rosette was attached correctly. The strain gauge location was marked on the specimen; the strain gauge would be located between the two slots closest to the load and in line with the bottom of the slots, as shown in Figure 3-13. Then, a cone shaped Dremel bit, three different grit sandpaper, and a buffer Dremel bit were used to grind off the mill scale and surface debris, leaving a smooth surface for the rosette to be applied. The area was then cleaned using a cotton swab and acetone.

Once the surface was prepared, the exact location of the rosette was located by scoring the plate using a razor blade and a square. The surface was roughened using sandpaper to provide something for the adhesive to grip onto. The rosette was lined up to the intersection of the scored lines, and the rosette wires were taped down to the plate to keep it in place. The area on the plate and the rosette were cleaned with acetone. Once the acetone dried, adhesive was applied to the rosette and was quickly and accurately placed on the intersection of the scored lines. Pressure was applied to the rosette to ensure the adhesive took to the plate.

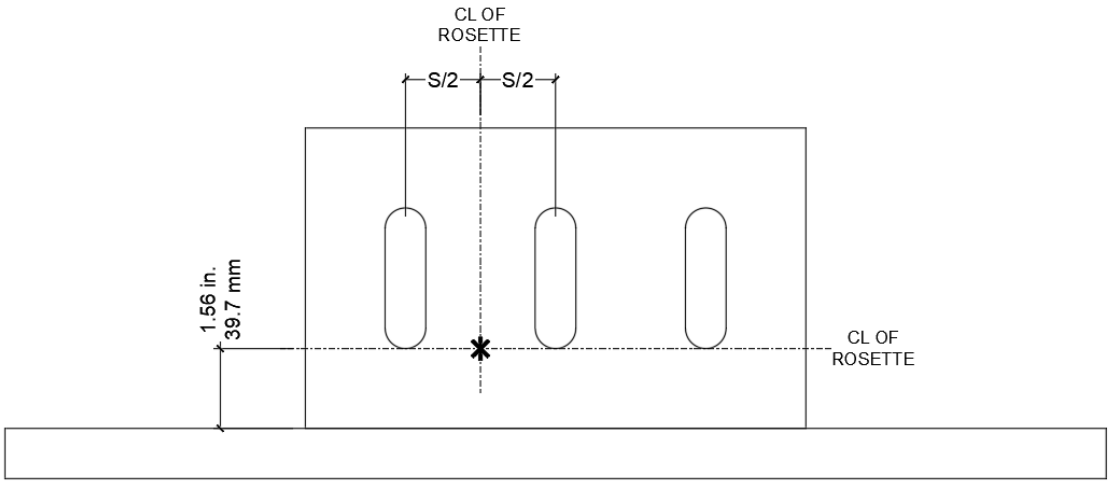

Figure 3-13: Location of Rosette.

The specimens were then documented through a series of pictures. These pictures served as a baseline for each test, providing a visual representation of their condition and the instrumentation used. The specimens were pictured at several different viewpoints and were accompanied by their test ID card, which included the test number, the date tested, and the test name per the established naming convention. To be consistent between the specimens, the same series of pictures were taken in front of a white background.

Moving to the test setup, each test had their own set of specific requirements. Each test required a specific number of shim plates, a specific length tension-controlled bolt, and a specific length of sandwich plate. The number of shim plates were based on the bolt position for the test; one shim plate was needed for the bolts positioned at 100%, and five shim plates were needed for the bolts positioned at 0%. The length of the tension-controlled bolts was dependent on the number of shim plates used for the test; the 5¼ in. (133 mm) long bolts were used for the 100% bolt position, and the 3½ in. (88.9 mm) long bolts were used for the 0% bolt position. The length of the sandwich plates was

dependent on the specimen's slot spacing; the 2 ft-0 in. (610 mm) long plates were used for the 3-in. (76.2 mm) spacing, and the 2 ft-3 in. (686 mm) long plates were used for the 4½-in. (144 mm) spacing.

Once those items were acquired, the shim plates were set down and aligned with the bolt holes in the beam flange. The specimen was set on top of the shim stack and then the eight tension-controlled bolts were placed through the specimen, shim stack, and the beam flange with the nuts and washers placed on loosely. Then, one sandwich plate was positioned behind the specimen, allowing for the bolts to be pushed in through the back of the assembly. When the bolt was pushed through the sandwich plate and the specimen, a washer was set on each bolt. This washer was used as a barrier for the rosette so it would not get damaged during the test. While there were some tests that did not have rosettes, the washers were still used in order to be consistent. After setting the second sandwich plate into the bolts, through the front of the assembly, the nuts and washers were loosely placed on the ends of the bolts.

The next step was to attach the yoke assembly to the test assembly. The threaded rod and yoke assembly were pulled out closer to the specimen to provide slack during the fit-up process. The two sandwich plates slid inside the yoke assembly, and the yoke shim was pushed in between them, until the bolt holes lined up. To aid in the bolt hole alignment process, the back end of a spud wrench was pushed through one of the bolt holes and moved the different plates around until they were lined up. A bolt was placed through the open bolt hole, the spud wrench was taken out for another bolt to be placed through. The nuts and washers were then loosely placed on the ends of the bolts.

Since the slotted holes in the test specimen were oriented perpendicular to the load, the bolts connecting the sandwich plates to the specimen had the ability to slide down the slots. After lifting the sandwich plates within the slots to be level, the bolts were finger tightened. Then, for tests with one to three shim plates, the nuts on the yoke bolts were tightened using a channel lock and a 1⅝ in. (41.3 mm) box wrench. After ensuring the sandwich plates were still level, the bolts in the specimen and sandwich plates were lightly tightened using spud wrenches. Then, the threaded rod was pulled snug to the yoke assembly, and the nut on the threaded rod was finger-tightened to the back of the actuator. The tension-controlled bolts through the specimen, shim stack, and beam flange were finger-tightened, and then fully tightened using a shear wrench, as seen in Figure 3-14. The bolts were tightened in a certain order for each test, as seen in Figure 3-15.

Figure 3-14: TONE Shear Wrench.

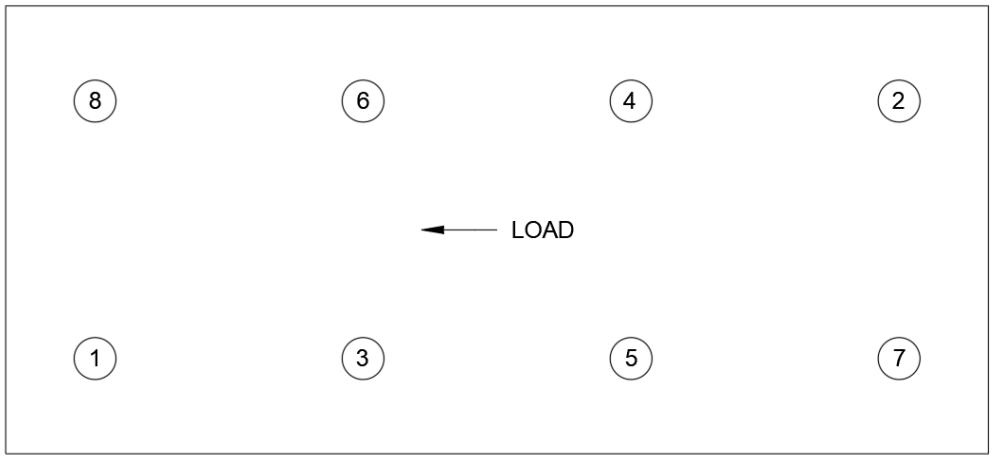

Figure 3-15: Typical TC Bolt Tightening Order.

For the tests that required four or five shim plates under the specimen, the procedure was slightly modified to account for slipping between the plates. Before tightening the bolts for the sandwich plates and the yoke assembly, the tension-controlled bolts in the specimen, shim plates, and beam flange were finger-tightened. Then, the actuator was turned on and pulled on the assembly up to a load of ½ kip (2.2 kN) to allow the shim plates to shift. Then, the tension-controlled bolts were fully tightened using a shear wrench in a slightly different order, as seen in Figure 3-16. The load from the actuator was released and the actuator was turned off once the tension-controlled bolts were tightened. Then, just as was done for the tests with fewer shim plates, the nuts on the yoke bolts were tightened using a channel lock and a box wrench and the bolts in the specimen and sandwich plates were lightly tightened using spud wrenches.

Once the plates were bolted together, the instrumentation equipment was set up and connected. For the tests that had rosettes, the rosette wires were connected to the data acquisition system. Then, the LVDTs were set up on the beam flange; LVDT 1 was oriented horizontally, resting in the LVDT stabilizer that was on the extended single plate

of the specimen assembly, and LVDT 2 was oriented vertically, touching the base plate of the specimen assembly.

Then, the test IDs were placed on the specimen, the LVDTs, and the plexiglass shield. The shield was cleaned and placed over the test assembly with a white backdrop behind the assembly, resting against it. There were two shop lights that were placed around the assembly to eliminate as many shadows as possible to help in achieving a visual on what happens during the test. There were two cameras that were set up to record the tests, one in front of the test, and the other on top of the plexiglass shield. To start the test, pictures were taken from both cameras and were set to record.

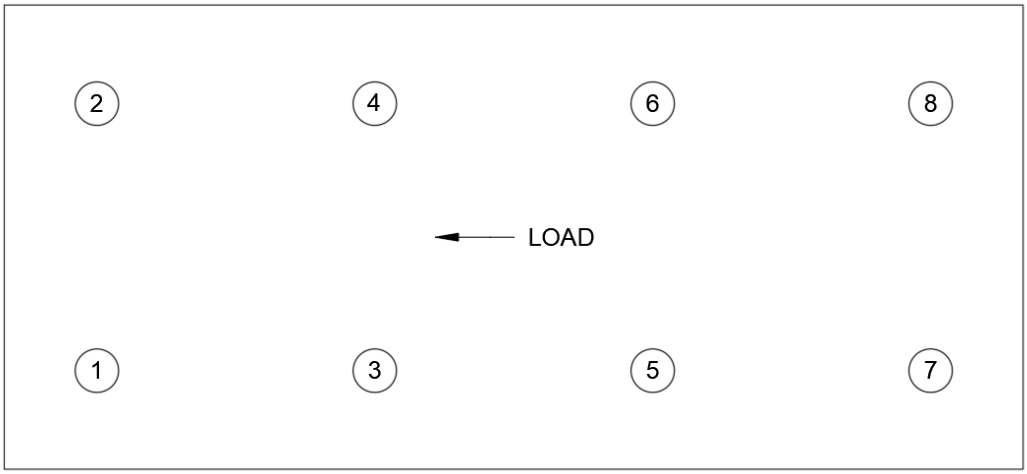

Figure 3-16: TC Bolt Tightening Order for Lower Bolt Group Positions.

3.4.2 Test Loading

When setup was complete, the actuator was turned on, and the load cell, rosettes, and LVDTs were checked to ensure they were reading. To ensure the data acquisition system was reading the numbers correctly, the readings from the LVDTs were called out and matched with the ones in the data acquisition system. Load was applied as monotonically as possible. The amount of load per step was not constant due to the actuator controls. Load measurements were announced during the test for the research team to hear.

The tests ended when one of two outcomes happened: there was sufficient shear deformation seen in the extended plate and it was not gathering more load, or the capacity of the load cell was reached. Once one of those two outcomes occurred, the actuator would be released. The data were saved by the data acquisition system.

3.4.3 Post-Test Procedure

Upon completion of a test, pictures were taken of the deformed test specimen and the camera recordings were turned off. The plexiglass shield was removed, and the test IDs were removed and saved for post-test pictures of the specimen. The LVDTs were removed from the specimen, and the rosette wires were disconnected.

The test specimen was then removed from the beam and placed on a table with a white background for post-test pictures. The post-test picture series included all the same angles from the pre-test pictures, as well as some focused on specific behaviors that were observed on the specimen.

Chapter 4: Experimental Results

Each test in the experimental program yielded both qualitative and quantitative data. The qualitative data consisted of the initial observations during the tests, as well as observations on the specimen behavior after watching the video recordings taken of each test. The quantitative data consisted of load, displacement, and strain data gathered through the data acquisition system. This chapter will discuss general observations and present the data gathered from the tests.

4.1 Observed Specimen Behavior

Each specimen was seen to behave in two ways: bolt bearing and plate flexure. The different specimens demonstrated different levels of each of those behaviors, with trends following the location of the bolts within the slotted holes. The specimens with bolts positioned closer to the weld displayed more bolt bearing behavior, while the specimens with bolts positioned farthest from the weld displayed more plate flexure behavior. The different levels of each behavior seen in the different test specimens are described in Table 4-1. The specimens that displayed plate flexure also experienced cusping at the bottoms of the slotted holes. As the specimens were loaded and the plate started to deform, the slotted holes started collapsing, creating cusps. There were also several different behaviors that were observed in the different specimens; some of the behaviors were seen in a couple of the tests, while others were seen in the majority of the tests.

Table 4-1: Observed Specimen Behaviors.

TEST ID	OBSERVED BOLT BEARING	OBSERVED PLATE FLEXURE
S30P100	Minimal	Moderate
S30P075	Minimal	Significant
S30P050	Extreme	Extreme
S30P025	Extreme	Extreme
S30P000	Extreme	Significant
S35P100	Moderate	Significant
S35P075	Significant	Extreme
S35P050	Moderate	Significant
S35P025	Moderate	Moderate
S35P000	Significant	Minimal
S40P100	Minimal	Moderate
S40P075	Moderate	Moderate
S40P050	Moderate	Moderate
S40P025	Significant	Moderate
S40P000	Significant	Minimal
S45P100	Moderate	Moderate
S45P075	Moderate	Moderate
S45P050	Moderate	Minimal
S45P025	Significant	Minimal
S45P000	Significant	Minimal

Plate tearing at the bottom of the slots in the direction of the load was observed in two of the tests: S30P050 and S35P075. Since there was no trend in the bolt position or the slot spacing, the plate tearing was determined to be due to the extreme loading of the specimens. Once the slots were no longer able to deform due to the cusping, the plate started tearing to allow for further deformation.

The top corner of the non-loaded edge of the specimen turned up in all the tests, except S40P000, S45P025, and S45P000. The tests that did not display this behavior had lower bolt positions, greater slot spacings, and displayed more bolt bearing than plate

flexure. A possible explanation for this is that the plate could behave as a frame while in flexure, resulting in the upward turn of the plate material on the specimens that displayed a lot of plate flexure. This behavior, as seen in Figure 4-1, could have been seen in more of the tests if more load was applied to the specimens.

Local out-of-plane plate buckling was also seen in the different tests in the experimental program. There were two areas of the plate where the local buckling was observed: the bottom of the loaded edge on the shear tab, and the top of the shear tab near the loaded edge. Both behaviors can be seen in Figure 4-2. The local out-of-plane buckling at the bottom of the loaded edge was seen at each spacing with bolt group positions at 100%, 75%, and 50%, as well as test S30P025. The magnitude of the buckling depended on the bolt group position, the slot spacing, the loading applied to the specimen. The specimens with lower bolt group positions and greater slot spacings experienced less buckling than the specimens with higher bolt group positions and smaller slot spacings.

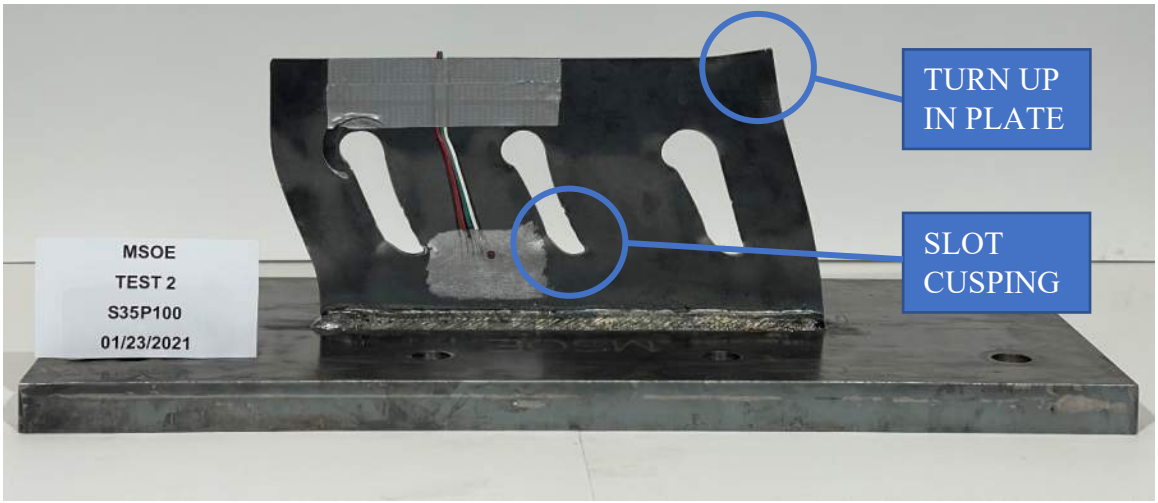

Figure 4-1: Example of Slot Cusping and Plate Turn Up.

Finally, the local out-of-plane buckling at the top of the shear tab near the loaded edge was observed in every test. The top of the single plate was seen to buckle towards one of the sandwich plates. This behavior could be attributed to a possible eccentricity from the washers that were placed in between the single plate and the sandwich plate to avoid crushing the rosettes during the tests.

Pictures of the test specimens before and after testing can be found in Appendices D and E, respectively. These pictures are provided to enable the reader to compare the before and after results of the tests, as well as to see the different behaviors that were observed during the experimental initiative.

Figure 4-2: Local Out-of-Plane Buckling on Loaded Edge (Left) and Top of Specimen (Right).

4.2 Shear Tab Displacement Data

The shear tab displacement data were gathered from LVDT 1, which measured the lateral displacement at the top of the plate during the tests. The data provided consistent trends for the different specimens and their configurations throughout the experimental program, allowing these data to be the focus for the analysis. There were, however, various elements in the data gathered that provided challenges when making observations and conclusions.

One of the elements occurred at the start of the data collection. As the tests were prepared to begin, the instrumentation and the data collection system were turned on before any load was applied to the specimen. Since the data collection system was running before the test began, there were a lot of extra data points that fluttered around the 0 kip (0 kN) line in the graphs. Since the beginning data were not useful for the analysis phase, they were omitted and not used in the analysis of this project.

Other elements that had to be addressed are the noise and spikes found in the lateral displacement data. Two different aspects of the test setup could have caused the fuzziness of the data: issues with the LVDT or signal conditioner, or the LVDT stabilizer setup. There could have been issues with how the LVDT or signal conditioner was reading or outputting the data gathered, causing fluttering of the data points to occur. There also could have been an issue with the LVDT stabilizer setup. Due to the LVDT being confined in the nut, there is a possibility that the LVDT was getting caught on the nut at some points, gathering data that were not representative of the test. Even though noise and lateral spikes were seen throughout the data for the different tests, the general trends of each data set can be seen. Chapter 5 will discuss the steps taken to minimize the

noise in the data to show the trends in the data more clearly, as well as how the steps contributed to the analysis phase.

The final general element for the lateral displacement data is the crossing pattern that occurs in the horizontal portion of the data, which has been called out in Figure 4-3. This crossing pattern could be the result of a LVDT or signal conditioner issue, or pauses between loadings during the tests. These pauses could be from unusually long breaks between the manual loading of the specimen or breaks during the test to observe the behavior of the specimen after a noise was heard or unexpected plate behavior was occurring. When the pauses between loads become too great, load could be released from the specimen, lessening the deformation of the specimen, causing the LVDT to read lower lateral displacements.

Figure 4-3 shows the raw data for load versus lateral displacement for all five bolt group positions at 3-in. (76.2 mm) spacing. The trends seen in this graph are similar to the trends seen at the other slot spacings. The first trend describes how the specimen deforms during the experiment. The data sets consist of a near-vertical section, starting at the bottom of the plot, where load is quickly applied with little lateral deformation. Then, there is a turning point where, at a certain load, the lateral deformation drastically increases. Finally, there is a near-horizontal section of the data set where the load is slowly applied with great lateral deformation. The other trend seen at this spacing, as well as the others, is when the bolt group is positioned closer to the weld, the capacity of the specimen increases.

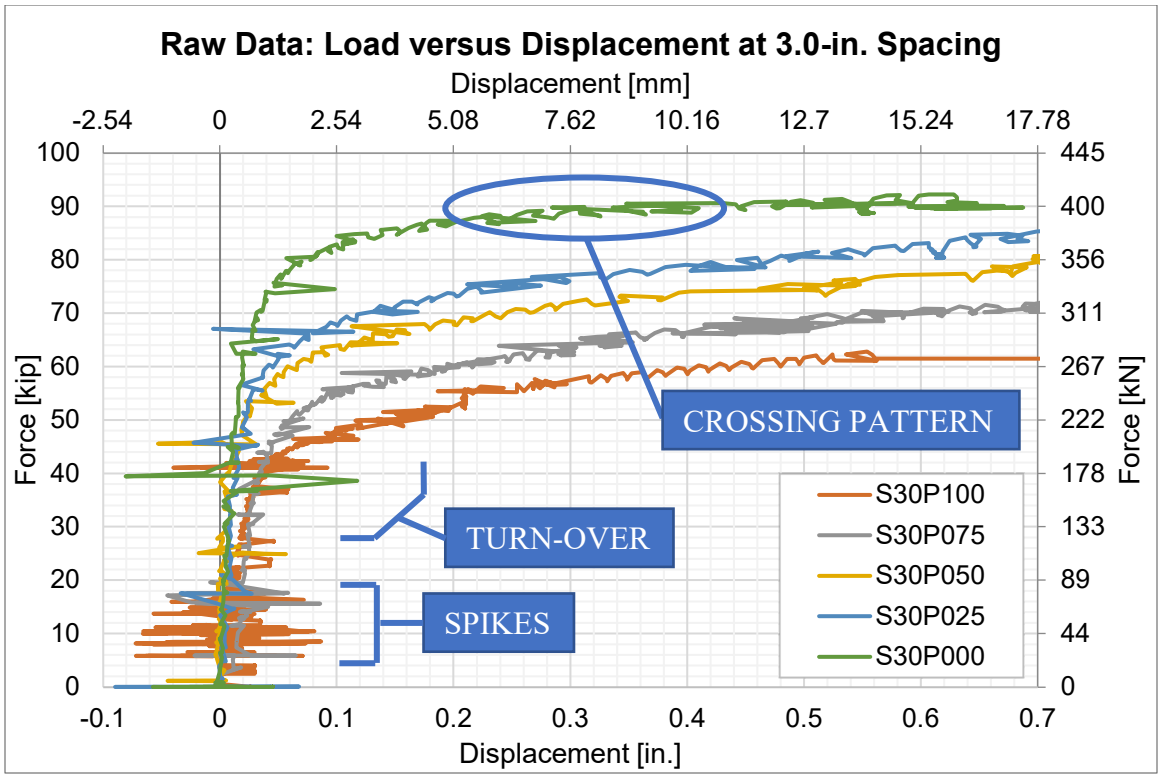

Figure 4-3: Raw Data at 3.0-in. Spacing.

While the trends for the 3-in. (76.2 mm) spacing are true for the other three spacings, there are a few differences that the other three spacings share. The graphs at 3½ in. (88.9 mm), 4 in. (102 mm), and 4½ in. (114 mm) spacings can be found in Figure 4-4, Figure 4-5, and Figure 4-6, respectively. It can be observed that the specimens with bolt group positions of 100% and 75% are similar in magnitude when comparing the capacities and lateral displacement. Additionally, some of the specimens with the 0% and 25% bolt group positions reached the capacity of the load cell before significant deformation was observed, rendering these specimens partially documented. Additionally, data from tests S35P050, S40P025, and S45P075 contained a horizontal shift near the bottom of the graph. Upon reviewing the videos of the tests, the shift was determined to be from LVDT 1 settling into the LVDT stabilizer.

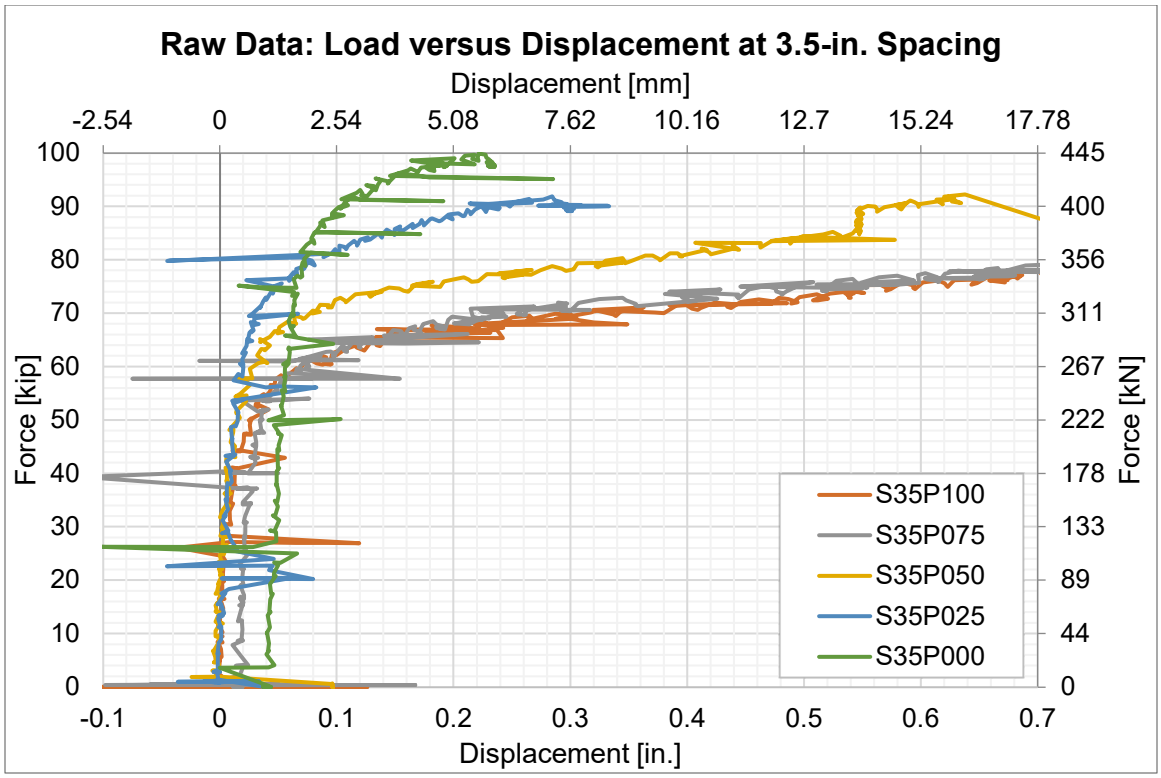

Figure 4-4: Raw Data at 3.5-in. Spacing.

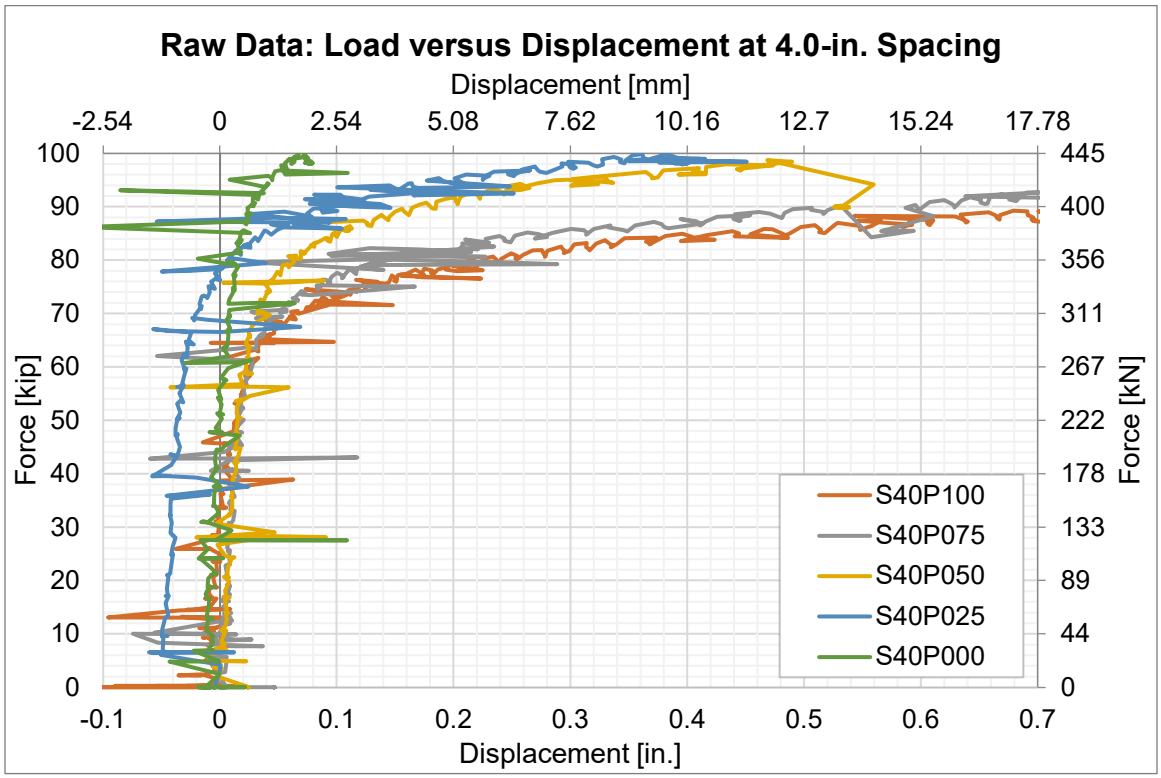

Figure 4-5: Raw Data at 4.0-in. Spacing.

The specimens at the 4½ in. (114 mm) spacing displayed even more differences than the other spacings. Three out of the five specimens reached the load cell capacity before significant lateral displacement was observed, rendering those three specimens partially documented. In test S45P075, there was a horizontal shift in the data at around 80 kips (356 kN). However, after reviewing the video of the test, there was no visible shift of the specimen, so the shift in data was determined to be from the LVDT or signal conditioner issue. Finally, in test S45P000, there was little noise in the data but there was a significant horizontal shift in the data around 88 kips (391 kN). After reviewing the video, the plate is seen to be slightly deforming throughout the test, but the reason for the sudden shift in lateral displacement is unknown.

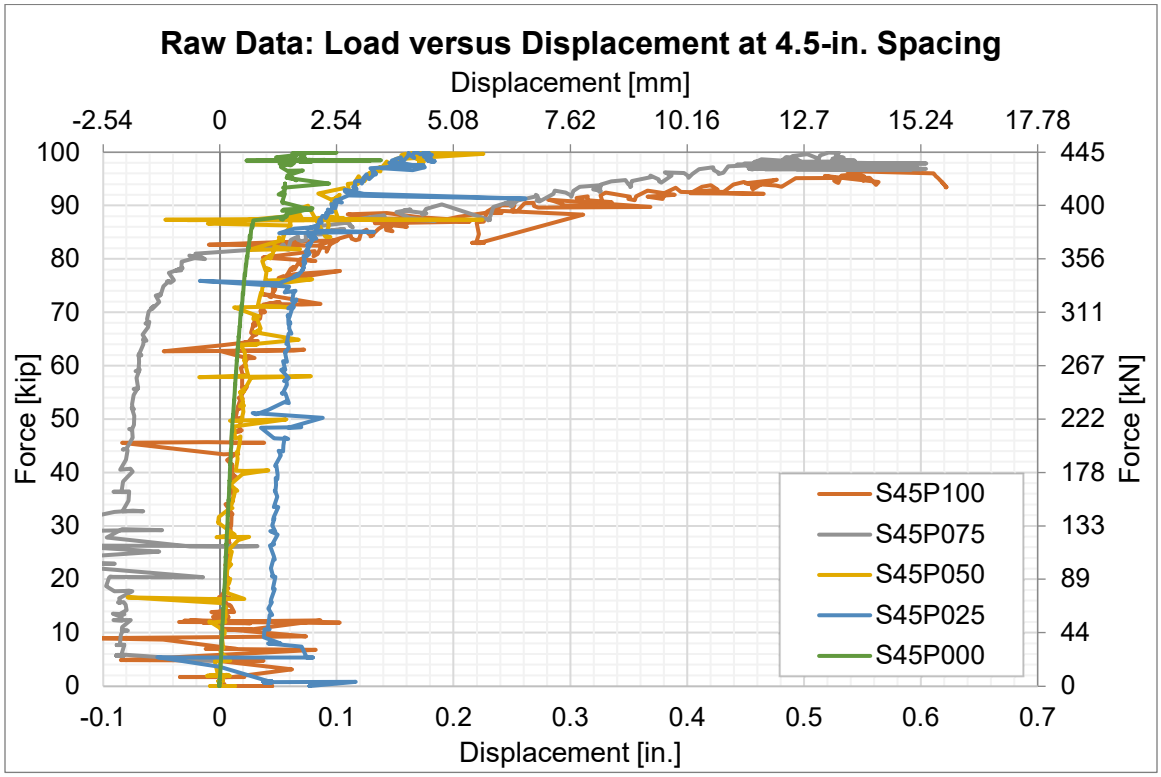

Figure 4-6: Raw Data at 4.5-in. Spacing.

4.3 Base Plate Uplift Data

As aforementioned, a fixed condition was assumed for the connection between the specimen base plate and the supporting beam. In an effort to determine whether the assumed fixity was achieved during the different tests, an LVDT was used to measure the vertical displacement of the base plate. The data from LVDT 2 were minimal for each test, with a maximum vertical displacement out of the twenty specimens tested of less than 0.005 in. (0.13 mm). The minimal vertical displacement seen in each test indicates that the goal of fixity was achieved in this experimental program. Representative graphs of the applied load versus the vertical displacement data for each test can be found in Appendix F.

4.4 Rosette Data

To observe the relative deformation behavior of the specimens between the long-slotted holes, strain data were collected from the rosettes that were attached to 14 of the 20 tests. The strain data, compared to the load applied for its respective test, produced a similar trend for each test where these data were gathered. At the beginning of each test, the strains in all three directions read around zero strain. Once the plate started experiencing significant shear deformation, the strains started increasing, veering away from the zero-strain line. The two strains taken at 45-degree angles increased exponentially in magnitude, while the perpendicular strain slightly increased in magnitude once the plate deformation caused the plate to stretch. During some of the tests, the deformation created too much tension in the rosette wires, causing the wires to detach from the plate. Horizontal lines at the end of the strain data can be seen on the

graphs where this sudden detachment occurred. The graphs of the load versus strain gauge data can be found in Appendix G.

Chapter 5: Data Analysis

Due to the amount of data gathered from this experimental initiative, two types of analyses were utilized: qualitative and quantitative. The qualitative analysis consists of conclusions made from observations documented during the test or seen in the video recording after the test. The quantitative analysis consists of conclusions based on numerical operations, and made possible through MATLAB software programming, from the data gathered during the experiment. The load versus horizontal shear tab displacement data were determined to be the most useful set of data to be analyzed and were used for the quantitative analysis. The data from the base plate uplift and strain gauges were not determined to be beneficial and were omitted from the data analysis.

5.1 Qualitative Analysis

There were several different behaviors observed throughout testing that provide insight into how the long slots affect the single plate at the different bolt group locations. Comparing the observed behaviors to what was expected proves useful when determining the factors that need to be implemented in the design procedure. The main behaviors observed were plate flexure, bolt bearing, local buckling, and the turning up of the plate corner.

As can be seen in post-test pictures in Appendix E, bolt bearing and plate flexure were easy to distinguish once the tests were complete. Table 5-1 provides the behaviors for each test specimen and the magnitude at which they were seen, compared to what was expected from the calculations performed before testing began. A trend can be seen where the specimens with bolts placed at higher positions had greater plate flexure, which also correlated to what was expected. It can also be seen that as the bolt group was placed

at the lower positions, bolt bearing was more prominent and correlated with what was expected. The middle bolt positions – 25%, 50%, and 75% – had a greater mixture between the two behaviors, rendering it difficult to decide which behavior governed. Overall, the trends found in this comparison prove the assumptions made in the design of the connection were correct with respect to which behaviors were going to be most noticeable.

Table 5-1: Comparison of Expected and Tested Specimen Behavior.

TEST ID	EXPECTED FAILURE MODE	OBSERVATIONS	
		PLATE FLEXURE	BOLT BEARING
S30P100	Bolt Plate Flexure	Moderate	Minimal
S30P075	Bolt Plate Flexure	Significant	Moderate
S30P050	Bolt Plate Flexure	Extreme	Extreme
S30P025	Plate Shear Rupture	Extreme	Extreme
S30P000	Plate Shear Rupture	Significant	Extreme
S35P100	Bolt Plate Flexure	Significant	Moderate
S35P075	Bolt Plate Flexure	Extreme	Significant
S35P050	Bolt Bearing/Bolt Plate Flexure	Significant	Moderate
S35P025	Bolt Bearing/Bolt Plate Flexure	Moderate	Moderate
S35P000	Plate Shear Rupture	Minimal	Significant
S40P100	Bolt Plate Flexure	Moderate	Moderate
S40P075	Bolt Plate Flexure	Moderate	Moderate
S40P050	Bolt Bearing/Bolt Plate Flexure	Moderate	Moderate
S40P025	Bolt Bearing/Bolt Plate Flexure	Moderate	Moderate
S40P000	Bolt Bearing	Minimal	Significant
S45P100	Bolt Plate Flexure	Moderate	Moderate
S45P075	Bolt Bearing/Bolt Plate Flexure	Moderate	Moderate
S45P050	Bolt Bearing/Bolt Plate Flexure	Minimal	Moderate
S45P025	Bolt Bearing/Bolt Plate Flexure	Minimal	Significant
S45P000	Bolt Bearing	Minimal	Significant

5.2 Quantitative Analysis

There were several different analysis methods considered for this project due to the complexity of the problem. After careful deliberation, the method thought to best represent the data and produce solid conclusions was to compare the horizontal displacement of the shear tab to the load applied to the specimen to compare the tested capacity to the expected capacity. As seen in Chapter 4, the raw data produced general trends, but contained noise in the graphs that made it difficult to find a capacity. An example of the noise can be seen in Figure 5-1. This was mitigated by a two-part process; first, the data were manually filtered for obvious outlier points in the data, and then were filtered using a MATLAB code to smooth out the curve further.

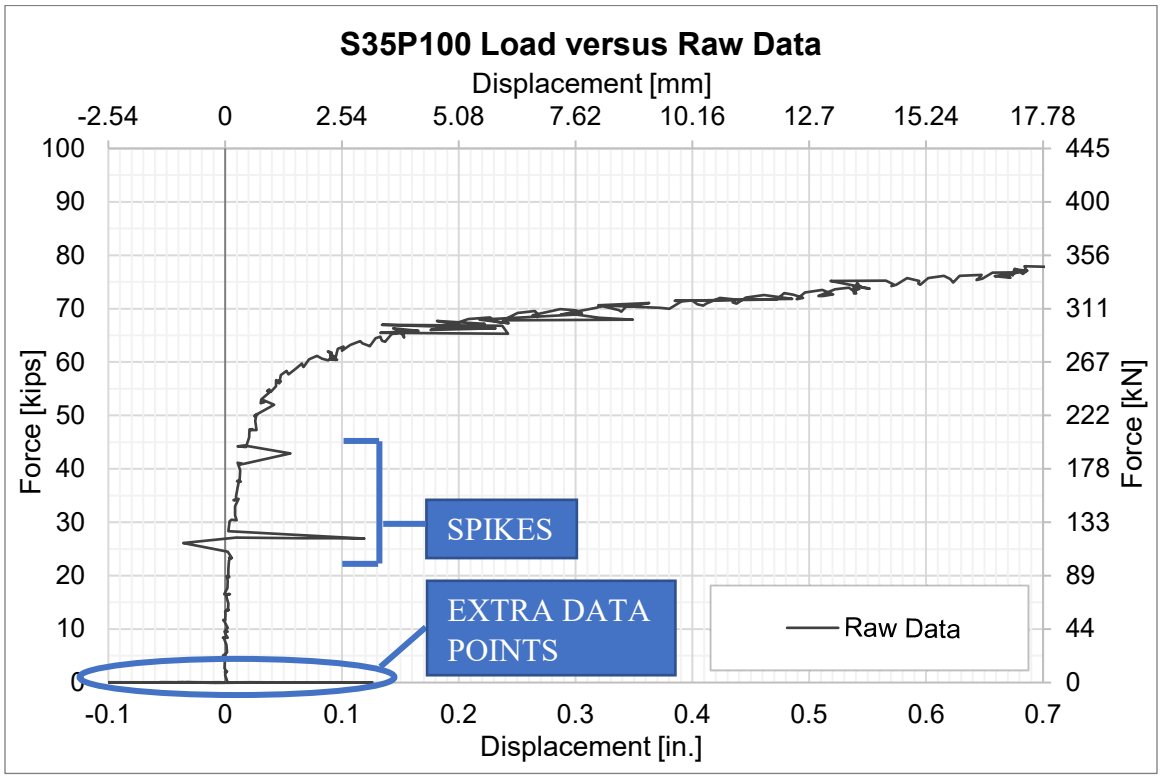

Figure 5-1: Example Raw Data versus Load.

After determining that the raw data contained too much noise to effectively analyze the data, the data for each test were combed through to find the greatest outliers that did not fit the data. The points chosen to be omitted were determined following a review of video footage for that test to ensure the spikes in data could not be explained by an event that happened during the test, such as a shift in the base plate or the LVDT moving out of place. Spikes caused by something that happened during the test were left in the data to ensure they were considered. There were also data points omitted from the prefiltered data at the start of the tests, found at the bottom of the graph. While the tests were starting, the equipment was turned on and their outputs were fluttering before load was applied. These data points were not rendered useful and were omitted from the prefiltered data. A comparison of the raw data to the prefiltered data can be found in Figure 5-2.

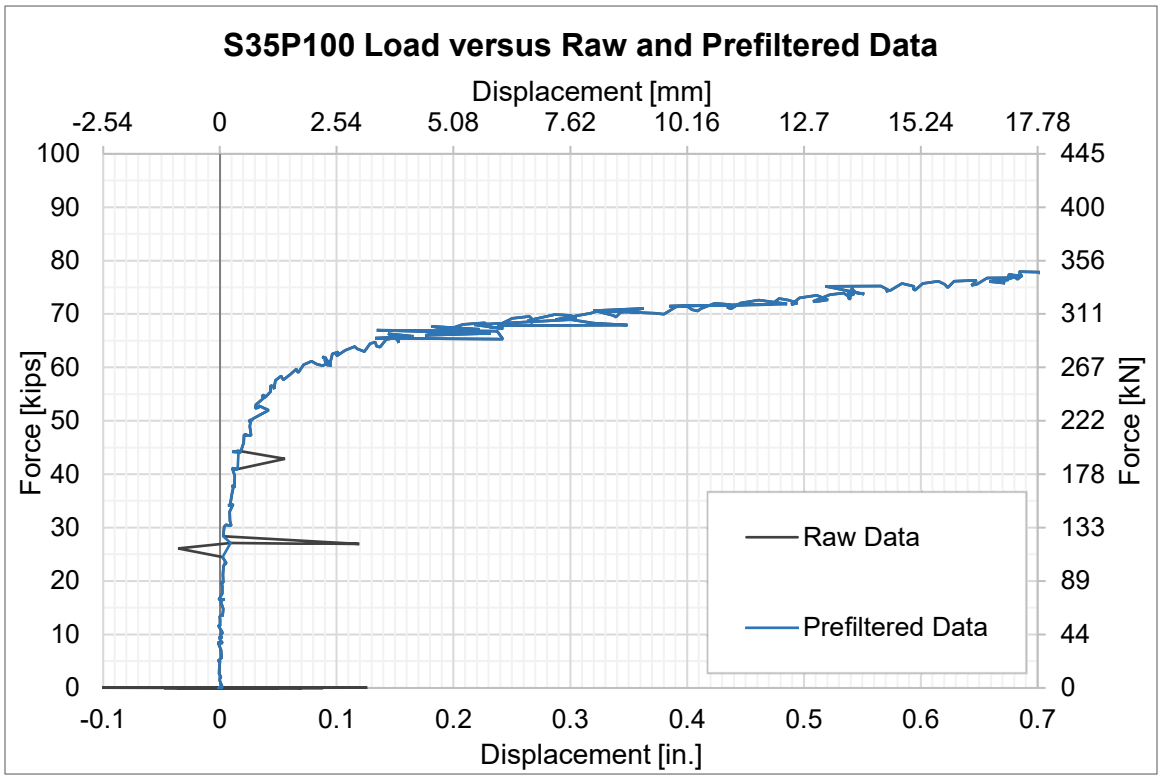

Figure 5-2: Example Raw and Prefiltered Data versus Load.

5.2.1 MATLAB

The last step to filtering the test data was to run it through a MATLAB code. This code was created to ensure the trend of the data remained intact while eliminating the noise that made it difficult to analyze. Two different codes were used: one for test S30P100, and the other for the remaining nineteen tests. The code for most of the tests has the data going through two filters, while the other code has those data going through three filters. This is due to the excess noise found in S30P100; when putting that test through two filters, the trend line was not representative of the data, so a third was put in the code to further smooth out the line.

The two different filters are the Butterworth filter and the Median filter. Both filters work to eliminate the noise in the data while keeping the numbers in the same range as the original data set. The code for S30P100 includes a second Median filter that further reduces the noise found in that data set. After the data were put through the filters, there was a curve fitting function and a smoothing parameter that were implemented in the code that fits the filtered data to a curve, enabling the data to illustrate its original trend through the graphs created. A comparison of each step of the data can be seen in Figure 5-3. The codes used for this process can be found in Appendices H and I.

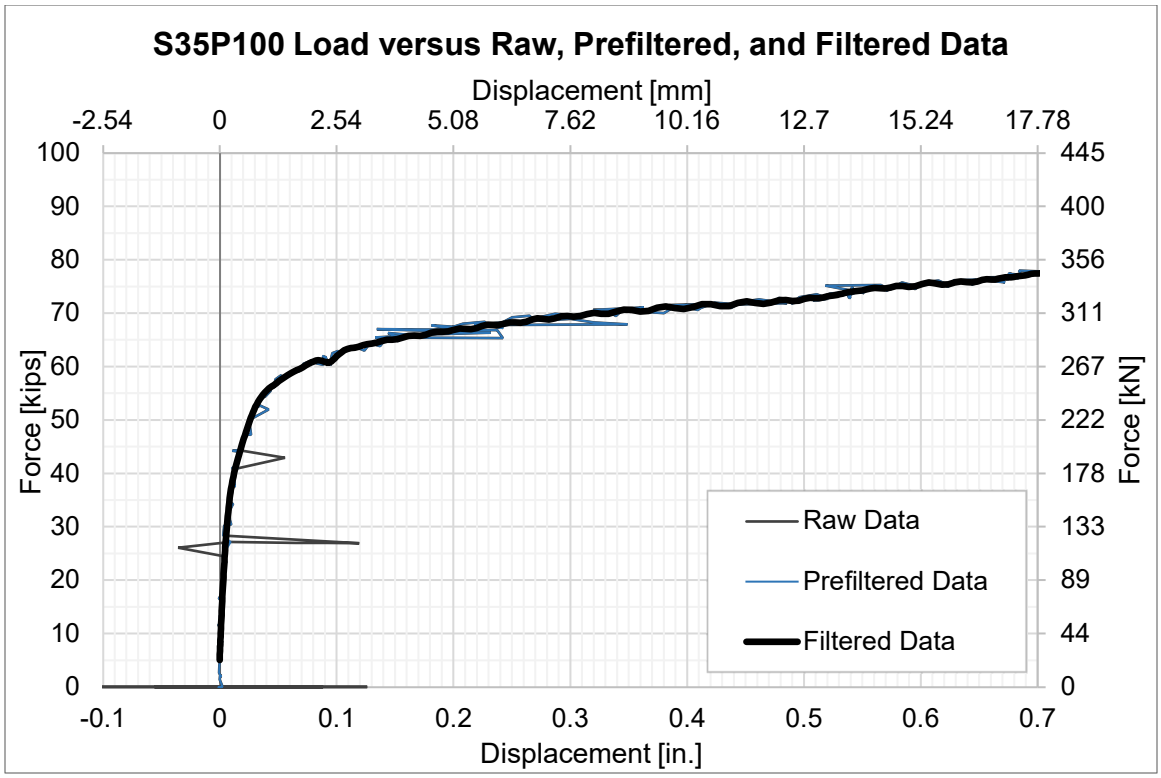

Figure 5-3: Example Raw, Prefiltered, and Filtered Data versus Load.

Once all the displacement data were filtered using the MATLAB code, they were compared to the load applied to each specimen. The trends found in Chapter 4 are better illustrated in the filtered graphs, found in Figure 5-4, Figure 5-5, Figure 5-6, and Figure 5-7. A wave-like behavior near the tail end of most of the curves, as well as dips in the force seen by the specimen, can be seen in those graphs. The movement in the trendline is due to how the different filters adjusted to smoothing out the curve while taking the unavoidable noise in the data into consideration.

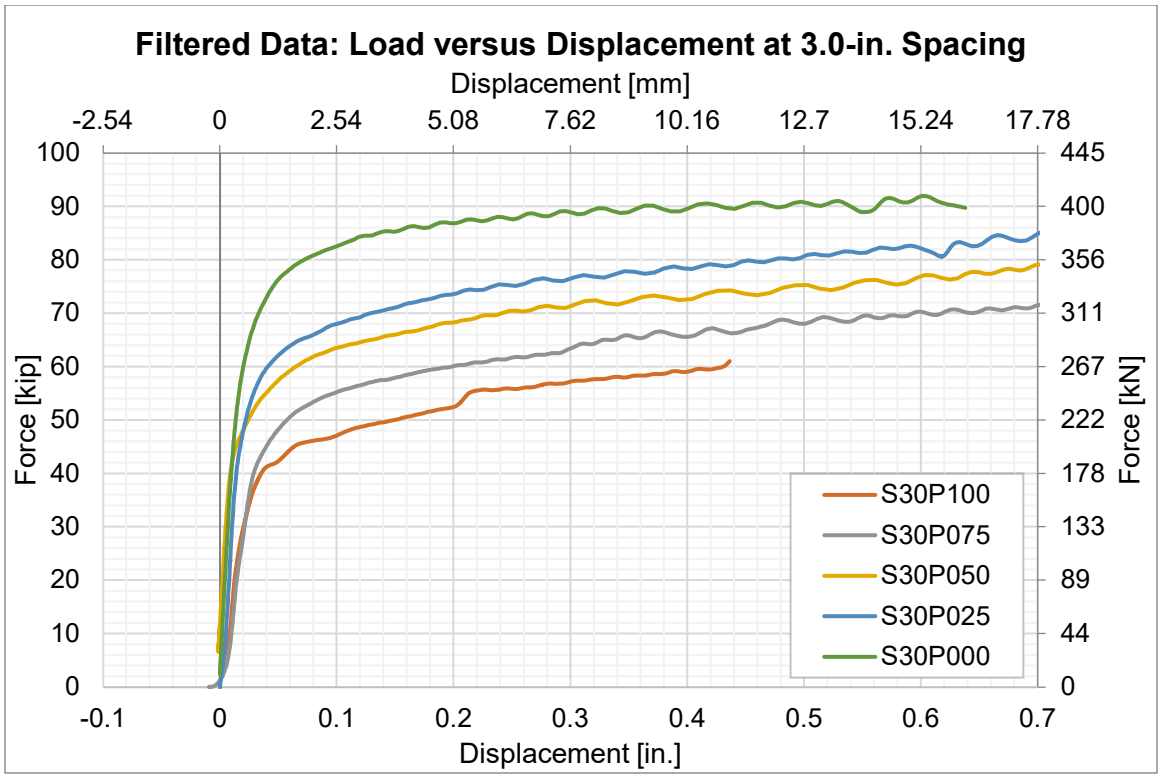

Figure 5-4: Filtered Data at 3.0-in. Spacing.

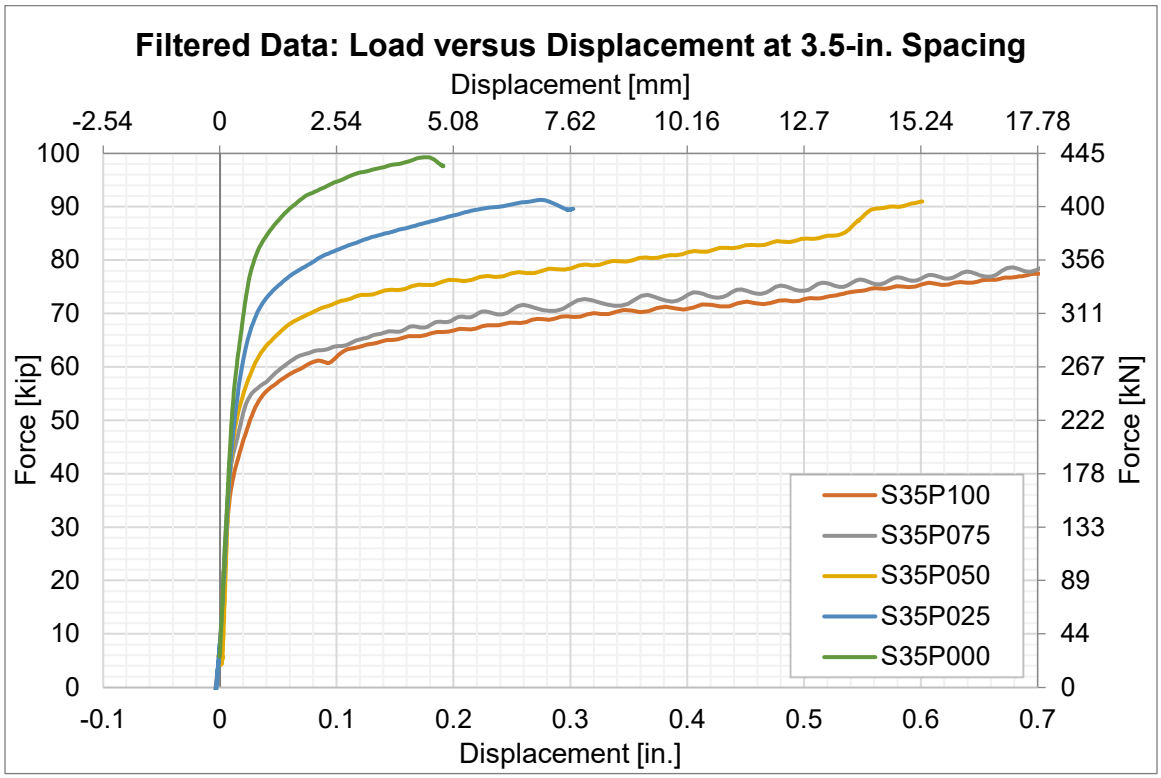

Figure 5-5: Filtered Data at 3.5-in. Spacing.

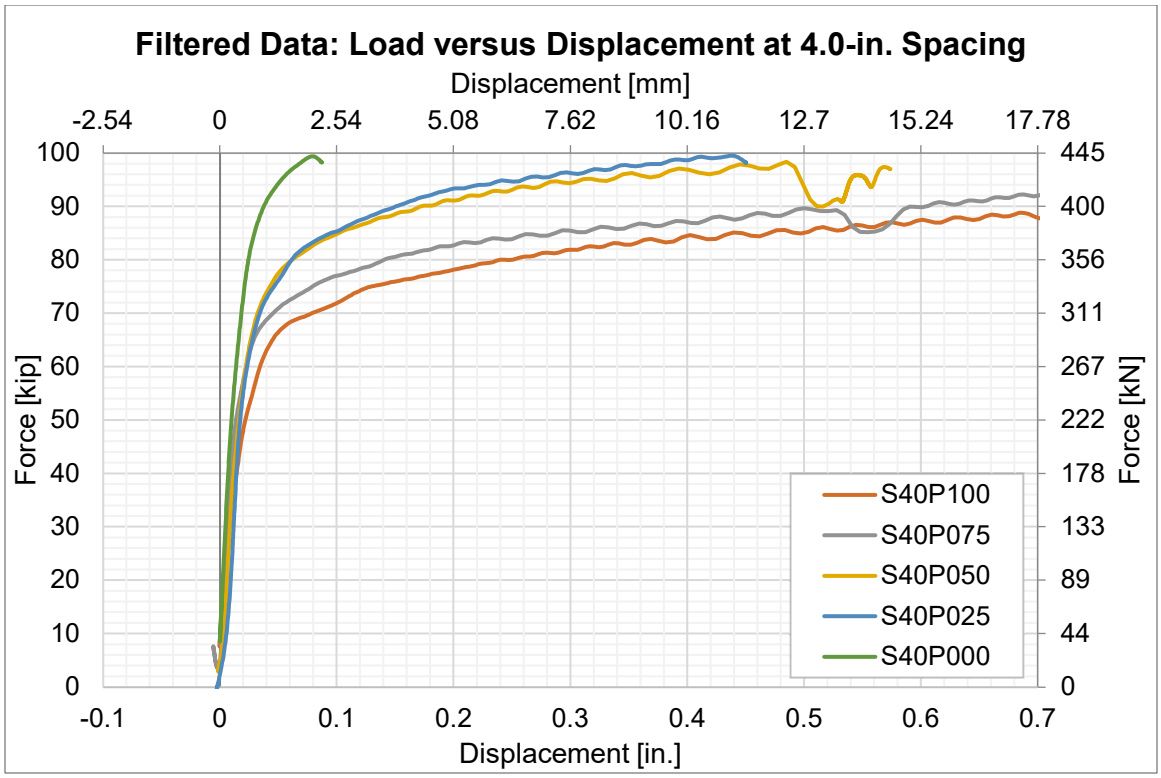

Figure 5-6: Filtered Data at 4.0-in. Spacing.

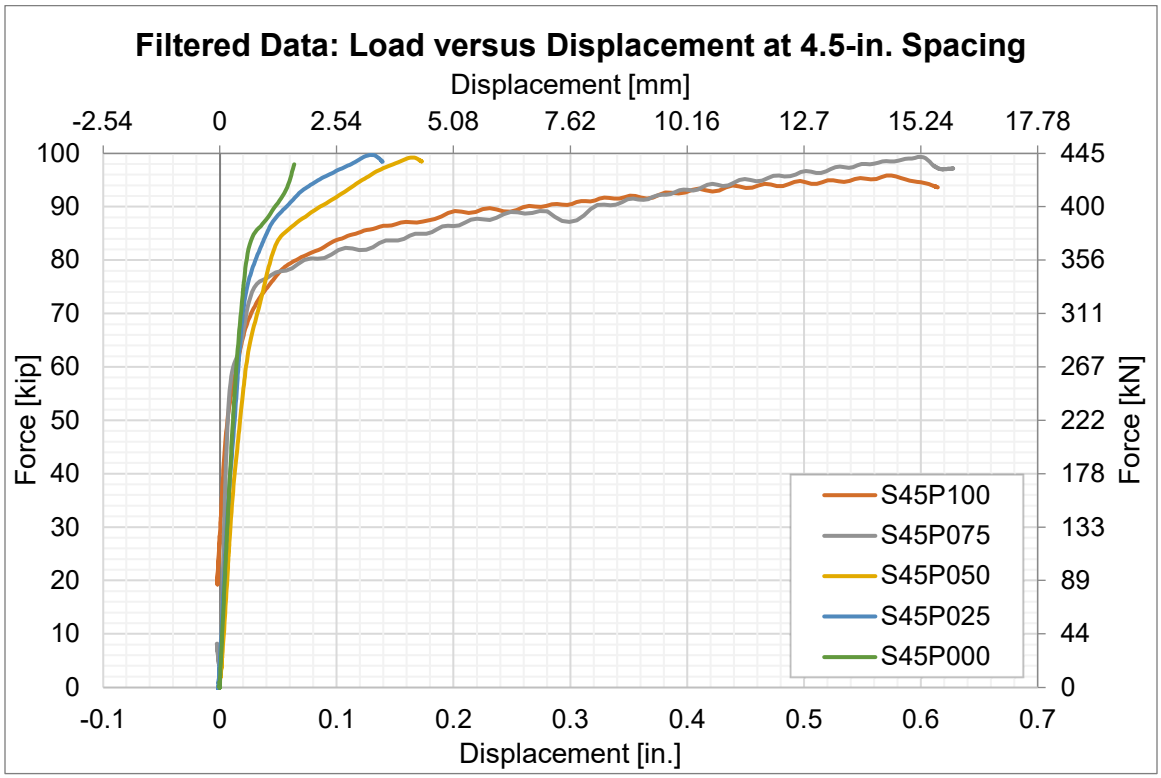

Figure 5-7: Filtered Data at 4.5-in. Spacing.

5.2.2 Capacity Determination

With the trend lines produced from the filtering process, the capacities of each specimen were determined. Careful consideration was put into finding the capacity since there was no clear or consistent way of defining failure for all twenty specimens. The method used to determine the capacity was a combination of numerical interpolation of the data and graphical analysis. It was assumed that the failure point would be found where the graph started to turn over, which is an indication that the plate has yielded, that plate flexure started to take over, and that the plate experienced significant loss of stiffness.

By observing the trend lines for each test, a turning point can be seen; finding that general location on the graph was the first step of determining the capacity. The next step was to turn to the data points for each graph and find the range of forces at the turning point on the graph. A percent difference was taken for each horizontal displacement value, which was a comparison of a point and the point prior.

Due to the variability between the different tests, it was difficult to determine the point where the graph turned that was consistent with all twenty data sets. There were ranges in each data set that had an increased percent difference around the turning point location seen on their respective graphs. There was discussion on which point to choose: the point with the highest percent difference, the first point at the range, the last point at the range, or the middle of the range. After deliberation and comparison of the data from the different tests, the data point with the highest percent difference to the point prior was determined to be the best representation of the turning point. The highest percent

difference was determined to indicate the greatest change, illustrating the turning point in the curve from elastic to plastic deformation in the specimens.

A comparison of the failure points for each specimen can be found in Figure 5-8. This graph illustrates the general trend of increased capacity as the bolt position moves closer to the welded edge for each slot spacing. However, the positions farthest from the welded edge have the most uncertainty, which can be seen by the overlap in capacities for the 3½ in. (88.9 mm) and 4 in. (102 mm) slot spacing specimens at the 100% and 75% positions.

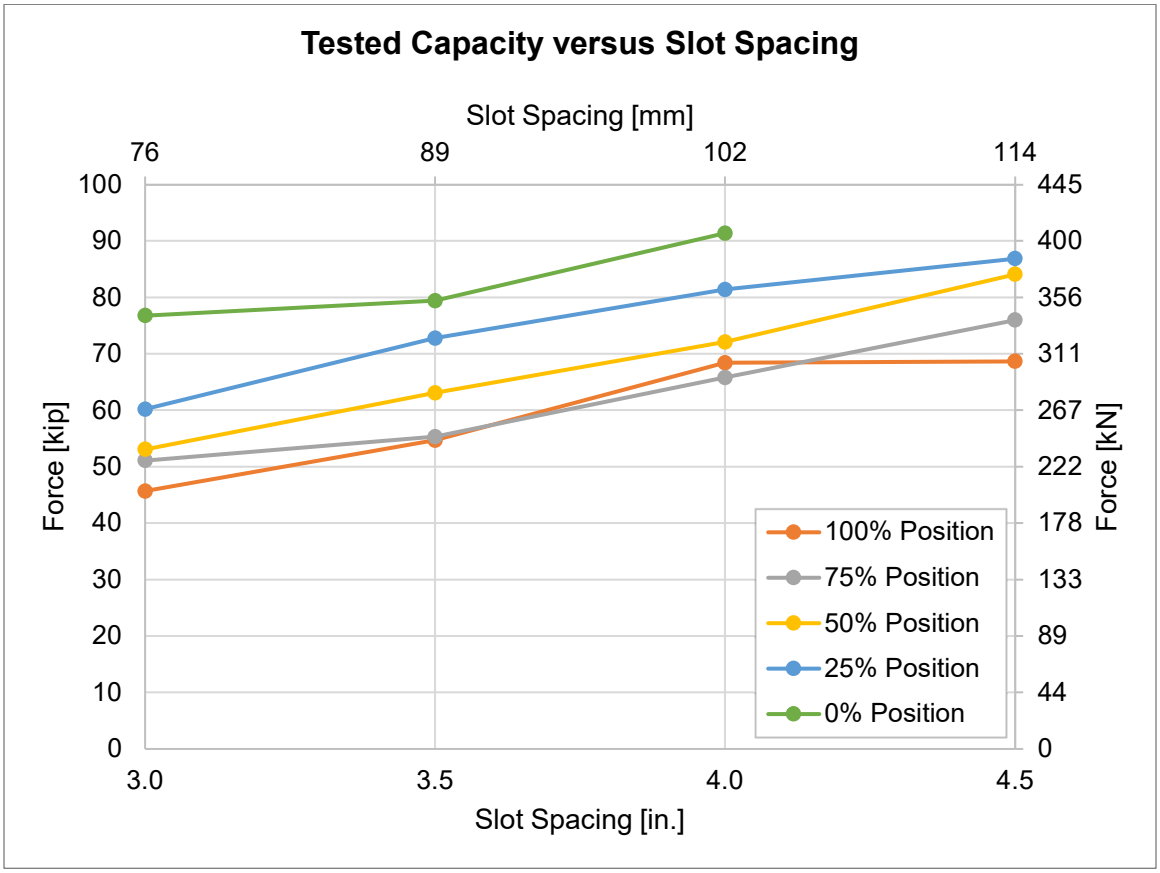

Figure 5-8: Tested Capacity versus Slot Spacing.

5.2.3 Comparison of Data

The following plots in Figure 5-9 through Figure 5-28 illustrate the comparisons between the expected and tested capacities, as well as the different stages of the filtering process, for each specimen in this experimental initiative. Each plot consists of the raw data, prefiltered data, filtered data, and the points of the expected and tested capacities for that specimen.

The expected and tested capacities can be compared to each other on each plot. By comparing those two capacities, it can be observed that the gap, which defines the percent difference between the two capacities, begins to decrease as the bolt group position moves farther from the welded edge. Further comparison of the different graphs provides a trend between the increase in capacity of the specimen as the bolt group is positioned closer to the welded edge.

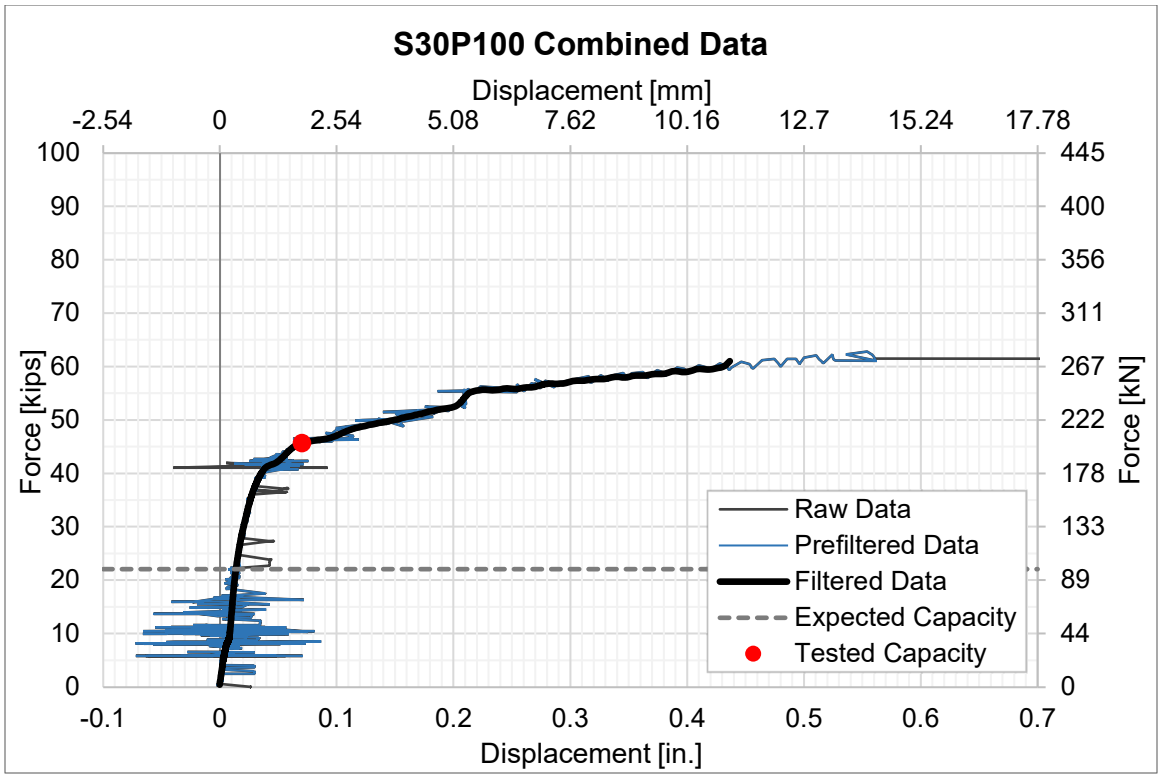

Figure 5-9: Combined Data for S30P100.

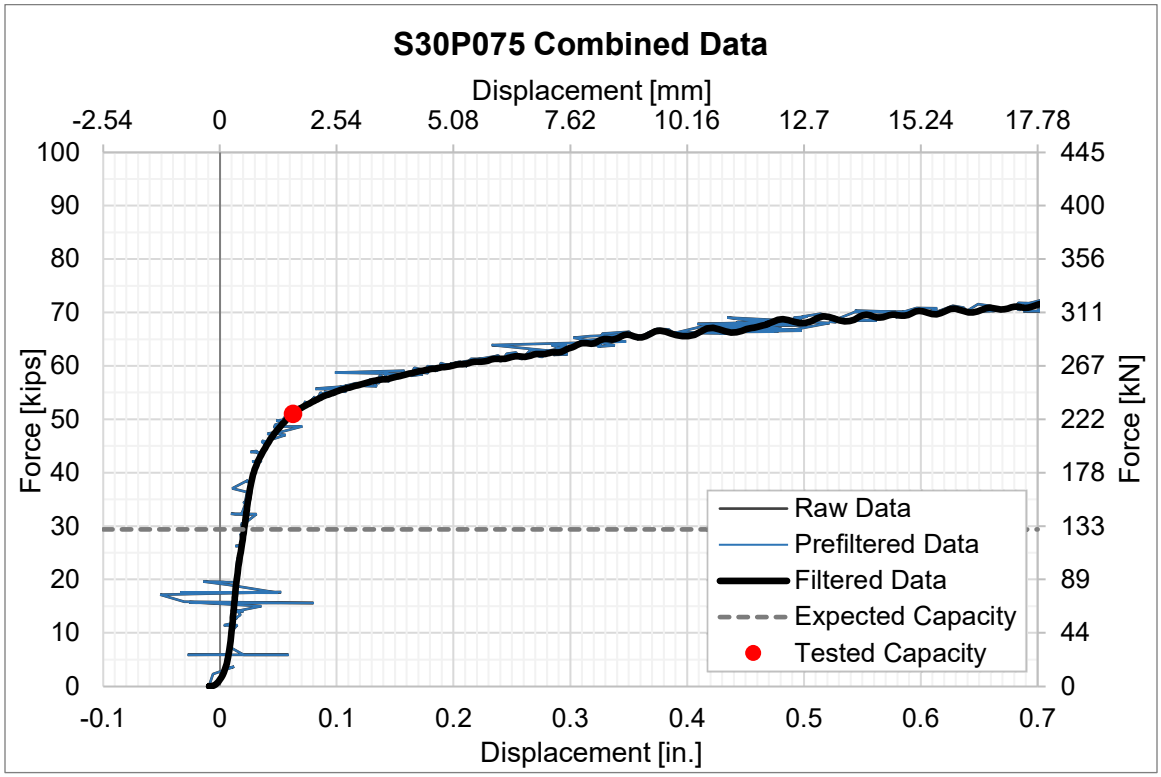

Figure 5-10: Combined Data for S30P075.

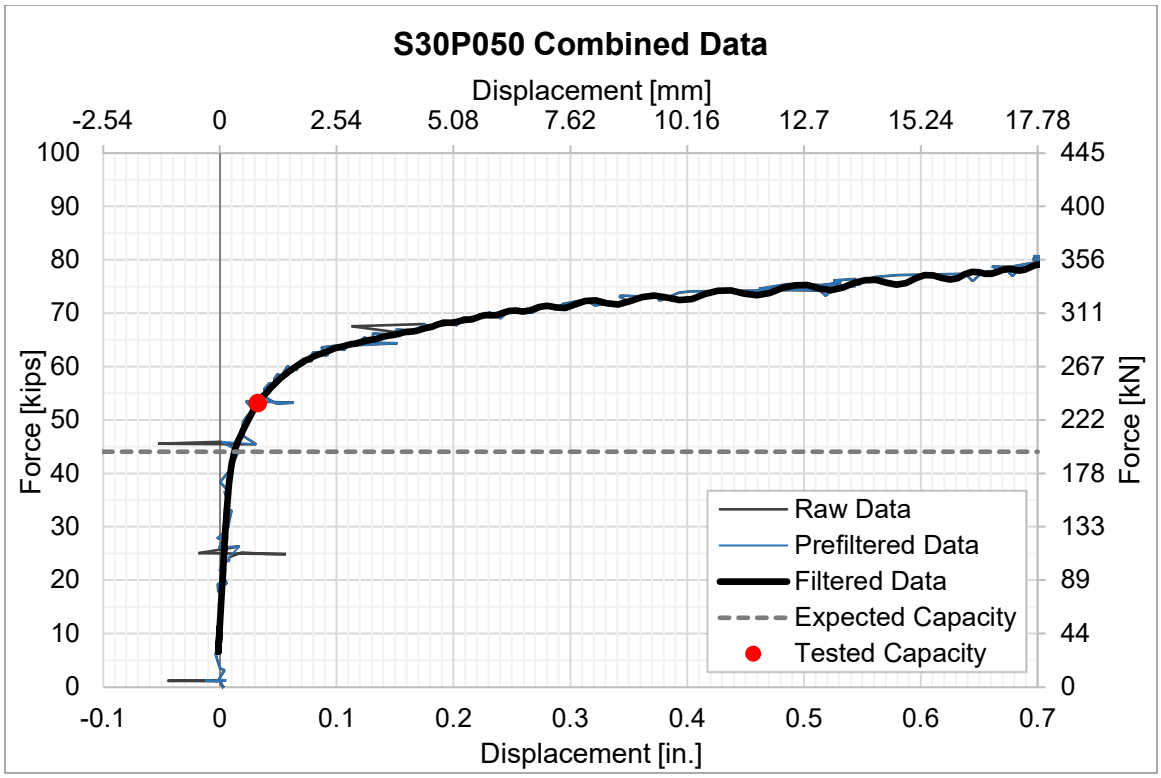

Figure 5-11: Combined Data for S30P050.

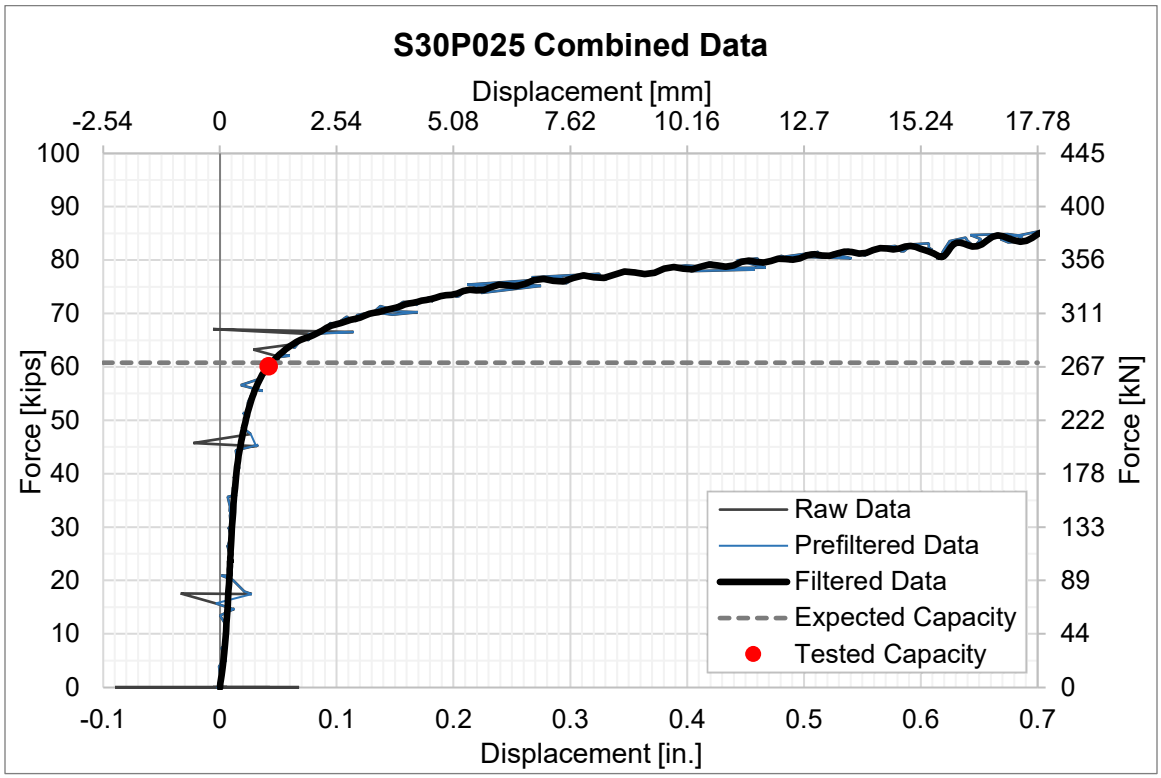

Figure 5-12: Combined Data for S30P025.

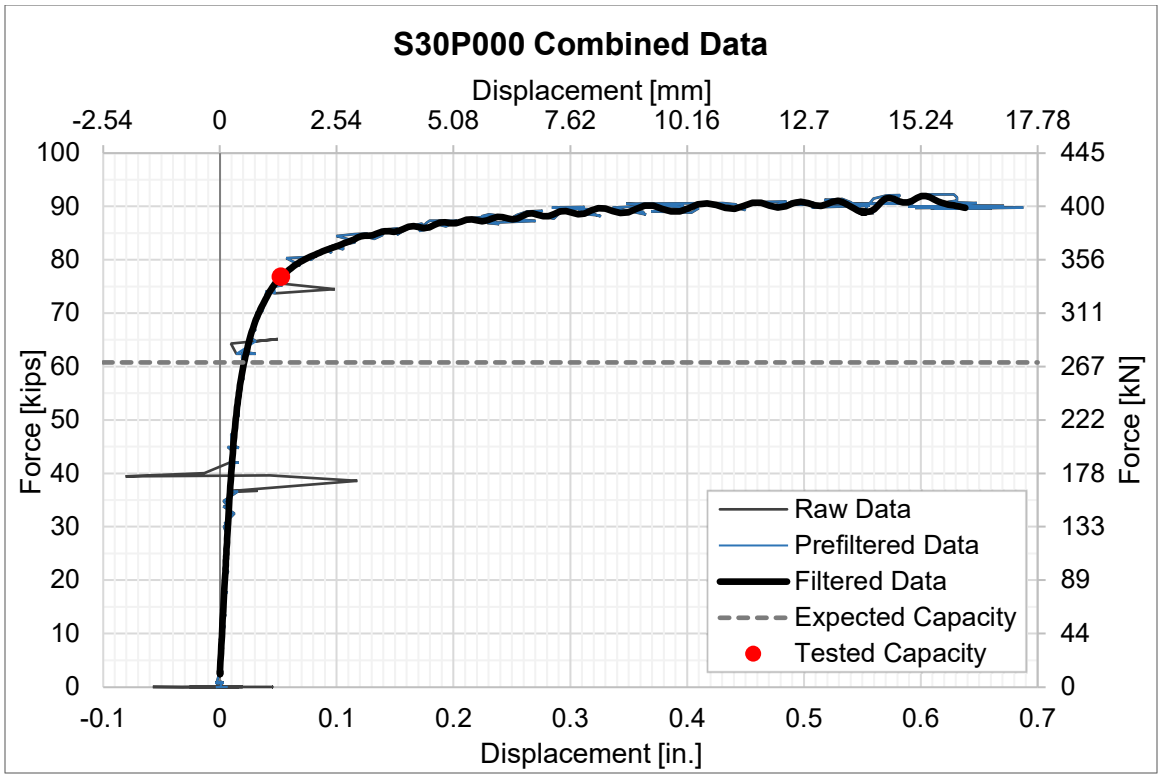

Figure 5-13: Combined Data for S30P000.

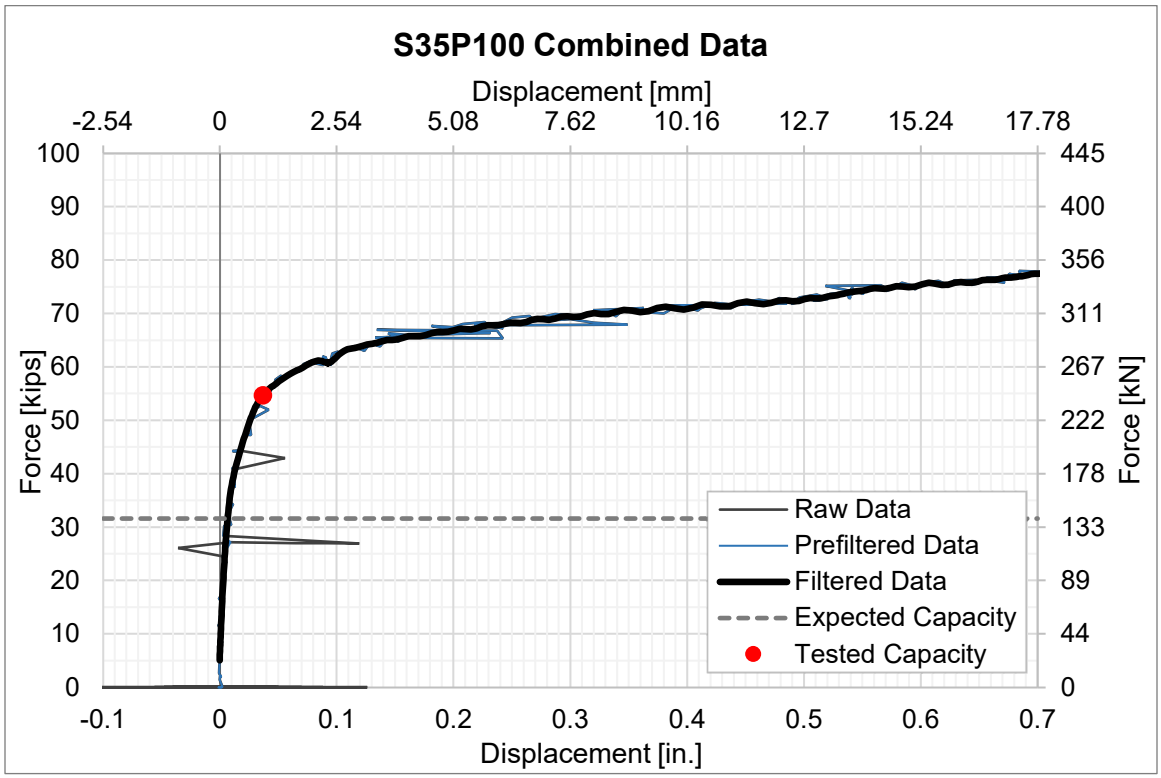

Figure 5-14: Combined Data for S35P100.

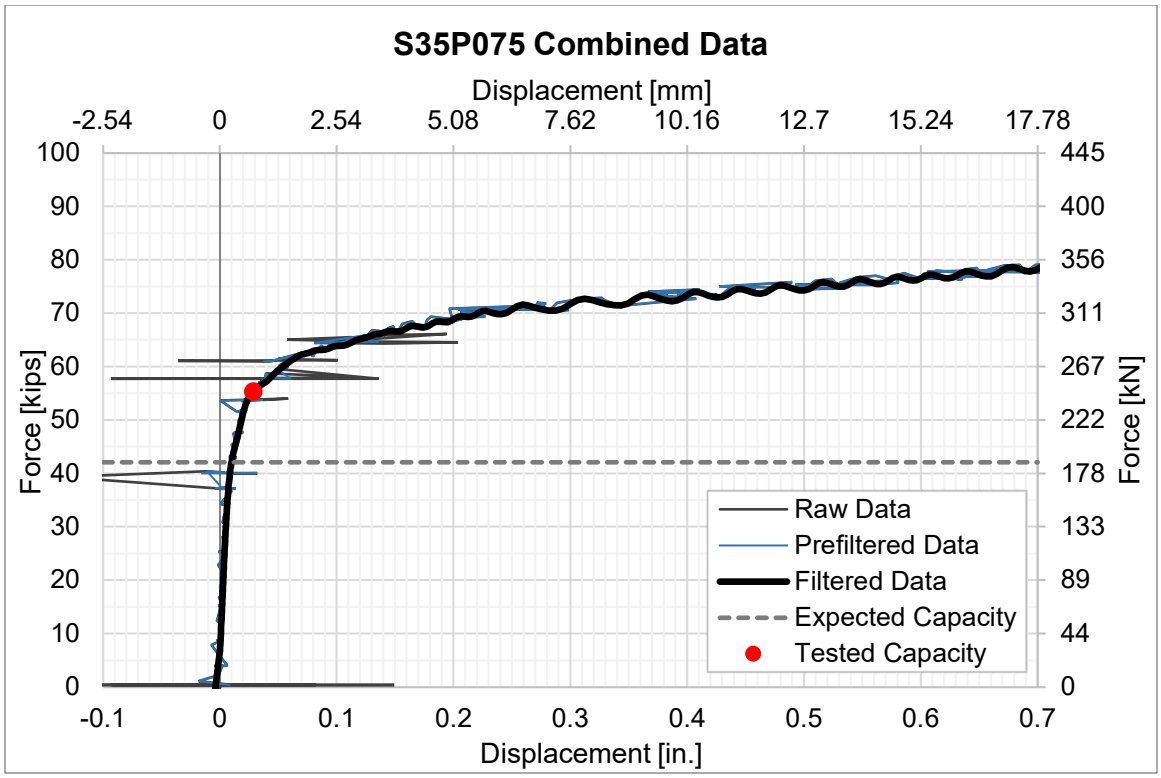

Figure 5-15: Combined Data for S35P075.

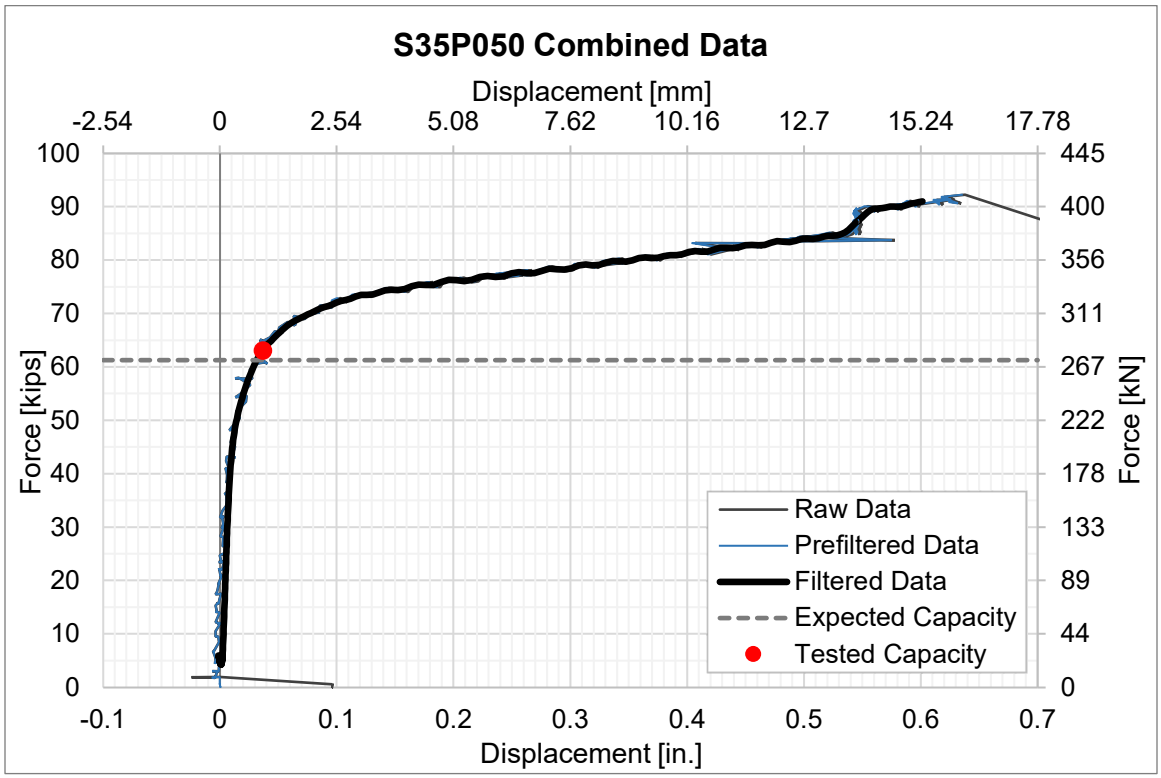

Figure 5-16: Combined Data for S35P050.

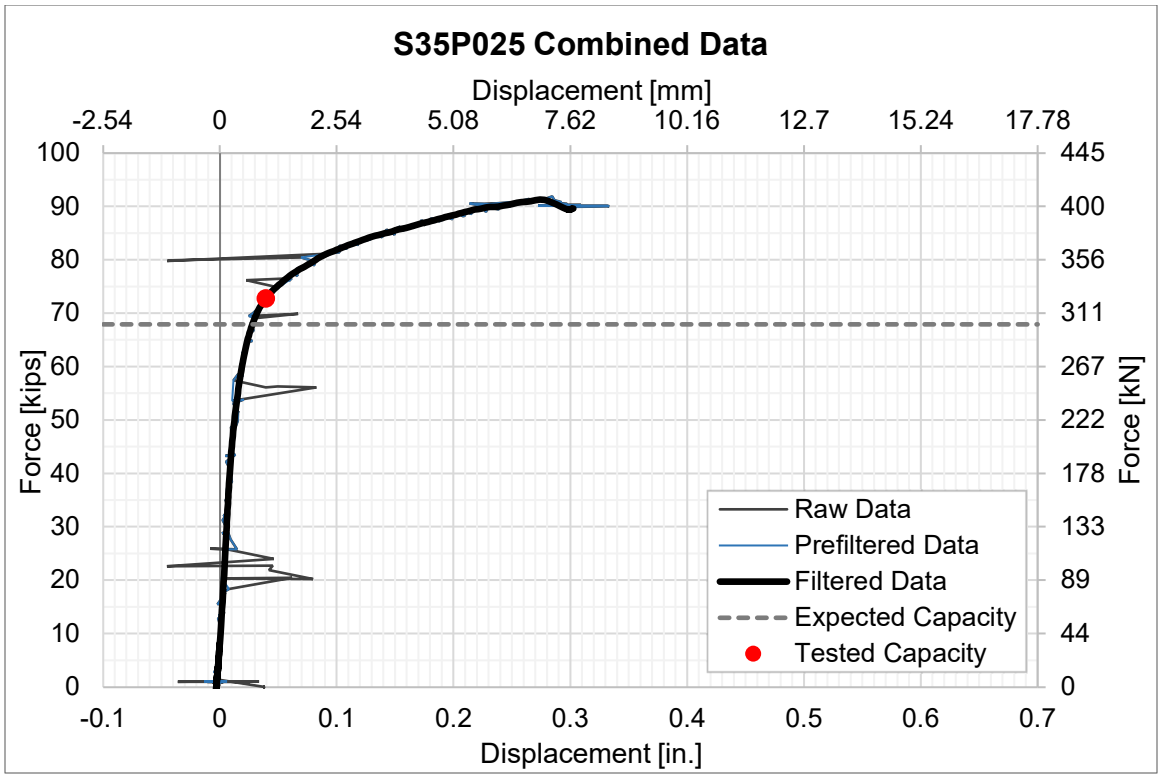

Figure 5-17: Combined Data for S35P025.

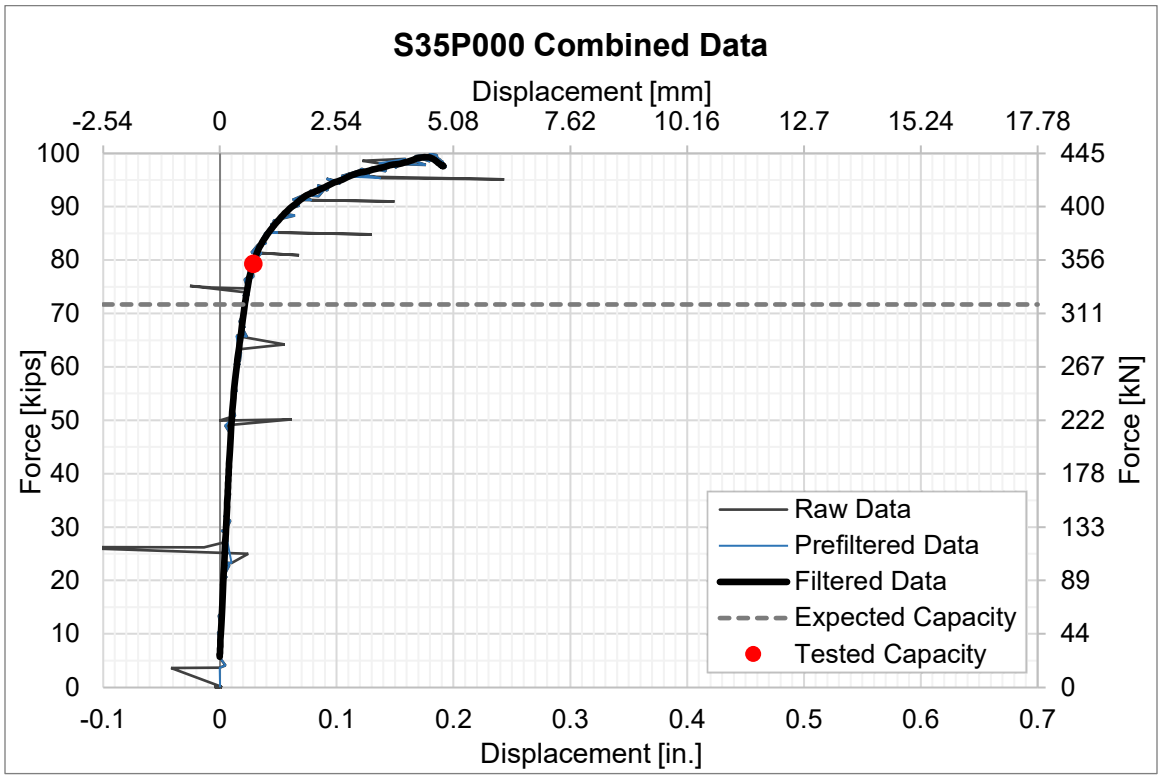

Figure 5-18: Combined Data for S35P000.

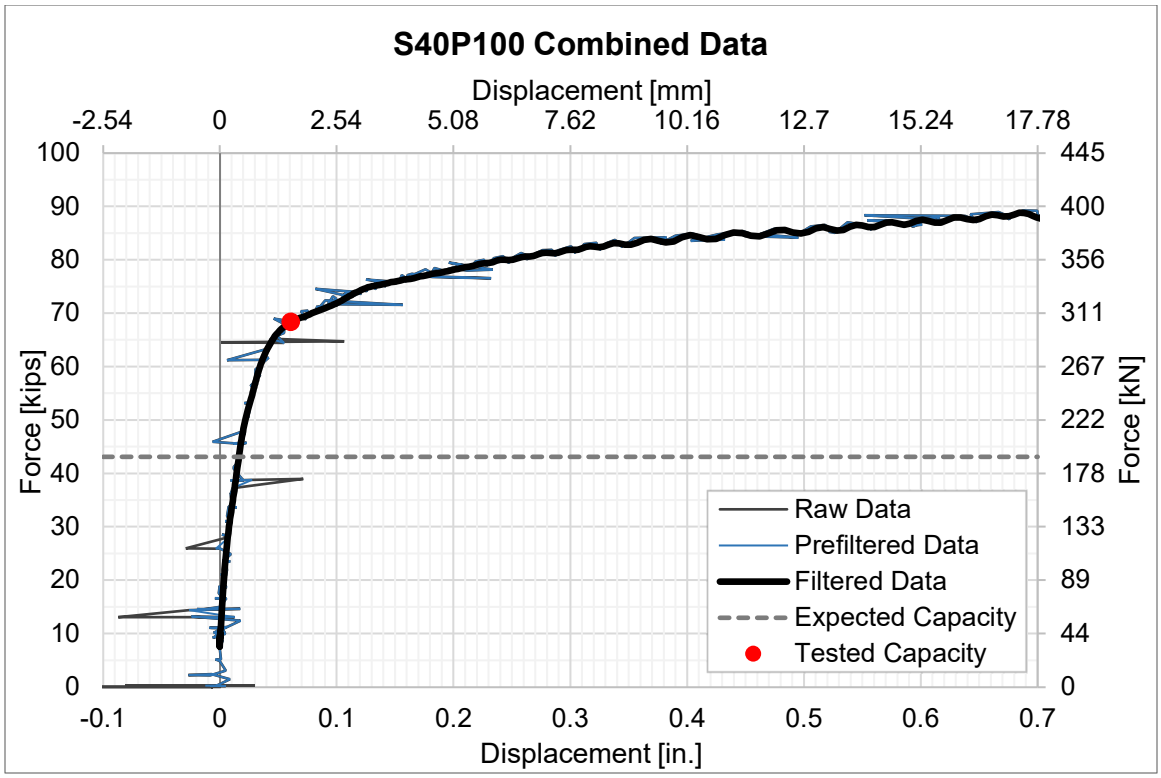

Figure 5-19: Combined Data for S40P100.

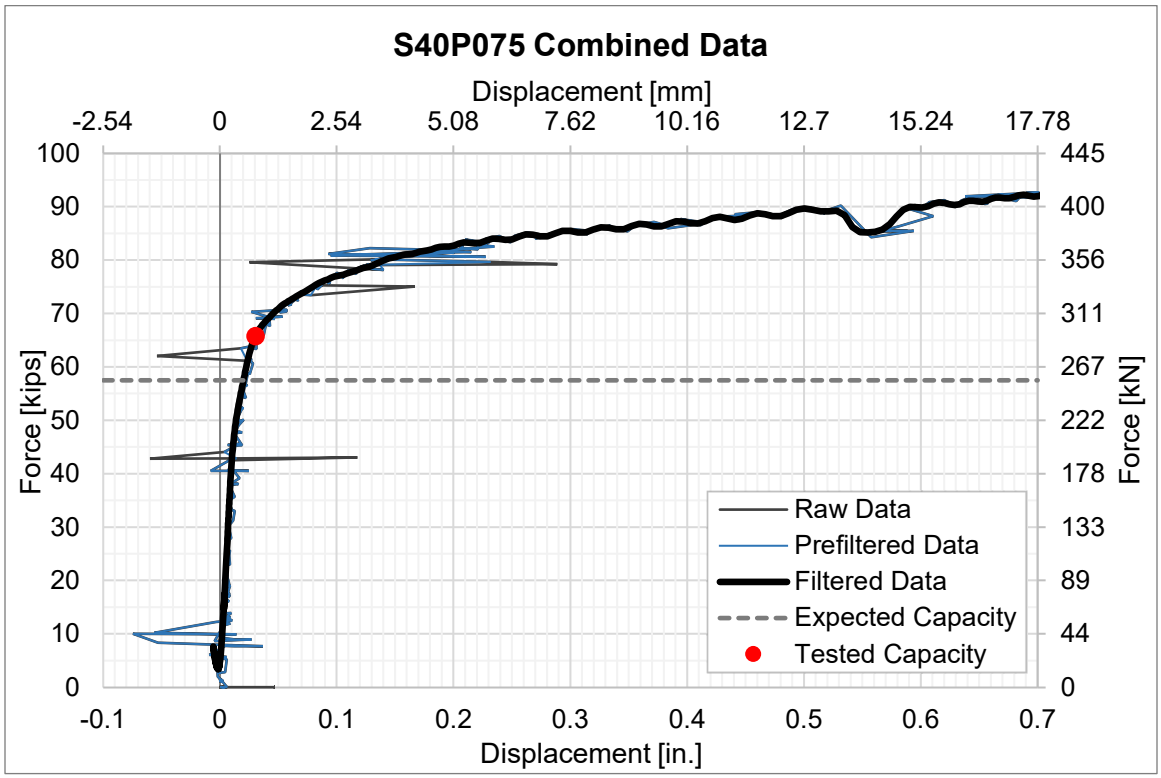

Figure 5-20: Combined Data for S40P075.

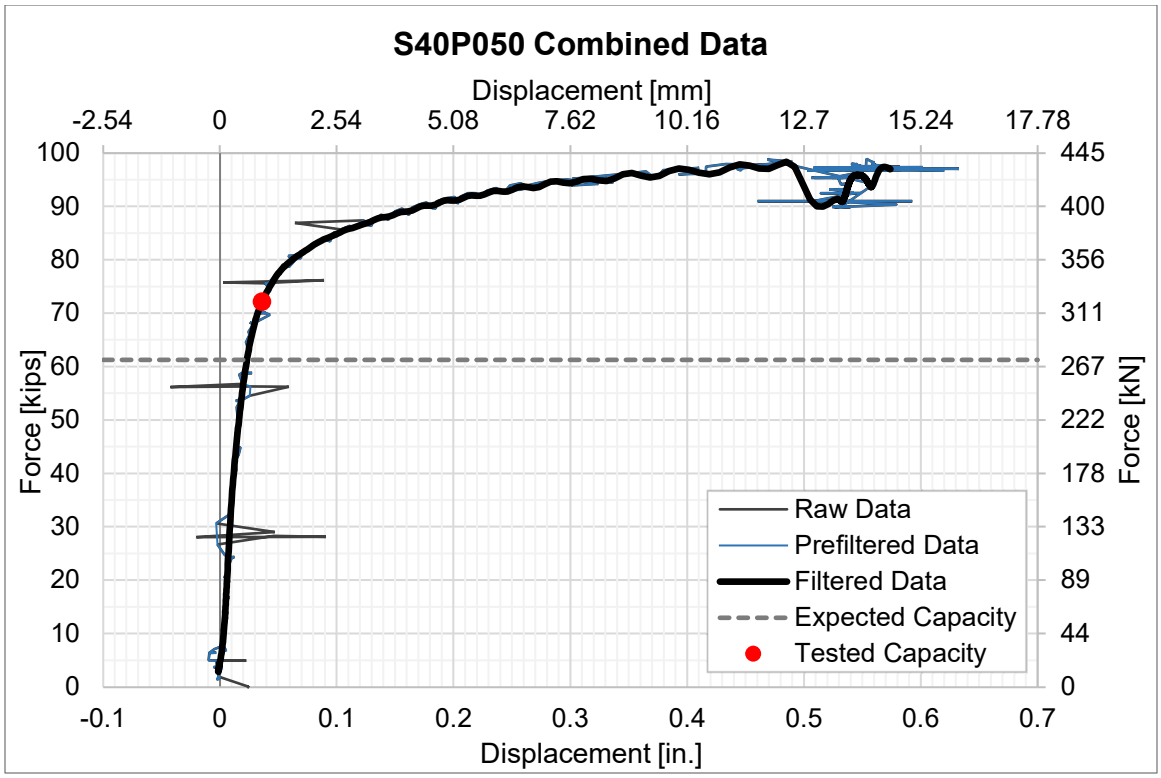

Figure 5-21: Combined Data for S40P050.

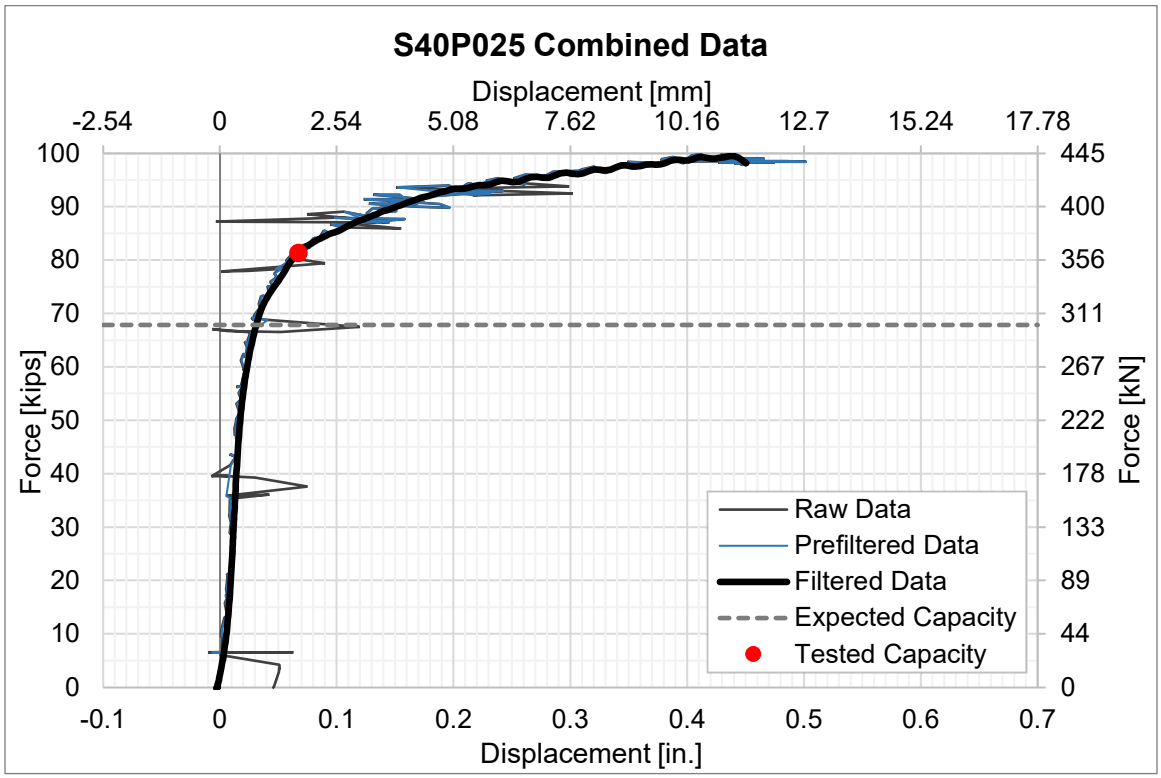

Figure 5-22: Combined Data for S40P025.

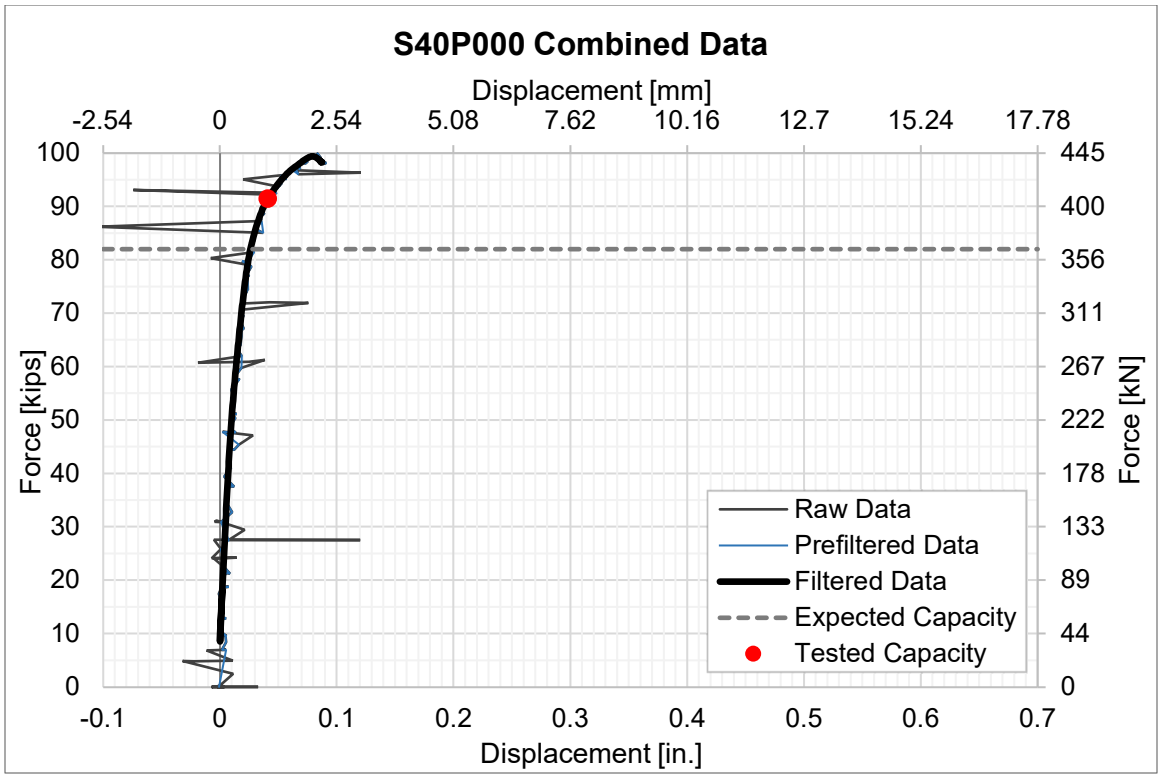

Figure 5-23: Combined Data for S40P000.

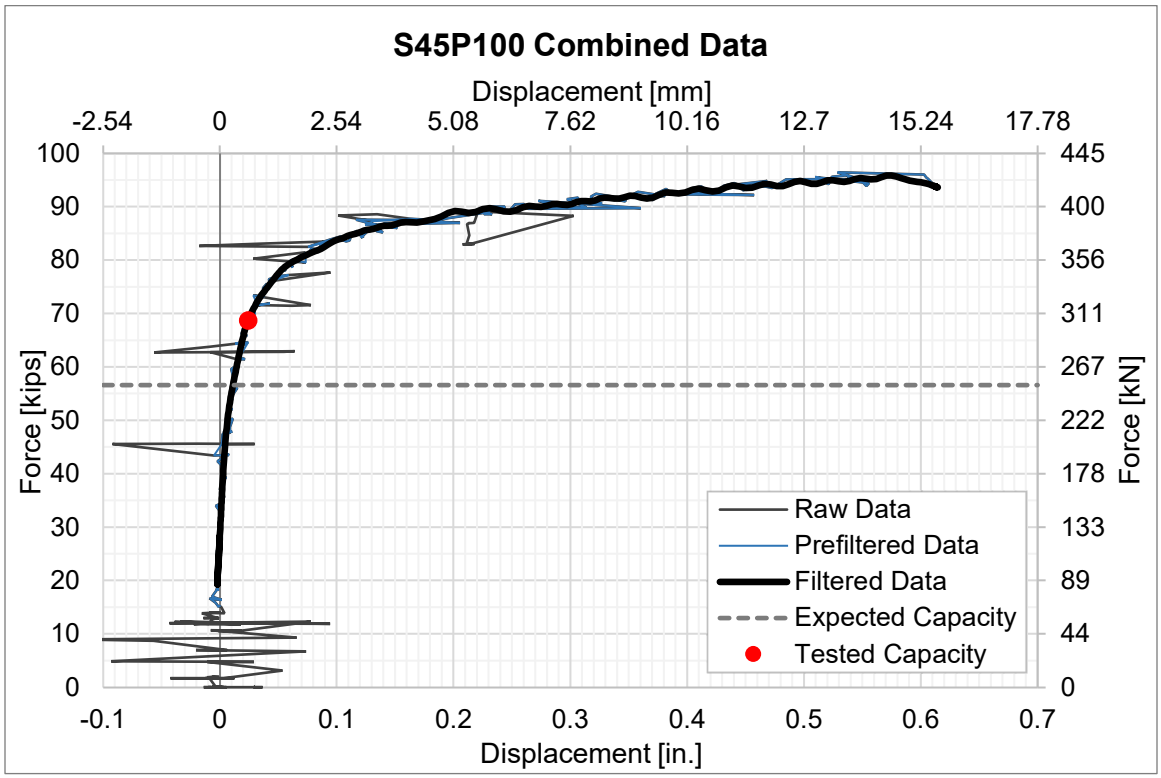

Figure 5-24: Combined Data for S45P100.

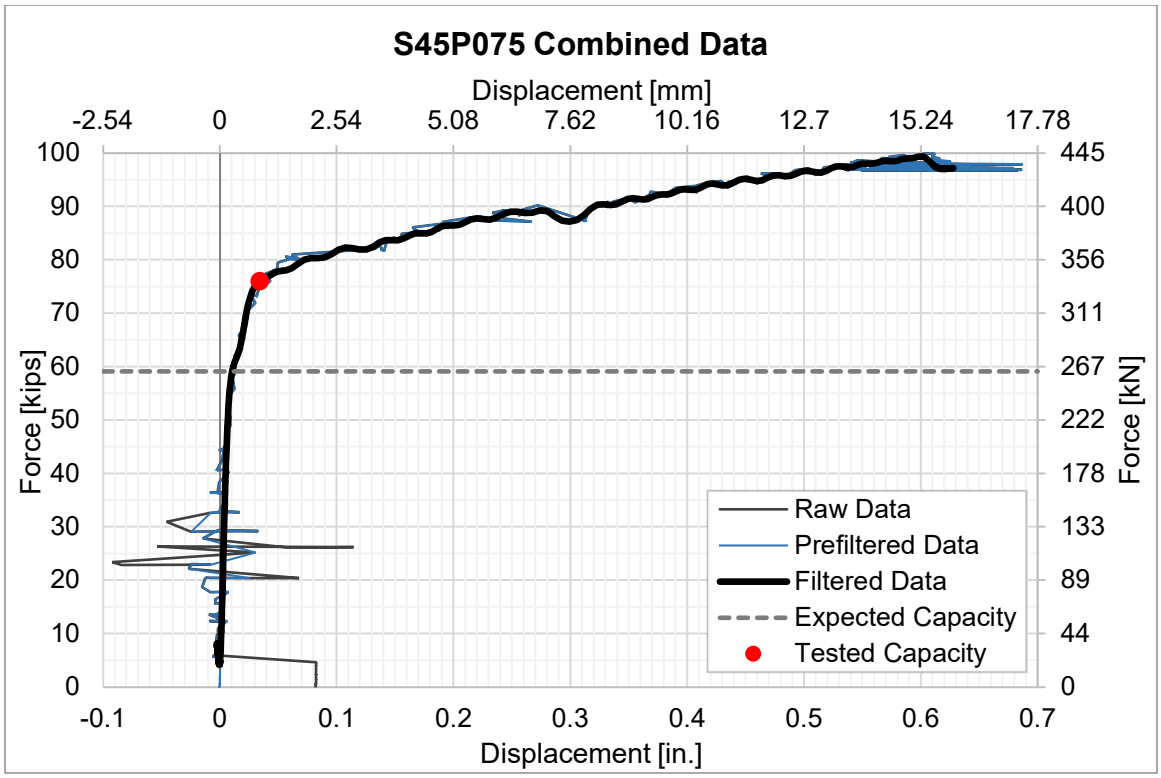

Figure 5-25: Combined Data for S45P075.

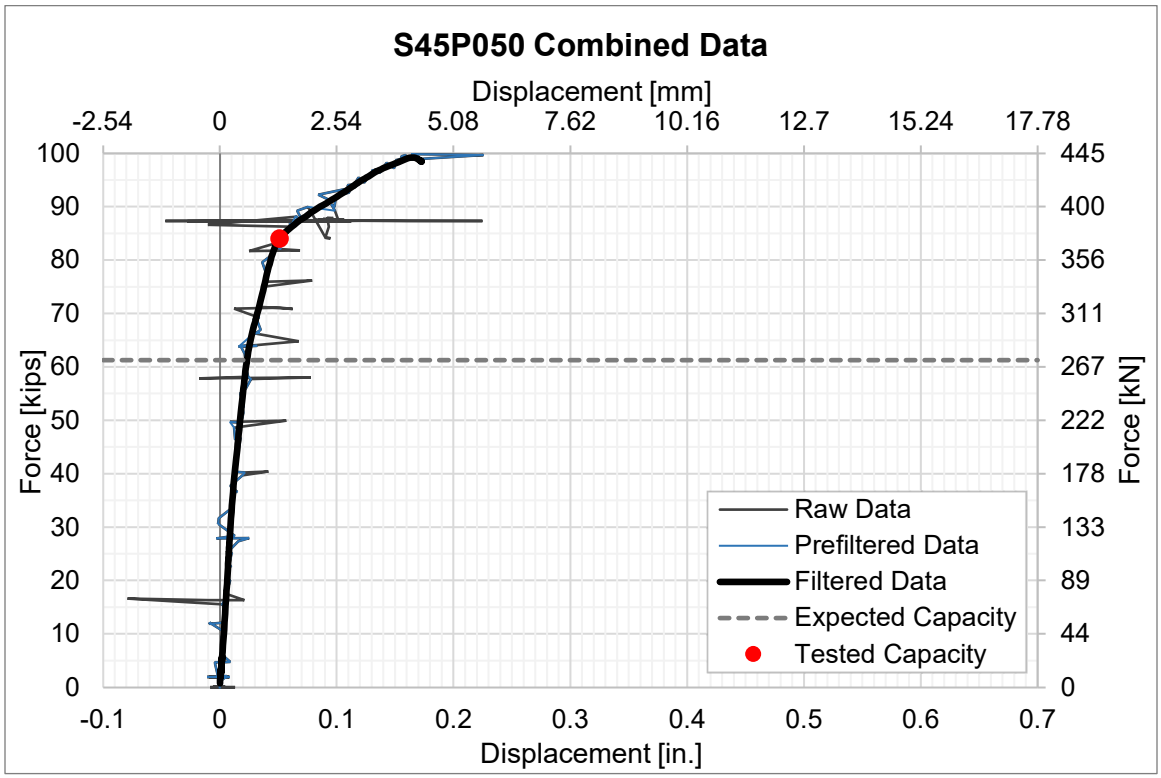

Figure 5-26: Combined Data for S45P050.

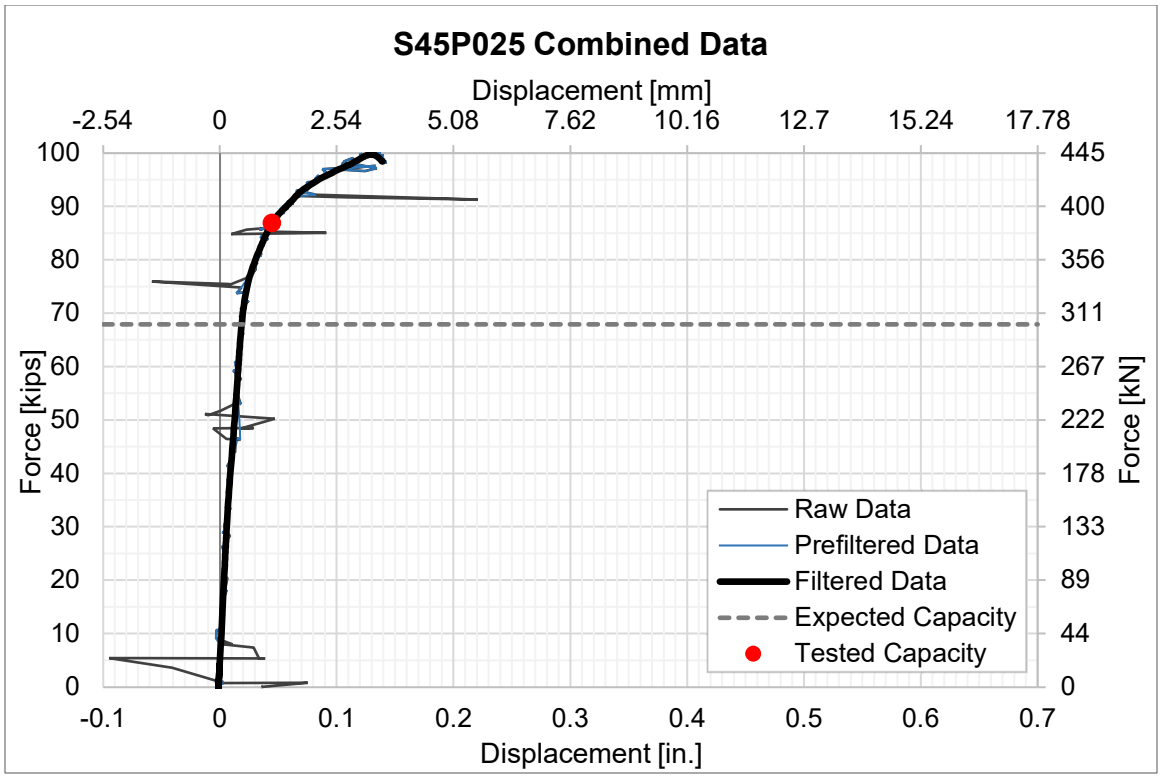

Figure 5-27: Combined Data for S45P025.

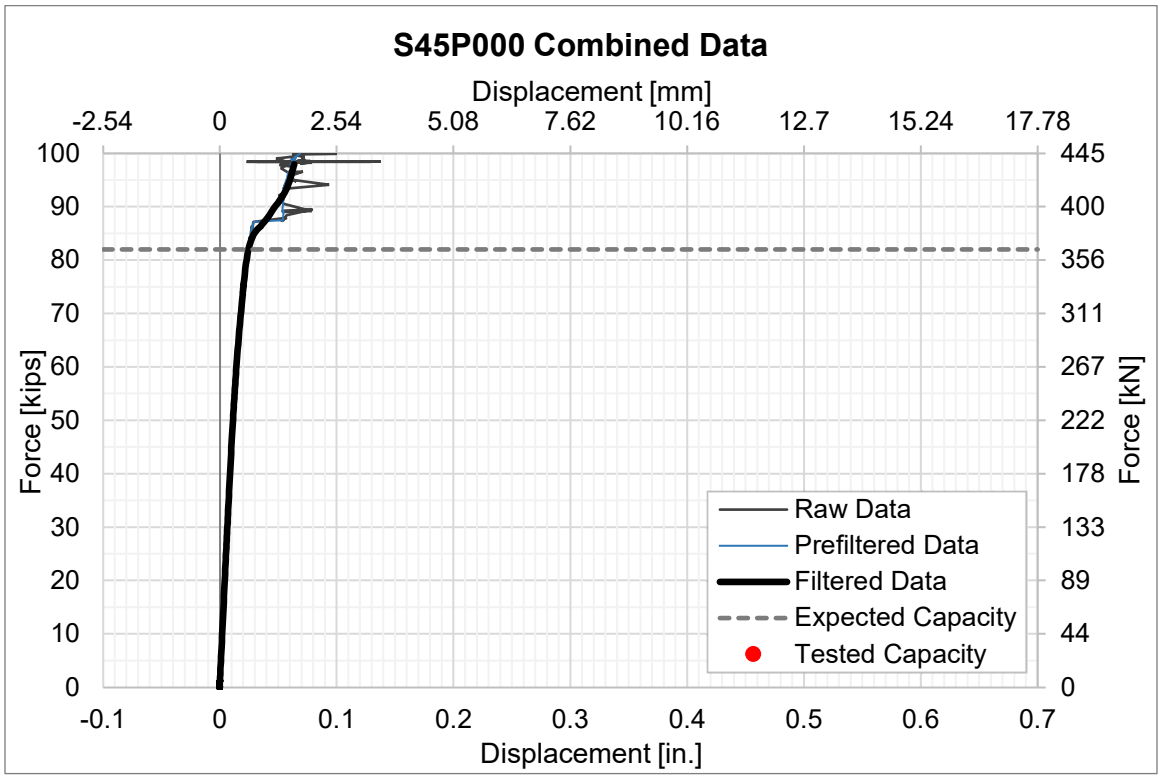

Figure 5-28: Combined Data for S45P000.

When comparing the expected to the tested capacities for each specimen, it can be seen that the vast majority of the tested capacities exceed what was expected, which is shown in Table 5-2. There were two exceptions: specimens S30P25 and S45P000. The expected capacity for specimen S30P25 is greater than the tested capacity by 1%; a tested capacity was not obtained for S45P000, so there is nothing to compare against. While most of the tested capacities are greater than the expected, the order of magnitude of that difference decreases as the bolt group position moves farther from the welded edge. This proves the need for an adjusted design procedure for these types of connections.

Table 5-2: Comparison of Expected and Tested Capacities.

TEST ID	EXPECTED CAPACITY kip (kN)	TESTED CAPACITY kip (kN)	PERCENT DIFFERENCE
S30P100	22.1 (98.1)	45.7 (203)	107%
S30P075	29.4 (131)	51.1 (227)	73.8%
S30P050	44.1 (196)	53.1 (236)	20.4%
S30P025	60.8 (270)	60.2 (268)	-0.99%
S30P000	60.8 (270)	76.8 (342)	26.3%
S35P100	31.6 (141)	54.7 (243)	73.1%
S35P075	42.1 (187)	55.3 (246)	31.4%
S35P050	61.3 (273)	63.1 (281)	2.94%
S35P025	67.9 (302)	72.8 (324)	7.22%
S35P000	71.7 (319)	79.4 (353)	10.7%
S40P100	43.1 (192)	68.4 (304)	58.7%
S40P075	57.5 (256)	65.8 (293)	14.4%
S40P050	61.3 (273)	72.1 (321)	17.6%
S40P025	67.9 (302)	81.4 (362)	19.4%
S40P000	82.0 (365)	91.4 (407)	11.5%
S45P100	56.6 (252)	68.7 (306)	21.4%
S45P075	59.1 (263)	76.0 (338)	28.6%
S45P050	61.3 (273)	84.1 (374)	37.2%
S45P025	67.9 (302)	86.9 (387)	28.0%
S45P000	82.0 (365)	N/A	N/A

Chapter 6: Discussion and Conclusions

There are many aspects of this research and experimental initiative that went well and resulted in new information and lessons learned. However, there were many more aspects of this initiative that could be improved and added in the future to bring the results that were desired at the conception of the project. This chapter discusses the pros and cons form this project and provides ideas for how this initiative can be improved upon in future studies.

6.1 Conclusions

There were several aspects of this project that were successful, including the several types of data gathered, the testing procedure that was followed, and the organization between the two different projects. The first one to note is the data gathered for this project. Not only were there quantitative data gathered from the rosettes, LVDTs, and the load cell, there were also qualitative data gathered through pictures and videos. The quantitative data that were gathered either confirmed the theories made about the project or provided new information to analyze. The qualitative data provided a way to document aspects that either cannot be put into words or would have been missed or overlooked in the experiment. The pictures taken of the specimens enabled the team to see the changes that occurred during the test after the material was recycled or discarded. The videos taken of the individual tests provided the opportunity to watch the tests over and over to figure out what happened at a specific point of the test, while also showing different point of views that would not have been attainable during the tests.

The documentation throughout this project was also successful. Having summaries of what happened during each test, quantitative data gathered for each test,

and videos of the tests used to answer questions from the initial test and the quantitative data was extremely helpful during the analysis phase. Adding to documentation, the step-by-step procedure for the test setup was successful. The procedure eliminated a lot of variability that could have occurred between the 20 different tests. It also allowed for improvements to be made on later tests, such as taking note of something that should be done differently for the remainder of the tests.

However, there were many lessons learned throughout this experimental initiative that can prove useful in future initiatives. Taking note of what was learned through this round of testing can enable further rounds of testing to gather more information to better understand the behavior of these single plate shear connections. Examples of the information learned through testing include anchorage of the specimens, location points for LVDTs and their setup, and location points for rosettes.

During some of the tests where the bolts were positioned near the weld, plate slipping was observed at the plate specimens and shim plates. The slipping was observed through loud noises during the test, seeing the plates shift in the recordings of the test, and by noticing the spikes in horizontal displacement data. The reason for the shift, discovered through watching the test recordings, was due to the anchorage of the specimen to the supporting beam. As aforementioned, the anchorage method was revised to accommodate for this behavior. However, the experimental initiative would have been more consistent if the anchorage method was used for each test.

Additionally, there were some lessons learned from setting up the LVDTs and where they were located. The LVDT holder used to keep the LVDT in place on the shear tab caused the LVDT to be confined within the nut, providing outputs that did not match

the behavior of the specimen during testing. This can be seen when the LVDT would get stuck in the nut and would read values that did not make sense for the observed behavior of the specimen. The second LVDT that gathered the base plate uplift measurements was useful in confirming the assumptions at the beginning of the initiative but did not contribute as much when analyzing the plate behavior. However, if that LVDT was used to gather horizontal displacement measurements of the sandwich plates, the data could be compared to the horizontal displacement of the shear tab to observe the relative displacements due to flexure and bearing independently. These data could provide answers to which behavior happens first and which is more prominent at the different bolt hole locations.

There were several lessons learned from using the rosettes during this experimental initiative. First, the location of the rosette did not provide enough information on the plate behavior. After observing the behavior of the plate, there are other locations that may provide more beneficial data: on the top, middle, and bottom edges of the slots. The data from these distinct locations could answer questions about what the plate around the slots experiences during the tests as well as provide a better approximation on how the plate sections between the slots act – as a cantilever, a frame, or another system.

Several conclusions can be made from the trends found through the analyzed data. First, a positive correlation was found between the connection capacity and the bolt group position: as the bolt group was positioned closer to the weld, the connection's capacity increased; as the bolt group was positioned farther from the weld, the connection's capacity decreased. Another trend found from the data analysis illustrates the different

amounts of flexural and bearing behavior exhibited by the shear tab. As the bolt group was positioned closer to the weld, the plate exhibited more bearing behavior than flexural; as the bolt group was positioned farther from the weld, the plate exhibited more flexural behavior than bearing.

Finally, there was a general trend found between the expected capacities and the tested capacities. For each specimen configuration, the same set of calculations were performed with the bolt group position and slot spacing changed for their respective tests. It was observed that at the 75% and 100% bolt group positions, the expected capacities were lower than the tested capacities by over 30%. Due to the gap between the tested and expected capacities, it was concluded that the design procedure was considerably conservative when designing the connections at those positions. However, the expected and tested capacities at the 0%, 25% and 50% bolt group positions were a lot closer in magnitude, roughly between 10% and 25%. While the calculations are conservative, it can be concluded that the design procedure is adequate for these positions. However, these trends confirm that the adapted design procedure used in this experimental initiative has the potential to be adjusted further to provide a more efficient and standard design for shear tabs with long-slotted holes.

6.2 Future Research

Due to the limitations of this project, and it being the first attempt at answering the questions around this experimental initiative, further research and testing should be completed. More work should be done to gain a better understanding of the plate behavior and to gather more informative data to allow for a more in-depth analysis. There

are many aspects of the project that can be added to and modified; the different ideas mentioned were determined through lessons learned throughout the experiment.

The first aspect that should be considered would be to limit the variables for testing to one: bolt position or slot spacing. Having the two different variables limited the number of specimens for each configuration. On that same note, incorporating several specimens with the same configuration would be beneficial. This would provide a better way to compare the trends in plate behavior, as well as allow more control over the variables for the different tests.

Another aspect of the project that could be modified would be in the setup of the specimen. First, the shear tab should increase in thickness to better represent what is seen in the field. Due to the capacity of the equipment used, the shear tabs for this project were ¼ in. (6.35 mm) thick. This plate likely saw different limit states that a thicker plate would see at the same stages in loading. Additionally, to better simulate the real-world application of these shear tabs, the base plate could be welded to an embed plate embedded in concrete. This would bring in different limit states to consider but would be more useful when understanding what happens.

The specimen configuration could also be modified for future testing. In this initial round of testing, the shear tab consisted of three rows of bolts in the slotted holes. The effects that more rows of bolts could have on the behavior of the plate was not considered for this project. Observing the shear tab with an increased number of bolt rows could be beneficial in understanding the plate behavior with the slotted holes; the increase in bolt rows could better portray what happens to the plate sections between the

slots. This configuration would also be useful when comparing to the plate configurations that are found in the field.

One of the biggest modifications that would be beneficial would be the number of rosettes used and their placement. As was previously mentioned, the placement for this test was not ideal in learning the latest information about how the plate sections behave. Various locations on the shear tab should be considered where more information can be gathered. The rosettes could be placed along the edges of the slots, closer to the top of the plate, and at the top of the non-loaded edge. The attachment of the rosettes located closer to the slot and farther from the welded edge will need significant consideration due to the amount of bending that may occur. The rosettes located at the top of the non-loaded edge could be useful in fully understanding why that area is rotated up during the tests. Additionally, several rosettes should be considered per test specimen to capture the different behavior at those distinct locations.

Finally, the creation of an inelastic finite element model should be considered in conjunction with the experimental testing. The results from the finite element model could be used to predict the behavior that should be observed in the experiment, as well as validate the observed behaviors during testing. The model could also be used to manipulate other variables not originally considered to observe their effects on the plate behavior without testing in the lab at that time. Creating additional models to simulate a framing system or cantilever beams could be beneficial to compare to the behavior seen during testing. Incorporating an inelastic finite element model would be a great addition to the data gathered on these types of connections and could answer a lot of questions that may be extremely difficult to observe during experimental testing.

References

American Concrete Institute (ACI). (2010). *Specification for Tolerance of Concrete Construction and Materials*. ACI 117-10. American Concrete Institute. Farmington Hills, Michigan.

American Institute of Steel Construction (AISC). (2016a). *Code of Standard Practice for Steel Buildings and Bridges*. ANSI/AISC 303-16. American Institute of Steel Construction. Chicago, Illinois.

American Institute of Steel Construction (AISC). (2016b). *Specification for Structural Steel Buildings*. ANSI/AISC 360-16. American Institute of Steel Construction. Chicago, Illinois.

Astaneh, A., Call, S. and McMullin, K. M. (1989). Design of Single Plate Shear Connections. *Engineering Journal*, AISC, Vol. 26, 21-32.

Electrical4U. (2021, April 16). Butterworth Filter: What is it? (Design & Applications). Electrical4U. https://www.electrical4u.com/butterworth-filter/.

Man, J. C. Y., Grondin, G. Y., and Driver, R. G. (2006). *Beam-to-Column Shear Connections with Slotted Holes* (Structural Engineering Report No. 260). University of Alberta, Department of Civil & Environmental Engineering. https://doi.org/10.7939/R3FF3M04W.

Muir, L. S. and Hewitt, C. M. (2009). Design of Unstiffened Extended Single-Plate Shear Connections. *Engineering Journal,* AISC, Vol. 46*,* 67-80.

Muir, L. S. and Thornton, W. A. (2011). The Development of a New Design Procedure for Conventional Single-Plate Shear Connections. *Engineering Journal*, AISC, Vol. 48, 141-152.

Ohki, M., Zervakis, M. E., Venetsanopoulos, A. N., and Leondes, C. T. (2021). Median Filters. Science Direct. https://www.sciencedirect.com/topics/engineering/median-filters.

Peterson, C. (2014). "Analysis of Long-Slotted Holes in Single Plate Connections." Master of Science in Structural Engineering (MSST) Capstone Paper, Milwaukee School of Engineering.

Sherman, D. R. and Ghorbanpoor, A. (2002). *Design of Extended Shear Tabs* (Report No. 3095). American Institute of Steel Construction. https://www.aisc.org/globalassets/aisc/research-library/design-of-extended-shear-tabs.pdf

Taxon, D. (2021). *Effect of Slot Spacing on Single Plate Connections with Long Slots*. Master of Science in Structural Engineering (MSAE) Capstone Project Report, Milwaukee School of Engineering. https://milwaukee.ent.sirsi.net/client/en_US/search/asset/2708/0

Wollenslegel, B. (2020). *Behavior of Extra-Long Slots.* Master's thesis, University of Cincinnati. https://etd.ohiolink.edu/.

Appendix A. Test Data from MAI

MAI METALLURGICAL ASSOCIATES, INC.

Tensile Test Report

MAI Report No:	220-3-235 REV1	**Date:**	January 15, 2021
Client:	Milwaukee School of Engineering	**Contact:**	Dr. Christopher Raebel
P.O. No:	Verbal	**Date Rec'd:**	December 22, 2020
Description:	Grade 50 Steel		

Property	11201407-P101 Sample1	11201407-P101 Sample2	112010407-P101 Sample3	112010407-P101 Sample4	ASTM A36
Test Bar Dimensions					
Width, inch	0.507	0.500	0.500	0.488	0.50
Thickness, inch	0.248	0.247	0.249	0.248	Material Thickness
Gage Length, inches	2.00	2.00	2.00	2.00	2.0
Tensile Strength, psi	72,500	72,900	73,100	72,700	58,000 - 80,000
Yield Strength, psi (1)	62,600	62,200	63,200	62,200	36,000 min.
Yield/Tensile Ratio	0.86	0.86	0.86	0.86	Not Specified
Elongation, %	30	31	30	33	21 min.

Property	11201407-P101 Sample5	11201407-P101 Sample6	ASTM A36
Test Bar Dimensions			
Width, inch	0.481	0.480	0.50
Thickness, inch	0.247	0.248	Material Thickness
Gage Length, inches	2.00	2.00	2.0
Tensile Strength, psi	73,000	72,900	58,000 - 80,000
Yield Strength, psi (1)	63,300	62,400	36,000 min.
Yield/Tensile Ratio	0.87	0.86	Not Specified
Elongation, %	31	31	21 min.

(1): at 0.2% offset

Notes: The tensile properties of all of the samples are in conformance with both ASTM A36, "Standard Specification for Carbon Structural Steel," and ASTM A992, "Standard Specification for Structural Steel Shapes."

The stress-strain curves for these samples are provided as separate Excel spreadsheets.

Respectfully submitted,

Anthony J. D'Antuono
Senior Metallurgical Engineer
Technical Manager

MAI ▪ 1515 Paramount Drive ▪ Suite 1 ▪ Waukesha, WI 53186
Phone: 262-798-8098 ▪ 800-798-4966 ▪ FAX: 262-798-8099 ▪. e-mail: info@metassoc.com
www.metassoc.com

Appendix B. Sample Calculations

S30P100 Expected Capacity

Goemetry and Material Properties

Single Plate Properties

Single Plate Thickness	$t_p := .25in$	
Vertical Edge Distance	$L_v := 2in$	From center of long slot
Horizontal Edge Distance	$L_h := 3in$	From center of long slot
Yield Strength	$F_y := 62.65ksi$	From material test data
Ultimate Strength	$F_u := 72.85ksi$	From material test data
Modulus of Elasticity	$E := 29000ksi$	From material test data
Slot Length	$L_s := \left(2 + \frac{13}{16}\right)in = 2\frac{13}{16}in$	
Bolt Position Relative to Welded Edge	$P_b := 100\%$	

Bolt Properties

A325-N Bolts

Number of Slots in a Row	$n := 3$	
Nominal Bolt Diameter	$d_b := .75in$	
Slot Spacing	$s := 3in$	
Slot Width	$d_h := d_b + \frac{1}{16}in = \frac{13}{16}in$	
Location of Bolt Relative to Welded Edge	$L_e := \left(L_h - \frac{L_s}{2}\right) + \frac{d_h}{2} + P_b \cdot \left(L_s - d_h\right) = 4\,in$	
Location of Bolt Relative to Slot End	$L_b := \frac{d_h}{2} + P_b \cdot \left(L_s - d_h\right) = 2\frac{13}{32}in$	

Embed Plate Properties

Embed Plate Thickness	$t_e := 1in$	
Embed Plate Eccentricity	$e := L_e = 4\,in$	Distance to Bolts from Face of Support
Yield Stress	$F_{ye} := 50ksi$	
Ultimate Stres	$F_{ue} := 65ksi$	

Single Plate Checks

Plate Properties

Plate Depth

$$d_p := (n - 1)\cdot s + 2\cdot L_v = 10\,in$$

Gross Shear Area

$$A_{gv} := d_p \cdot t_p = 2.5\,in^2$$

Net Shear Area

$$A_{nv} := \left[d_p - (n)\cdot\left(d_h\right) - L_v\right]\cdot t_p = 1.39\,in^2$$

Number of Shear Planes

$$n_{sp} := 1$$

Plastic Section Modulus

$$Z_x := n_{sp}\cdot\frac{t_p\cdot d_p^{\,2}}{4} = 6.25\,in^3$$

Shear and Flexure Checks

Shear Yielding

$$R_{n.PlShearYield} := 0.6\cdot F_y\cdot A_{gv} = 94.0\cdot kip$$

EQN J4-3

Flexural Yielding

$$R_{n.PlFlexureYield} := \frac{F_y\cdot Z_x}{e} = 97.9\,kip$$

Combined Shear and Flexure Check

$$R_{n.PlShearFlexureYield} := \frac{1}{\sqrt{\left(\frac{1}{R_{n.PlShearYield}}\right)^2 + \left(\frac{1}{R_{n.PlFlexureYield}}\right)^2}}$$

$$R_{n.PlShearFlexureYield} = 67.8\,kip$$

Net Shear Rupture

$$R_{n.PlShearRupt} := 0.60\cdot F_u\cdot A_{nv} = 60.78\,kip$$

EQN J4-4

Buckling Checks

Flexural Coefficient

$$\lambda := \frac{d_p\cdot\sqrt{F_y\cdot\frac{in^2}{kip}}}{10\cdot t_p\cdot\sqrt{475 + 280\left(\frac{d_p}{e}\right)^2}} = 0.671$$

Muir and Hewitt Equation

Flexural Buckling Coefficient

$$Q := \begin{cases} 1.0 & \text{if } \lambda \le 0.7 \\ (1.34 - .486\lambda) & \text{if } 0.7 < \lambda \le 1.41 \\ \frac{1.3}{\lambda^2} & \text{if } \lambda > 1.41 \end{cases} = 1.00$$

Critical Buckling Stress

$$F_{bx} := F_y\cdot Q = 62.65\,ksi$$

Elastic Section Modulus

$$S_x := n_{sp}\cdot\frac{t_p\cdot d_p^{\,2}}{6} = 4.17\,in^3$$

Plate Buckling Strength

$$R_{n.PlBuckling} := \frac{F_{bx}\cdot S_x}{e} = 65.3\,kip$$

Block Shear Check

Gross Shear Length $L_{gv} := (n - 1) \cdot s + L_v = 8\ in$

Net Shear Length $L_{nv} := L_{gv} - (n - .5) \cdot d_h = 5.97\ in$

Gross Tension Length $L_{gt} := L_v = 2\ in$

Net Tension Length $L_{nt} := L_{gt} - \frac{L_s}{2} = 0.59375\ in$

Gross Shear Area $A_{gv} := L_{gv} \cdot t_p = 2\ in^2$

Net Shear Area $A_{nv} := L_{nv} \cdot t_p = 1.49\ in^2$

Gross Tension Area $A_{gt} := L_{gt} \cdot t_p = 0.5\ in^2$

Net Tension Area $A_{nt} := L_{nt} \cdot t_p = 0.15 \cdot in^2$

Block Shear Capacity $R_{n.PlBlockShear} := F_u \cdot A_{nt} + min(0.6 \cdot F_u \cdot A_{nv}, 0.6 \cdot F_y \cdot A_{gv})$ EQN J4-5

$R_{n.PlBlockShear} = 76.04\ kip$

Bolt Checks

Bolt Shear

Area of Bolt $A_{bolt} := \pi \cdot \frac{d_b^2}{4} = 0.44\ in^2$

Bolt Shear Stress $F_{nv} := 54ksi$ AISC Table J3.2, P. 16.1-129

Number of Shear Planes $n_{sp} := 2$ 2 Sandwich Plates

Bolt Shear Strength $R_{n.BoltShear} := n \cdot n_{sp} \cdot F_{nv} \cdot A_{bolt} = 143.14 \cdot kip$ EQN J3-1

Plate Bearing/Tearout at Bottom Bolt

Clear Edge Distance $L_{c.pl} := L_v - \frac{d_h}{2} = 1.59\ in$

Number of Shear Planes $n_{sp} := 1$

Bolt Tearout Strength $R_{n.BoltTearout.PlBot} := n_{sp} \cdot 1 \cdot L_{c.pl} \cdot t_p \cdot F_u = 29.03 \cdot kip$ EQN J3-6F

Bolt Bearing Strength $R_{n.BoltBearing.PlBot} := n_{sp} \cdot 2 \cdot d_b \cdot t_p \cdot F_u = 27.32 \cdot kip$ EQN J3-6E

Botom Bolt Capacity $R_{n.Bolt.PlBottom} := min(R_{n.BoltTearout.PlBot}, R_{n.BoltBearing.PlBot})$

$R_{n.Bolt.PlBottom} = 27.32\ kip$

Plate Bearing/Tearout at Remaining Bolts

Clear Distance Between Slots

$$L_{c.pl} := s - d_h = 2.19\ in$$

Number of Shear Planes

$$n_{sp} := 1$$

Bolt Tearout Strength

$$R_{n.BoltTearout.PlMid} := (n-1)\cdot n_{sp}\cdot 1\cdot L_{c.pl}\, t_p\cdot F_u = 79.68\cdot kip$$ EQN J3-6F

Bolt Bearing Strength

$$R_{n.BoltBearing.PlMid} := (n-1)\cdot n_{sp}\cdot 2\cdot d_b\cdot t_p\cdot F_u = 54.64\cdot kip$$ EQN J3-6E

Remaining Bolt Capacity

$$R_{n.Bolt.PlMid} := min\left(R_{n.BoltTearout.PlMid}, R_{n.BoltBearing.PlMid}\right)$$

$$R_{n.Bolt.PlMid} = 54.64\ kip$$

Plate Flexure at Bottom Bolt

Clear Edge Distance

$$L_{c.pl} := L_v - \frac{d_h}{2} = 1.59375\ in$$

Elastic Section Modulus

$$S_x := \frac{t_p\cdot L_{c.pl}^{\,2}}{6} = 0.105835\ in^3$$

"Beam" Span Length

$$Span := L_b - \frac{13}{32}in = 2\ in$$

$$Span := \begin{cases} 0.001in & if\ Span \le 0 \\ Span & if\ Span > 0 \end{cases} = 2\cdot in$$

Used 0.001 in. in equation to avoid dividing by 0

Plate Flexure Capacity at Bottom Bolt

$$R_{n.BoltPlFlexure.Bot} := \frac{F_y\cdot S_x}{Span} = 3.32\cdot kip$$

Plate Flexure at Remaining Bolts

Clear Distance Between Slots

$$L_{c.pl} := s - d_h = 2.19\ in$$

Elastic Section Modulus

$$S_x := \frac{t_p\cdot L_{c.pl}^{\,2}}{4} = 0.3\ in^3$$

"Beam" Span Length

$$Span := L_b - \frac{13}{32}in = 2\ in$$

$$Span := \begin{cases} 0.001in & if\ Span \le 0 \\ Span & if\ Span > 0 \end{cases} = 2\cdot in$$

Used 0.001 in. in equation to avoid dividing by 0

Plate Flexure Capacity at Remaining Bolts

$$R_{n.BoltPlFlexure.Mid} := \frac{(n-1)F_y\cdot S_x}{Span} = 18.74\cdot kip$$

Single Plate to Embed Plate Weld

Minimum Weld Metal Strength

$$F_{EXX} := 70ksi$$

Effective Weld Length

$$L_w := d_p - 2 \cdot .25in = 9.5\,in$$

Minimum Plate Thickness

$$t_{min} := min\left(t_p, t_e\right) = 0.25\,in$$

Minimum Weld Sixe

$$w_{min} := \begin{cases} \frac{1}{4}in & if\ t_{min} \le .75in \\ \frac{3}{16}in & if\ t_{min} \le .5in \\ \frac{1}{8}in & if\ t_{min} \le .25in \\ \frac{5}{16}in & otherwise \end{cases} = \frac{1}{8} \cdot in$$

Design Weld Size

$$w_{des} := max\left(w_{min}, Ceil\left(\frac{5 \cdot t_{min}}{8}, \frac{1}{16}in\right)\right) = \frac{3}{16}\,in$$

Design Weld Size

$$w_{des} := \frac{1}{4}in$$

Resultant Load Angle

$$\theta := atan\left[\frac{\left(\frac{3 \cdot e}{L_w^{\,2}}\right)}{\left(\frac{1}{2L_w}\right)}\right] = 68.4 \cdot deg$$

Weld Directional Increase

$$F := 1 + 0.5 \cdot \left(sin(\theta)^{1.5}\right) = 1.45$$

Weld Strength

$$F_w := F \cdot 0.6 \cdot F_{EXX} = 60.83 \cdot ksi$$

Weld Stress

$$F_{w.des} := \frac{F_w}{\sqrt{2}} = 43.01\,ksi$$

Combined Weld Stress

$$F_{r.all} := w_{des} \cdot F_{w.des} = 10.75 \cdot kpi$$

Start of Solve Block

Given

$$F_{r.all} = \sqrt{\left(\frac{P}{2 \cdot L_w}\right)^2 + \left(P \cdot e \cdot \frac{3}{L_w^{\,2}}\right)^2}$$

$$P := Find(P)\ float, 5 \rightarrow (-902338.0 \cdot in \cdot plf \quad 902338.0 \cdot in \cdot plf)$$

Weld Strength

$$R_{n.weld} := max(P) = 75.2 \cdot kip$$

S30P100 Expected Capacity Summary

$R_{n.PlShearYield} = 93.98\,kip$

$R_{n.PlFlexureYield} = 97.89\,kip$

$R_{n.PlShearFlexureYield} = 67.79\,kip$

$R_{n.PlShearRupt} = 60.78\,kip$

$R_{n.PlBuckling} = 65.26\,kip$

$R_{n.PlBlockShear} = 76.04\,kip$

$R_{n.BoltShear} = 143.14\,kip$

$R_{n.BoltTearout.PlBot} = 29.03\,kip$

$R_{n.BoltTearout.PlMid} = 79.68\,kip$

$R_{n.BoltTearout} := R_{n.BoltTearout.PlBot} + R_{n.BoltTearout.PlMid} = 108.71\,kip$

$R_{n.BoltBearing.PlBot} = 27.32\,kip$

$R_{n.BoltBearing.PlMid} = 54.64\,kip$

$R_{n.BoltBearing} := R_{n.BoltBearing.PlBot} + R_{n.BoltBearing.PlMid} = 81.96\,kip$

$R_{n.BoltPlFlexure.Bot} = 3.32\,kip$

$R_{n.BoltPlFlexure.Mid} = 18.74\,kip$

$R_{n.Bolt.PlFlexure} := R_{n.BoltPlFlexure.Bot} + R_{n.BoltPlFlexure.Mid} = 22.05\,kip$

$$R_{n.Bolt.Bot} := \begin{pmatrix} R_{n.BoltTearout.PlBot} \\ R_{n.BoltBearing.PlBot} \\ R_{n.BoltPlFlexure.Bot} \end{pmatrix} = \begin{pmatrix} 29.03 \\ 27.32 \\ 3.32 \end{pmatrix} kip$$

$$R_{n.Bolt.Mid} := \begin{pmatrix} R_{n.BoltTearout.PlMid} \\ R_{n.BoltBearing.PlMid} \\ R_{n.BoltPlFlexure.Mid} \end{pmatrix} = \begin{pmatrix} 79.68 \\ 54.64 \\ 18.74 \end{pmatrix} kip$$

$R_{n.Bolts} := min(R_{n.Bolt.Bot}) + min(R_{n.Bolt.Mid}) = 22.05\,kip$

$R_{n.weld} = 75.19\,kip$

$w_{des} = \frac{1}{4}\,in$

$s = 3\,in$ $\quad P_b = 100 \cdot \%$ $\quad Capacity = 22.05\,kip$ $\quad Capacity = 98.09 \cdot kN$ $\quad LimitState = \begin{pmatrix} \text{"R.Bolt.PLFlexure"} \\ \text{"R.Bolts"} \end{pmatrix}$

S35P100 Expected Capacity Summary

$R_{n.PlShearYield} = 103.37\,kip$

$R_{n.PlFlexureYield} = 118.45\,kip$

$R_{n.PlShearFlexureYield} = 77.88\,kip$

$R_{n.PlShearRupt} = 71.71\,kip$

$R_{n.PlBuckling} = 78.97\,kip$

$R_{n.PlBlockShear} = 86.96\,kip$

$R_{n.BoltShear} = 143.14\,kip$

$R_{n.BoltTearout.PlBot} = 29.03\,kip$

$R_{n.BoltTearout.PlMid} = 97.89\,kip$

$R_{n.BoltTearout} := R_{n.BoltTearout.PlBot} + R_{n.BoltTearout.PlMid} = 126.92\,kip$

$R_{n.BoltBearing.PlBot} = 27.32\,kip$

$R_{n.BoltBearing.PlMid} = 54.64\,kip$

$R_{n.BoltBearing} := R_{n.BoltBearing.PlBot} + R_{n.BoltBearing.PlMid} = 81.96\,kip$

$R_{n.BoltPlFlexure.Bot} = 3.32\,kip$

$R_{n.BoltPlFlexure.Mid} = 28.28\,kip$

$R_{n.Bolt.PlFlexure} := R_{n.BoltPlFlexure.Bot} + R_{n.BoltPlFlexure.Mid} = 31.6\,kip$

$$R_{n.Bolt.Bot} := \begin{pmatrix} R_{n.BoltTearout.PlBot} \\ R_{n.BoltBearing.PlBot} \\ R_{n.BoltPlFlexure.Bot} \end{pmatrix} = \begin{pmatrix} 29.03 \\ 27.32 \\ 3.32 \end{pmatrix} kip$$

$$R_{n.Bolt.Mid} := \begin{pmatrix} R_{n.BoltTearout.PlMid} \\ R_{n.BoltBearing.PlMid} \\ R_{n.BoltPlFlexure.Mid} \end{pmatrix} = \begin{pmatrix} 97.89 \\ 54.64 \\ 28.28 \end{pmatrix} kip$$

$R_{n.Bolts} := min\left(R_{n.Bolt.Bot}\right) + min\left(R_{n.Bolt.Mid}\right) = 31.6\,kip$

$R_{n.weld} = 89.89\,kip$

$w_{des} = \frac{1}{4}\,in$

$s = 3.5\,in$

$P_b = 100 \cdot \%$

$Capacity = 31.6\,kip$

$Capacity = 140.55 \cdot kN$

$$LimitState = \begin{pmatrix} \text{"R.Bolt.PLFlexure"} \\ \text{"R.Bolts"} \end{pmatrix}$$

S40P100 Expected Capacity Summary

$R_{n.PlShearYield} = 112.77\,kip$

$R_{n.PlFlexureYield} = 140.96\,kip$

$R_{n.PlShearFlexureYield} = 88.06\,kip$

$R_{n.PlShearRupt} = 82.64\,kip$

$R_{n.PlBuckling} = 93.97\,kip$

$R_{n.PlBlockShear} = 97.89\,kip$

$R_{n.BoltShear} = 143.14\,kip$

$R_{n.BoltTearout.PlBot} = 29.03\,kip$

$R_{n.BoltTearout.PlMid} = 116.1\,kip$

$R_{n.BoltTearout} := R_{n.BoltTearout.PlBot} + R_{n.BoltTearout.PlMid} = 145.13\,kip$

$R_{n.BoltBearing.PlBot} = 27.32\,kip$

$R_{n.BoltBearing.PlMid} = 54.64\,kip$

$R_{n.BoltBearing} := R_{n.BoltBearing.PlBot} + R_{n.BoltBearing.PlMid} = 81.96\,kip$

$R_{n.BoltPlFlexure.Bot} = 3.32\,kip$

$R_{n.BoltPlFlexure.Mid} = 39.78\,kip$

$R_{n.Bolt.PlFlexure} := R_{n.BoltPlFlexure.Bot} + R_{n.BoltPlFlexure.Mid} = 43.1\,kip$

$$R_{n.Bolt.Bot} := \begin{pmatrix} R_{n.BoltTearout.PlBot} \\ R_{n.BoltBearing.PlBot} \\ R_{n.BoltPlFlexure.Bot} \end{pmatrix} = \begin{pmatrix} 29.03 \\ 27.32 \\ 3.32 \end{pmatrix} kip$$

$$R_{n.Bolt.Mid} := \begin{pmatrix} R_{n.BoltTearout.PlMid} \\ R_{n.BoltBearing.PlMid} \\ R_{n.BoltPlFlexure.Mid} \end{pmatrix} = \begin{pmatrix} 116.1 \\ 54.64 \\ 39.78 \end{pmatrix} kip$$

$R_{n.Bolts} := min\left(R_{n.Bolt.Bot}\right) + min\left(R_{n.Bolt.Mid}\right) = 43.1\,kip$

$R_{n.weld} = 105.39\,kip$

$w_{des} = \frac{1}{4}\,in$

$s = 4\,in$ $\quad Capacity = 43.1\,kip$ $\quad Capacity = 191.71 \cdot kN$ $\quad LimitState = \begin{pmatrix} \text{"R.Bolt.PLFlexure"} \\ \text{"R.Bolts"} \end{pmatrix}$

$P_b = 100 \cdot \%$

S45P100 Expected Capacity Summary

$R_{n.PlShearYield} = 122.17\,kip$

$R_{n.PlFlexureYield} = 165.44\,kip$

$R_{n.PlShearFlexureYield} = 98.28\,kip$

$R_{n.PlShearRupt} = 93.57\,kip$

$R_{n.PlBuckling} = 110.13\,kip$

$R_{n.PlBlockShear} = 108.82\,kip$

$R_{n.BoltShear} = 143.14\,kip$

$R_{n.BoltTearout.PlBot} = 29.03\,kip$

$R_{n.BoltTearout.PlMid} = 134.32\,kip$

$R_{n.BoltTearout} := R_{n.BoltTearout.PlBot} + R_{n.BoltTearout.PlMid} = 163.34\,kip$

$R_{n.BoltBearing.PlBot} = 27.32\,kip$

$R_{n.BoltBearing.PlMid} = 54.64\,kip$

$R_{n.BoltBearing} := R_{n.BoltBearing.PlBot} + R_{n.BoltBearing.PlMid} = 81.96\,kip$

$R_{n.BoltPlFlexure.Bot} = 3.32\,kip$

$R_{n.BoltPlFlexure.Mid} = 53.24\,kip$

$R_{n.Bolt.PlFlexure} := R_{n.BoltPlFlexure.Bot} + R_{n.BoltPlFlexure.Mid} = 56.56\,kip$

$$R_{n.Bolt.Bot} := \begin{pmatrix} R_{n.BoltTearout.PlBot} \\ R_{n.BoltBearing.PlBot} \\ R_{n.BoltPlFlexure.Bot} \end{pmatrix} = \begin{pmatrix} 29.03 \\ 27.32 \\ 3.32 \end{pmatrix} kip$$

$$R_{n.Bolt.Mid} := \begin{pmatrix} R_{n.BoltTearout.PlMid} \\ R_{n.BoltBearing.PlMid} \\ R_{n.BoltPlFlexure.Mid} \end{pmatrix} = \begin{pmatrix} 134.32 \\ 54.64 \\ 53.24 \end{pmatrix} kip$$

$R_{n.Bolts} := min\left(R_{n.Bolt.Bot}\right) + min\left(R_{n.Bolt.Mid}\right) = 56.56\,kip$

$R_{n.weld} = 121.55\,kip$

$w_{des} = \frac{1}{4}\,in$

$s = 4.5\,in$

$P_b = 100 \cdot \%$

$Capacity = 56.56\,kip$ $Capacity = 251.59 \cdot kN$ $LimitState = \begin{pmatrix} \text{"R.Bolt.PLFlexure"} \\ \text{"R.Bolts"} \end{pmatrix}$

S30P075 Expected Capacity Summary

$R_{n.PlShearYield} = 93.98\,kip$

$R_{n.PlFlexureYield} = 111.88\,kip$

$R_{n.PlShearFlexureYield} = 71.96\,kip$

$R_{n.PlShearRupt} = 60.78\,kip$

$R_{n.PlBuckling} = 74.58\,kip$

$R_{n.PlBlockShear} = 76.04\,kip$

$R_{n.BoltShear} = 143.14\,kip$

$R_{n.BoltTearout.PlBot} = 29.03\,kip$

$R_{n.BoltTearout.PlMid} = 79.68\,kip$

$R_{n.BoltTearout} := R_{n.BoltTearout.PlBot} + R_{n.BoltTearout.PlMid} = 108.71\,kip$

$R_{n.BoltBearing.PlBot} = 27.32\,kip$

$R_{n.BoltBearing.PlMid} = 54.64\,kip$

$R_{n.BoltBearing} := R_{n.BoltBearing.PlBot} + R_{n.BoltBearing.PlMid} = 81.96\,kip$

$R_{n.BoltPlFlexure.Bot} = 4.42\,kip$

$R_{n.BoltPlFlexure.Mid} = 24.98\,kip$

$R_{n.Bolt.PlFlexure} := R_{n.BoltPlFlexure.Bot} + R_{n.BoltPlFlexure.Mid} = 29.4\,kip$

$$R_{n.Bolt.Bot} := \begin{pmatrix} R_{n.BoltTearout.PlBot} \\ R_{n.BoltBearing.PlBot} \\ R_{n.BoltPlFlexure.Bot} \end{pmatrix} = \begin{pmatrix} 29.03 \\ 27.32 \\ 4.42 \end{pmatrix} kip$$

$$R_{n.Bolt.Mid} := \begin{pmatrix} R_{n.BoltTearout.PlMid} \\ R_{n.BoltBearing.PlMid} \\ R_{n.BoltPlFlexure.Mid} \end{pmatrix} = \begin{pmatrix} 79.68 \\ 54.64 \\ 24.98 \end{pmatrix} kip$$

$R_{n.Bolts} := min(R_{n.Bolt.Bot}) + min(R_{n.Bolt.Mid}) = 29.4\,kip$

$R_{n.weld} = 83.42\,kip$

$w_{des} = \frac{1}{4}\,in$

$s = 3\,in$

$P_b = 75 \cdot \%$

$Capacity = 29.4\,kip$ $\quad Capacity = 130.79 \cdot kN$ $\quad LimitState = \begin{pmatrix} \text{"R.Bolt.PLFlexure"} \\ \text{"R.Bolts"} \end{pmatrix}$

S35P075 Expected Capacity Summary

$R_{n.PlShearYield} = 103.37\,kip$

$R_{n.PlFlexureYield} = 135.37\,kip$

$R_{n.PlShearFlexureYield} = 82.16\,kip$

$R_{n.PlShearRupt} = 71.71\,kip$

$R_{n.PlBuckling} = 90.25\,kip$

$R_{n.PlBlockShear} = 86.96\,kip$

$R_{n.BoltShear} = 143.14\,kip$

$R_{n.BoltTearout.PlBot} = 29.03\,kip$

$R_{n.BoltTearout.PlMid} = 97.89\,kip$

$R_{n.BoltTearout} := R_{n.BoltTearout.PlBot} + R_{n.BoltTearout.PlMid} = 126.92\,kip$

$R_{n.BoltBearing.PlBot} = 27.32\,kip$

$R_{n.BoltBearing.PlMid} = 54.64\,kip$

$R_{n.BoltBearing} := R_{n.BoltBearing.PlBot} + R_{n.BoltBearing.PlMid} = 81.96\,kip$

$R_{n.BoltPlFlexure.Bot} = 4.42\,kip$

$R_{n.BoltPlFlexure.Mid} = 37.71\,kip$

$R_{n.Bolt.PlFlexure} := R_{n.BoltPlFlexure.Bot} + R_{n.BoltPlFlexure.Mid} = 42.13\,kip$

$$R_{n.Bolt.Bot} := \begin{pmatrix} R_{n.BoltTearout.PlBot} \\ R_{n.BoltBearing.PlBot} \\ R_{n.BoltPlFlexure.Bot} \end{pmatrix} = \begin{pmatrix} 29.03 \\ 27.32 \\ 4.42 \end{pmatrix} kip$$

$$R_{n.Bolt.Mid} := \begin{pmatrix} R_{n.BoltTearout.PlMid} \\ R_{n.BoltBearing.PlMid} \\ R_{n.BoltPlFlexure.Mid} \end{pmatrix} = \begin{pmatrix} 97.89 \\ 54.64 \\ 37.71 \end{pmatrix} kip$$

$R_{n.Bolts} := min\left(R_{n.Bolt.Bot}\right) + min\left(R_{n.Bolt.Mid}\right) = 42.13\,kip$

$R_{n.weld} = 99.22\,kip$

$w_{des} = \frac{1}{4}\,in$

$s = 3.5\,in$

$P_b = 75 \cdot \%$

$Capacity = 42.13\,kip$ $Capacity = 187.4 \cdot kN$ $LimitState = \begin{pmatrix} \text{"R.Bolt.PLFlexure"} \\ \text{"R.Bolts"} \end{pmatrix}$

S40P075 Expected Capacity Summary

$R_{n.PlShearYield} = 112.77\,kip$

$R_{n.PlFlexureYield} = 161.1\,kip$

$R_{n.PlShearFlexureYield} = 92.38\,kip$

$R_{n.PlShearRupt} = 82.64\,kip$

$R_{n.PlBuckling} = 107.4\,kip$

$R_{n.PlBlockShear} = 97.89\,kip$

$R_{n.BoltShear} = 143.14\,kip$

$R_{n.BoltTearout.PlBot} = 29.03\,kip$

$R_{n.BoltTearout.PlMid} = 116.1\,kip$

$R_{n.BoltTearout} := R_{n.BoltTearout.PlBot} + R_{n.BoltTearout.PlMid} = 145.13\,kip$

$R_{n.BoltBearing.PlBot} = 27.32\,kip$

$R_{n.BoltBearing.PlMid} = 54.64\,kip$

$R_{n.BoltBearing} := R_{n.BoltBearing.PlBot} + R_{n.BoltBearing.PlMid} = 81.96\,kip$

$R_{n.BoltPlFlexure.Bot} = 4.42\,kip$

$R_{n.BoltPlFlexure.Mid} = 53.04\,kip$

$R_{n.Bolt.PlFlexure} := R_{n.BoltPlFlexure.Bot} + R_{n.BoltPlFlexure.Mid} = 57.46\,kip$

$$R_{n.Bolt.Bot} := \begin{pmatrix} R_{n.BoltTearout.PlBot} \\ R_{n.BoltBearing.PlBot} \\ R_{n.BoltPlFlexure.Bot} \end{pmatrix} = \begin{pmatrix} 29.03 \\ 27.32 \\ 4.42 \end{pmatrix} kip$$

$$R_{n.Bolt.Mid} := \begin{pmatrix} R_{n.BoltTearout.PlMid} \\ R_{n.BoltBearing.PlMid} \\ R_{n.BoltPlFlexure.Mid} \end{pmatrix} = \begin{pmatrix} 116.1 \\ 54.64 \\ 53.04 \end{pmatrix} kip$$

$R_{n.Bolts} := min\left(R_{n.Bolt.Bot}\right) + min\left(R_{n.Bolt.Mid}\right) = 57.46\,kip$

$R_{n.weld} = 115.71\,kip$

$w_{des} = \frac{1}{4}\,in$

$s = 4\,in$

$P_b = 75 \cdot \%$

$Capacity = 57.46\,kip$ $Capacity = 255.62 \cdot kN$ $LimitState = \begin{pmatrix} \text{"R.Bolt.PLFlexure"} \\ \text{"R.Bolts"} \end{pmatrix}$

S45P075 Expected Capacity Summary

$R_{n.PlShearYield} = 122.17\,kip$

$R_{n.PlFlexureYield} = 189.07\,kip$

$R_{n.PlShearFlexureYield} = 102.61\,kip$

$R_{n.PlShearRupt} = 93.57\,kip$

$R_{n.PlBuckling} = 126.05\,kip$

$R_{n.PlBlockShear} = 108.82\,kip$

$R_{n.BoltShear} = 143.14\,kip$

$R_{n.BoltTearout.PlBot} = 29.03\,kip$

$R_{n.BoltTearout.PlMid} = 134.32\,kip$

$R_{n.BoltTearout} := R_{n.BoltTearout.PlBot} + R_{n.BoltTearout.PlMid} = 163.34\,kip$

$R_{n.BoltBearing.PlBot} = 27.32\,kip$

$R_{n.BoltBearing.PlMid} = 54.64\,kip$

$R_{n.BoltBearing} := R_{n.BoltBearing.PlBot} + R_{n.BoltBearing.PlMid} = 81.96\,kip$

$R_{n.BoltPlFlexure.Bot} = 4.42\,kip$

$R_{n.BoltPlFlexure.Mid} = 70.99\,kip$

$R_{n.Bolt.PlFlexure} := R_{n.BoltPlFlexure.Bot} + R_{n.BoltPlFlexure.Mid} = 75.41\,kip$

$$R_{n.Bolt.Bot} := \begin{pmatrix} R_{n.BoltTearout.PlBot} \\ R_{n.BoltBearing.PlBot} \\ R_{n.BoltPlFlexure.Bot} \end{pmatrix} = \begin{pmatrix} 29.03 \\ 27.32 \\ 4.42 \end{pmatrix} kip$$

$$R_{n.Bolt.Mid} := \begin{pmatrix} R_{n.BoltTearout.PlMid} \\ R_{n.BoltBearing.PlMid} \\ R_{n.BoltPlFlexure.Mid} \end{pmatrix} = \begin{pmatrix} 134.32 \\ 54.64 \\ 70.99 \end{pmatrix} kip$$

$R_{n.Bolts} := min\left(R_{n.Bolt.Bot}\right) + min\left(R_{n.Bolt.Mid}\right) = 59.06\,kip$

$R_{n.weld} = 132.75\,kip$

$w_{des} = \frac{1}{4}\,in$

$s = 4.5\,in$

$P_b = 75 \cdot \%$

$Capacity = 59.06\,kip$ $Capacity = 262.7 \cdot kN$ $LimitState = (\text{"R.Bolts"})$

S30P050 Expected Capacity Summary

$R_{n.PlShearYield} = 93.98\,kip$

$R_{n.PlFlexureYield} = 130.52\,kip$

$R_{n.PlShearFlexureYield} = 76.26\,kip$

$R_{n.PlShearRupt} = 60.78\,kip$

$R_{n.PlBuckling} = 87.01\,kip$

$R_{n.PlBlockShear} = 76.04\,kip$

$R_{n.BoltShear} = 143.14\,kip$

$R_{n.BoltTearout.PlBot} = 29.03\,kip$

$R_{n.BoltTearout.PlMid} = 79.68\,kip$

$R_{n.BoltTearout} := R_{n.BoltTearout.PlBot} + R_{n.BoltTearout.PlMid} = 108.71\,kip$

$R_{n.BoltBearing.PlBot} = 27.32\,kip$

$R_{n.BoltBearing.PlMid} = 54.64\,kip$

$R_{n.BoltBearing} := R_{n.BoltBearing.PlBot} + R_{n.BoltBearing.PlMid} = 81.96\,kip$

$R_{n.BoltPlFlexure.Bot} = 6.63\,kip$

$R_{n.BoltPlFlexure.Mid} = 37.47\,kip$

$R_{n.Bolt.PlFlexure} := R_{n.BoltPlFlexure.Bot} + R_{n.BoltPlFlexure.Mid} = 44.1\,kip$

$$R_{n.Bolt.Bot} := \begin{pmatrix} R_{n.BoltTearout.PlBot} \\ R_{n.BoltBearing.PlBot} \\ R_{n.BoltPlFlexure.Bot} \end{pmatrix} = \begin{pmatrix} 29.03 \\ 27.32 \\ 6.63 \end{pmatrix} kip$$

$$R_{n.Bolt.Mid} := \begin{pmatrix} R_{n.BoltTearout.PlMid} \\ R_{n.BoltBearing.PlMid} \\ R_{n.BoltPlFlexure.Mid} \end{pmatrix} = \begin{pmatrix} 79.68 \\ 54.64 \\ 37.47 \end{pmatrix} kip$$

$R_{n.Bolts} := min(R_{n.Bolt.Bot}) + min(R_{n.Bolt.Mid}) = 44.1\,kip$

$R_{n.weld} = 93.22\,kip$

$w_{des} = \frac{1}{4}\,in$

$s = 3\,in$

$P_b = 50 \cdot \%$

$Capacity = 44.1\,kip$ $\quad Capacity = 196.19 \cdot kN$ $\quad LimitState = \begin{pmatrix} \text{"R.Bolt.PLFlexure"} \\ \text{"R.Bolts"} \end{pmatrix}$

S35P050 Expected Capacity Summary

$R_{n.PlShearYield} = 103.37\,kip$

$R_{n.PlFlexureYield} = 157.93\,kip$

$R_{n.PlShearFlexureYield} = 86.49\,kip$

$R_{n.PlShearRupt} = 71.71\,kip$

$R_{n.PlBuckling} = 105.29\,kip$

$R_{n.PlBlockShear} = 86.96\,kip$

$R_{n.BoltShear} = 143.14\,kip$

$R_{n.BoltTearout.PlBot} = 29.03\,kip$

$R_{n.BoltTearout.PlMid} = 97.89\,kip$

$R_{n.BoltTearout} := R_{n.BoltTearout.PlBot} + R_{n.BoltTearout.PlMid} = 126.92\,kip$

$R_{n.BoltBearing.PlBot} = 27.32\,kip$

$R_{n.BoltBearing.PlMid} = 54.64\,kip$

$R_{n.BoltBearing} := R_{n.BoltBearing.PlBot} + R_{n.BoltBearing.PlMid} = 81.96\,kip$

$R_{n.BoltPlFlexure.Bot} = 6.63\,kip$

$R_{n.BoltPlFlexure.Mid} = 56.56\,kip$

$R_{n.Bolt.PlFlexure} := R_{n.BoltPlFlexure.Bot} + R_{n.BoltPlFlexure.Mid} = 63.19\,kip$

$$R_{n.Bolt.Bot} := \begin{pmatrix} R_{n.BoltTearout.PlBot} \\ R_{n.BoltBearing.PlBot} \\ R_{n.BoltPlFlexure.Bot} \end{pmatrix} = \begin{pmatrix} 29.03 \\ 27.32 \\ 6.63 \end{pmatrix} kip$$

$$R_{n.Bolt.Mid} := \begin{pmatrix} R_{n.BoltTearout.PlMid} \\ R_{n.BoltBearing.PlMid} \\ R_{n.BoltPlFlexure.Mid} \end{pmatrix} = \begin{pmatrix} 97.89 \\ 54.64 \\ 56.56 \end{pmatrix} kip$$

$R_{n.Bolts} := min(R_{n.Bolt.Bot}) + min(R_{n.Bolt.Mid}) = 61.27\,kip$

$R_{n.weld} = 110.1\,kip$

$w_{des} = \frac{1}{4}\,in$

$s = 3.5\,in$

$P_b = 50 \cdot \%$

$Capacity = 61.27\,kip$ $Capacity = 272.53 \cdot kN$ $LimitState = (\text{"R.Bolts"})$

S40P050 Expected Capacity Summary

$R_{n.PlShearYield} = 112.77\,kip$

$R_{n.PlFlexureYield} = 187.95\,kip$

$R_{n.PlShearFlexureYield} = 96.7\,kip$

$R_{n.PlShearRupt} = 82.64\,kip$

$R_{n.PlBuckling} = 125.3\,kip$

$R_{n.PlBlockShear} = 97.89\,kip$

$R_{n.BoltShear} = 143.14\,kip$

$R_{n.BoltTearout.PlBot} = 29.03\,kip$

$R_{n.BoltTearout.PlMid} = 116.1\,kip$

$R_{n.BoltTearout} := R_{n.BoltTearout.PlBot} + R_{n.BoltTearout.PlMid} = 145.13\,kip$

$R_{n.BoltBearing.PlBot} = 27.32\,kip$

$R_{n.BoltBearing.PlMid} = 54.64\,kip$

$R_{n.BoltBearing} := R_{n.BoltBearing.PlBot} + R_{n.BoltBearing.PlMid} = 81.96\,kip$

$R_{n.BoltPlFlexure.Bot} = 6.63\,kip$

$R_{n.BoltPlFlexure.Mid} = 79.57\,kip$

$R_{n.Bolt.PlFlexure} := R_{n.BoltPlFlexure.Bot} + R_{n.BoltPlFlexure.Mid} = 86.2\,kip$

$$R_{n.Bolt.Bot} := \begin{pmatrix} R_{n.BoltTearout.PlBot} \\ R_{n.BoltBearing.PlBot} \\ R_{n.BoltPlFlexure.Bot} \end{pmatrix} = \begin{pmatrix} 29.03 \\ 27.32 \\ 6.63 \end{pmatrix} kip$$

$$R_{n.Bolt.Mid} := \begin{pmatrix} R_{n.BoltTearout.PlMid} \\ R_{n.BoltBearing.PlMid} \\ R_{n.BoltPlFlexure.Mid} \end{pmatrix} = \begin{pmatrix} 116.1 \\ 54.64 \\ 79.57 \end{pmatrix} kip$$

$R_{n.Bolts} := min\left(R_{n.Bolt.Bot}\right) + min\left(R_{n.Bolt.Mid}\right) = 61.27\,kip$

$R_{n.weld} = 127.5\,kip$

$w_{des} = \frac{1}{4}\,in$

$s = 4\,in$

$P_b = 50 \cdot \%$

$Capacity = 61.27\,kip$ $Capacity = 272.53 \cdot kN$ $LimitState = (\text{"R.Bolts"})$

S45P050 Expected Capacity Summary

$R_{n.PlShearYield} = 122.17\,kip$

$R_{n.PlFlexureYield} = 220.58\,kip$

$R_{n.PlShearFlexureYield} = 106.87\,kip$

$R_{n.PlShearRupt} = 93.57\,kip$

$R_{n.PlBuckling} = 147.05\,kip$

$R_{n.PlBlockShear} = 108.82\,kip$

$R_{n.BoltShear} = 143.14\,kip$

$R_{n.BoltTearout.PlBot} = 29.03\,kip$

$R_{n.BoltTearout.PlMid} = 134.32\,kip$

$R_{n.BoltTearout} := R_{n.BoltTearout.PlBot} + R_{n.BoltTearout.PlMid} = 163.34\,kip$

$R_{n.BoltBearing.PlBot} = 27.32\,kip$

$R_{n.BoltBearing.PlMid} = 54.64\,kip$

$R_{n.BoltBearing} := R_{n.BoltBearing.PlBot} + R_{n.BoltBearing.PlMid} = 81.96\,kip$

$R_{n.BoltPlFlexure.Bot} = 6.63\,kip$

$R_{n.BoltPlFlexure.Mid} = 106.49\,kip$

$R_{n.Bolt.PlFlexure} := R_{n.BoltPlFlexure.Bot} + R_{n.BoltPlFlexure.Mid} = 113.12\,kip$

$$R_{n.Bolt.Bot} := \begin{pmatrix} R_{n.BoltTearout.PlBot} \\ R_{n.BoltBearing.PlBot} \\ R_{n.BoltPlFlexure.Bot} \end{pmatrix} = \begin{pmatrix} 29.03 \\ 27.32 \\ 6.63 \end{pmatrix} kip$$

$$R_{n.Bolt.Mid} := \begin{pmatrix} R_{n.BoltTearout.PlMid} \\ R_{n.BoltBearing.PlMid} \\ R_{n.BoltPlFlexure.Mid} \end{pmatrix} = \begin{pmatrix} 134.32 \\ 54.64 \\ 106.49 \end{pmatrix} kip$$

$R_{n.Bolts} := min\left(R_{n.Bolt.Bot}\right) + min\left(R_{n.Bolt.Mid}\right) = 61.27\,kip$

$R_{n.weld} = 145.28\,kip$

$w_{des} = \frac{1}{4}\,in$

$s = 4.5\,in$

$P_b = 50 \cdot \%$

$Capacity = 61.27\,kip$ $Capacity = 272.53 \cdot kN$ $LimitState = (\text{"R.Bolts"})$

S30P025 Expected Capacity Summary

$R_{n.PlShearYield} = 93.98\,kip$

$R_{n.PlFlexureYield} = 156.63\,kip$

$R_{n.PlShearFlexureYield} = 80.58\,kip$

$R_{n.PlShearRupt} = 60.78\,kip$

$R_{n.PlBuckling} = 104.42\,kip$

$R_{n.PlBlockShear} = 76.04\,kip$

$R_{n.BoltShear} = 143.14\,kip$

$R_{n.BoltTearout.PlBot} = 29.03\,kip$

$R_{n.BoltTearout.PlMid} = 79.68\,kip$

$R_{n.BoltTearout} := R_{n.BoltTearout.PlBot} + R_{n.BoltTearout.PlMid} = 108.71\,kip$

$R_{n.BoltBearing.PlBot} = 27.32\,kip$

$R_{n.BoltBearing.PlMid} = 54.64\,kip$

$R_{n.BoltBearing} := R_{n.BoltBearing.PlBot} + R_{n.BoltBearing.PlMid} = 81.96\,kip$

$R_{n.BoltPlFlexure.Bot} = 13.26\,kip$

$R_{n.BoltPlFlexure.Mid} = 74.95\,kip$

$R_{n.Bolt.PlFlexure} := R_{n.BoltPlFlexure.Bot} + R_{n.BoltPlFlexure.Mid} = 88.21\,kip$

$$R_{n.Bolt.Bot} := \begin{pmatrix} R_{n.BoltTearout.PlBot} \\ R_{n.BoltBearing.PlBot} \\ R_{n.BoltPlFlexure.Bot} \end{pmatrix} = \begin{pmatrix} 29.03 \\ 27.32 \\ 13.26 \end{pmatrix} kip$$

$$R_{n.Bolt.Mid} := \begin{pmatrix} R_{n.BoltTearout.PlMid} \\ R_{n.BoltBearing.PlMid} \\ R_{n.BoltPlFlexure.Mid} \end{pmatrix} = \begin{pmatrix} 79.68 \\ 54.64 \\ 74.95 \end{pmatrix} kip$$

$R_{n.Bolts} := min\left(R_{n.Bolt.Bot}\right) + min\left(R_{n.Bolt.Mid}\right) = 67.9\,kip$

$R_{n.weld} = 104.78\,kip$

$w_{des} = \frac{1}{4}\,in$

$s = 3\,in$

$P_b = 25 \cdot \%$

$Capacity = 60.78\,kip$ $Capacity = 270.38 \cdot kN$ $LimitState = (\text{"Cap.PLShearRupt"})$

S35P025 Expected Capacity Summary

$R_{n.PlShearYield} = 103.37\,kip$

$R_{n.PlFlexureYield} = 189.52\,kip$

$R_{n.PlShearFlexureYield} = 90.75\,kip$

$R_{n.PlShearRupt} = 71.71\,kip$

$R_{n.PlBuckling} = 126.34\,kip$

$R_{n.PlBlockShear} = 86.96\,kip$

$R_{n.BoltShear} = 143.14\,kip$

$R_{n.BoltTearout.PlBot} = 29.03\,kip$

$R_{n.BoltTearout.PlMid} = 97.89\,kip$

$R_{n.BoltTearout} := R_{n.BoltTearout.PlBot} + R_{n.BoltTearout.PlMid} = 126.92\,kip$

$R_{n.BoltBearing.PlBot} = 27.32\,kip$

$R_{n.BoltBearing.PlMid} = 54.64\,kip$

$R_{n.BoltBearing} := R_{n.BoltBearing.PlBot} + R_{n.BoltBearing.PlMid} = 81.96\,kip$

$R_{n.BoltPlFlexure.Bot} = 13.26\,kip$

$R_{n.BoltPlFlexure.Mid} = 113.12\,kip$

$R_{n.Bolt.PlFlexure} := R_{n.BoltPlFlexure.Bot} + R_{n.BoltPlFlexure.Mid} = 126.39\,kip$

$$R_{n.Bolt.Bot} := \begin{pmatrix} R_{n.BoltTearout.PlBot} \\ R_{n.BoltBearing.PlBot} \\ R_{n.BoltPlFlexure.Bot} \end{pmatrix} = \begin{pmatrix} 29.03 \\ 27.32 \\ 13.26 \end{pmatrix} kip$$

$$R_{n.Bolt.Mid} := \begin{pmatrix} R_{n.BoltTearout.PlMid} \\ R_{n.BoltBearing.PlMid} \\ R_{n.BoltPlFlexure.Mid} \end{pmatrix} = \begin{pmatrix} 97.89 \\ 54.64 \\ 113.12 \end{pmatrix} kip$$

$R_{n.Bolts} := min\left(R_{n.Bolt.Bot}\right) + min\left(R_{n.Bolt.Mid}\right) = 67.9\,kip$

$R_{n.weld} = 122.56\,kip$

$w_{des} = \frac{1}{4}\,in$

$s = 3.5\,in$

$P_b = 25 \cdot \%$

$Capacity = 67.9\,kip$ $Capacity = 302.03 \cdot kN$ $LimitState = (\text{"R.Bolts"})$

S40P025 Expected Capacity Summary

$R_{n.PlShearYield} = 112.77\,kip$

$R_{n.PlFlexureYield} = 225.54\,kip$

$R_{n.PlShearFlexureYield} = 100.86\,kip$

$R_{n.PlShearRupt} = 82.64\,kip$

$R_{n.PlBuckling} = 150.36\,kip$

$R_{n.PlBlockShear} = 97.89\,kip$

$R_{n.BoltShear} = 143.14\,kip$

$R_{n.BoltTearout.PlBot} = 29.03\,kip$

$R_{n.BoltTearout.PlMid} = 116.1\,kip$

$R_{n.BoltTearout} := R_{n.BoltTearout.PlBot} + R_{n.BoltTearout.PlMid} = 145.13\,kip$

$R_{n.BoltBearing.PlBot} = 27.32\,kip$

$R_{n.BoltBearing.PlMid} = 54.64\,kip$

$R_{n.BoltBearing} := R_{n.BoltBearing.PlBot} + R_{n.BoltBearing.PlMid} = 81.96\,kip$

$R_{n.BoltPlFlexure.Bot} = 13.26\,kip$

$R_{n.BoltPlFlexure.Mid} = 159.13\,kip$

$R_{n.Bolt.PlFlexure} := R_{n.BoltPlFlexure.Bot} + R_{n.BoltPlFlexure.Mid} = 172.39\,kip$

$$R_{n.Bolt.Bot} := \begin{pmatrix} R_{n.BoltTearout.PlBot} \\ R_{n.BoltBearing.PlBot} \\ R_{n.BoltPlFlexure.Bot} \end{pmatrix} = \begin{pmatrix} 29.03 \\ 27.32 \\ 13.26 \end{pmatrix} kip$$

$$R_{n.Bolt.Mid} := \begin{pmatrix} R_{n.BoltTearout.PlMid} \\ R_{n.BoltBearing.PlMid} \\ R_{n.BoltPlFlexure.Mid} \end{pmatrix} = \begin{pmatrix} 116.1 \\ 54.64 \\ 159.13 \end{pmatrix} kip$$

$R_{n.Bolts} := min\left(R_{n.Bolt.Bot}\right) + min\left(R_{n.Bolt.Mid}\right) = 67.9\,kip$

$R_{n.weld} = 140.62\,kip$

$w_{des} = \frac{1}{4}\,in$

$s = 4\,in$

$P_b = 25 \cdot \%$

$Capacity = 67.9\,kip$ $Capacity = 302.03 \cdot kN$ $LimitState = (\text{"R.Bolts"})$

S45P025 Expected Capacity Summary

$R_{n.PlShearYield} = 122.17\,kip$

$R_{n.PlFlexureYield} = 264.7\,kip$

$R_{n.PlShearFlexureYield} = 110.92\,kip$

$R_{n.PlShearRupt} = 93.57\,kip$

$R_{n.PlBuckling} = 176.46\,kip$

$R_{n.PlBlockShear} = 108.82\,kip$

$R_{n.BoltShear} = 143.14\,kip$

$R_{n.BoltTearout.PlBot} = 29.03\,kip$

$R_{n.BoltTearout.PlMid} = 134.32\,kip$

$R_{n.BoltTearout} := R_{n.BoltTearout.PlBot} + R_{n.BoltTearout.PlMid} = 163.34\,kip$

$R_{n.BoltBearing.PlBot} = 27.32\,kip$

$R_{n.BoltBearing.PlMid} = 54.64\,kip$

$R_{n.BoltBearing} := R_{n.BoltBearing.PlBot} + R_{n.BoltBearing.PlMid} = 81.96\,kip$

$R_{n.BoltPlFlexure.Bot} = 13.26\,kip$

$R_{n.BoltPlFlexure.Mid} = 212.97\,kip$

$R_{n.Bolt.PlFlexure} := R_{n.BoltPlFlexure.Bot} + R_{n.BoltPlFlexure.Mid} = 226.23\,kip$

$$R_{n.Bolt.Bot} := \begin{pmatrix} R_{n.BoltTearout.PlBot} \\ R_{n.BoltBearing.PlBot} \\ R_{n.BoltPlFlexure.Bot} \end{pmatrix} = \begin{pmatrix} 29.03 \\ 27.32 \\ 13.26 \end{pmatrix} kip$$

$$R_{n.Bolt.Mid} := \begin{pmatrix} R_{n.BoltTearout.PlMid} \\ R_{n.BoltBearing.PlMid} \\ R_{n.BoltPlFlexure.Mid} \end{pmatrix} = \begin{pmatrix} 134.32 \\ 54.64 \\ 212.97 \end{pmatrix} kip$$

$R_{n.Bolts} := min\left(R_{n.Bolt.Bot}\right) + min\left(R_{n.Bolt.Mid}\right) = 67.9\,kip$

$R_{n.weld} = 158.83\,kip$

$w_{des} = \frac{1}{4}\,in$

$s = 4.5\,in$

$P_b = 25 \cdot \%$

$Capacity = 67.9\,kip$ $Capacity = 302.03 \cdot kN$ $LimitState = (\text{"R.Bolts"})$

S30P000 Expected Capacity Summary

$R_{n.PlShearYield} = 93.98\,kip$

$R_{n.PlFlexureYield} = 195.78\,kip$

$R_{n.PlShearFlexureYield} = 84.72\,kip$

$R_{n.PlShearRupt} = 60.78\,kip$

$R_{n.PlBuckling} = 130.52\,kip$

$R_{n.PlBlockShear} = 76.04\,kip$

$R_{n.BoltShear} = 143.14\,kip$

$R_{n.BoltTearout.PlBot} = 29.03\,kip$

$R_{n.BoltTearout.PlMid} = 79.68\,kip$

$R_{n.BoltTearout} := R_{n.BoltTearout.PlBot} + R_{n.BoltTearout.PlMid} = 108.71\,kip$

$R_{n.BoltBearing.PlBot} = 27.32\,kip$

$R_{n.BoltBearing.PlMid} = 54.64\,kip$

$R_{n.BoltBearing} := R_{n.BoltBearing.PlBot} + R_{n.BoltBearing.PlMid} = 81.96\,kip$

$R_{n.BoltPlFlexure.Bot} = 6630.56\,kip$

$R_{n.BoltPlFlexure.Mid} = 37473.75\,kip$

$R_{n.Bolt.PlFlexure} := R_{n.BoltPlFlexure.Bot} + R_{n.BoltPlFlexure.Mid} = 44104.32\,kip$

$$R_{n.Bolt.Bot} := \begin{pmatrix} R_{n.BoltTearout.PlBot} \\ R_{n.BoltBearing.PlBot} \\ R_{n.BoltPlFlexure.Bot} \end{pmatrix} = \begin{pmatrix} 29.03 \\ 27.32 \\ 6630.56 \end{pmatrix} kip$$

$$R_{n.Bolt.Mid} := \begin{pmatrix} R_{n.BoltTearout.PlMid} \\ R_{n.BoltBearing.PlMid} \\ R_{n.BoltPlFlexure.Mid} \end{pmatrix} = \begin{pmatrix} 79.68 \\ 54.64 \\ 37473.75 \end{pmatrix} kip$$

$R_{n.Bolts} := min\left(R_{n.Bolt.Bot}\right) + min\left(R_{n.Bolt.Mid}\right) = 81.96\,kip$

$R_{n.weld} = 117.96\,kip$

$w_{des} = \frac{1}{4}\,in$

$s = 3\,in$

$P_b = 0 \cdot \%$

$Capacity = 60.78\,kip$ $Capacity = 270.38 \cdot kN$ $LimitState = (\text{"Cap.PLShearRupt"})$

S35P000 Expected Capacity Summary

$R_{n.PlShearYield} = 103.37\,kip$

$R_{n.PlFlexureYield} = 236.9\,kip$

$R_{n.PlShearFlexureYield} = 94.74\,kip$

$R_{n.PlShearRupt} = 71.71\,kip$

$R_{n.PlBuckling} = 157.93\,kip$

$R_{n.PlBlockShear} = 86.96\,kip$

$R_{n.BoltShear} = 143.14\,kip$

$R_{n.BoltTearout.PlBot} = 29.03\,kip$

$R_{n.BoltTearout.PlMid} = 97.89\,kip$

$R_{n.BoltTearout} := R_{n.BoltTearout.PlBot} + R_{n.BoltTearout.PlMid} = 126.92\,kip$

$R_{n.BoltBearing.PlBot} = 27.32\,kip$

$R_{n.BoltBearing.PlMid} = 54.64\,kip$

$R_{n.BoltBearing} := R_{n.BoltBearing.PlBot} + R_{n.BoltBearing.PlMid} = 81.96\,kip$

$R_{n.BoltPlFlexure.Bot} = 6630.56\,kip$

$R_{n.BoltPlFlexure.Mid} = 56562.43\,kip$

$R_{n.Bolt.PlFlexure} := R_{n.BoltPlFlexure.Bot} + R_{n.BoltPlFlexure.Mid} = 63192.99\,kip$

$$R_{n.Bolt.Bot} := \begin{pmatrix} R_{n.BoltTearout.PlBot} \\ R_{n.BoltBearing.PlBot} \\ R_{n.BoltPlFlexure.Bot} \end{pmatrix} = \begin{pmatrix} 29.03 \\ 27.32 \\ 6630.56 \end{pmatrix} kip$$

$$R_{n.Bolt.Mid} := \begin{pmatrix} R_{n.BoltTearout.PlMid} \\ R_{n.BoltBearing.PlMid} \\ R_{n.BoltPlFlexure.Mid} \end{pmatrix} = \begin{pmatrix} 97.89 \\ 54.64 \\ 56562.43 \end{pmatrix} kip$$

$R_{n.Bolts} := min\left(R_{n.Bolt.Bot}\right) + min\left(R_{n.Bolt.Mid}\right) = 81.96\,kip$

$R_{n.weld} = 136.19\,kip$

$w_{des} = \frac{1}{4}\,in$

$s = 3.5\,in$ $\quad Capacity = 71.71\,kip$ $\quad Capacity = 318.99\,kN$ $\quad LimitState = (\text{"Cap.PLShearRupt"})$

$P_b = 0\cdot\%$

S40P000 Expected Capacity Summary

$R_{n.PlShearYield} = 112.77\,kip$

$R_{n.PlFlexureYield} = 281.93\,kip$

$R_{n.PlShearFlexureYield} = 104.7\,kip$

$R_{n.PlShearRupt} = 82.64\,kip$

$R_{n.PlBuckling} = 187.95\,kip$

$R_{n.PlBlockShear} = 97.89\,kip$

$R_{n.BoltShear} = 143.14\,kip$

$R_{n.BoltTearout.PlBot} = 29.03\,kip$

$R_{n.BoltTearout.PlMid} = 116.1\,kip$

$R_{n.BoltTearout} := R_{n.BoltTearout.PlBot} + R_{n.BoltTearout.PlMid} = 145.13\,kip$

$R_{n.BoltBearing.PlBot} = 27.32\,kip$

$R_{n.BoltBearing.PlMid} = 54.64\,kip$

$R_{n.BoltBearing} := R_{n.BoltBearing.PlBot} + R_{n.BoltBearing.PlMid} = 81.96\,kip$

$R_{n.BoltPlFlexure.Bot} = 6630.56\,kip$

$R_{n.BoltPlFlexure.Mid} = 79566.72\,kip$

$R_{n.Bolt.PlFlexure} := R_{n.BoltPlFlexure.Bot} + R_{n.BoltPlFlexure.Mid} = 86197.28\,kip$

$$R_{n.Bolt.Bot} := \begin{pmatrix} R_{n.BoltTearout.PlBot} \\ R_{n.BoltBearing.PlBot} \\ R_{n.BoltPlFlexure.Bot} \end{pmatrix} = \begin{pmatrix} 29.03 \\ 27.32 \\ 6630.56 \end{pmatrix} kip$$

$$R_{n.Bolt.Mid} := \begin{pmatrix} R_{n.BoltTearout.PlMid} \\ R_{n.BoltBearing.PlMid} \\ R_{n.BoltPlFlexure.Mid} \end{pmatrix} = \begin{pmatrix} 116.1 \\ 54.64 \\ 79566.72 \end{pmatrix} kip$$

$R_{n.Bolts} := min\left(R_{n.Bolt.Bot}\right) + min\left(R_{n.Bolt.Mid}\right) = 81.96\,kip$

$R_{n.weld} = 154.4\,kip$

$w_{des} = \frac{1}{4}\,in$

$s = 4\,in$

$P_b = 0 \cdot \%$

$Capacity = 81.96\,kip$ $\quad Capacity = 364.56 \cdot kN$ $\quad LimitState = \begin{pmatrix} \text{"R.BoltBearing"} \\ \text{"R.Bolts"} \end{pmatrix}$

S45P000 Expected Capacity Summary

$R_{n.PlShearYield} = 122.17\,kip$

$R_{n.PlFlexureYield} = 330.87\,kip$

$R_{n.PlShearFlexureYield} = 114.6\,kip$

$R_{n.PlShearRupt} = 93.57\,kip$

$R_{n.PlBuckling} = 220.58\,kip$

$R_{n.PlBlockShear} = 108.82\,kip$

$R_{n.BoltShear} = 143.14\,kip$

$R_{n.BoltTearout.PlBot} = 29.03\,kip$

$R_{n.BoltTearout.PlMid} = 134.32\,kip$

$R_{n.BoltTearout} := R_{n.BoltTearout.PlBot} + R_{n.BoltTearout.PlMid} = 163.34\,kip$

$R_{n.BoltBearing.PlBot} = 27.32\,kip$

$R_{n.BoltBearing.PlMid} = 54.64\,kip$

$R_{n.BoltBearing} := R_{n.BoltBearing.PlBot} + R_{n.BoltBearing.PlMid} = 81.96\,kip$

$R_{n.BoltPlFlexure.Bot} = 6630.56\,kip$

$R_{n.BoltPlFlexure.Mid} = 106486.65\,kip$

$R_{n.Bolt.PlFlexure} := R_{n.BoltPlFlexure.Bot} + R_{n.BoltPlFlexure.Mid} = 113117.21\,kip$

$$R_{n.Bolt.Bot} := \begin{pmatrix} R_{n.BoltTearout.PlBot} \\ R_{n.BoltBearing.PlBot} \\ R_{n.BoltPlFlexure.Bot} \end{pmatrix} = \begin{pmatrix} 29.03 \\ 27.32 \\ 6630.56 \end{pmatrix} kip$$

$$R_{n.Bolt.Mid} := \begin{pmatrix} R_{n.BoltTearout.PlMid} \\ R_{n.BoltBearing.PlMid} \\ R_{n.BoltPlFlexure.Mid} \end{pmatrix} = \begin{pmatrix} 134.32 \\ 54.64 \\ 106486.65 \end{pmatrix} kip$$

$R_{n.Bolts} := min\left(R_{n.Bolt.Bot}\right) + min\left(R_{n.Bolt.Mid}\right) = 81.96\,kip$

$R_{n.weld} = 172.48\,kip$

$w_{des} = \frac{1}{4}\,in$

$s = 4.5\,in$

$P_b = 0 \cdot \%$

$Capacity = 81.96\,kip$ $Capacity = 364.56 \cdot kN$ $LimitState = \begin{pmatrix} \text{"R.BoltBearing"} \\ \text{"R.Bolts"} \end{pmatrix}$

Yoke Design

Plate P82 Checks

Plate Thickness	$t := .5in$	
Plate Width	$w := 10in$	
Plate Length	$l := 10.5in$	Portion of plate with notch is excluded
Plate Yield Stress	$F_y := 50ksi$	
Plate Ultimate Stress	$F_u := 65ksi$	
Number of Bolt Rows	$n_{Rows} := 1$	Parallel to Load
Number of Bolt Columns	$n_{Cols} := 2$	Perpendicular to Load
Number of Bolts	$N := n_{Rows} \cdot n_{Cols} = 2$	
Bolt Col Spacing	$s_h := 3in$	Horizontal Spacing
Bolt Row Spacing	$s_v := 0in$	Vertical Spacing
Bolt Strength	$F_{nv} := 54ksi$	A325 Bolt
Bolt Diameter	$d_b := 1in$	
Hole Diameter	$d_{hole} := d_b + \frac{1}{8}in = 1.13\,in$	
Horizontal Edge Distance	$l_h := 2in$	
Clear Horizontal Edge Distance	$l_{eh} := l_h - \frac{\left(d_b + \frac{1}{8}in\right)}{2} = 1.438\,in$	
Vertical Edge Distance	$l_v := \frac{w - s_v}{2} = 5\,in$	
Clear Vertical Edge Distance	$l_{ev} := l_v - \frac{\left(d_b + \frac{1}{8}in\right)}{2} = 4.438\,in$	
Applied Load	$P := 120kip$	Maximum actuator capacity

Tensile Yielding

Strength Reduction Factor $\phi := 0.9$

Gross Area $A_g := t \cdot w = 5\ in^2$

Tensile Yielding Capacity $Cap_{TenYield} := \phi \cdot F_y \cdot A_g = 225 \cdot kip$ Eqn. J4-1

Check $Check_{TenYield} := \begin{cases} \text{"OK"} & \text{if } Cap_{TenYield} \geq P \\ \text{"No Good"} & \text{otherwise} \end{cases} = \text{"OK"}$

Tensile Rupture

Strength Reduction Factor $\phi := 0.75$

Net Area $A_n := t \cdot \left(w - n_{Rows} \cdot d_{hole}\right) = 4.44\ in^2$

Shear Lag Factor $U := 1.0$ AISC Table D3.1, P. 16.1-30

Effective Area $A_e := U \cdot A_n = 4.44\ in^2$

Tensile Rupture Capacity $Cap_{TenRupt} := \phi \cdot F_u \cdot A_e = 216.33 \cdot kip$ Eqn. J4-2

Check $Check_{TenRupt} := \begin{cases} \text{"OK"} & \text{if } Cap_{TenRupt} \geq P \\ \text{"No Good"} & \text{otherwise} \end{cases} = \text{"OK"}$

Bearing at Bolt Hole

Strength Reduction Factor $\phi := 0.75$

Number of Shear Planes $N_{sp} := 2$

Capacity of Bolt Bearing $Cap_{BoltBearing} := N_{sp} \cdot N \cdot \phi \cdot 2.4 \cdot d_b \cdot t \cdot F_u = 234 \cdot kip$ Eqn. J3-6a

Check $Check_{BoltBearing} := \begin{cases} \text{"OK"} & \text{if } Cap_{BoltBearing} \geq P \\ \text{"No Good"} & \text{otherwise} \end{cases} = \text{"OK"}$

Tearout at Bolt Hole

Strength Reduction Factor $\phi := 0.75$

Number of Shear Planes $N_{sp} := 2$

Capacity of Bolt Tearout $Cap_{BoltTearout} := N_{sp} \cdot N \cdot \phi \cdot 1.2 \cdot l_{eh} \cdot t \cdot F_u = 168.19 \cdot kip$ Eqn. J3-6c

Check $Check_{BoltBearing} := \begin{cases} \text{"OK"} & \text{if } Cap_{BoltTearout} \geq P \\ \text{"No Good"} & \text{otherwise} \end{cases} = \text{"OK"}$

Block Shear Check

Shear Lag Factor $U_{bs} := 1.0$

Strength Reduction Factor $\phi := 0.75$

Failure Path: L-Shape

Shear Length $l_{Shear} := l_h + s_h = 5\ in$

Number of Shear Planes $n_{SP} := 1$

Number of Bolt Holes in Shear Plane $n_{BoltSP} := 1.5$

Net Shear Area $A_{nv} := t \cdot n_{SP} \cdot \left[l_{Shear} - n_{BoltSP} \cdot \left(d_{hole} + \frac{1}{16} in \right) \right] = 1.61\ in^2$

Gross Shear Area $A_{gv} := t \cdot n_{SP} \cdot l_{Shear} = 2.5\ in^2$

Tension Length $l_{Tension} := s_v + l_v = 5\ in$

Number of Bolt Holes in Tension Plane $n_{BoltTen} := .5$

Net Tension Area $A_{nt} := t \cdot \left[l_{Tension} - n_{BoltTen} \cdot \left(d_{hole} + \frac{1}{16} in \right) \right] = 2.2\ in^2$

$Cap_{BS1} := 0.60 \cdot F_u \cdot A_{nv} + U_{bs} \cdot F_u \cdot A_{nt} = 205.97 \cdot kip$ Eqn. J4-5

$Cap_{BS2} := 0.60 \cdot F_y \cdot A_{gv} + U_{bs} \cdot F_u \cdot A_{nt} = 218.2 \cdot kip$ Eqn. J4-5

Block Shear Capacity $Cap_{BS} := min\left(Cap_{BS1}, Cap_{BS2} \right) = 205.97 \cdot kip$

Check $Check_{BlockShear} := \begin{cases} \text{"OK"} & if\ Cap_{BS} \geq P \\ \text{"No Good"} & otherwise \end{cases} = \text{"OK"}$

Weld at Connection to P64

Strength Reduction Factor $\phi := 0.75$

Available Weld Length $l_{Weld} := 3in$

Number of Weld Lines $n_{Lines} := 8$

Weld Size $s_{Weld} := \frac{5}{16}in$

Effective Weld Length $l_{WeldEff} := n_{Lines} \cdot \left(l_{Weld} - 2 \cdot s_{Weld}\right) = 19\,in$

Electrode Grade $F_{EXX} := 70ksi$

Available Weld Strength $Cap_{Weld} := \phi \cdot 0.60 \cdot F_{EXX} \cdot \left(\frac{\sqrt{2}}{2}\right) \cdot s_{Weld} \cdot l_{WeldEff} = 132.25 \cdot kip$ Eqn. 8-1

Check $Check_{Weld} := \begin{cases} \text{"OK"} & \text{if } Cap_{Weld} \geq P \\ \text{"No Good"} & \text{otherwise} \end{cases} = \text{"OK"}$

Plate Reduced Section Yielding

Strength Reduction Factor $\phi := 0.90$

Length at Reduced Section $l_{Tension} := 6in$

Tension Area $A_{Tension} := t \cdot l_{Tension} = 3\,in^2$

Plate Yielding Capacity $Cap_{PlateYield} := \phi \cdot F_y \cdot A_{Tension} = 135 \cdot kip$

Check $Check_{PlateYield} := \begin{cases} \text{"OK"} & \text{if } Cap_{PlateYield} \geq P \\ \text{"No Good"} & \text{otherwise} \end{cases} = \text{"OK"}$

Sandwich Plate Design

Input

Plate Dimensions

Plate Length	$w := 24in$	
Plate Width	$b := 3.25in$	
Plate Thickness	$t := 1in$	
Gross Area	$A_g := b \cdot t = 3.25\,in^2$	
Horizontal Edge Distance	$L_h := 2in$	
Vertical Edge Distance	$L_v := 1.625in$	
Test Side Hole Spacing	$S_T := 3in$	
Test Side Bolt Diameter	$d_{bT} := \frac{3}{4}in$	
Test Side Number of Bolts	$N_T := 3$	
Test Side Hole Diameter	$d_{hT} := d_{bT} + \frac{1}{16}in = 0.81\,in$	
Yoke Side Hole Spacing	$S_Y := 3in$	
Yoke Side Bolt Diameter	$d_{bY} := 1in$	
Yoke Side Number of Bolts	$N_Y := 2$	
Yoke Side Hole Diameter	$d_{hY} := d_{bY} + \frac{1}{8}in = 1.13\,in$	

Material Properties

Yield Stress	$F_y := 50ksi$	
Ultimate Stress	$F_u := 65ksi$	
Bolt Strength	$F_{nv} := 54ksi$	A325 Bolt

Bolt Shear

Area of Test Side Bolt

$$A_{bT} := \frac{\pi \cdot d_{bT}^{2}}{4} = 0.44\ in^2$$

Area of Yoke Side Bolt

$$A_{bY} := \frac{\pi \cdot d_{bY}^{2}}{4} = 0.79\ in^2$$

Number of Shear Planes

$$N_{sp} := 2$$

Bolts are in double shear

Strength Reduction Factor

$$\phi := 0.75$$

Test Side Bolt Strength

$$Cap_{BoltShear.T} := \left(N_T \cdot N_{sp}\right) \cdot \phi \cdot F_{nv} \cdot A_{bT} = 107.35\ kip$$

Eqn J3-1

Yoke Side Bolt Strength

$$Cap_{BoltShear.Y} := \left(N_Y \cdot N_{sp}\right) \cdot \phi \cdot F_{nv} \cdot A_{bY} = 127.23\ kip$$

Eqn J3-1

Bearing and Tearout

Number of Shear Planes

$$N_{sp} := 2$$

Strength Reduction Factor

$$\phi := 0.75$$

Test Side Bearing

$$Cap_{BoltBearing.T} := N_{sp} \cdot N_T \cdot \phi \cdot 2.4 \cdot d_{bT} \cdot t \cdot F_u = 526.5\ kip$$

Eqn J3-6a

Test Side Clear Distance

$$L_c := L_h - 0.5 \cdot d_{hT} = 1.59\ in$$

Test Side Tearout

$$Cap_{BoltTearout.T} := N_{sp} \cdot N_T \cdot \phi \cdot 1.2 \cdot L_c \cdot t \cdot F_u = 559.41\ kip$$

Eqn J3-6c

Yoke Side Bearing

$$Cap_{BoltBearing.Y} := N_{sp} \cdot N_Y \cdot \phi \cdot 2.4 \cdot d_{bY} \cdot t \cdot F_u = 468\ kip$$

Eqn J3-6a

Yoke Side Clear Distance

$$L_c := L_h - 0.5 \cdot d_{hY} = 1.44\ in$$

Yoke Side Tearout

$$Cap_{BoltTearout.Y} := N_{sp} \cdot N_Y \cdot \phi \cdot 1.2 \cdot L_c \cdot t \cdot F_u = 336.37\ kip$$

Eqn J3-6c

Plate Tensile Yielding

Strength Reduction Factor $\phi := 0.90$

Tensile Yielding Capacity $Cap_{TensileYield} := \phi \cdot F_y \cdot A_g = 146.25\ kip$ Eqn J4-1

Plate Net Section Tensile Rupture

Test Side Net Area $A_{netT} := \left(b - d_{hT}\right)t = 2.44\ in^2$

Yoke Side Net Area $A_{netY} := \left(b - d_{hY}\right)t = 2.12\ in^2$

Strength Reduction Factor $\phi := 0.90$

Test Side Tensile Rupture Capacity $Cap_{TensileRupt.T} := \phi \cdot F_u \cdot A_{netT} = 142.59\ kip$ Eqn J4-2

Yoke Side Tensile Rupture Capacity $Cap_{TensileRupt.Y} := \phi \cdot F_u \cdot A_{netY} = 124.31\ kip$ Eqn J4-2

Block Shear Checks

Test Side Block Shear

Gross Shear Length $L_{gv} := \left(N_T - 1\right) \cdot S_T + L_h = 8\ in$

Net Shear Length $L_{nv} := L_{gv} - \left(N_T - .5\right) \cdot d_{hT} = 5.97\ in$

Gross Tension Length $L_{gt} := L_v = 1.63\ in$

Net Tension Length $L_{nt} := L_{gt} - \frac{d_{hT}}{2} = 1.21875\ in$

Gross Shear Area $A_{gv} := L_{gv} \cdot t = 8\ in^2$

Net Shear Area $A_{nv} := L_{nv} \cdot t = 5.97\ in^2$

Gross Tension Area $A_{gt} := L_{gt} \cdot t = 1.63\ in^2$

Net Tension Area $A_{nt} := L_{nt} \cdot t = 1.22 \cdot in^2$

Test Side Block Shear Capacity $Cap_{BlockShear.T} := F_u \cdot A_{nt} + min\left(0.6 \cdot F_u \cdot A_{nv}, 0.6 \cdot F_y \cdot A_{gv}\right)$ Eqn J4-5

$Cap_{BlockShear.T} = 312\ kip$

Block Shear Checks

Yoke Side Block Shear

Gross Shear Length $L_{gv} := \left(N_Y - 1\right) \cdot S_Y + L_h = 5\ in$

Net Shear Length $L_{nv} := L_{gv} - \left(N_Y - .5\right) \cdot d_{hY} = 3.31\ in$

Gross Tension Length $L_{gt} := L_v = 1.63\ in$

Net Tension Length $L_{nt} := L_{gt} - \frac{d_{hY}}{2} = 1.0625\ in$

Gross Shear Area $A_{gv} := L_{gv} \cdot t = 5\ in^2$

Net Shear Area $A_{nv} := L_{nv} \cdot t = 3.31\ in^2$

Gross Tension Area $A_{gt} := L_{gt} \cdot t = 1.63\ in^2$

Net Tension Area $A_{nt} := L_{nt} \cdot t = 1.06 \cdot in^2$

Test Side Block Shear Capacity $Cap_{BlockShear.Y} := F_u \cdot A_{nt} + min\left(0.6 \cdot F_u \cdot A_{nv}, 0.6 \cdot F_y \cdot A_{gv}\right)$ Eqn J4-5

Test Side	Yoke Side
$Cap_{BoltShear.T} = 107.35\ kip$	$Cap_{BoltShear.Y} = 127.23\ kip$
$Cap_{BoltBearing.T} = 526.5\ kip$	$Cap_{BoltBearing.Y} = 468\ kip$
$Cap_{BoltTearout.T} = 559.41\ kip$	$Cap_{BoltTearout.Y} = 336.37\ kip$
$Cap_{TensileRupt.T} = 142.59\ kip$	$Cap_{TensileRupt.Y} = 124.31\ kip$
$Cap_{BlockShear.T} = 312\ kip$	$Cap_{BlockShear.Y} = 198.25\ kip$

$Cap_{TensileYield} = 146.25\ kip$

Appendix C. Shop Drawings

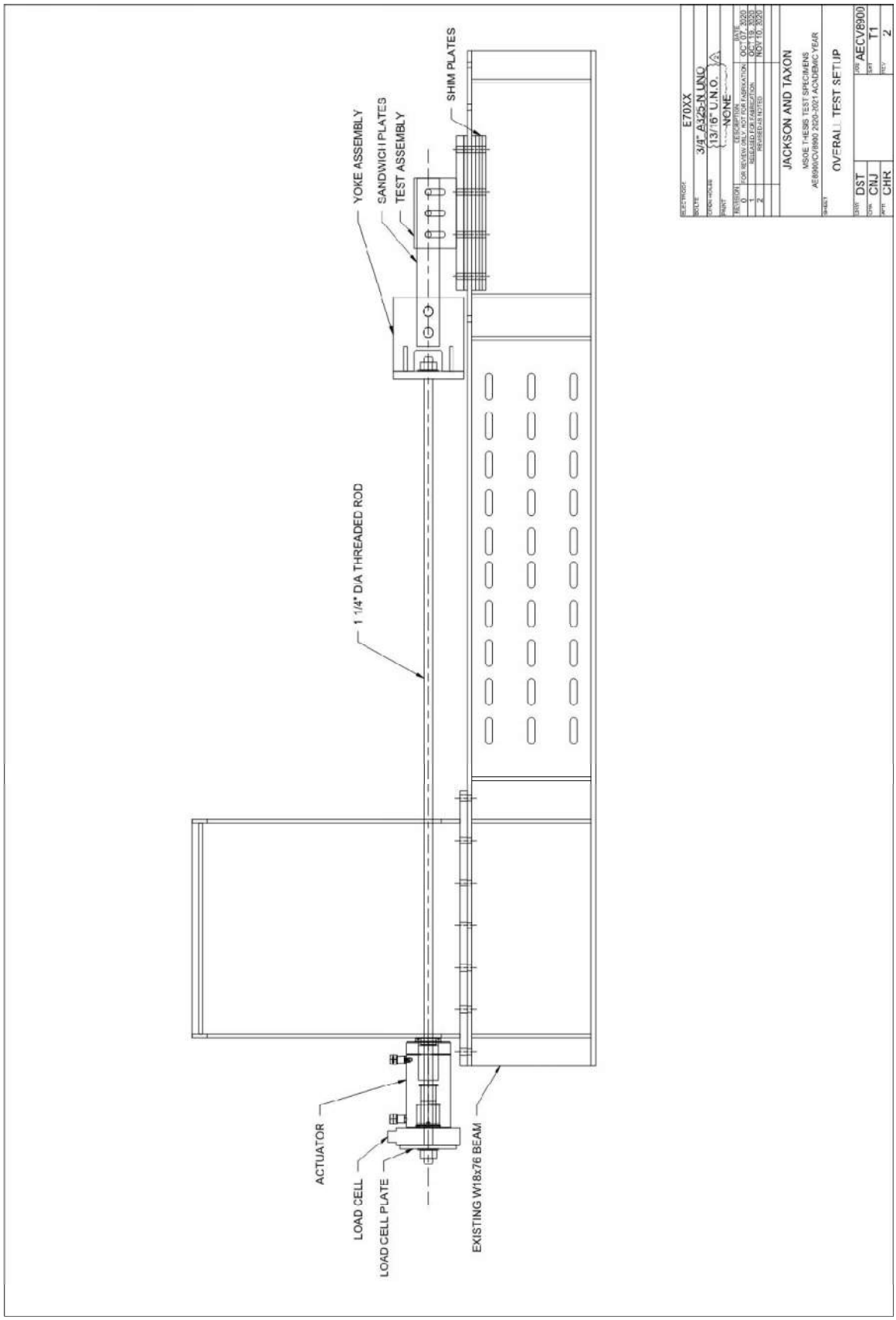
YOKE ASSEMBLY
SANDWICH PLATES
TEST ASSEMBLY
SHIM PLATES
1 1/4" DIA THREADED ROD
ACTUATOR
LOAD CELL
LOAD CELL PLATE
EXISTING W18x76 BEAM
ELECTRODE
E70XX
BOLTS
3/4" A325-N UNO
SPEC HOLES
13/16" U.N.O.
PAINT
NONE
DESCRIPTION
DATE
0
FOR REVIEW ONLY - NOT FOR FABRICATION
OCT 07 2020
1
INCLUDED AS NOTED
OCT 19 2020
2
REVISED AS NOTED
NOV 10 2020
JACKSON AND TAXON
MSOE THESIS TEST SPECIMENS
AE8990/CV8990 2020-2021 ACADEMIC YEAR
SHEET
OVERALL TEST SETUP
DSN DST
DRN CNJ
APP CHK
DRG AECV8900
SHT T1
REV 2

BILL OF MATERIALS

	MARK	NO. PIECES	SHAPE	LENGTH FEET	LENGTH INCHES	GRADE	WEIGHT	REMARKS
1	AST1	6	ASSEMELY					
2	P11	6	PL 1/4" x 6"	0	10	A572 50	26.5	
3	P12	21	PL 1" x 1'-0"	1	10	A572-50	1310.1	
						TOTAL WT	1335.5	

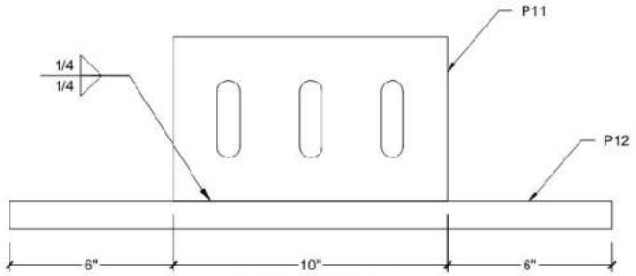

(6) ASSEMBLY AST1
ELEVATON

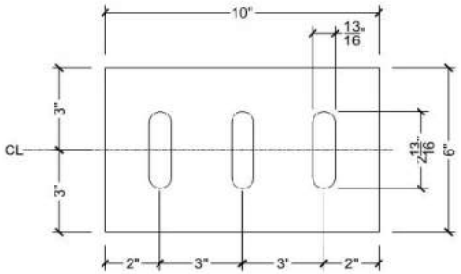

(6) PLATES P11

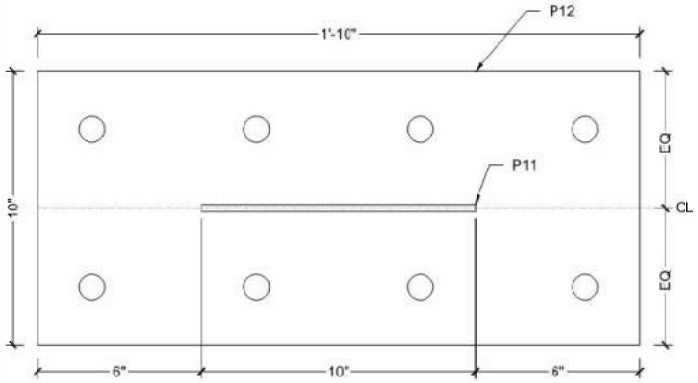

(6) ASSEMBLY AST1
TOP

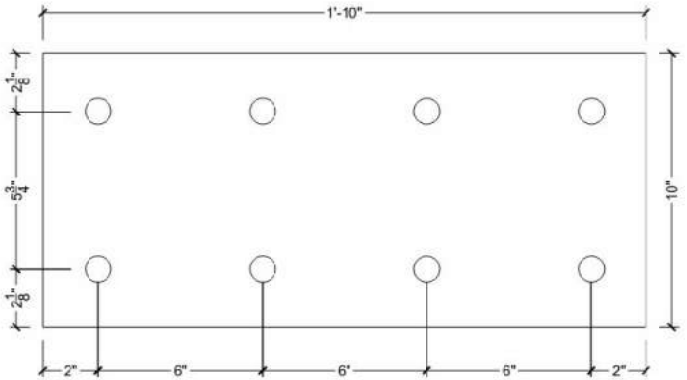

(21) PLATES P12

ELECTRODE	E70XX
BOLTS	3/4" A325-N UNO
OPEN HOLES	13/16" U.N.O.
PAINT	NONE

REVISION	DESCRIPTION	DATE
0	FOR REVIEW ONLY. NOT FOR FABRIKATION	OCT 07, 2020
1	RELEASED FOR FABRICATION	OCT 19, 2020
2	REVISED AS NOTED	NOV 10, 2020

JACKSON AND TAXON

MSOE THESIS TEST SPECIMENS
AE8990/CV8990 2020-2021 ACADEMIC YEAR

SHEET: TEST 1 SPECIMENS

DWN	DST	JOB	AECV8900
CHK	CNJ	SHT	1
APP	CHR	REV	2

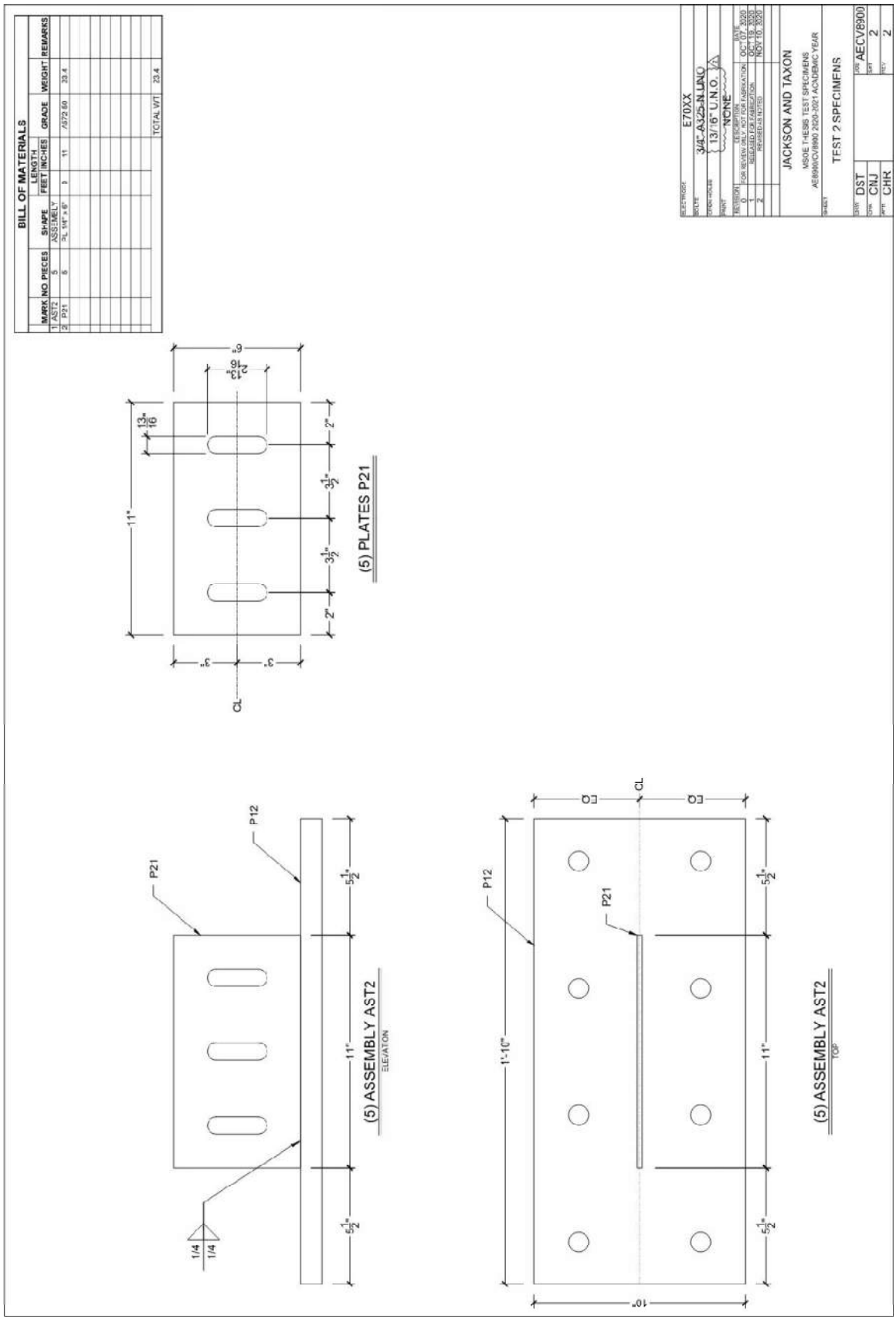
BILL OF MATERIALS
MARK NO. PIECES SHAPE LENGTH FEET INCHES GRADE WEIGHT REMARKS
1 AST2 5 ASSEMBLY
2 P21 5 PL 1/4" x 6" 1 11 A572 60 33.4
TOTAL WT 23.4
E70XX
3/4" A325-N UNO
13/16" U.N.O.
NONE
DESCRIPTION DATE
0 FOR REVIEW ONLY - NOT FOR FABRICATION OCT 07 2020
1 REVISED AS NOTED OCT 19 2020
2 REVISED AS NOTED NOV 10 2020
JACKSON AND TAXON
MSOE THESIS TEST SPECIMENS
AE8990/CV8990 2020-2021 ACADEMIC YEAR
TEST 2 SPECIMENS
DRW DST
CHK CNJ
APP CHK
DRG AECV8900
SHT 2
REV 2
(5) PLATES P21
(5) ASSEMBLY AST2
ELEVATION
(5) ASSEMBLY AST2
TOP
P21
P12
CL
11"
1'-10"
10"

BILL OF MATERIALS								
	MARK	NO. PIECES	SHAPE	LENGTH FEET	LENGTH INCHES	GRADE	WEIGHT	REMARKS
1	AST3	5	ASSEMELY					
2	P31	5	PL 1/4" x 6"	1	0	A572 50	25.5	
						TOTAL WT	25.5	

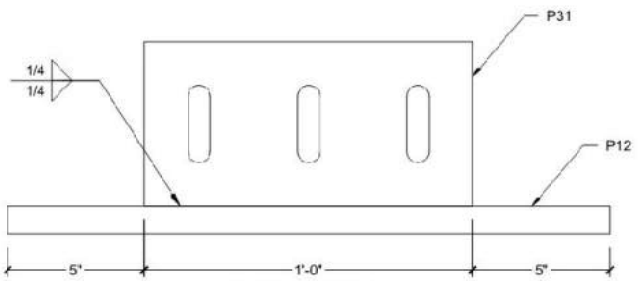

(5) ASSEMBLY AST3
ELEVATON

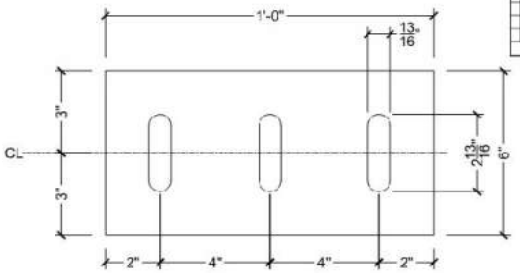

(5) PLATES P31

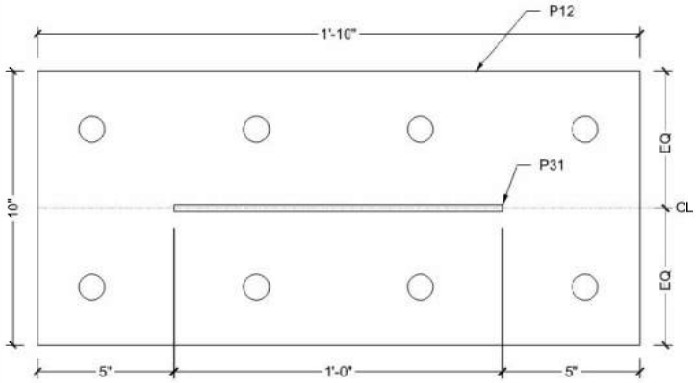

(5) ASSEMBLY AST3
TOP

ELECTRODE	E70XX
BOLTS	~~3/4" A325-N UNO~~
OPEN HOLES	13/16" U.N.O.
PAINT	~~NONE~~

REVISION	DESCRIPTION	DATE
0	FOR REVIEW ONLY. NOT FOR FABRIKATION	OCT 07, 2020
1	RELEASED FOR FABRICATION	OCT 19, 2020
2	REVISED AS NOTED	NOV 10, 2020

JACKSON AND TAXON

MSOE THESIS TEST SPECIMENS
AE8990/CV8990 2020-2021 ACADEMIC YEAR

SHEET: TEST 3 SPECIMENS

DWN	DST	JOB	AECV8900
CHK	CNJ	SHT	3
APP	CHR	REV	2

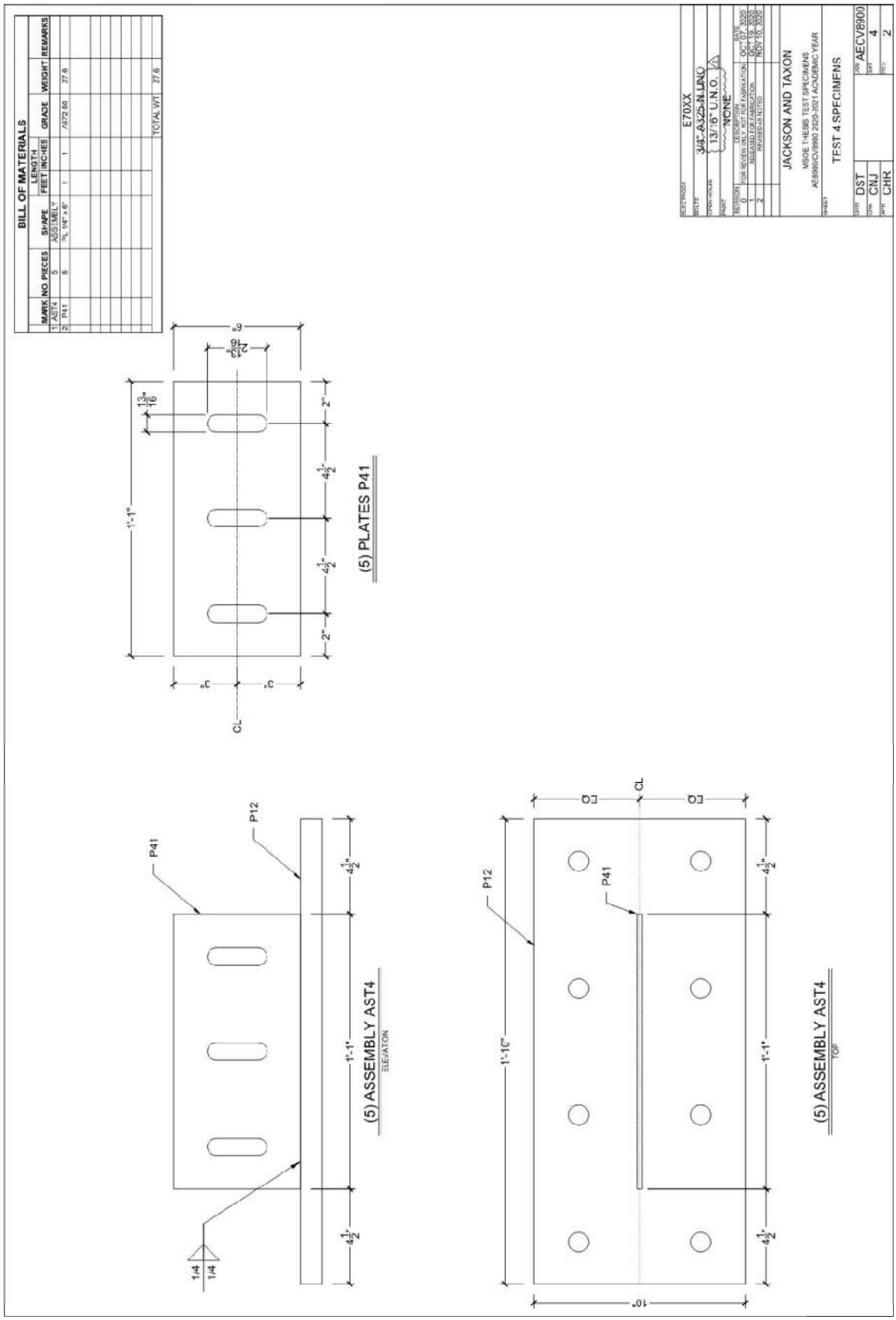
BILL OF MATERIALS
MARK NO PIECES SHAPE LENGTH FEET INCHES GRADE WEIGHT REMARKS
1 AST4 5 ASSEMBLY
2 P41 5 PL 1/4" x 6" 1 1 A572 50 27.6
TOTAL WT. 27.6
E70XX
3/4" A325-N UNO
13/16" U.N.O.
NONE
DESCRIPTION DATE
0 FOR REVIEW ONLY - NOT FOR FABRICATION OCT 07 2020
1 REVISED AS NOTED OCT 28 2020
2 REVISED AS NOTED NOV 10 2020
JACKSON AND TAXON
MSOE THESIS TEST SPECIMENS
AE8990/CV8990 2020-2021 ACADEMIC YEAR
TEST 4 SPECIMENS
DRW DST
CHK CNJ
APP CHR
DWG AECV8900
SHT 4
REV 2
(5) PLATES P41
(5) ASSEMBLY AST4
ELEVATION
(5) ASSEMBLY AST4
TOP
P41
P12
CL
1'-1"
1'-10"
10"
2"
4½"
13/16"

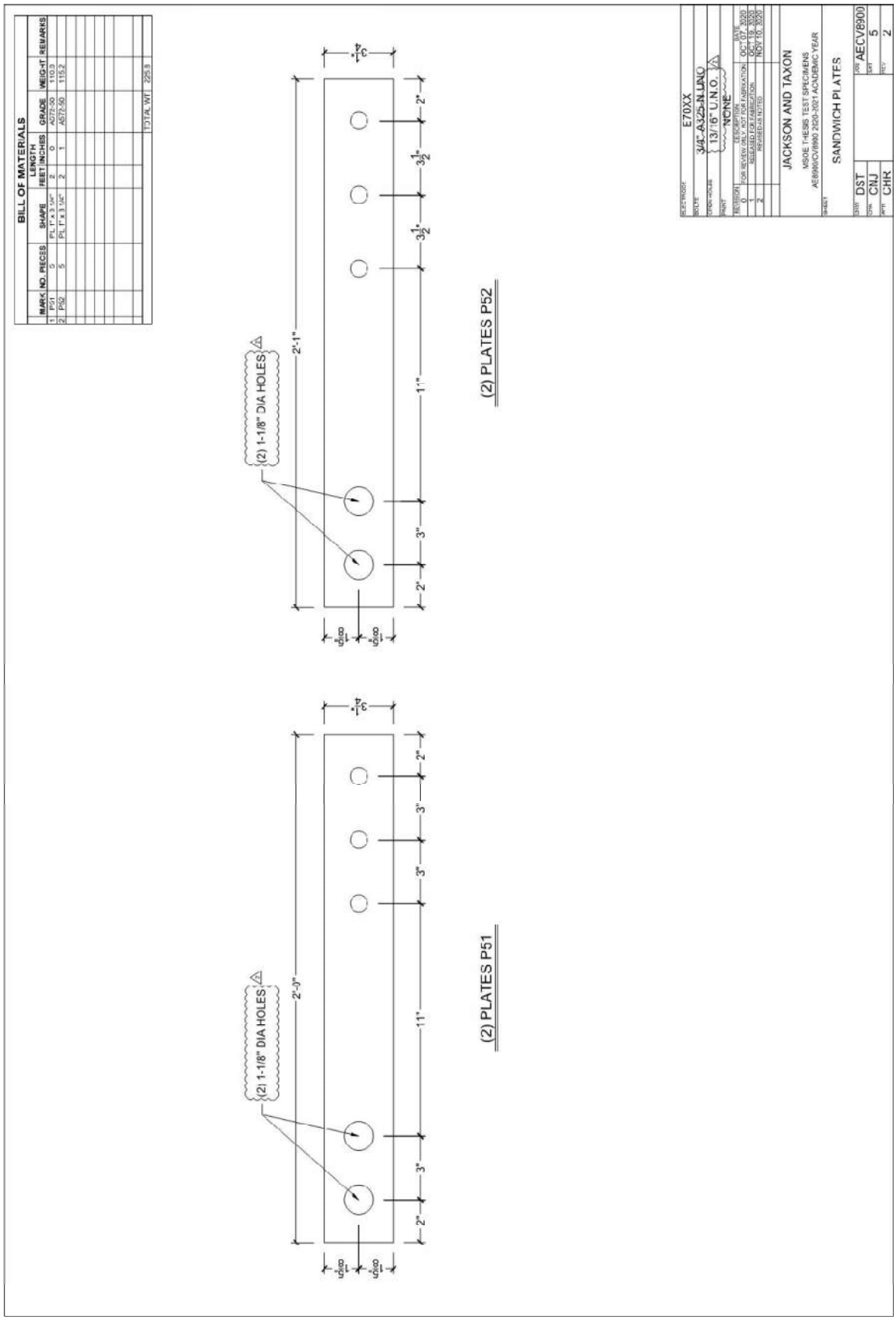
BILL OF MATERIALS
MARK NO. PIECES SHAPE LENGTH FEET INCHES GRADE WEIG-HT REMARKS
P51 5 PL 1" x 3 1/4" 2 0 A572-50 110.3
P52 5 PL 1" x 3 1/4" 2 1 A572-50 115.2
TOTAL WT 225.5
E70XX
3/4" A325-N UNO
13/16" U.N.O.
NONE
DESCRIPTION DATE
0 FOR REVIEW ONLY - NOT FOR FABRICATION OCT 07 2020
1 REVISED AS NOTED OCT 28 2020
2 REVISED AS NOTED NOV 10 2020
JACKSON AND TAXON
MSOE THESIS TEST SPECIMENS
AE8990/CV8990 2020-2021 ACADEMIC YEAR
SANDWICH PLATES
DRW AECV8900
SHT 5
REV 2
DST
CNJ
CHK
(2) 1-1/8" DIA HOLES
2'-0"
11"
2"
3"
3"
3"
2"
(2) PLATES P51
(2) 1-1/8" DIA HOLES
2'-1"
11"
2"
3"
3 1/2"
3 1/2"
2"
(2) PLATES P52

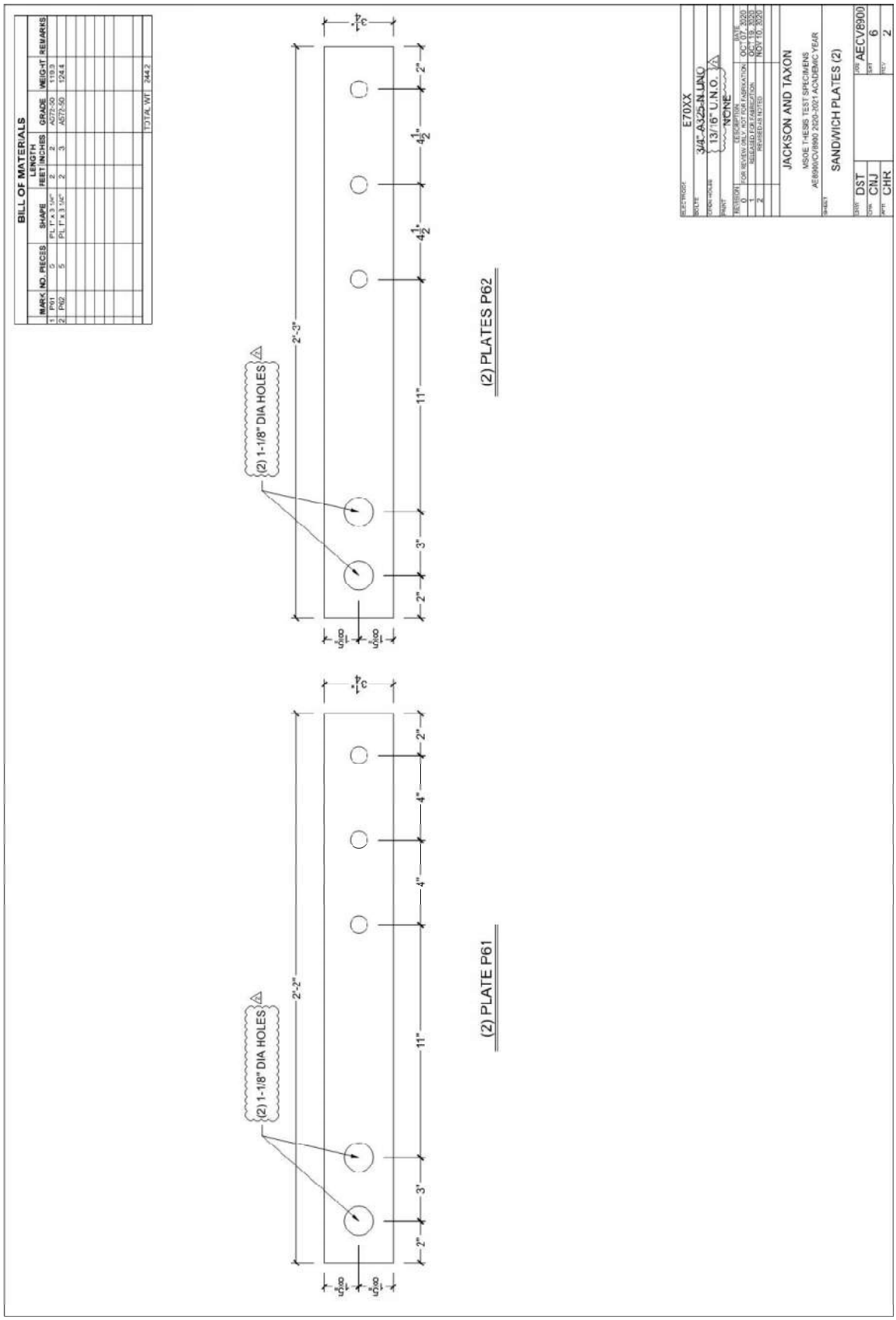
BILL OF MATERIALS
MARK NO. PIECES SHAPE LENGTH FEET INCHES GRADE WEIG-HT REMARKS
1 PI1 5 PL 1" x 3 1/4" 2 2 A572-50 1193
2 PI2 5 PL 1" x 3 1/4" 2 3 A572-50 1244
TOTAL WT 2437
(2) 1-1/8" DIA HOLES
2'-2"
11"
4"
3"
2"
(2) PLATE P61
2'-3"
4 1/2"
(2) PLATES P62
E70XX
3/4" A325-N UNO
13/16" U.N.O.
NONE
DESCRIPTION
FOR REVIEW ONLY - NOT FOR FABRICATION
REVISED AS NOTED
JACKSON AND TAXON
MSOE THESIS TEST SPECIMENS
AE8990/CV8990 2020-2021 ACADEMIC YEAR
SAND/WICH PLATES (2)
DST
CNJ
CHK
AECV8900
6
2

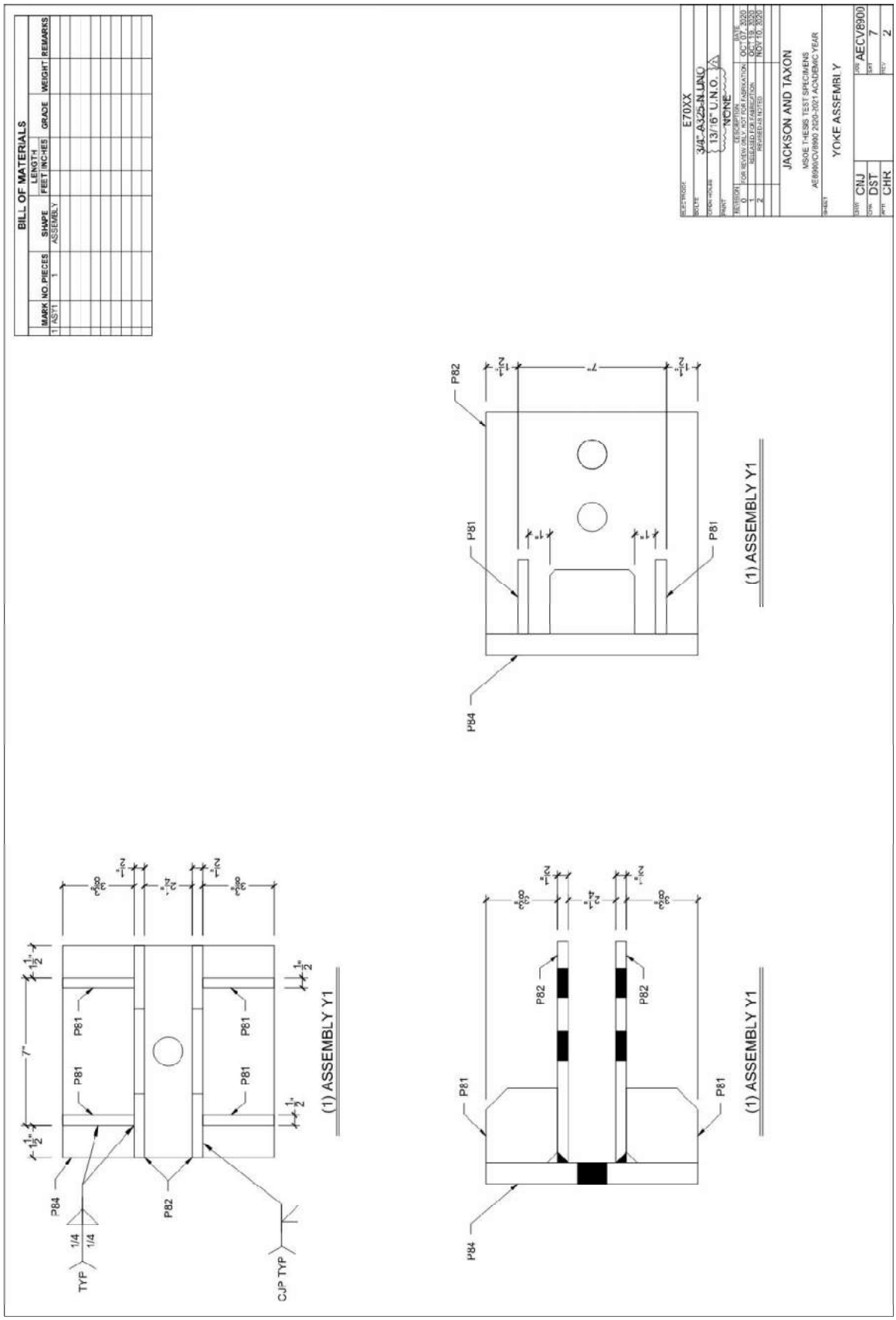
BILL OF MATERIALS
MARK
NO. PIECES
SHAPE
LENGTH
FEET INCHES
GRADE
WEIGHT
REMARKS
1 AST1
1
ASSEMBLY
E70XX
3/4" A325-N UNO
13/16" U.N.O.
NONE
DESCRIPTION
DATE
0 FOR REVIEW ONLY - NOT FOR FABRICATION OCT 07 2020
1 REVISED AS NOTED OCT 19 2020
2 REVISED AS NOTED NOV 10 2020
JACKSON AND TAXON
MSOE THESIS TEST SPECIMENS
AE8990/CV8990 2020-2021 ACADEMIC YEAR
YOKE ASSEMBLY
DRN CNJ
CHK DST
APP CHK
DRG AECV8900
SHT 7
REV 2
P81
P82
P84
7"
1 1/2"
1/2"
1/4
TYP
CJP TYP
(1) ASSEMBLY Y1

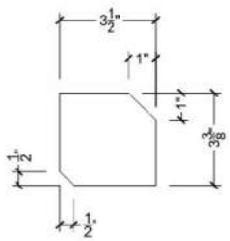

(4) PLATES P81

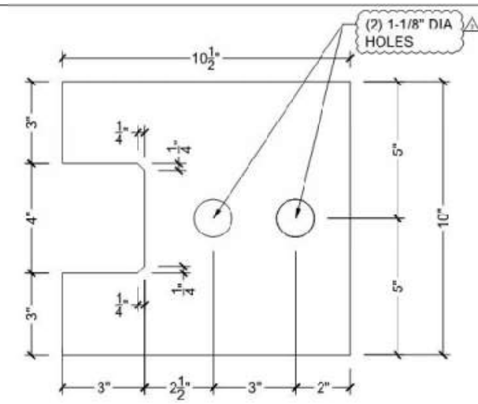

(2) PLATES P82

	BILL OF MATERIALS							
				LENGTH				
	MARK	NO. PIECES	SHAPE	FEET	INCHES	GRADE	WEIGHT	REMARKS
1	P81	4	PL 1/2" x 3 1/2"	0	3.375	A572-50	6.7	
2	P82	2	PL 1/2" x 10"	0	10.5	A572-50	29.8	BEVEL PLATE
3	P83	1	PL 1/4" x 8 1/2"	0	7	A572-50	4.2	
4	P84	1	PL 1" x 10"	0	10	A572-50	28.4	
						TOTAL WT	62.3	

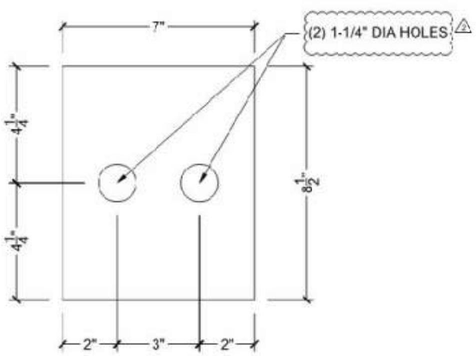

(1) PLATE P83

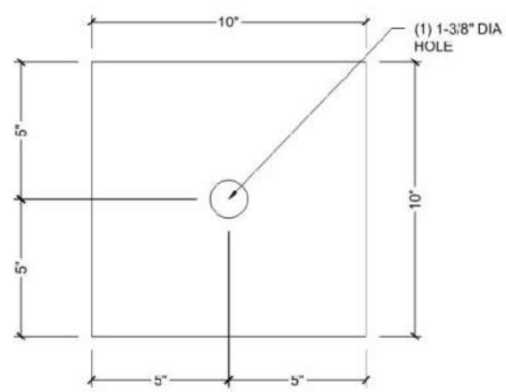

(1) PLATE P84

ELECTRODE	E70XX	
BOLTS	~~3/4" A325-N UNO~~	
OPEN HOLES	13/16" U.N.O.	
PAINT	NONE	
REVISION	DESCRIPTION	DATE
0	FOR REVIEW ONLY, NOT FOR FABRICATION	OCT 07, 2020
1	RELEASED FOR FABRICATION	OCT 19, 2020
2	REVISED AS NOTED	NOV 10, 2020

JACKSON AND TAXON

MSOE THESIS TEST SPECIMENS
AE8990/CV8990 2020-2021 ACADEMIC YEAR

SHEET: YOKE PLATES

DRW	CNJ	JOB	AECV8900
CHK	DST	SHT	8
APR	CHR	REV	2

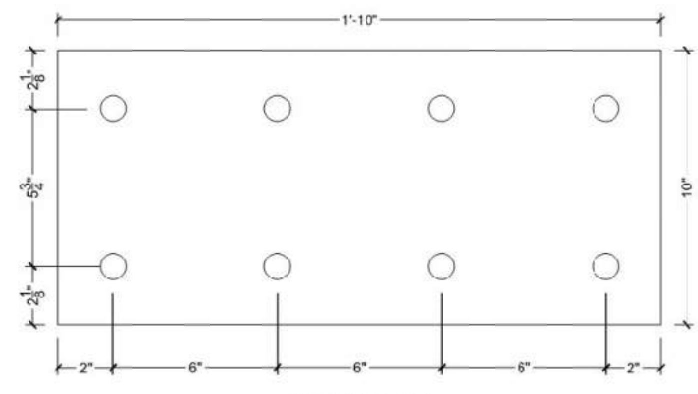

(5) PLATES P91

BILL OF MATERIALS

	MARK	NO PIECES	SHAPE	LENGTH FEET	LENGTH INCHES	GRADE	WEIGHT	REMARKS
1	P91	5	PL 1/2" x 10"	1	10	A572-50	156.0	
2	P92	8	PL 1/2" x 4"	1	10	A572-50	99.8	
3	P93	1	PL 1" x 8"	0	8	A572-50	18.1	
						TOTAL WT	273.9	

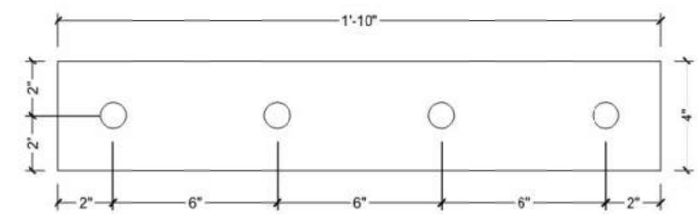

(8) PLATES P92

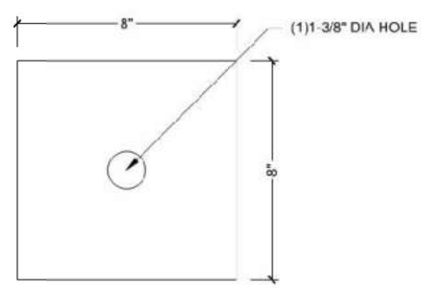

(1) PLATE P93

ELECTRODE	E70XX
BOLTS	~~3/4" A325-N UNO~~
OPEN HOLES	13/16" U.N.O.
PAINT	NONE

REVISION	DESCRIPTION	DATE
0	FOR REVIEW ONLY, NOT FOR FABRICATION	OCT 07, 2020
1	RELEASED FOR FABRICATION	OCT 19, 2020
2	REVISED AS NOTED	NOV 10, 2020

JACKSON AND TAXON

MSOE THESIS TEST SPECIMENS
AE8990/CV8990 2020-2021 ACADEMIC YEAR

SHEET: SHIM PLATES

DRW	DST	JOB	AECV8900
CHK	CNJ	SHT	9
APR	CHR	REV	2

Appendix D. Pre-Test Specimen Photos

Figure D-1: Front View of S30P100.

Figure D-2: Top View of S30P100.

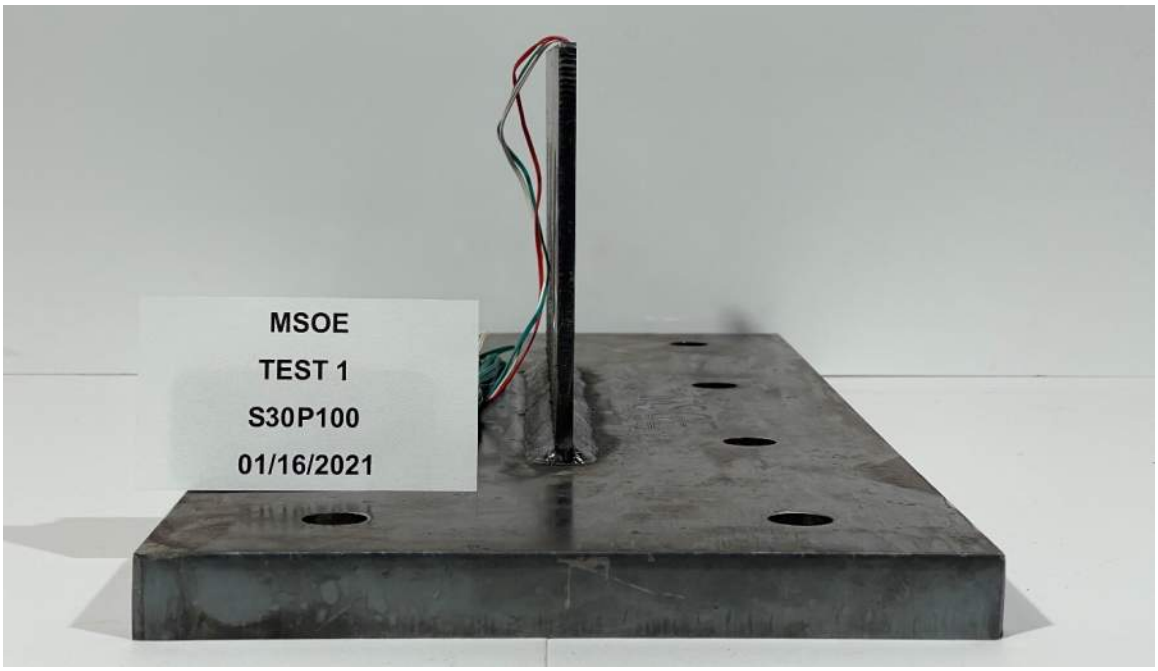

Figure D-3: Side View of S30P100.

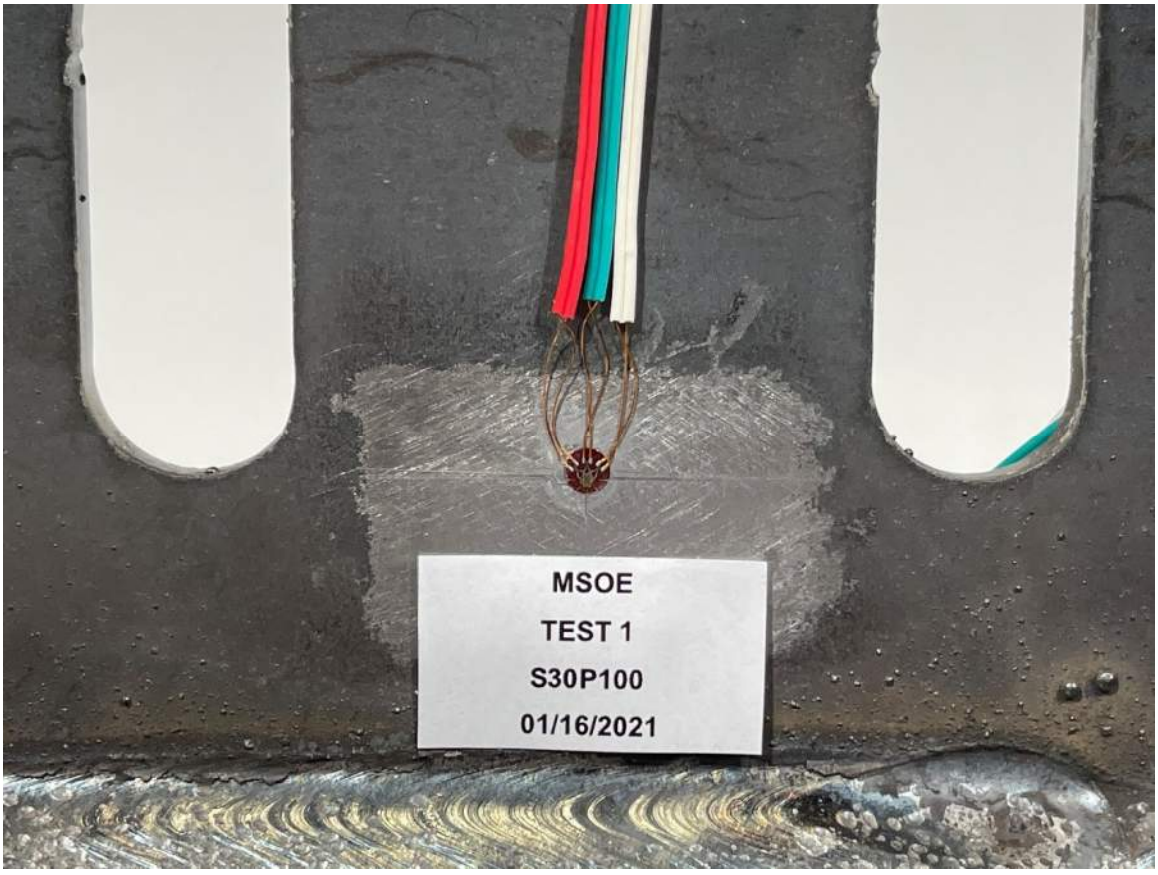

Figure D-4: Close-up View on Rosette of S30P100.

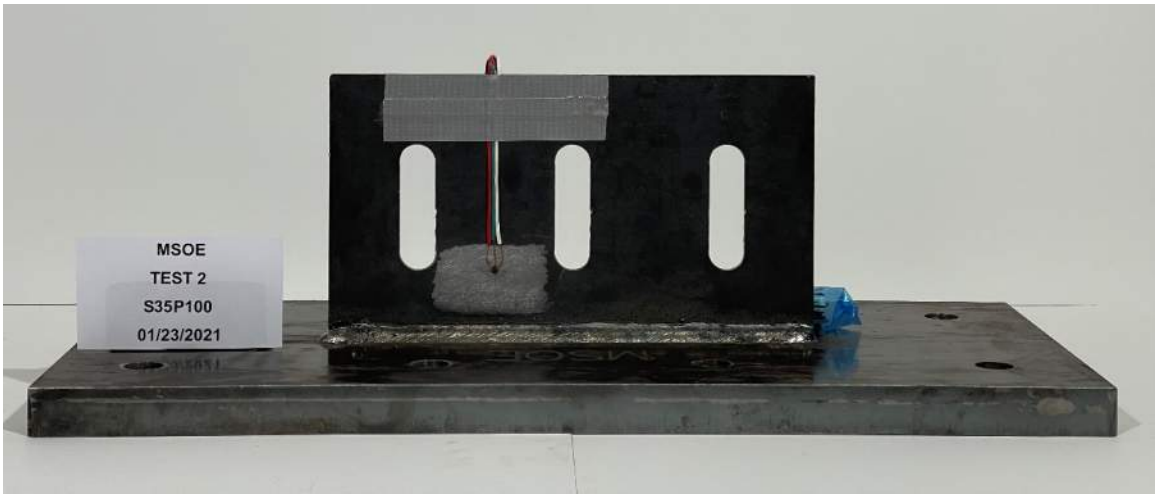

Figure D-5: Front View of S35P100.

Figure D-6: Top View of S35P100.

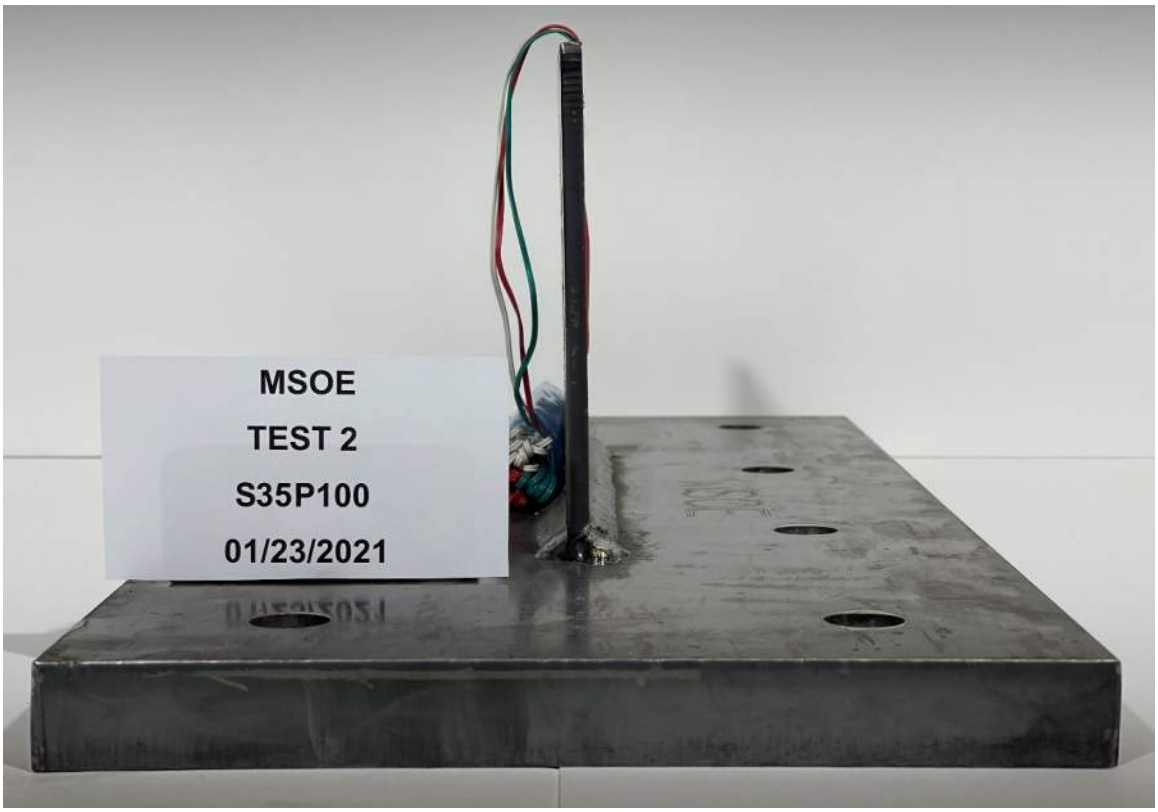

Figure D-7: Side View of S35P100.

Figure D-8: Close-up View on Rosette of S35P100.

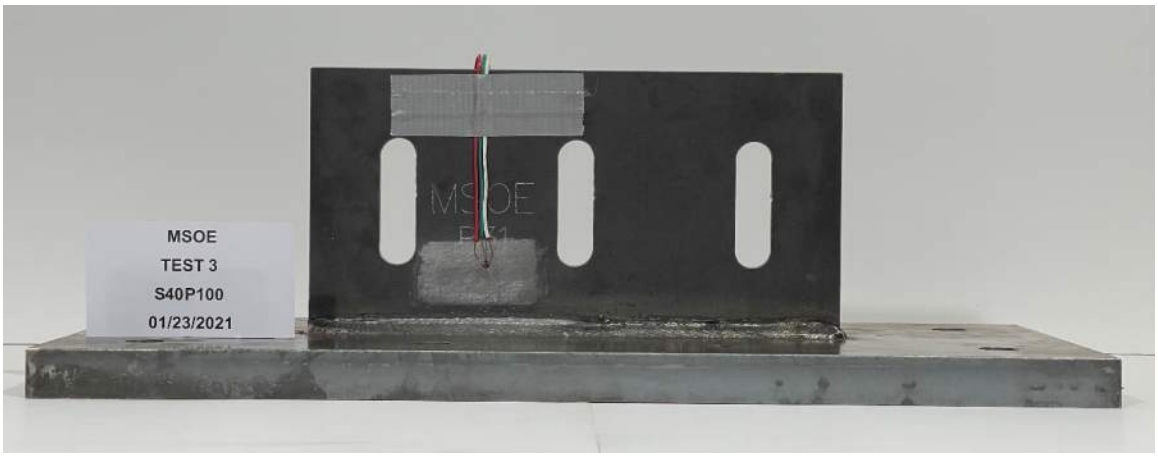

Figure D-9: Front View of S40P100.

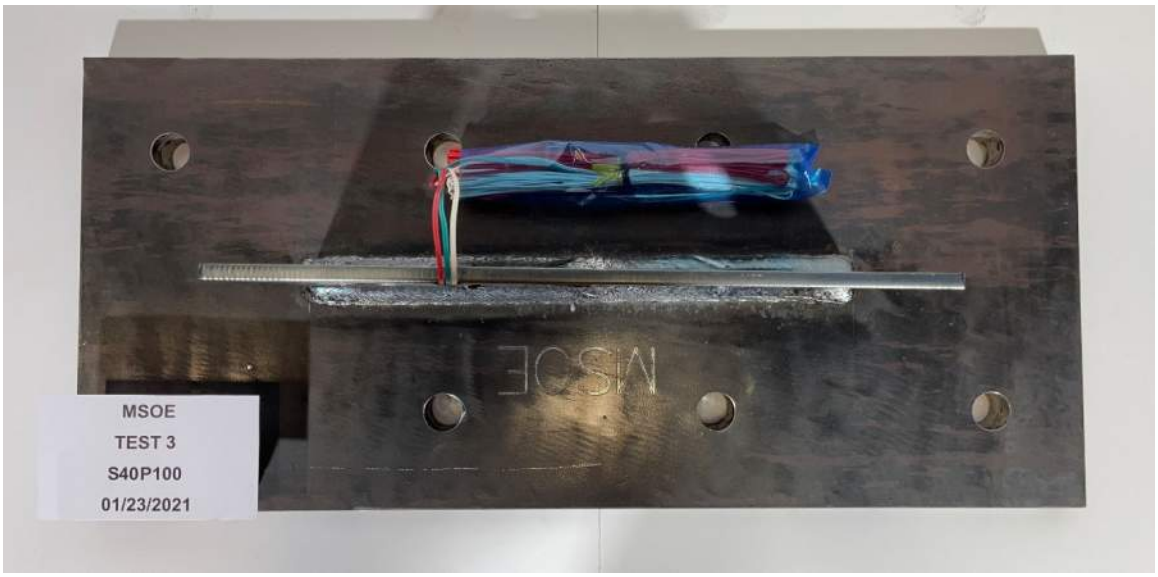

Figure D-10: Top View of S40P100.

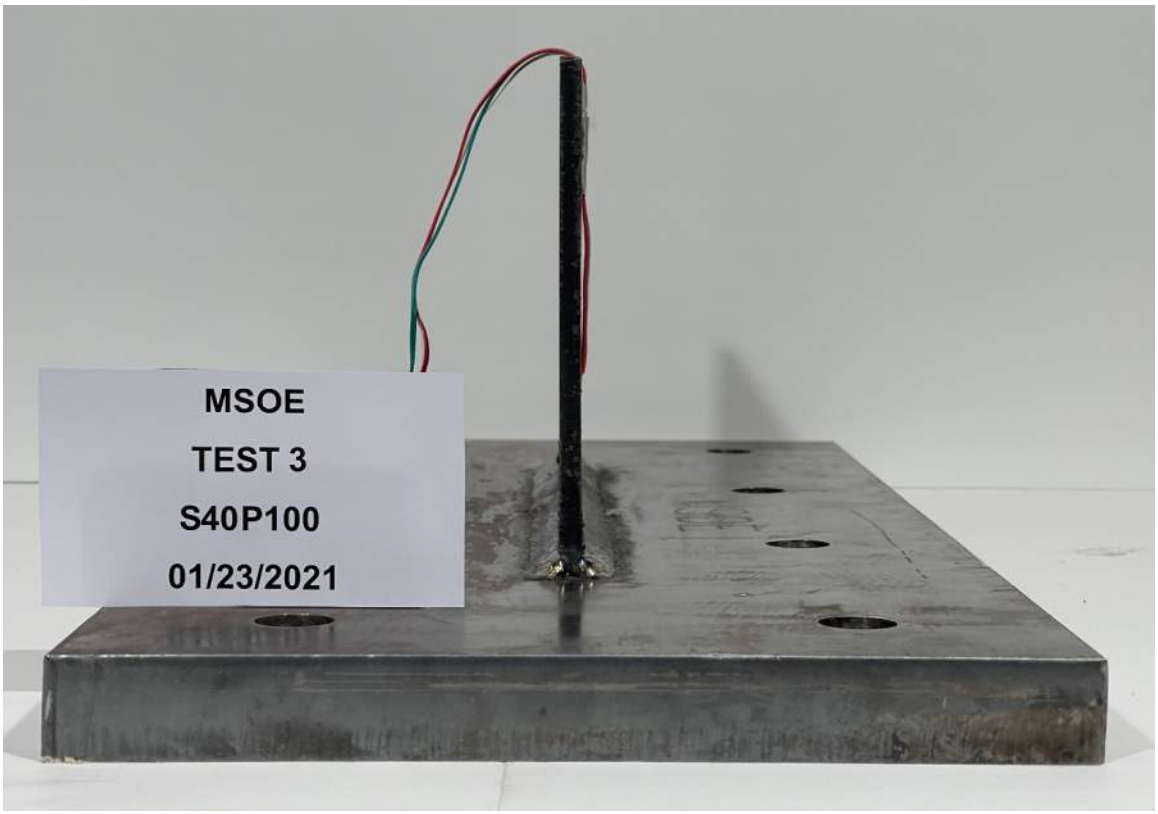

Figure D-11: Side View of S40P100.

Figure D-12: Close-up View on Rosette of S40P100.

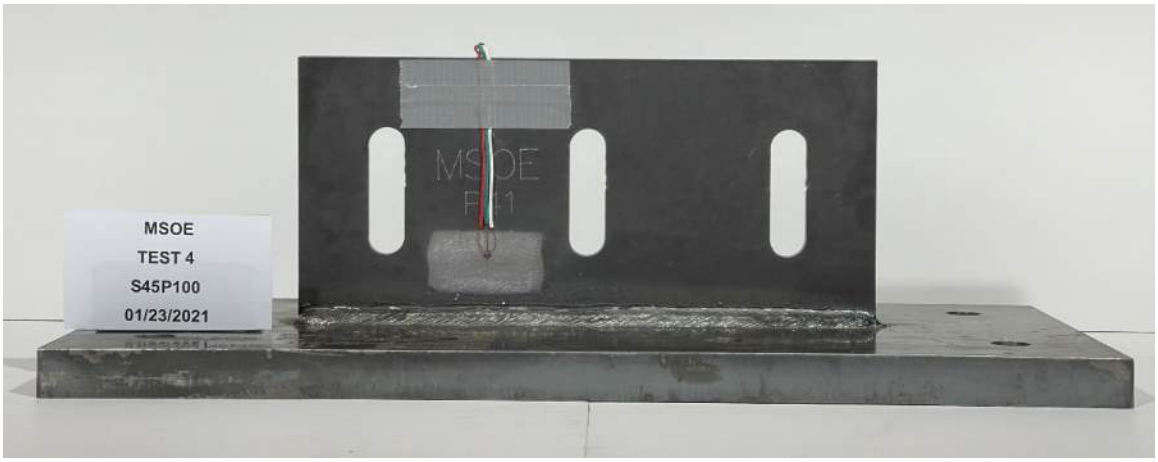

Figure D-13: Front View of S45P100.

Figure D-14: Top View of S45P100.

Figure D-15: Side View of S45P100.

Figure D-16: Close-up View on Rosette of S45P100.

Figure D-17: Front View of S30P075.

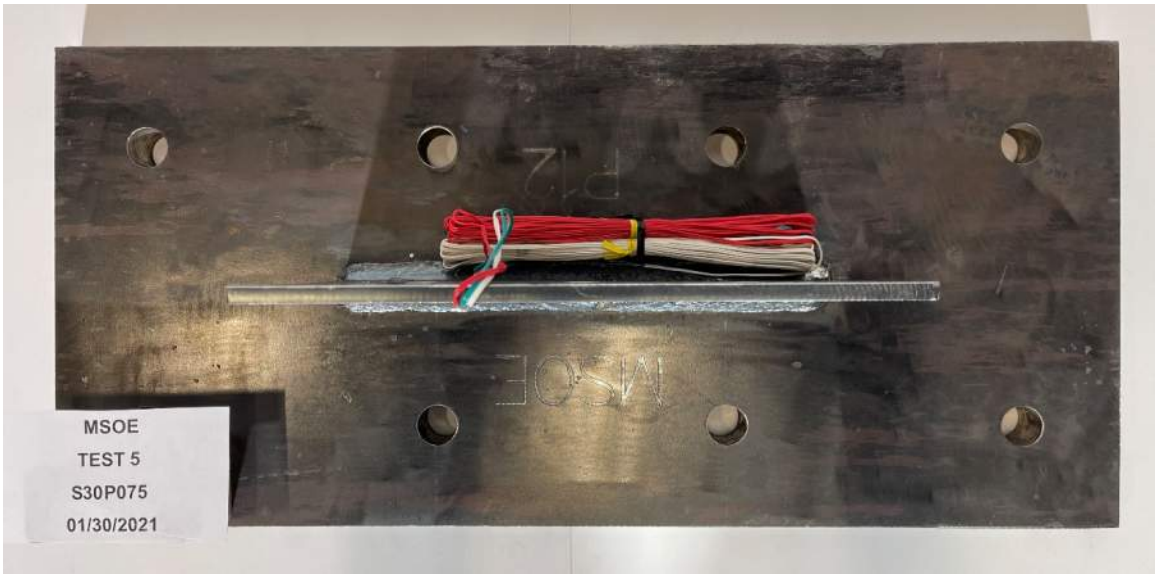

Figure D-18: Top View of S30P075.

Figure D-19: Side View of S30P075.

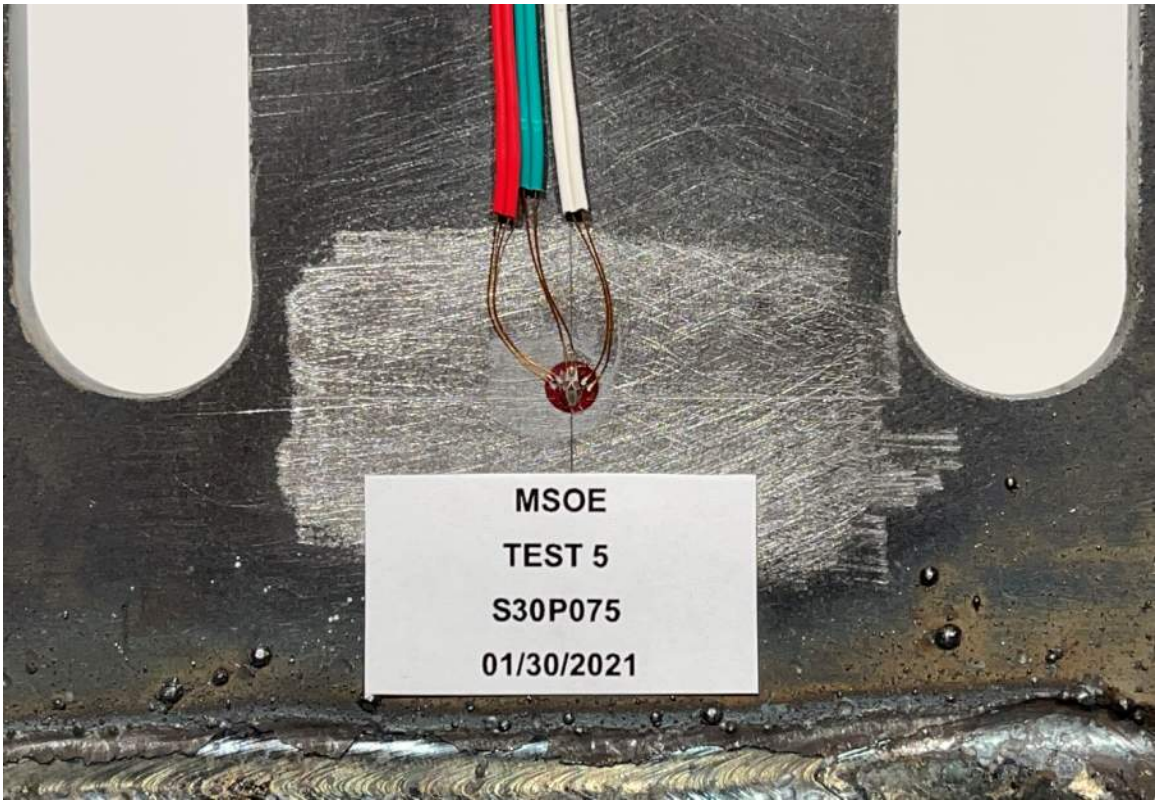

Figure D-20: Close-up View on Rosette of S30P075.

Figure D-21: Front View of S35P075.

Figure D-22: Top View of S35P075.

Figure D-23: Side View of S35P075.

Figure D-24: Front View of S40P075.

Figure D-25: Top View of S40P075.

Figure D-26: Side View of S40P075.

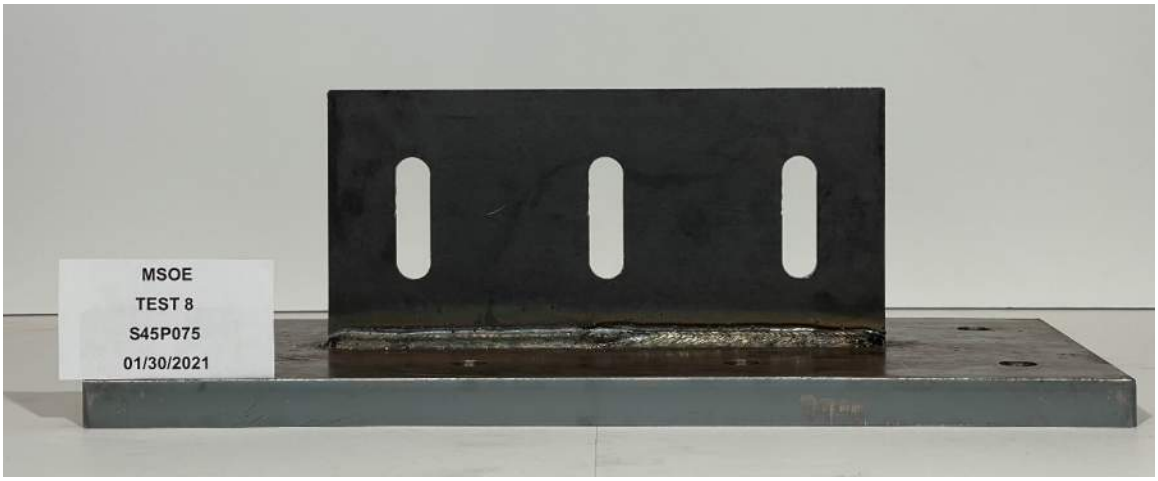

Figure D-27: Front View of S45P075.

Figure D-28: Top View of S45P075.

Figure D-29: Side View of S45P075.

Figure D-30: Front View of S30P050.

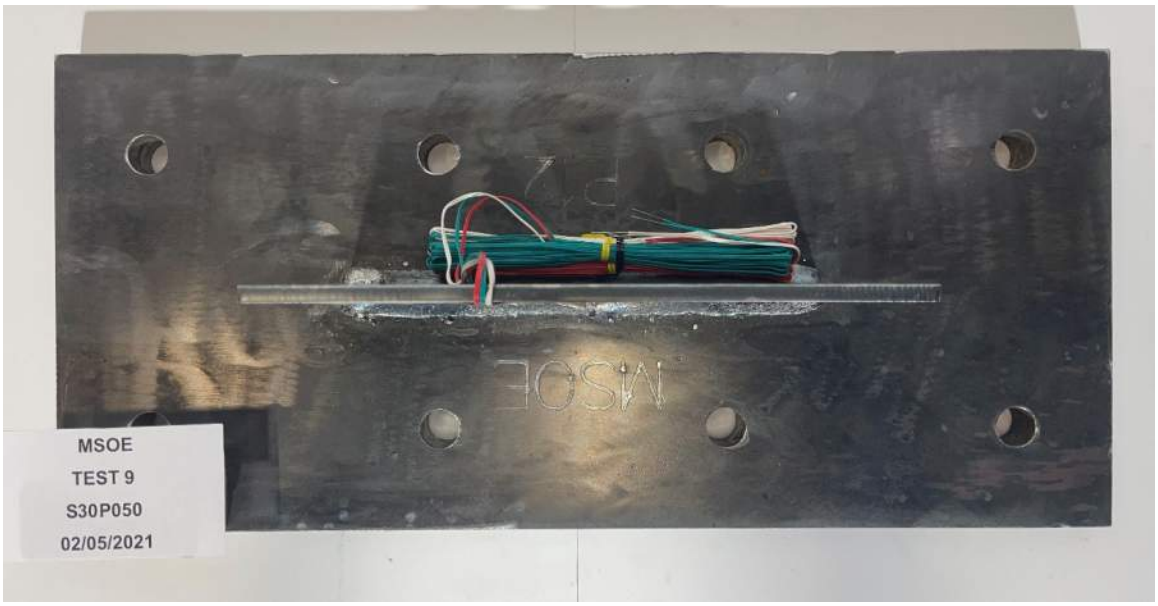

Figure D-31: Top View of S30P050.

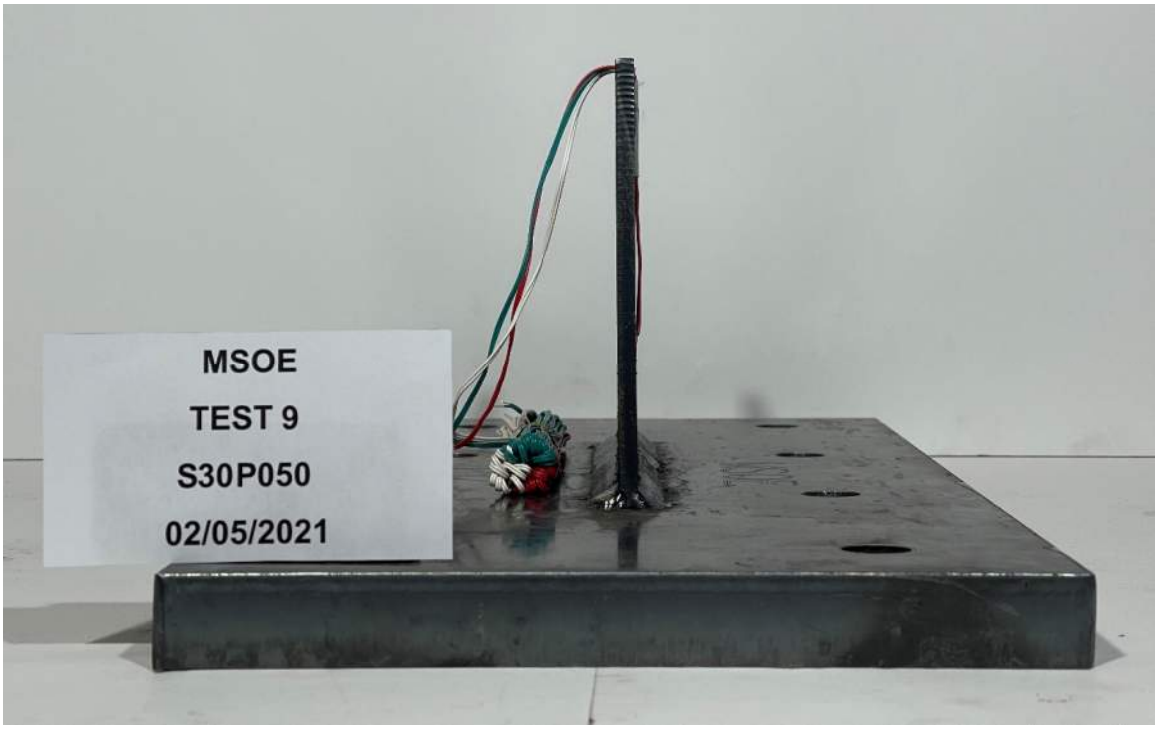

Figure D-32: Side View of S30P050.

Figure D-33: Close-up View on Rosette of S30P050.

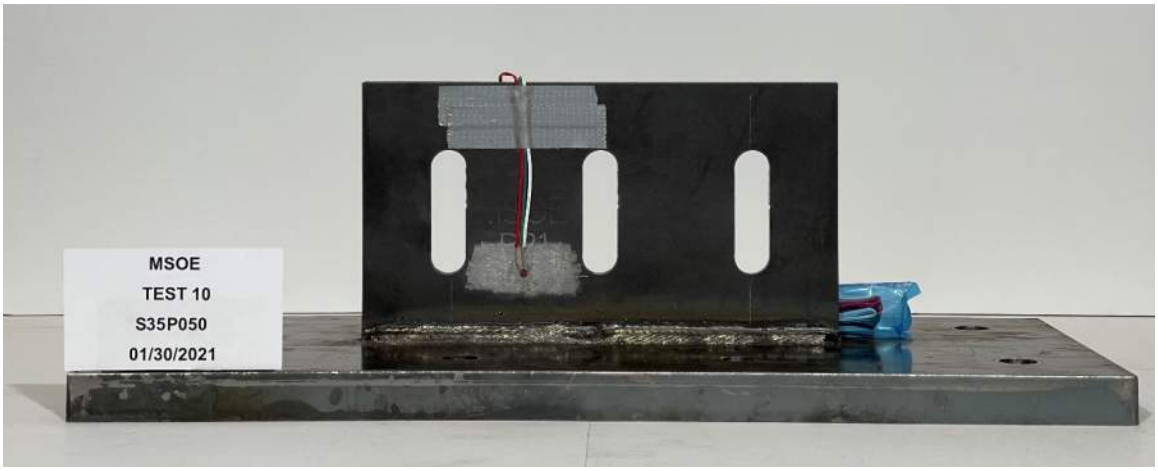

Figure D-34: Front View of S35P050.

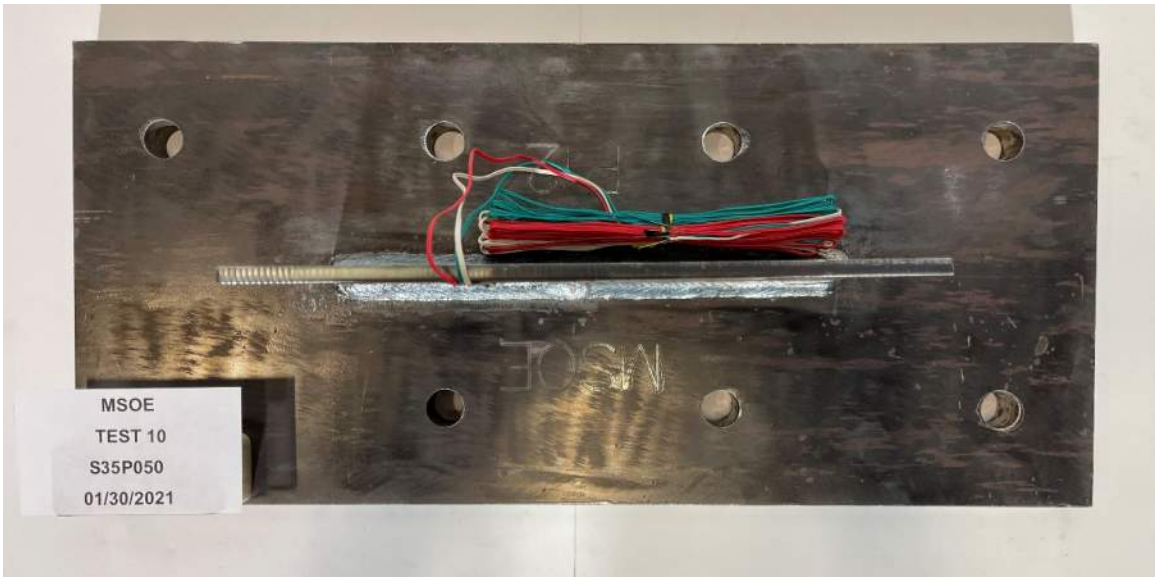

Figure D-35: Top View of S35P050.

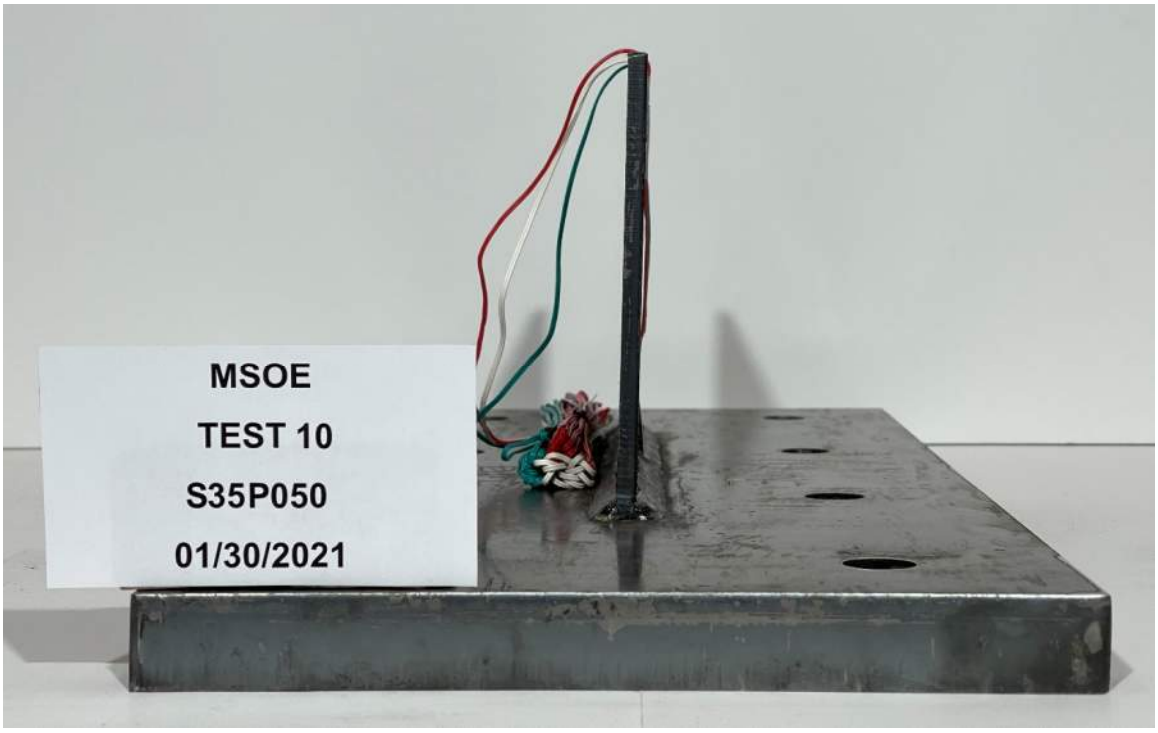

Figure D-36: Side View of S35P050.

Figure D-37: Close-up View on Rosette of S35P050.

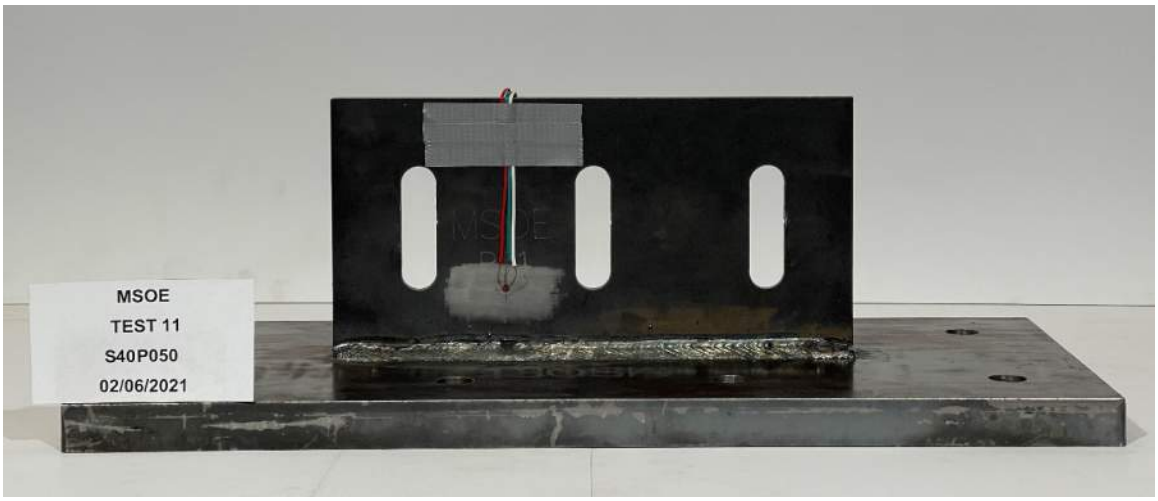

Figure D-38: Front View of S40P050.

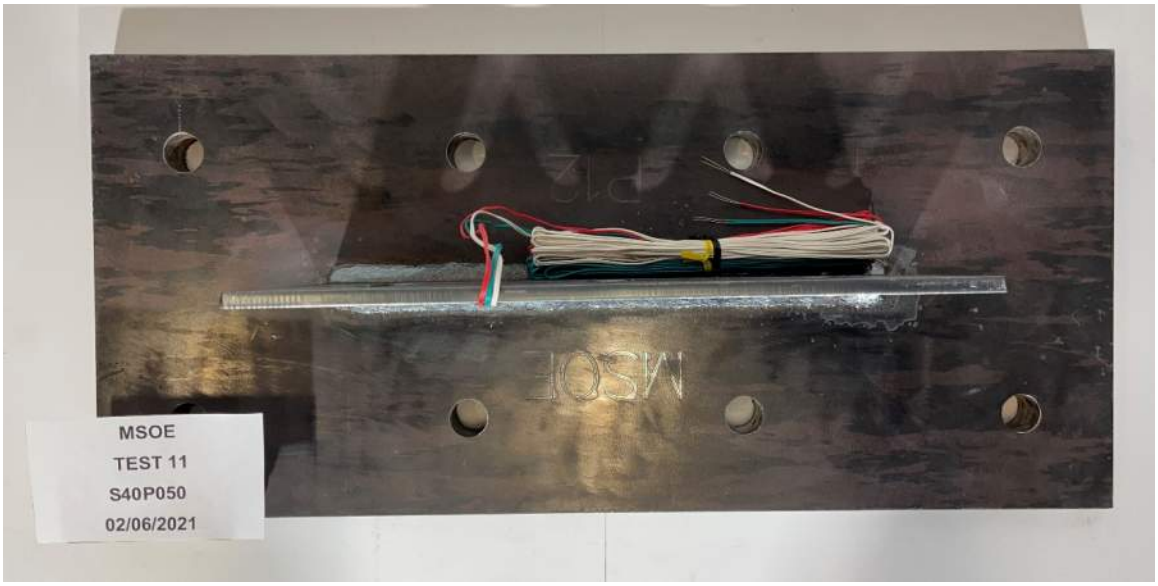

Figure D-39: Top View of S40P050.

Figure D-40: Side View of S40P050.

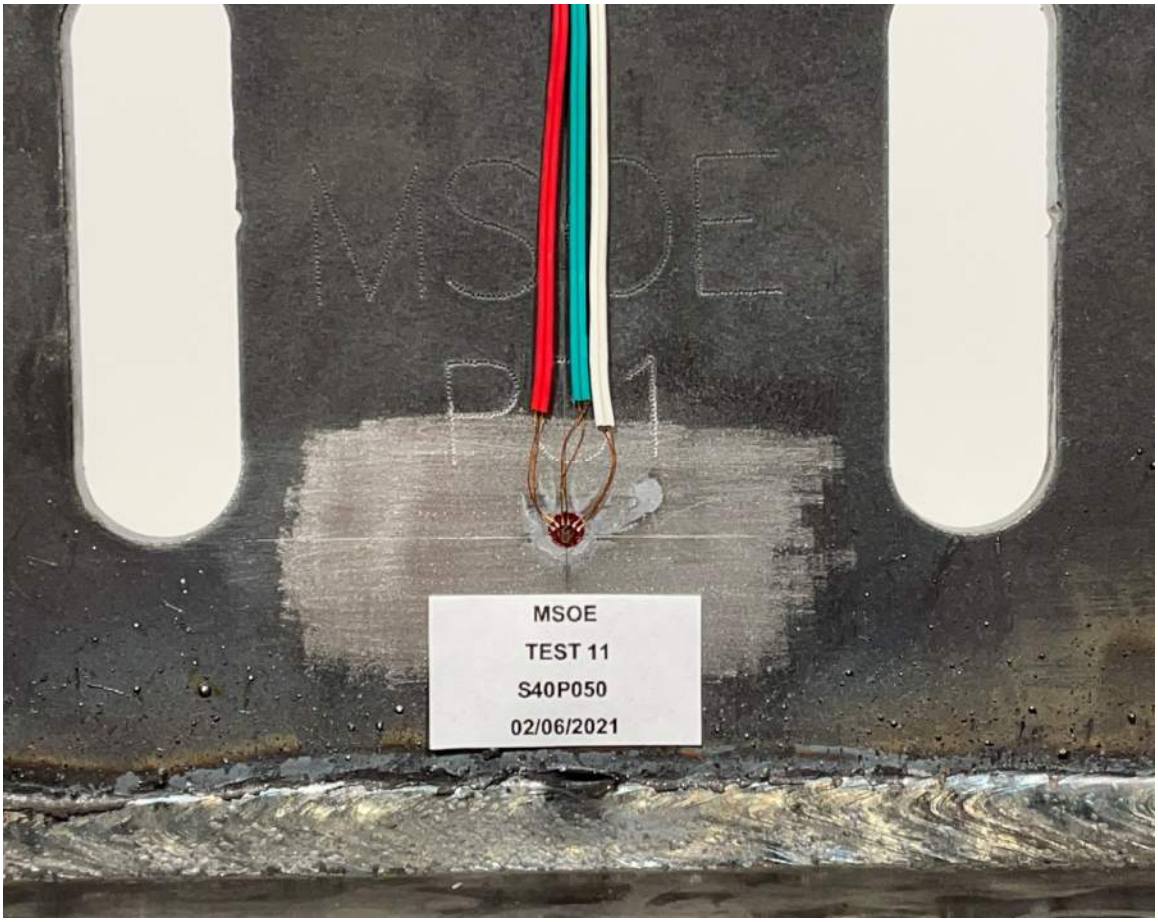

Figure D-41: Close-up View on Rosette of S40P050.

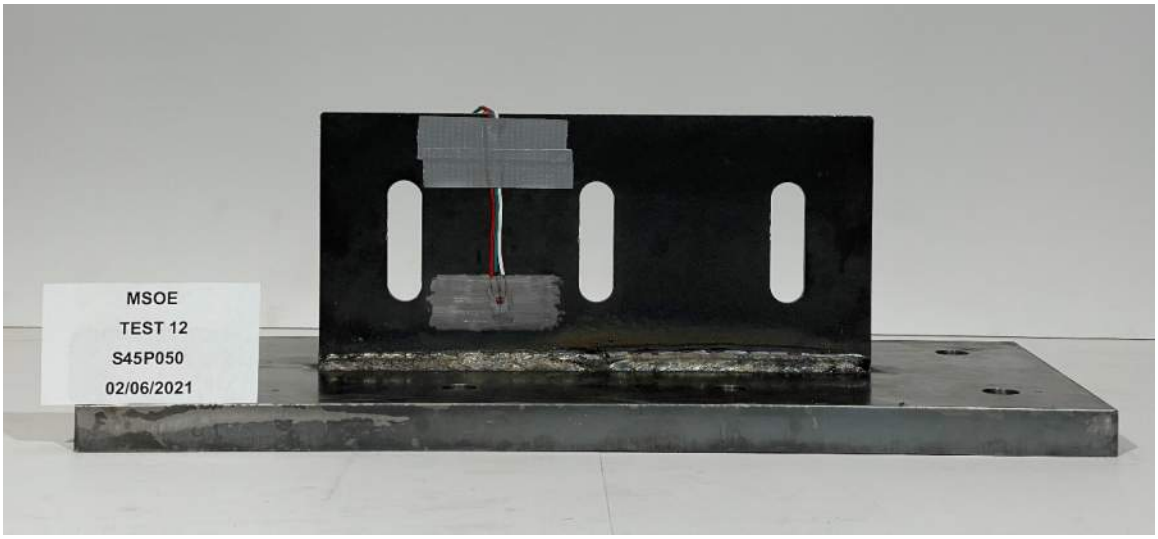

Figure D-42: Front View of S45P050.

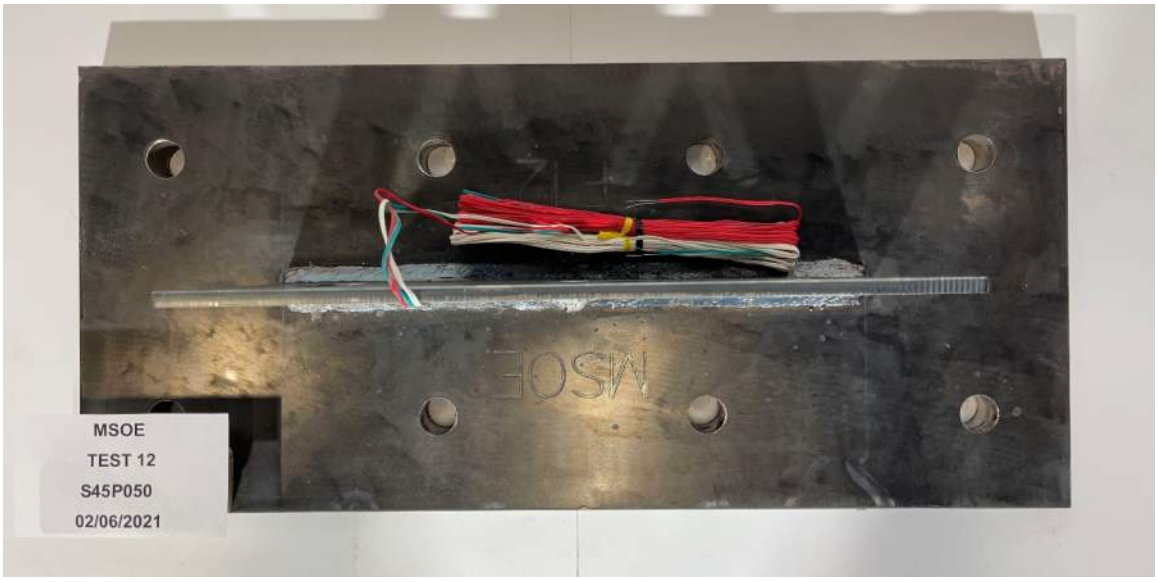

Figure D-43: Top View of S45P050.

Figure D-44: Side View of S45P050.

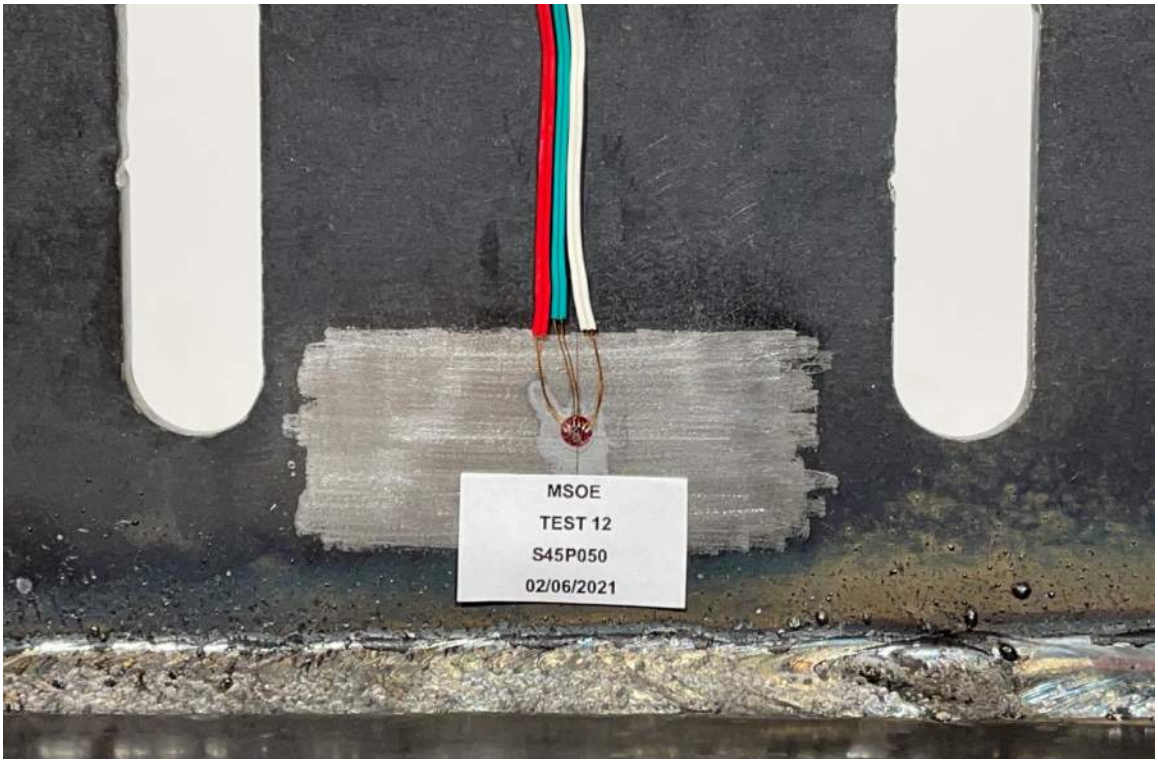

Figure D-45: Close-up View on Rosette of S45P050.

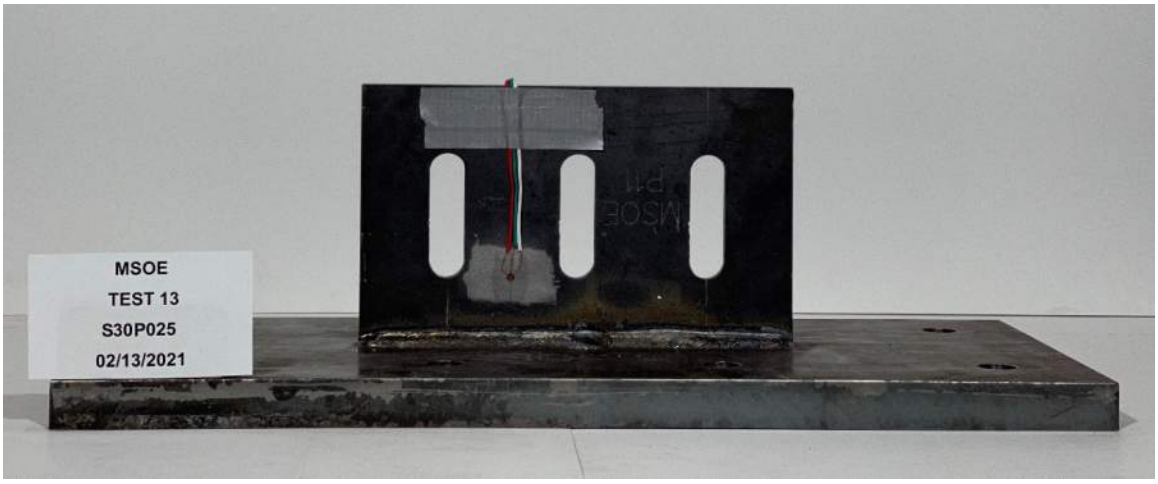

Figure D-46: Front View of S30P025.

Figure D-47: Top View of S30P025.

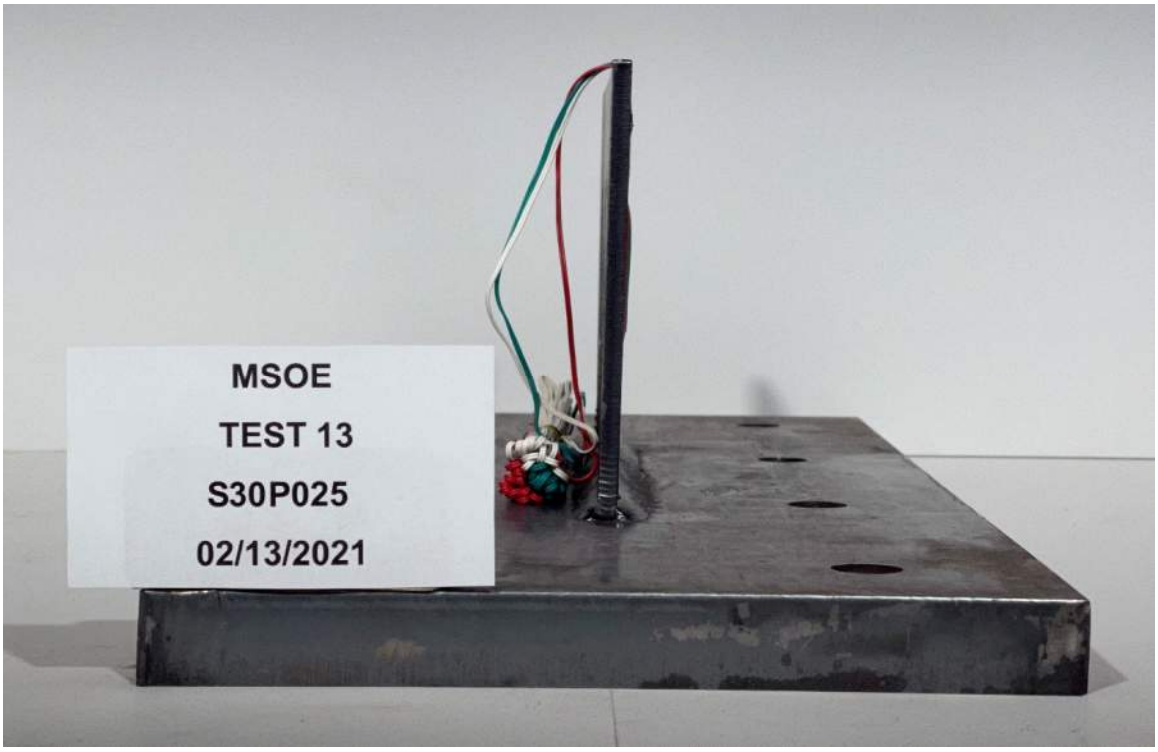

Figure D-48: Side View of S30P025.

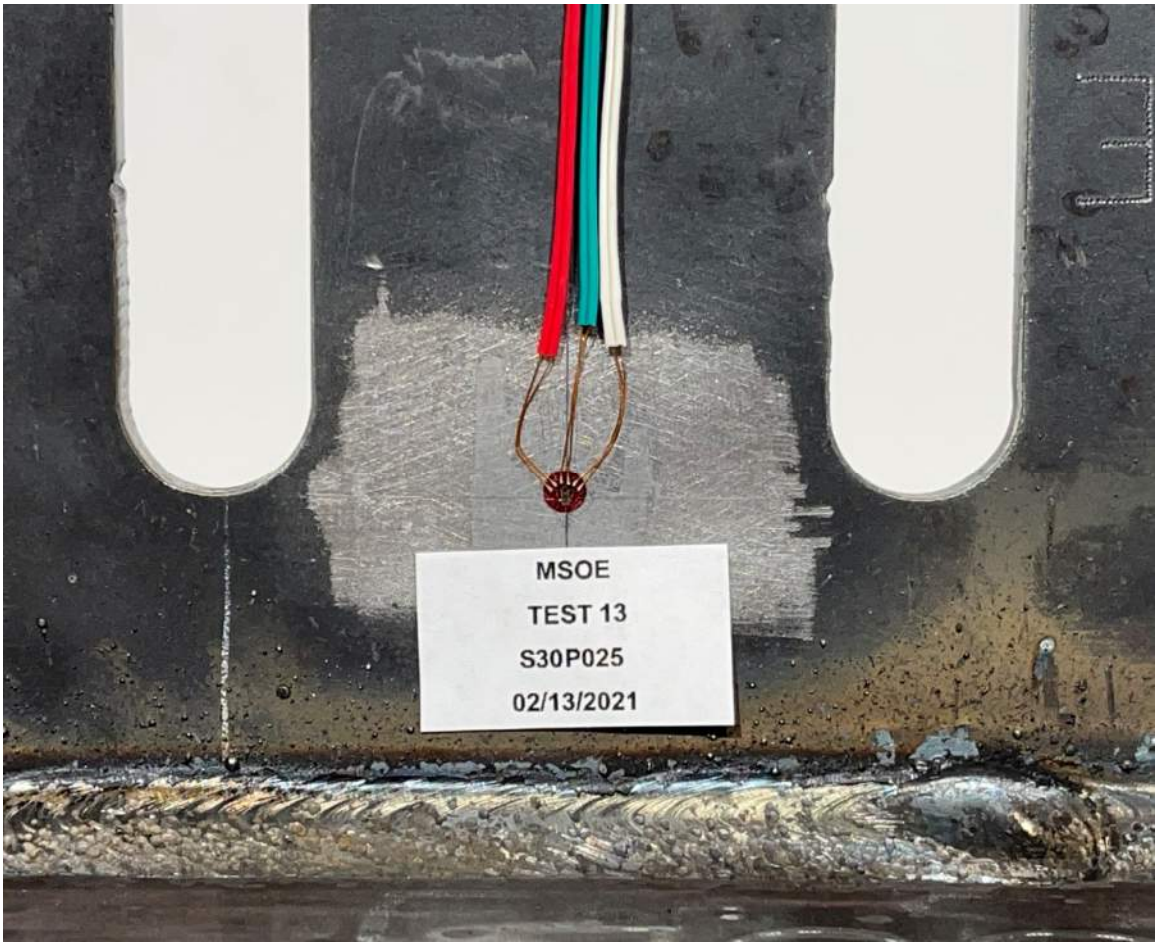

Figure D-49: Close-up View on Rosette of S30P025.

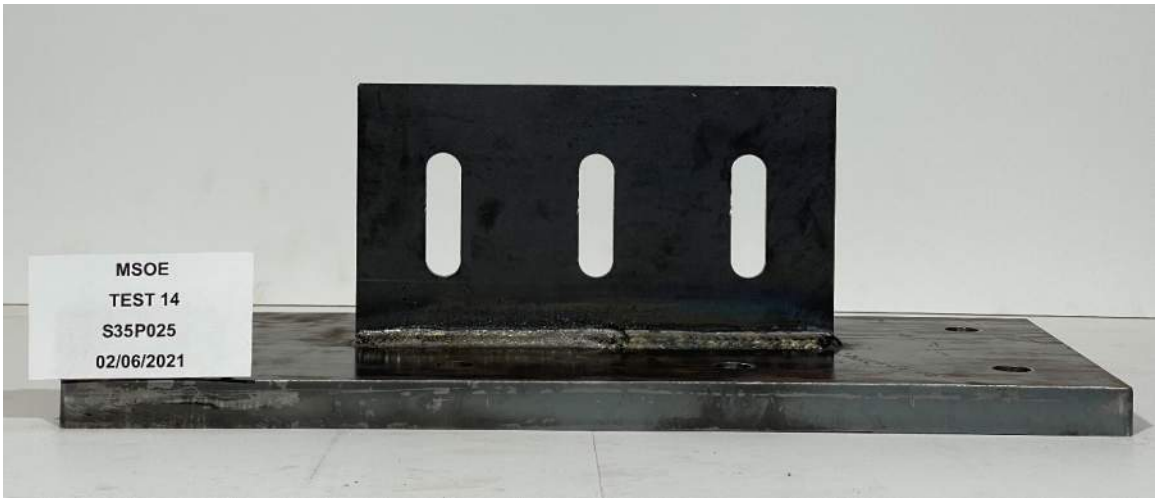

Figure D-50: Front View of S35P025.

Figure D-51: Top View of S35P025.

Figure D-52: Side View of S35P025.

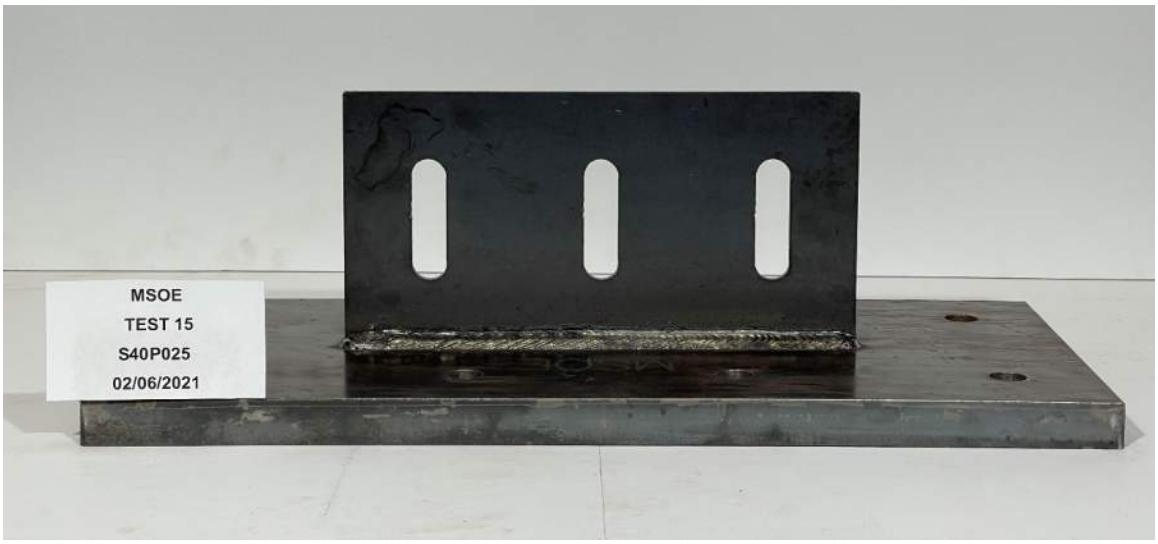

Figure D-53: Front View of S40P025.

Figure D-54: Top View of S40P025.

Figure D-55: Side View of S40P025.

Figure D-56: Front View of S45P025.

Figure D-57: Top View of S45P025.

Figure D-58: Side View of S45P025.

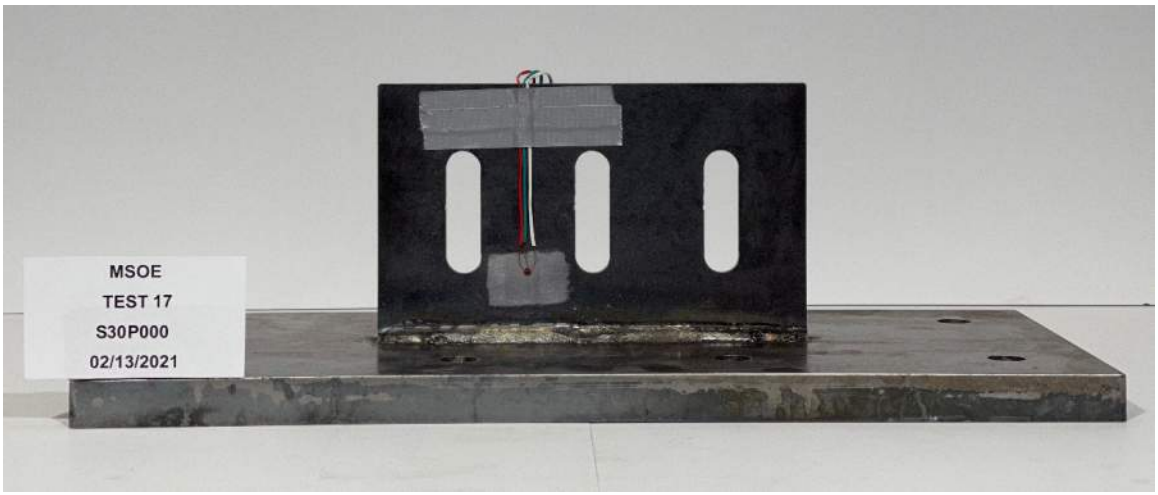

Figure D-59: Front View of S30P000.

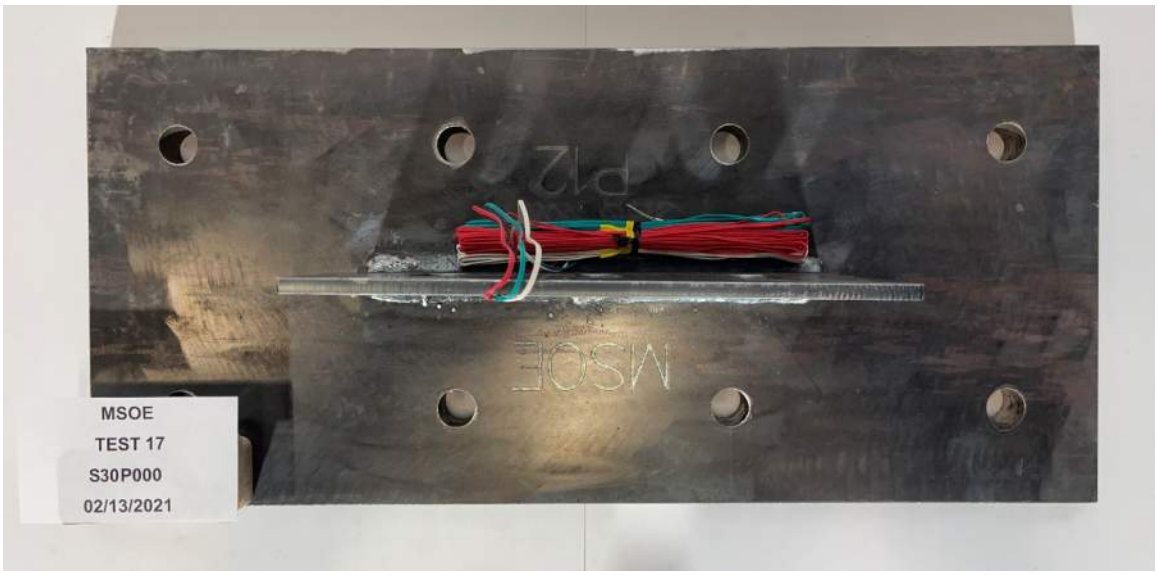

Figure D-60: Top View of S30P000.

Figure D-61: Side View of S30P000.

Figure D-62: Close-up View on Rosette of S30P000.

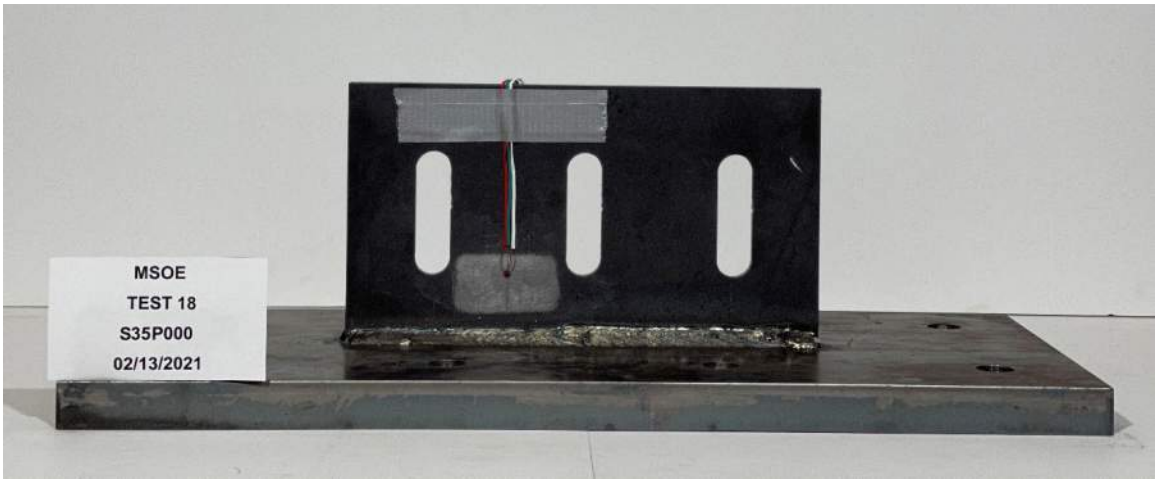

Figure D-63: Front View of S35P000.

Figure D-64: Top View of S35P000.

Figure D-65: Side View of S35P000.

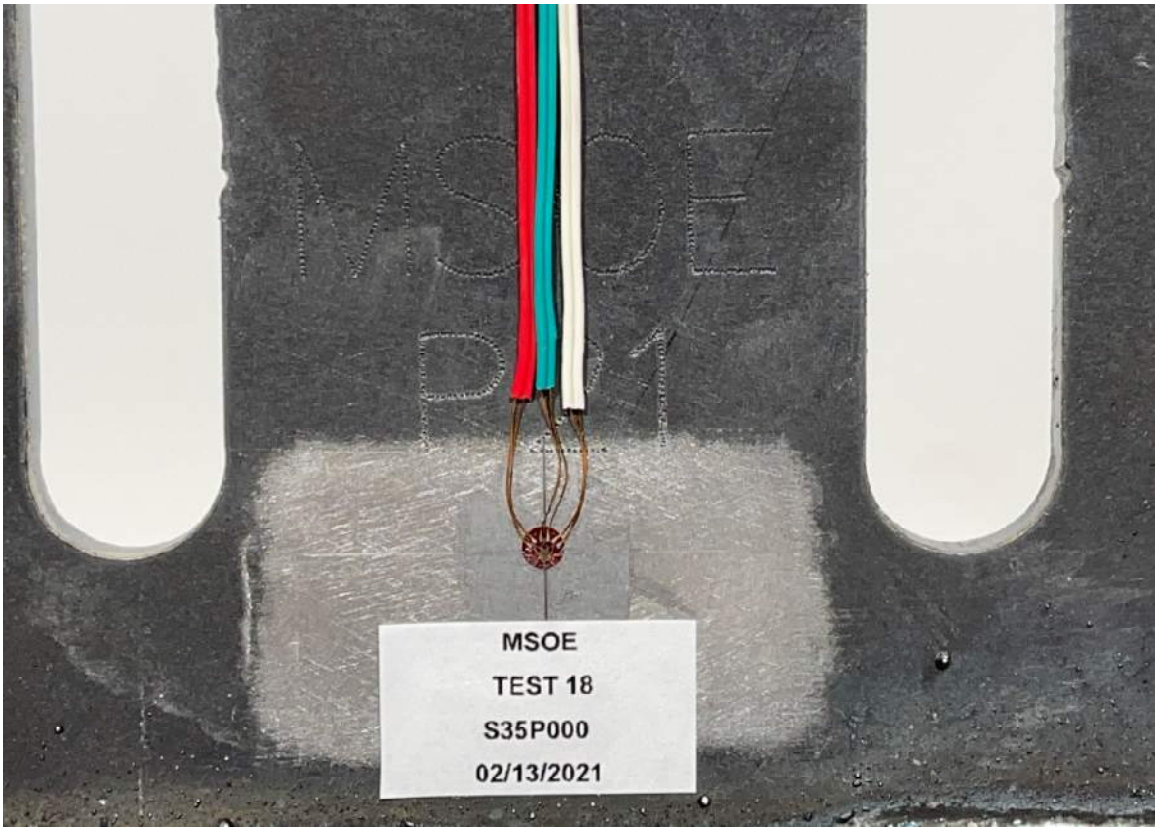

Figure D-66: Close-up View on Rosette of S35P000.

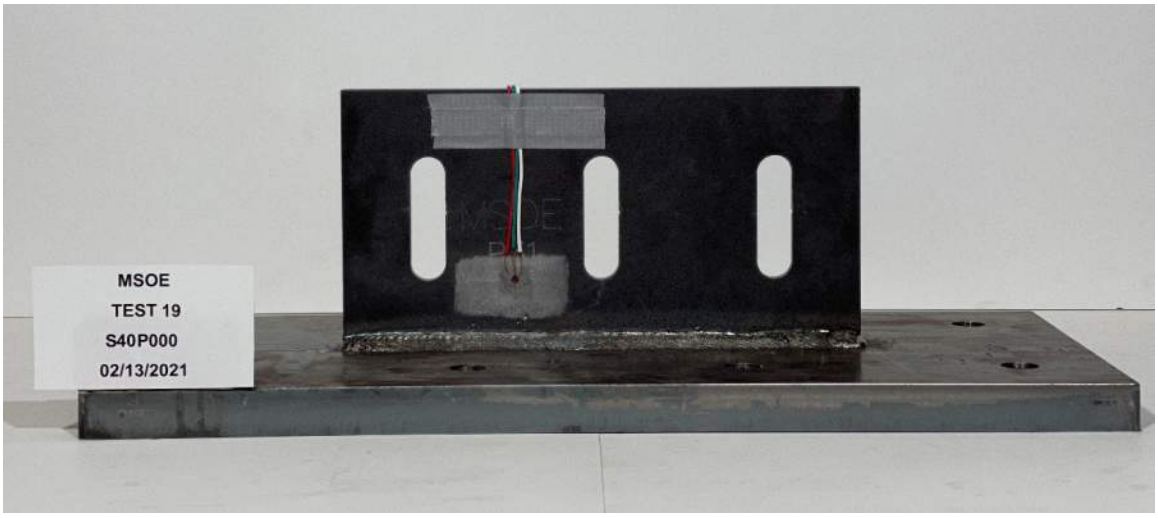

Figure D-67: Front View of S40P000.

Figure D-68: Top View of S40P000.

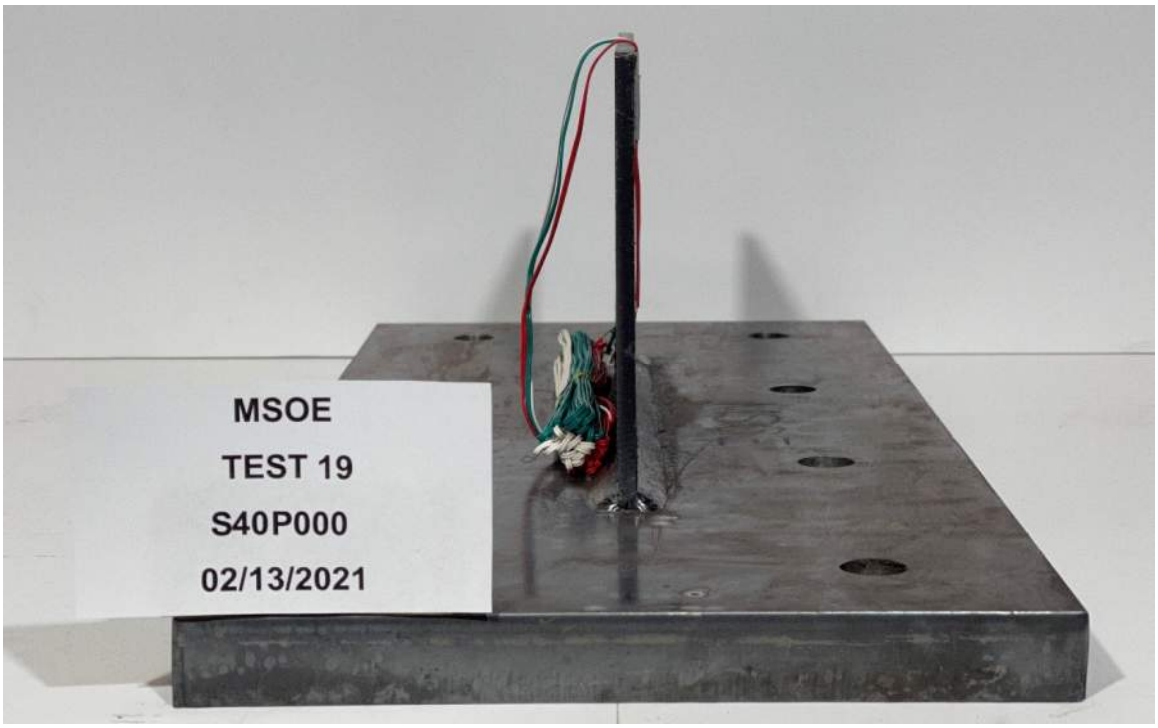

Figure D-69: Side View of S40P000.

Figure D-70: Close-up View on Rosette of S40P000.

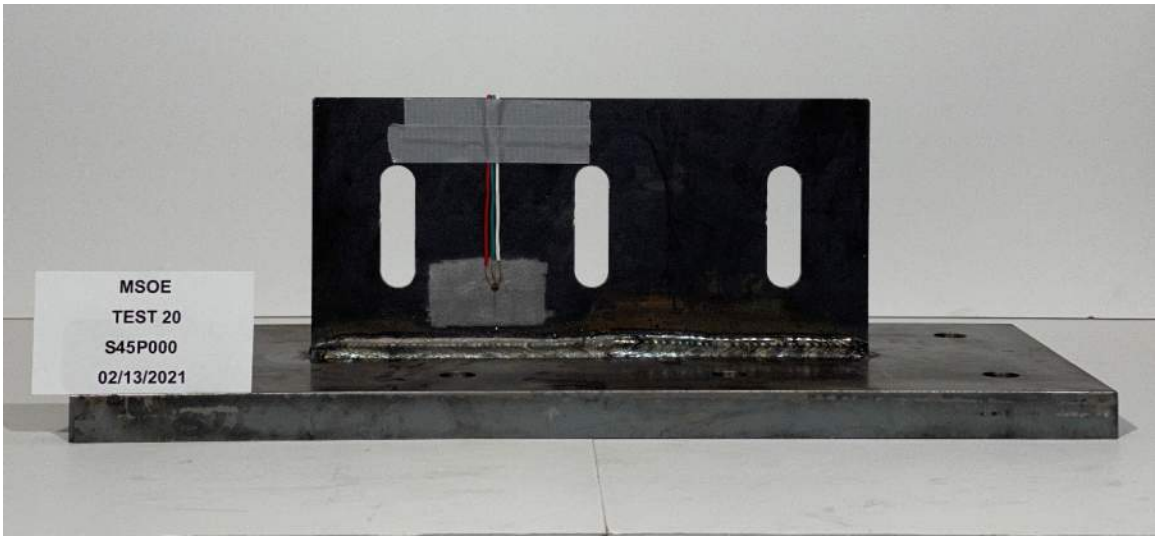

Figure D-71: Front View of S45P000.

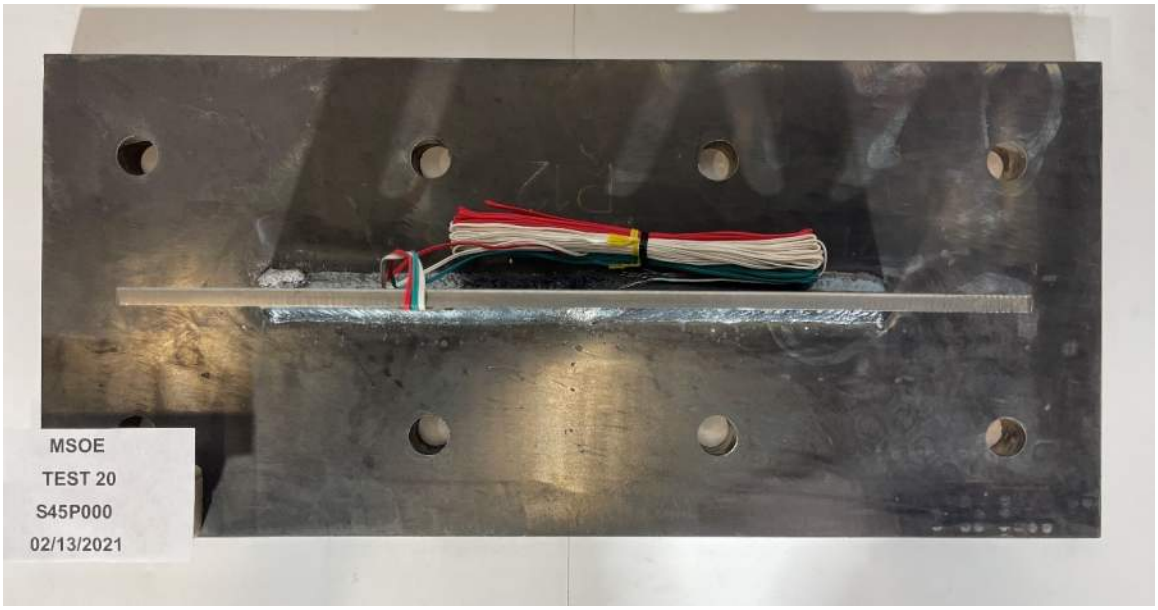

Figure D-72: Top View of S45P000.

Figure D-73: Side View of S45P000.

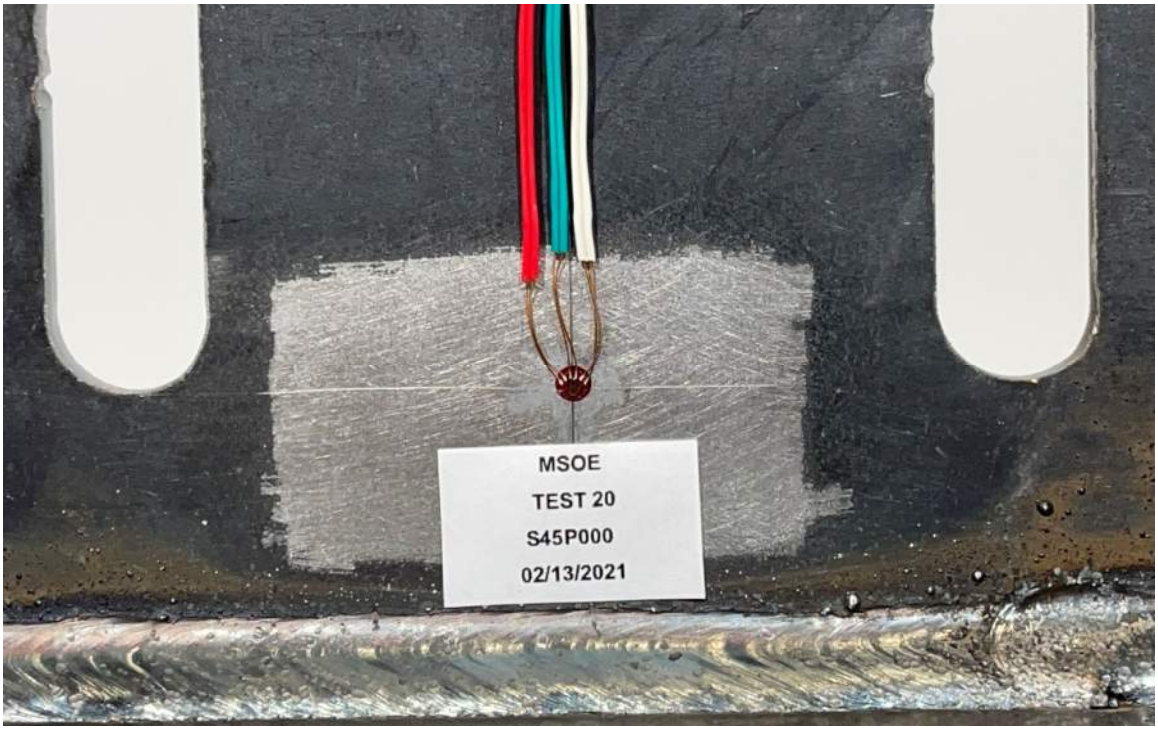

Figure D-74: Close-up View on Rosette of S45P000.

Appendix E. Post-Test Specimen Photos

Figure E-1: Front View of S30P100.

Figure E-2: Top View of S30P100.

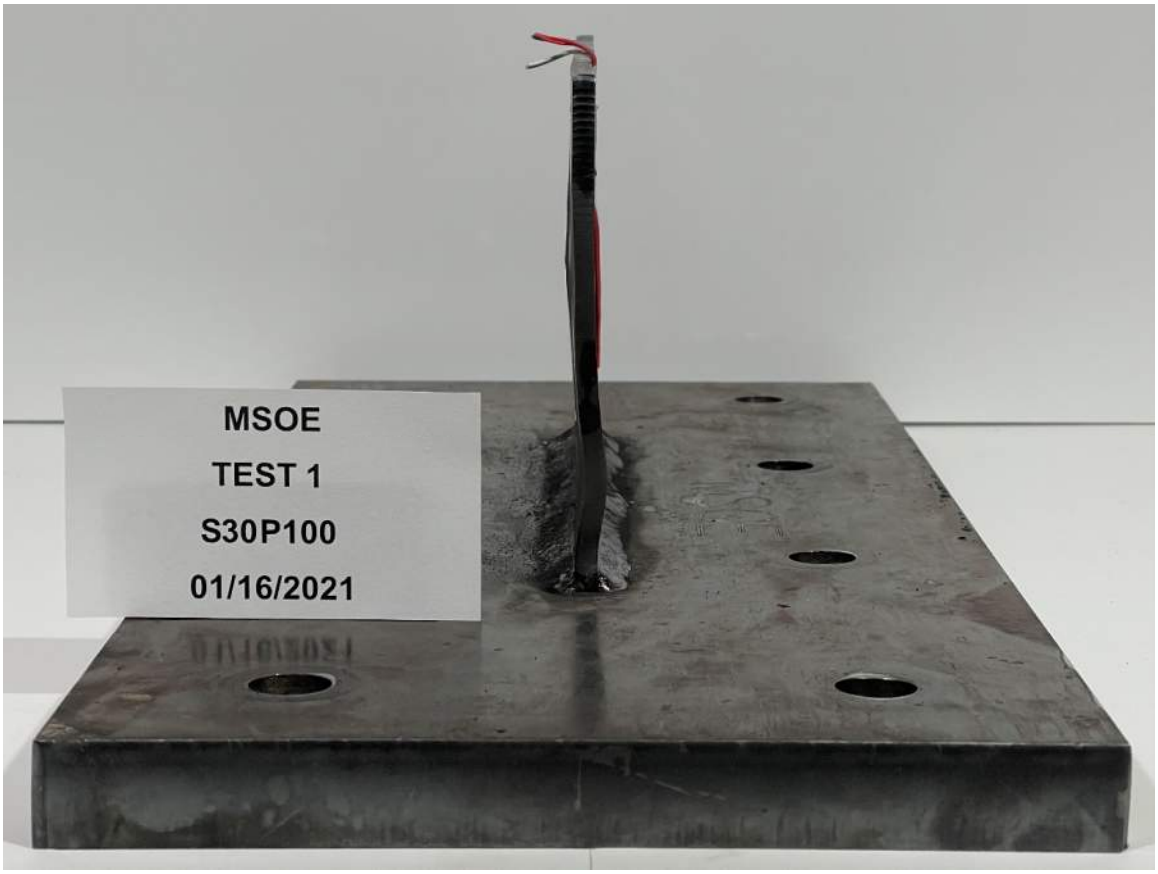

Figure E-3: Side View of S30P100.

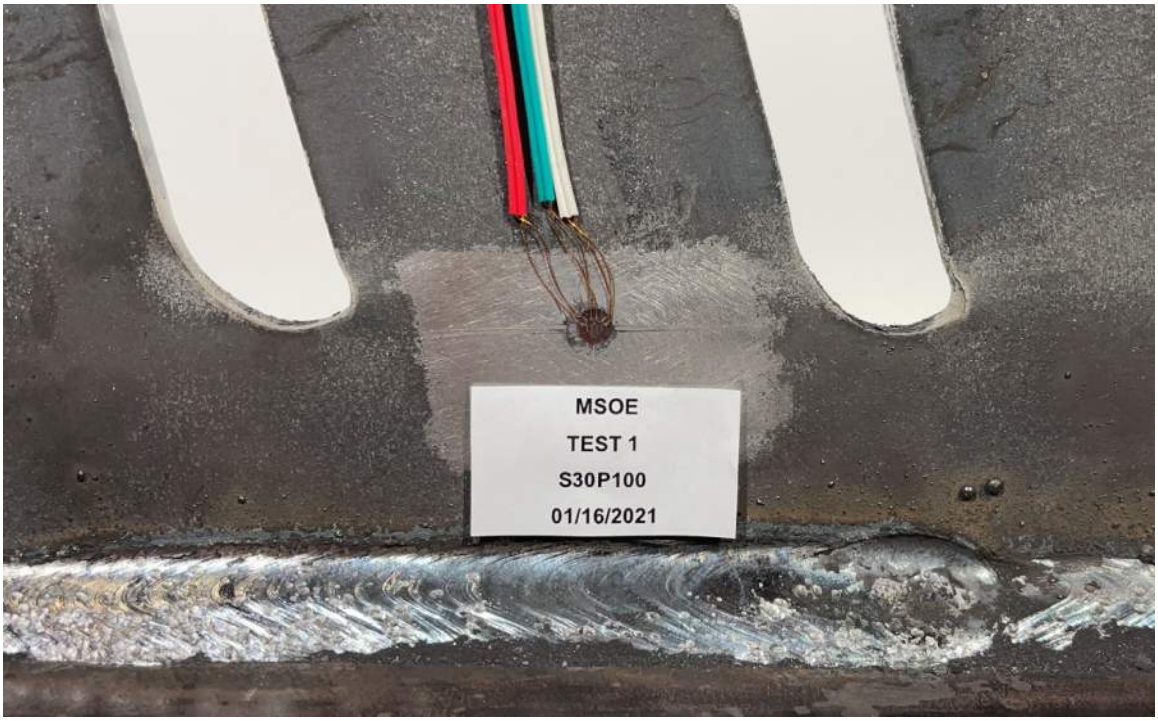

Figure E-4: Close-up View on Rosette of S30P100.

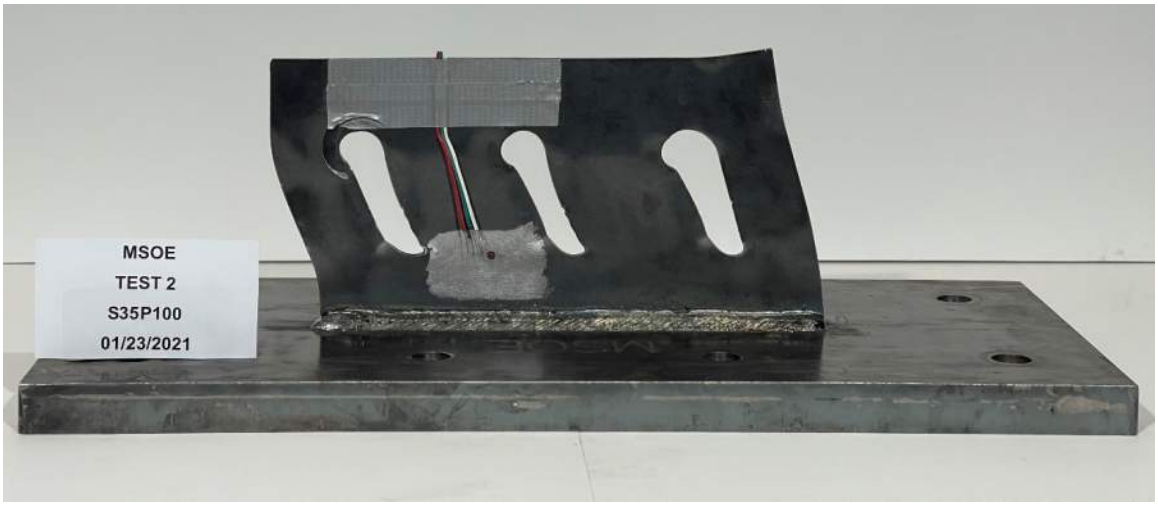

Figure E-5: Front View of S35P100.

Figure E-6: Top View of S35P100.

Figure E-7: Side View of S35P100.

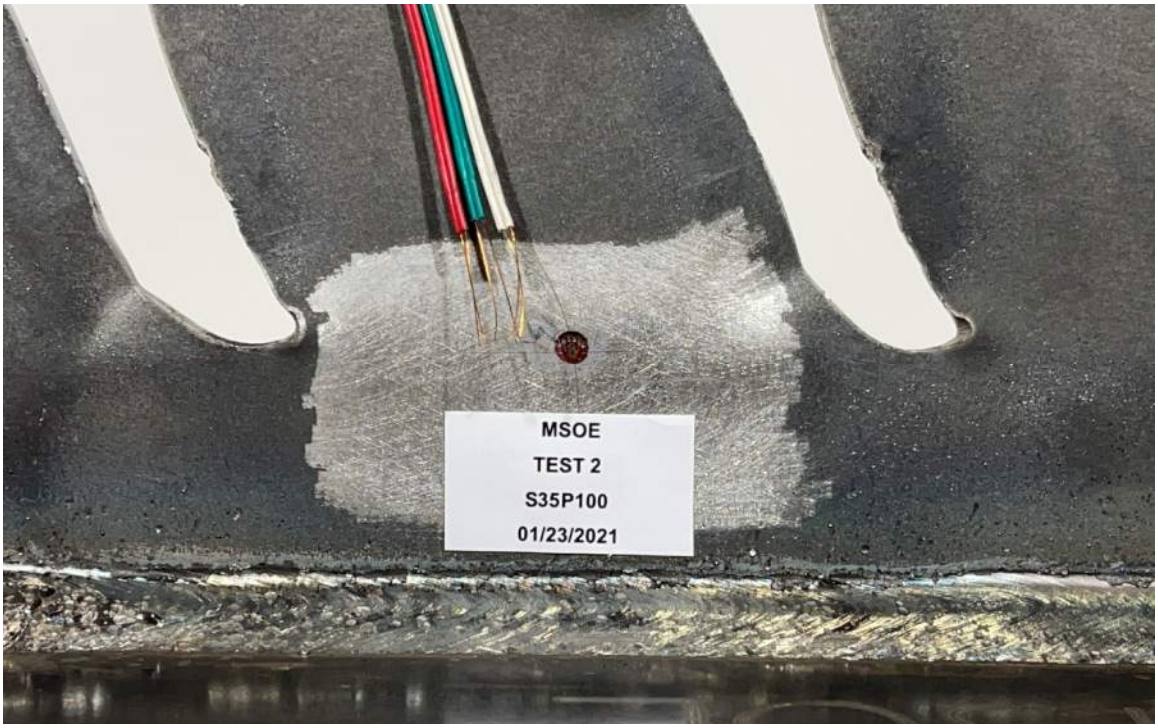

Figure E-8: Close-up View on Rosette of S35P100.

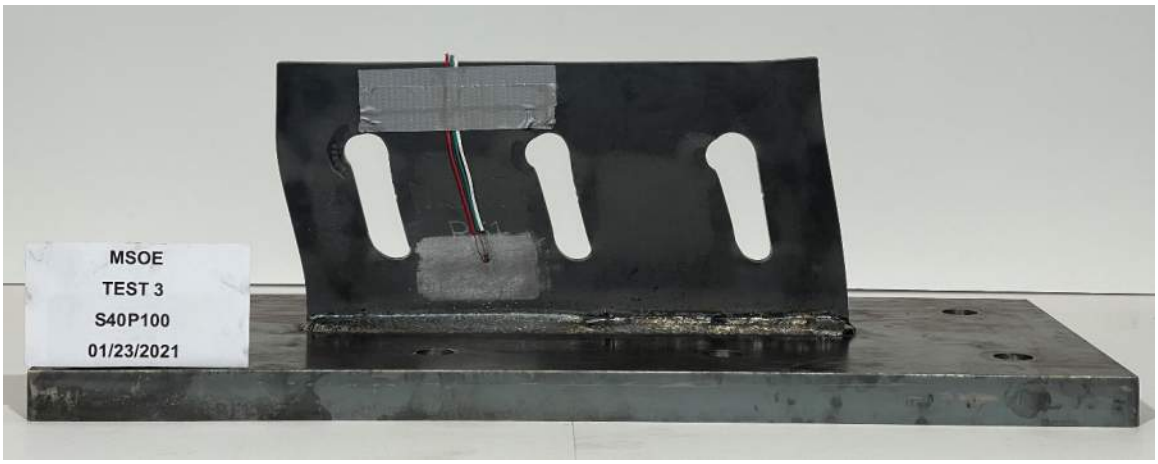

Figure E-9: Front View of S40P100.

Figure E-10: Top View of S40P100.

Figure E-11: Side View of S40P100.

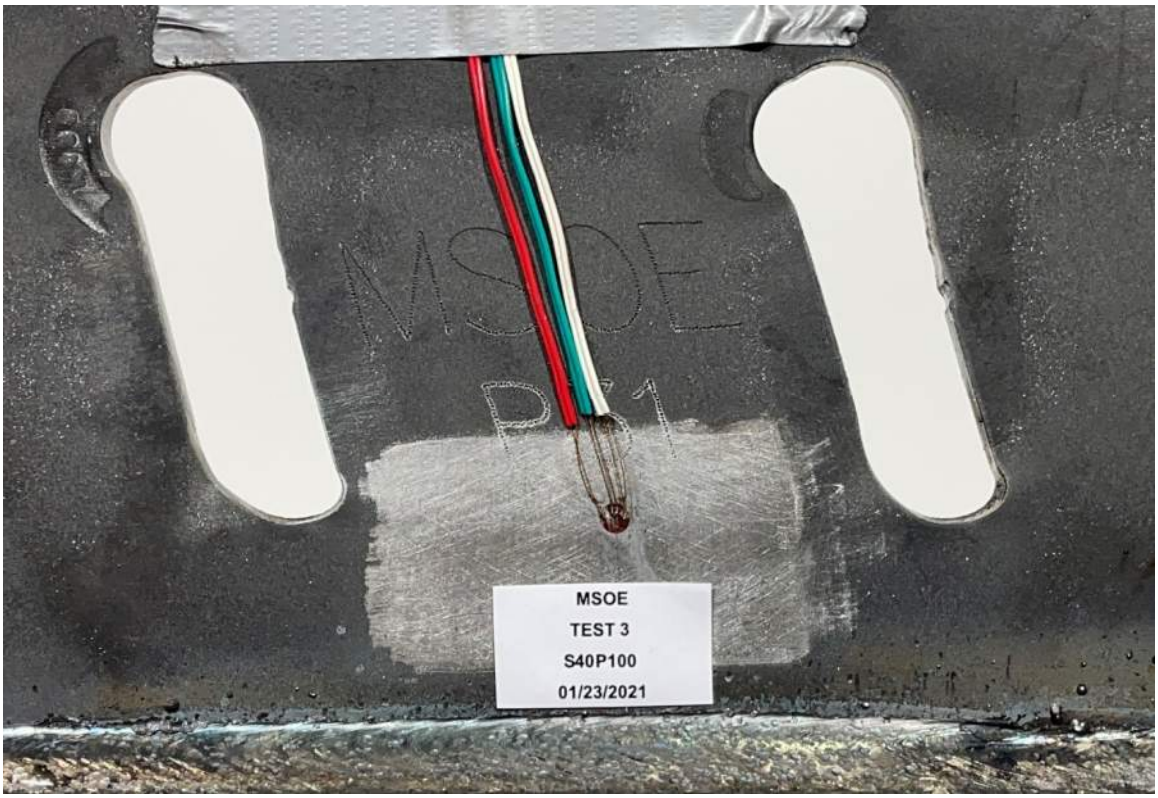

Figure E-12: Close-up View on Rosette of S40P100.

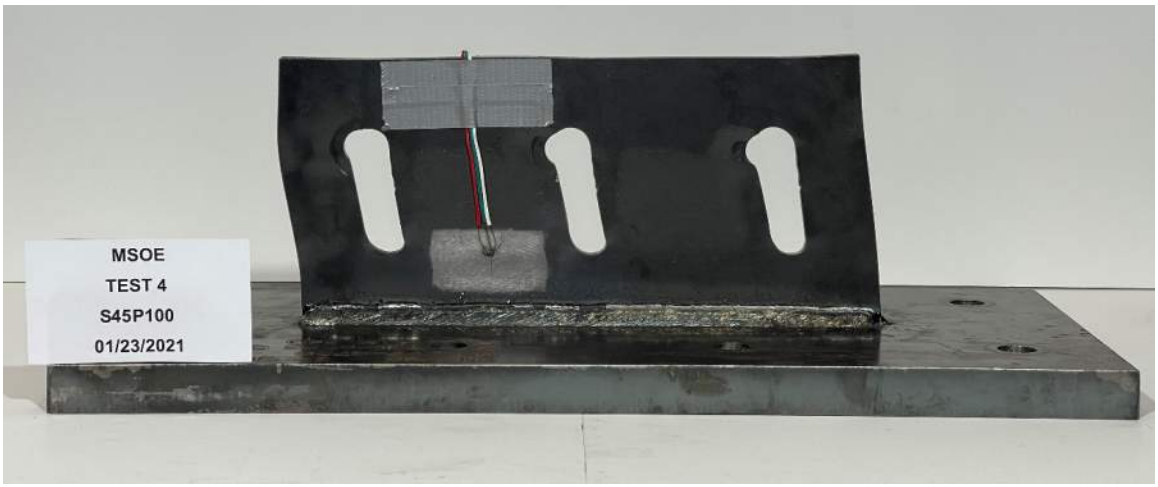

Figure E-13: Front View of S45P100.

Figure E-14: Top View of S45P100.

Figure E-15: Side View of S45P100.

Figure E-16: Close-up View on Rosette of S45P100.

Figure E-17: Front View of S30P075.

Figure E-18: Top View of S30P075.

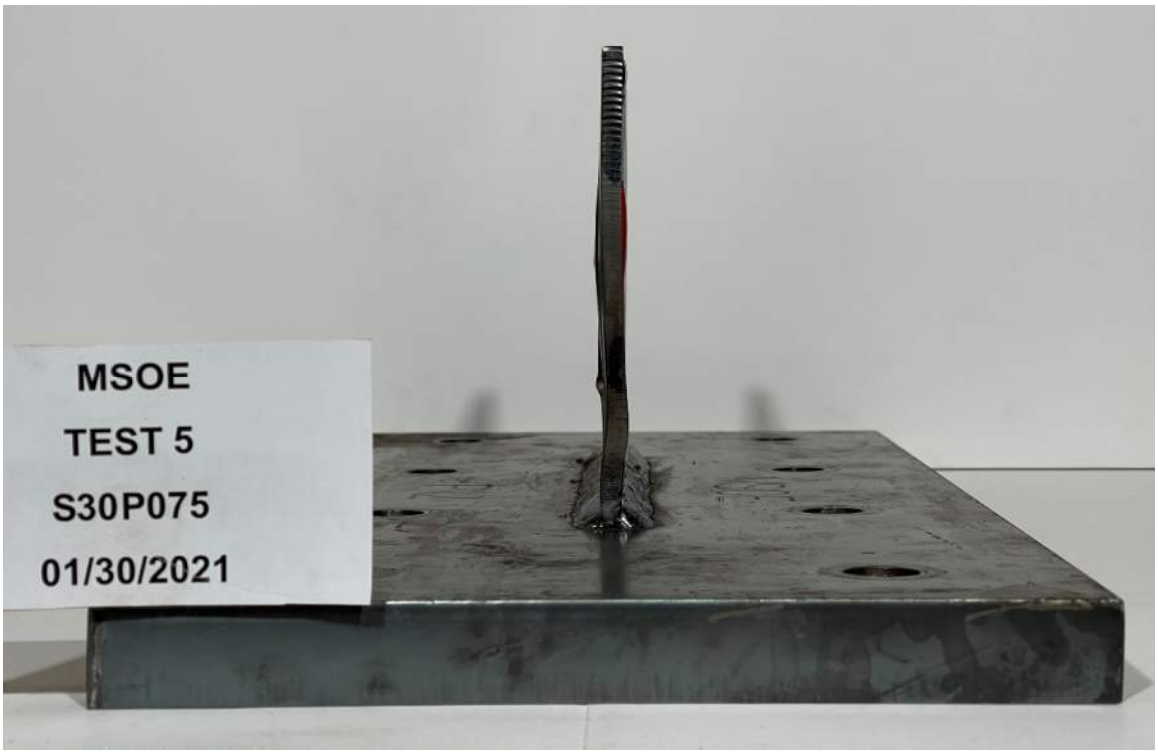

Figure E-19: Side View of S30P075.

Figure E-20: Close-up View on Rosette of S30P075.

Figure E-21: Front View of S35P075.

Figure E-22: Top View of S35P075.

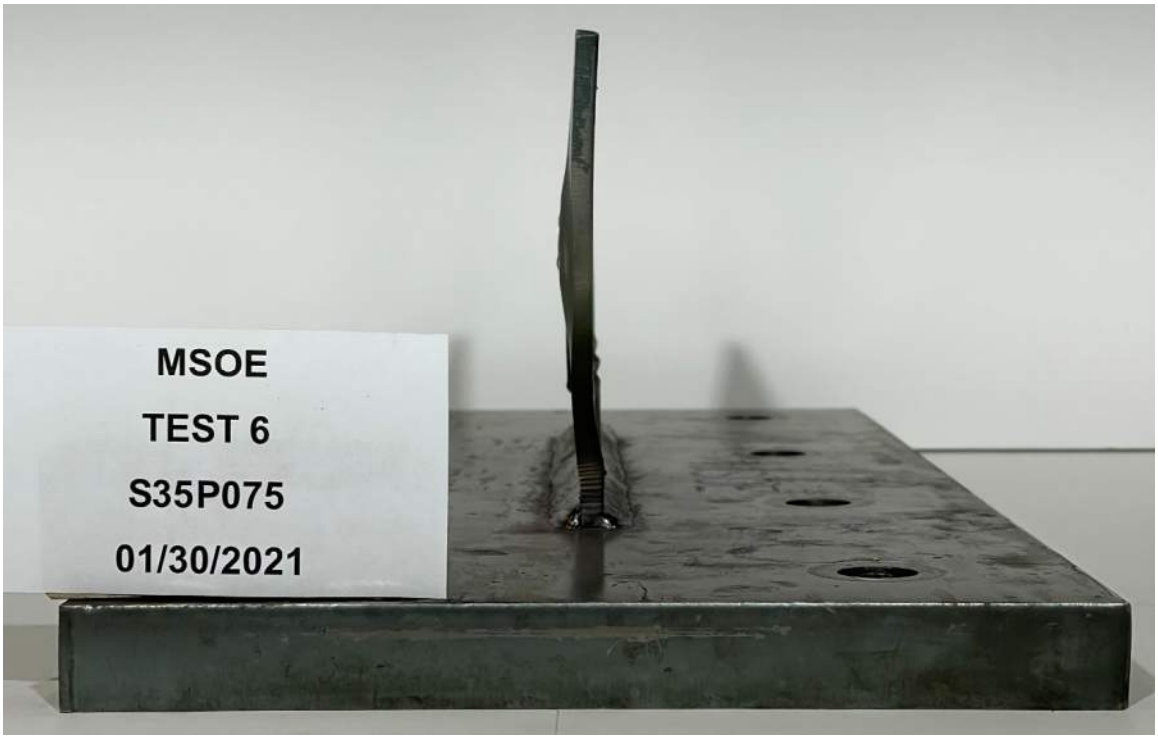

Figure E-23: Side View of S35P075.

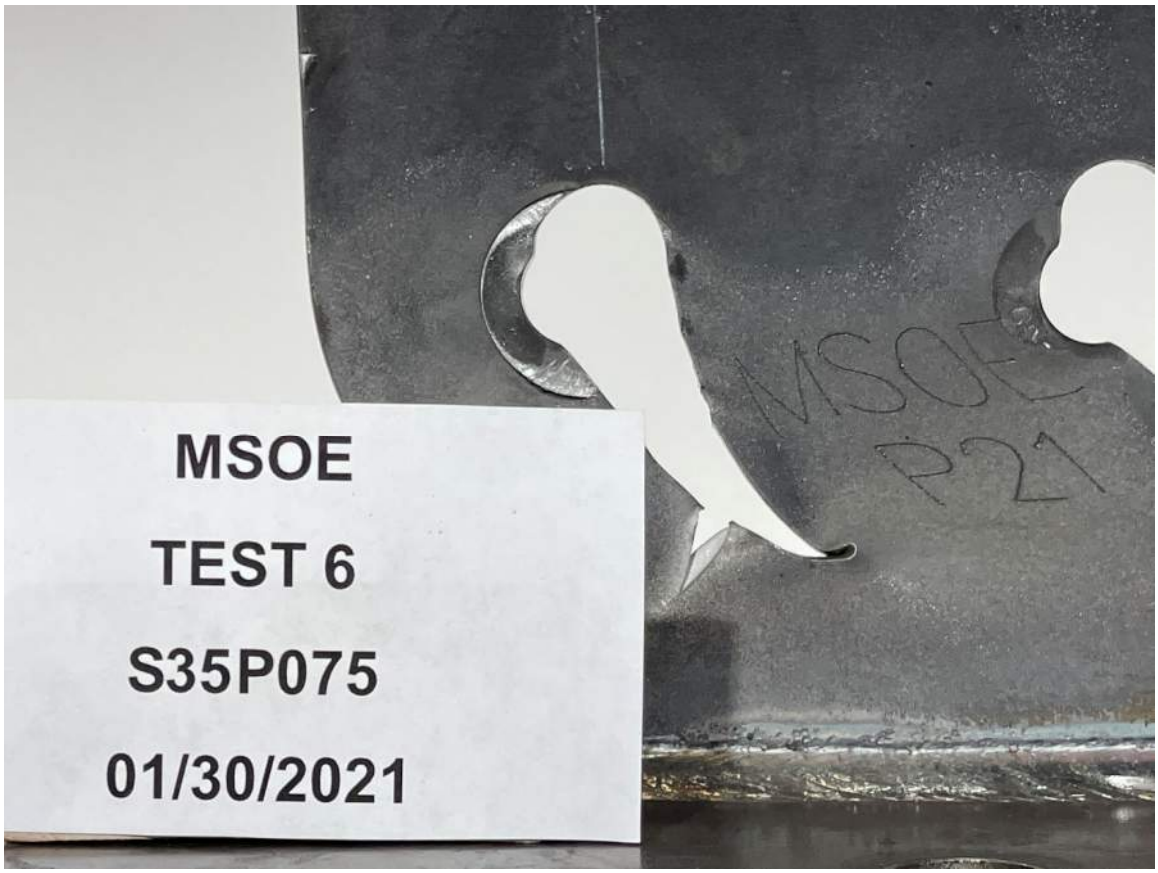

Figure E-24: Close-up View on Plate Tear of S35P075.

Figure E-25: Front View of S40P075.

Figure E-26: Top View of S40P075.

Figure E-27: Side View of S40P075.

Figure E-28: Front View of S45P075.

Figure E-29: Top View of S45P075.

Figure E-30: Side View of S45P075.

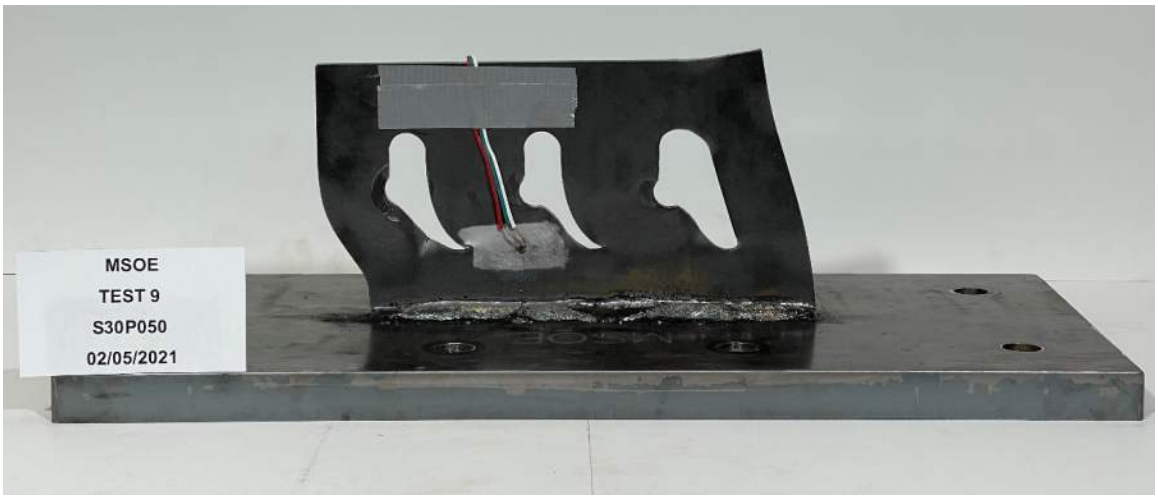

Figure E-31: Front View of S30P050.

Figure E-32: Top View of S30P050.

Figure E-33: Side View of S30P050.

Figure E-34: Close-up View on Rosette of S30P050.

Figure E-35: Close-up View on Plate Tear of S30P050.

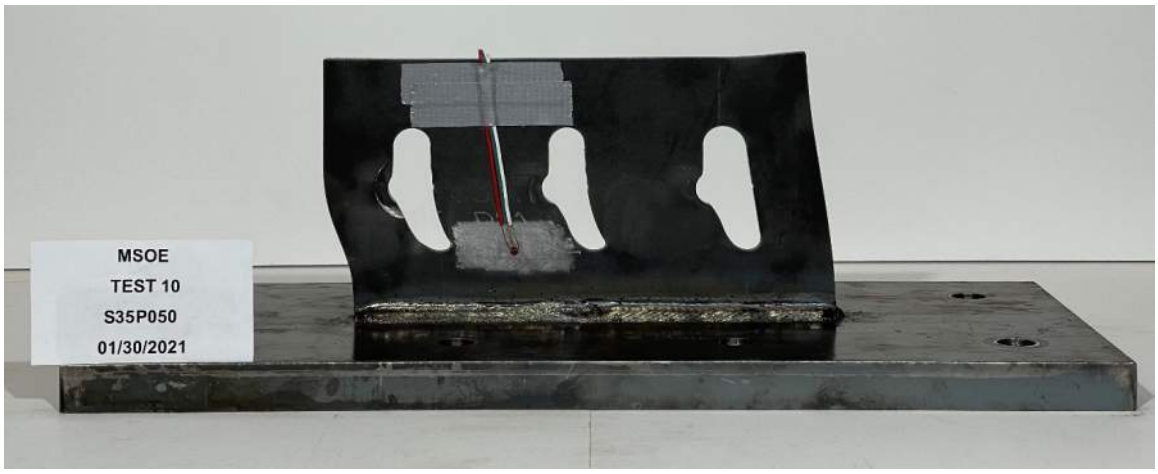

Figure E-36: Front View of S35P050.

Figure E-37: Top View of S35P050.

Figure E-38: Side View of S35P050.

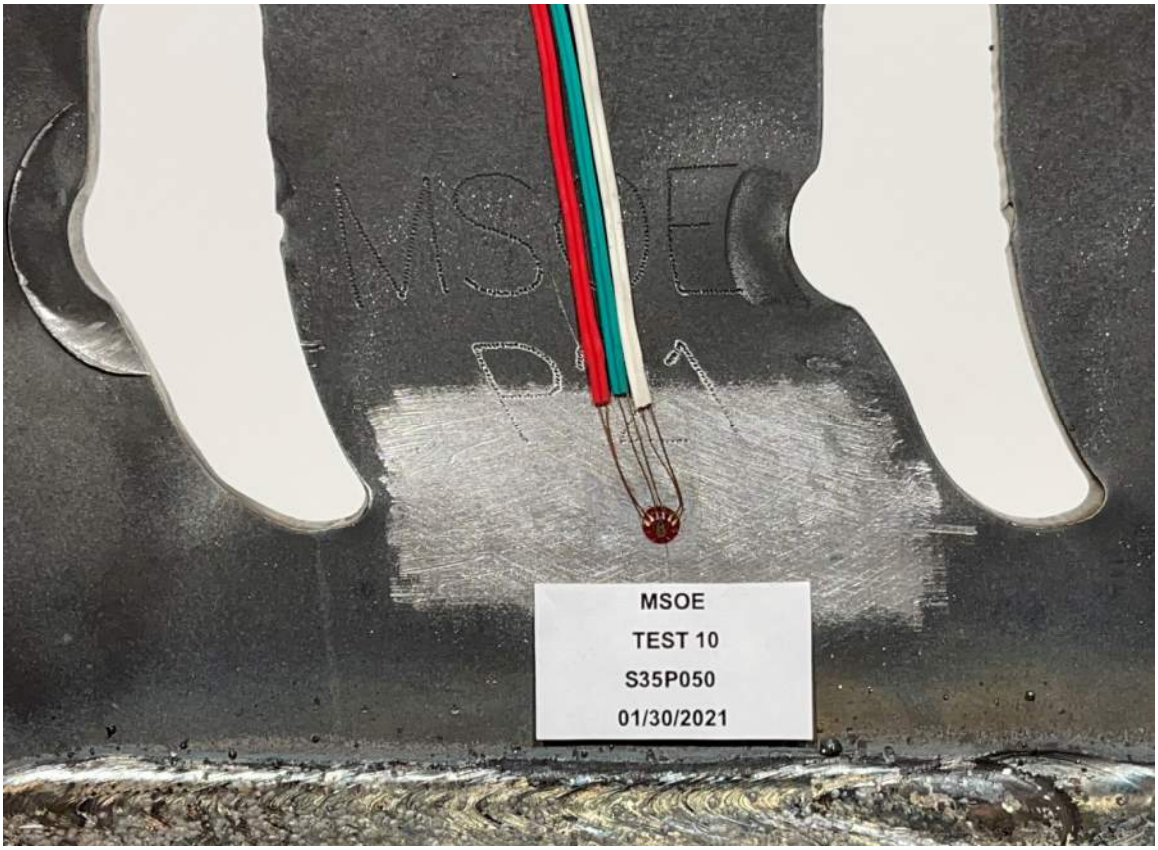

Figure E-39: Close-up View on Rosette of S35P050.

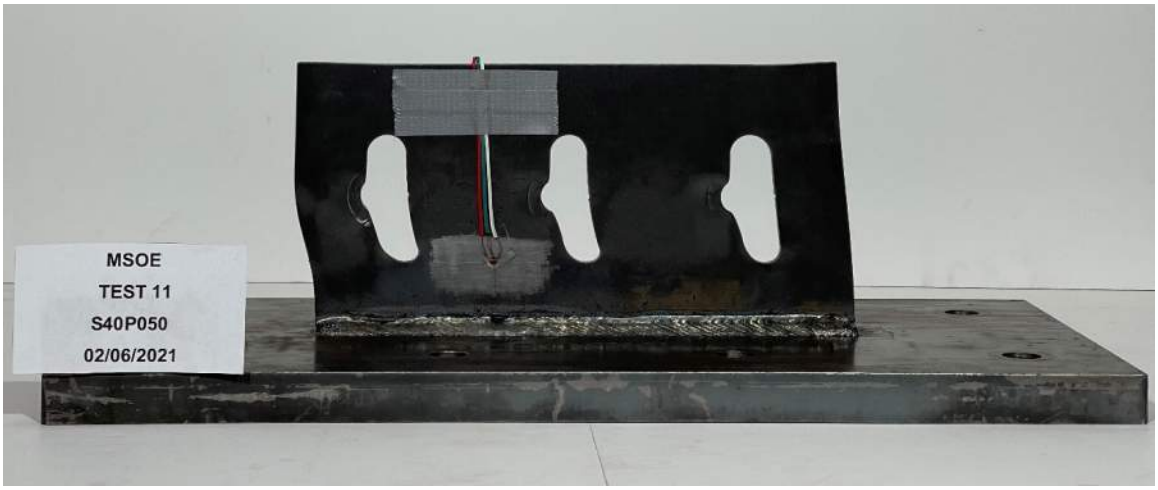

Figure E-40: Front View of S40P050.

Figure E-41: Top View of S40P050.

Figure E-42: Side View of S40P050.

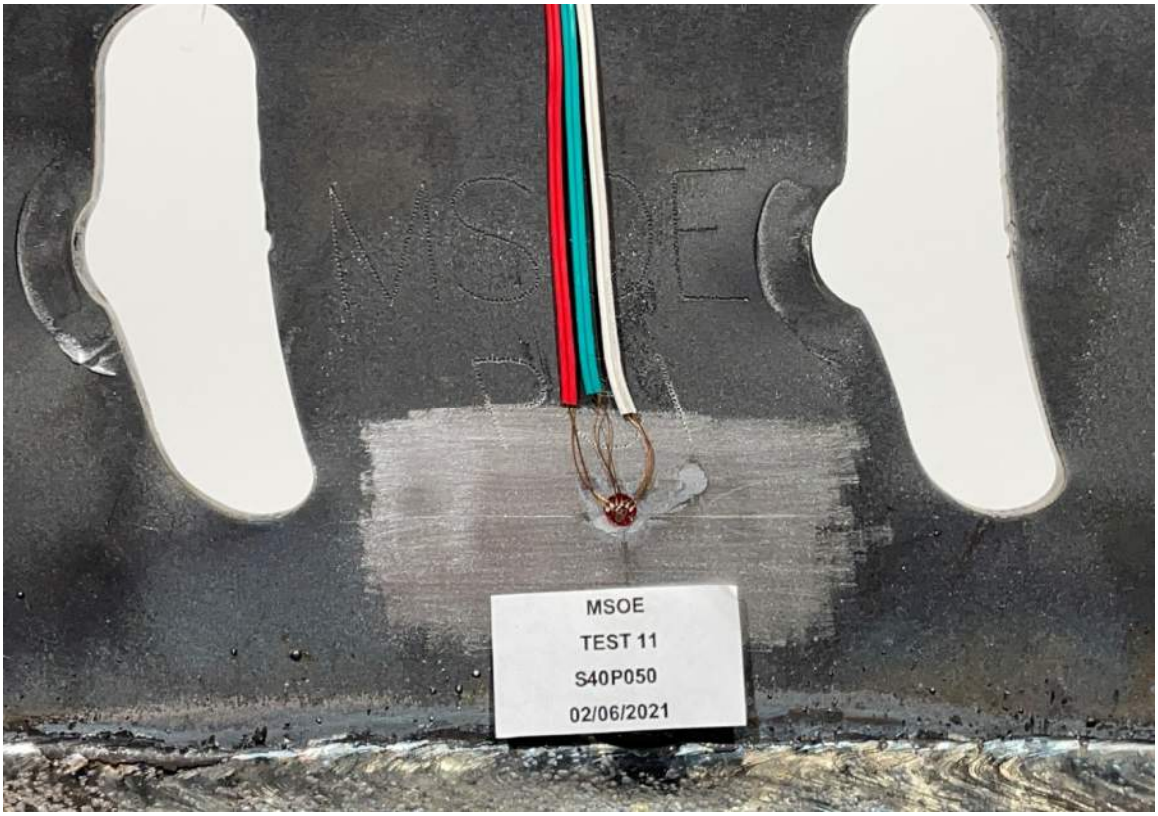

Figure E-43: Close-up View on Rosette of S40P050.

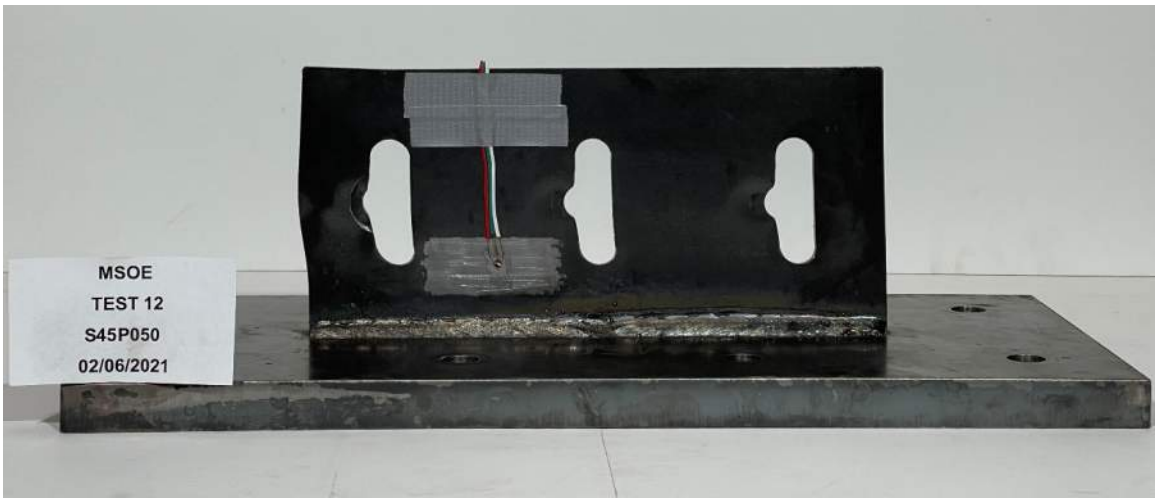

Figure E-44: Front View of S45P050.

Figure E-45: Top View of S45P050.

Figure E-46: Side View of S45P050.

Figure E-47: Close-up View on Rosette of S45P050.

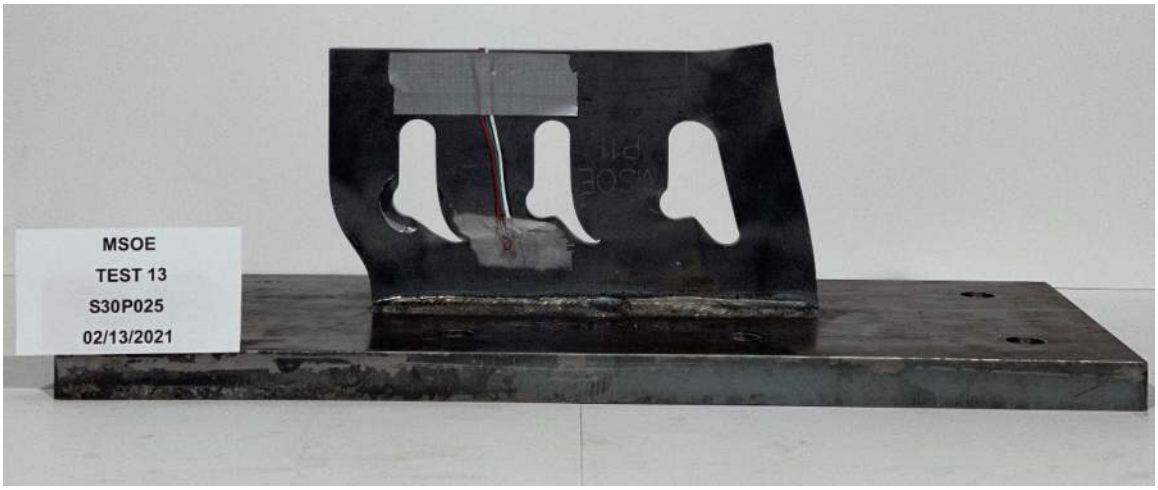

Figure E-48: Front View of S30P025.

Figure E-49: Top View of S30P025.

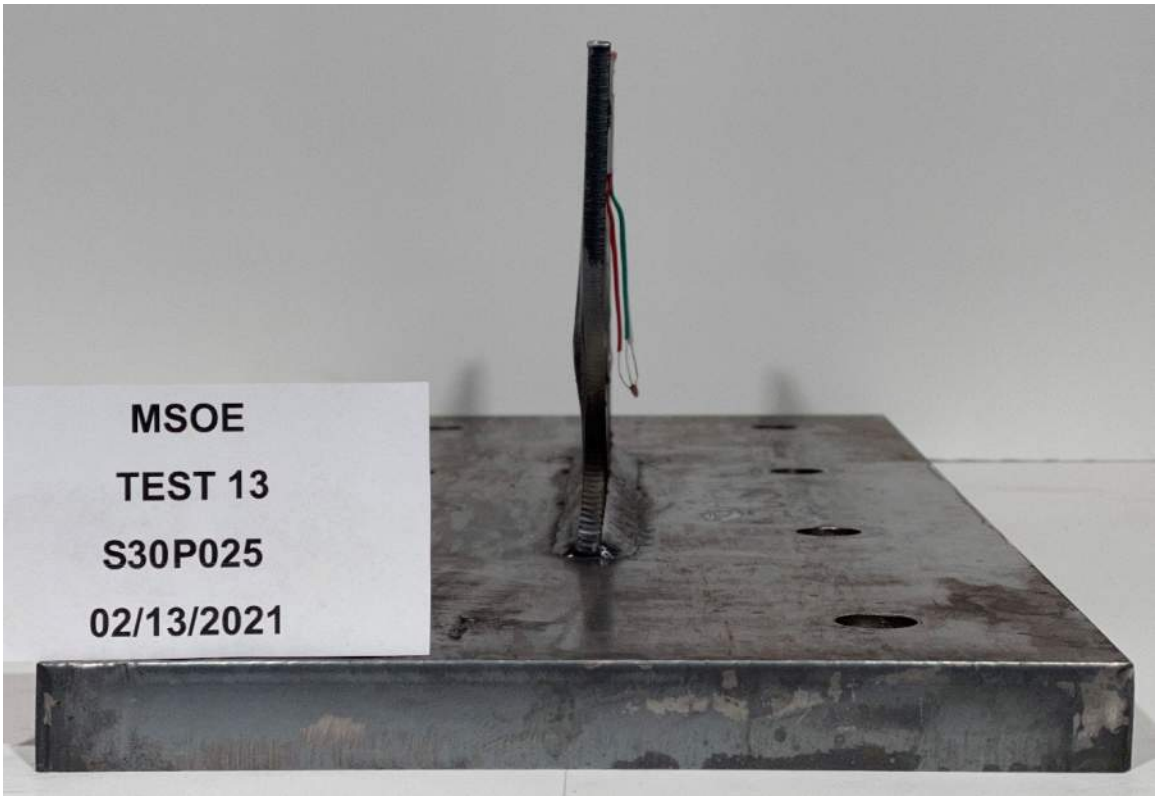

Figure E-50: Side View of S30P025.

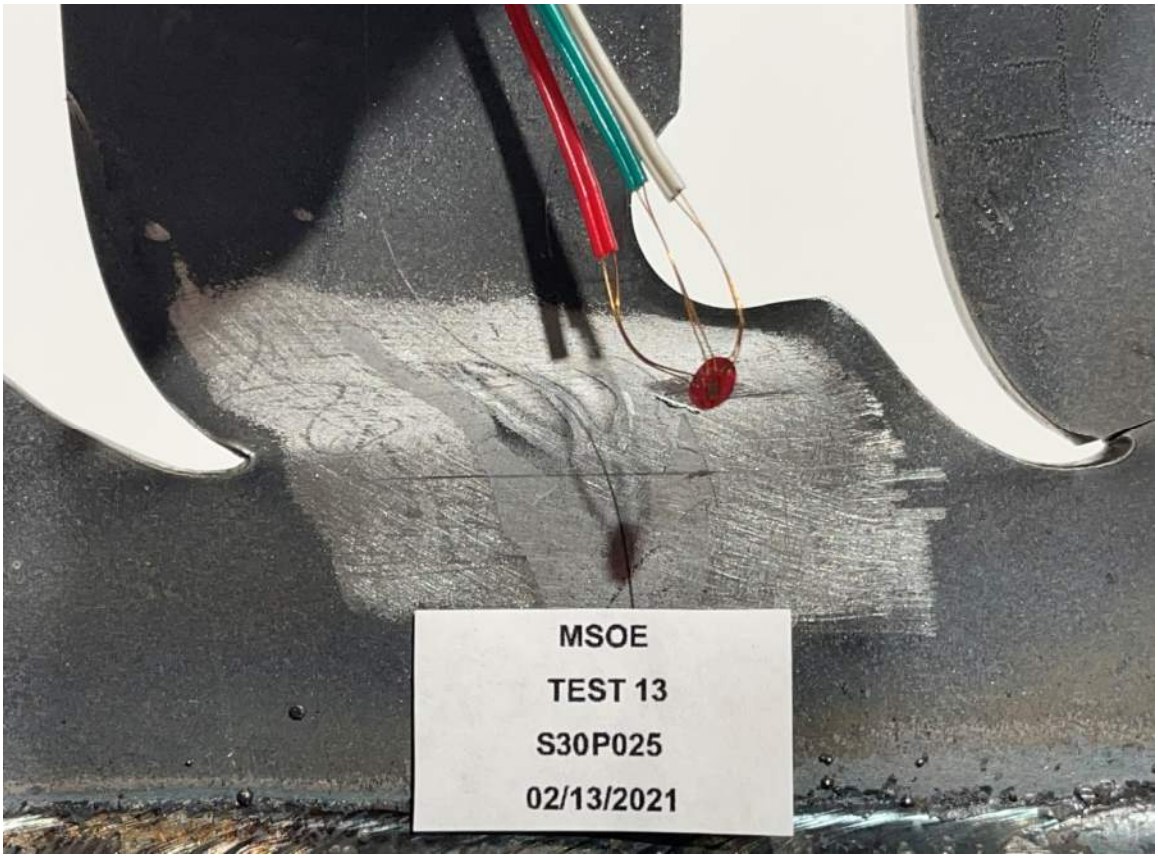

Figure E-51: Close-up View on Rosette of S30P025.

Figure E-52: Front View of S35P025.

Figure E-53: Top View of S35P025.

Figure E-54: Side View of S35P025.

Figure E-55: Front View of S40P025.

Figure E-56: Top View of S40P025.

Figure E-57: Side View of S40P025.

Figure E-58: Front View of S45P025.

Figure E-59: Top View of S45P025.

Figure E-60: Side View of S45P025.

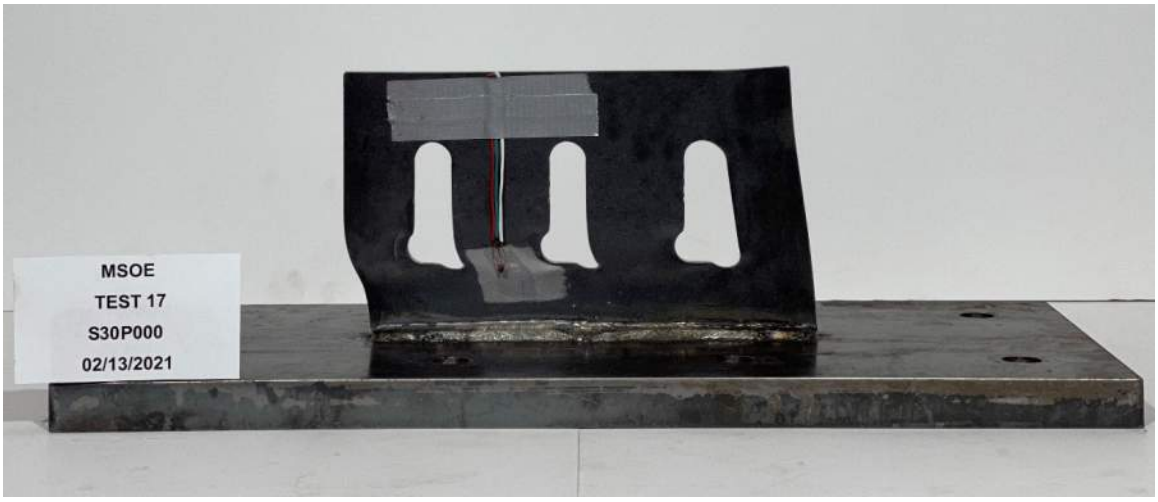

Figure E-61: Front View of S30P000.

Figure E-62: Top View of S30P000.

Figure E-63: Side View of S30P000.

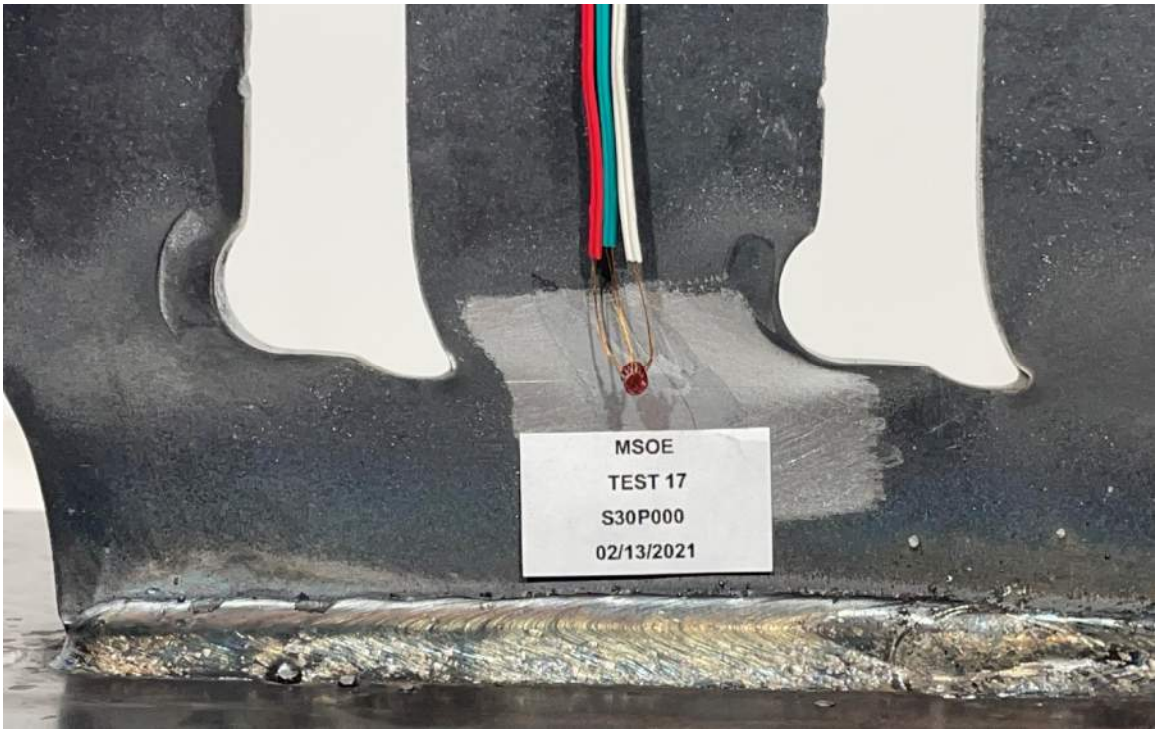

Figure E-64: Close-up View on Rosette of S30P000.

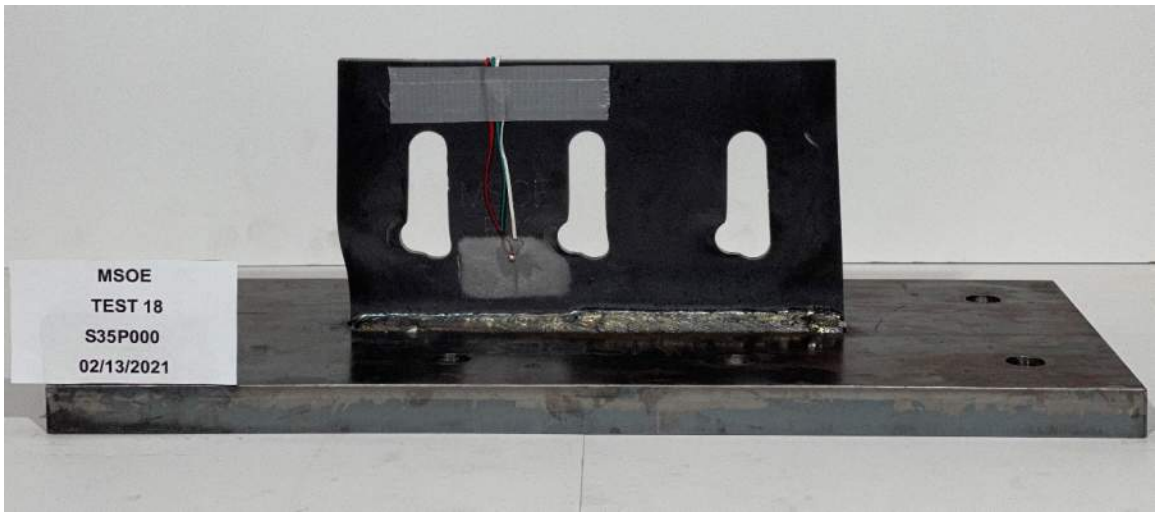

Figure E-65: Front View of S35P000.

Figure E-66: Top View of S35P000.

Figure E-67: Side View of S35P000.

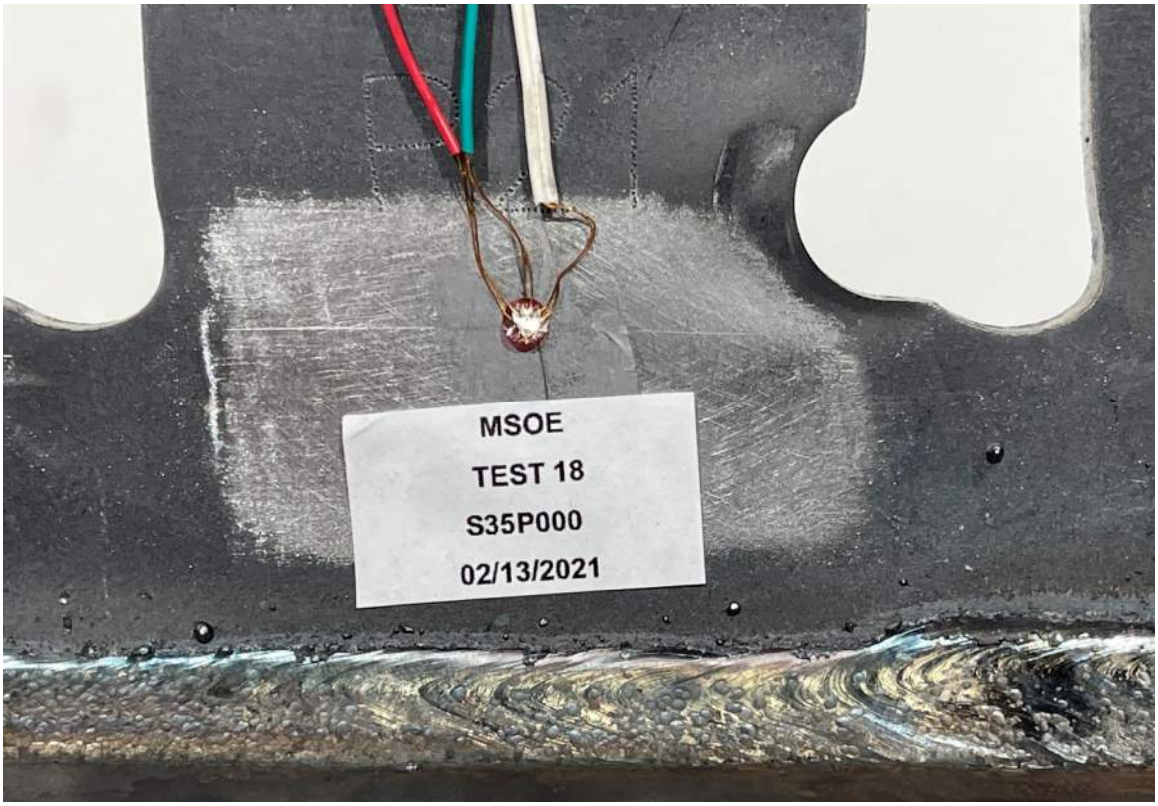

Figure E-68: Close-up View on Rosette of S35P000.

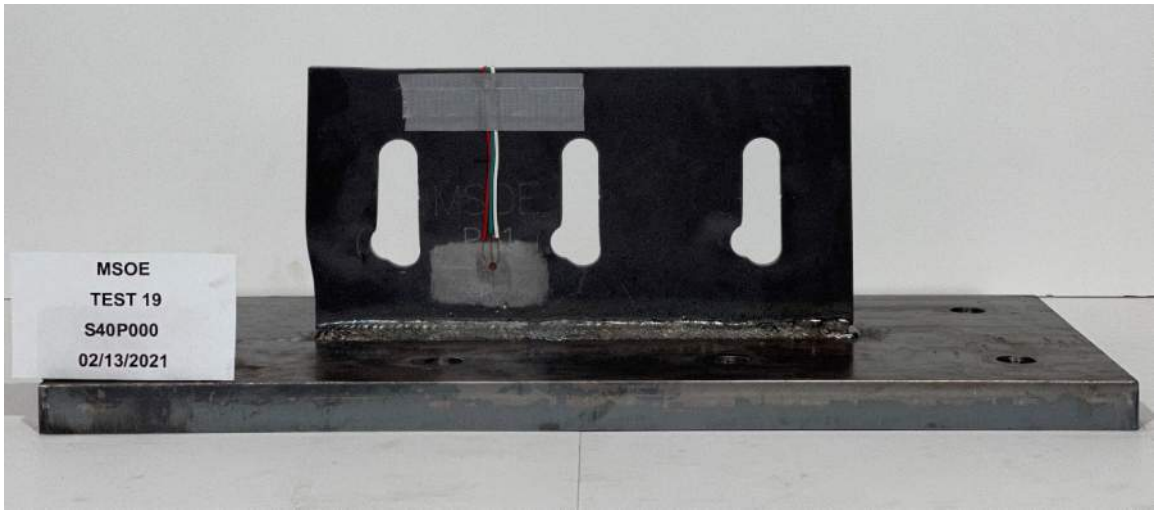

Figure E-69: Front View of S40P000.

Figure E-70: Top View of S40P000.

Figure E-71: Side View of S40P000.

Figure E-72: Close-up View on Rosette of S40P000.

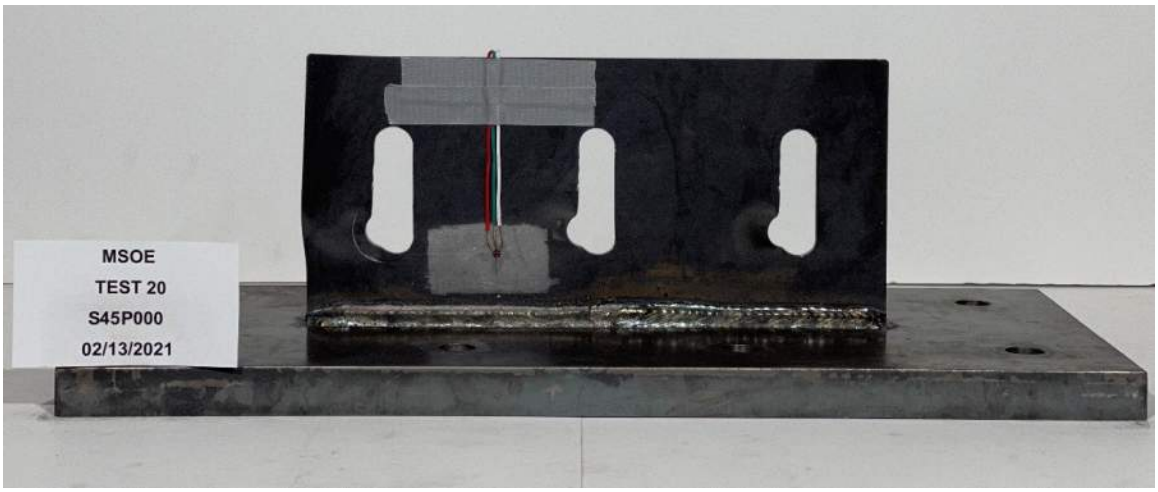

Figure E-73: Front View of S45P000.

Figure E-74: Top View of S45P000.

Figure E-75: Side View of S45P000.

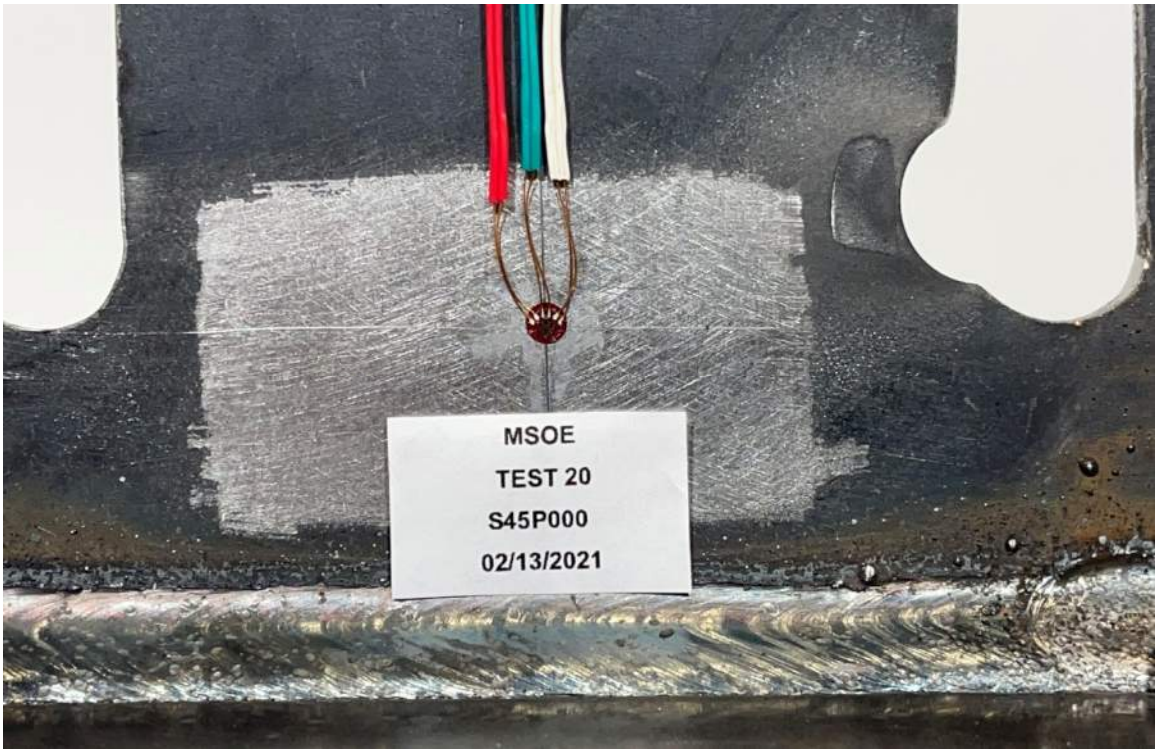

Figure E-76: Close-up View on Rosette of S45P000.

Appendix F. Load versus Base Plate Uplift Graphs

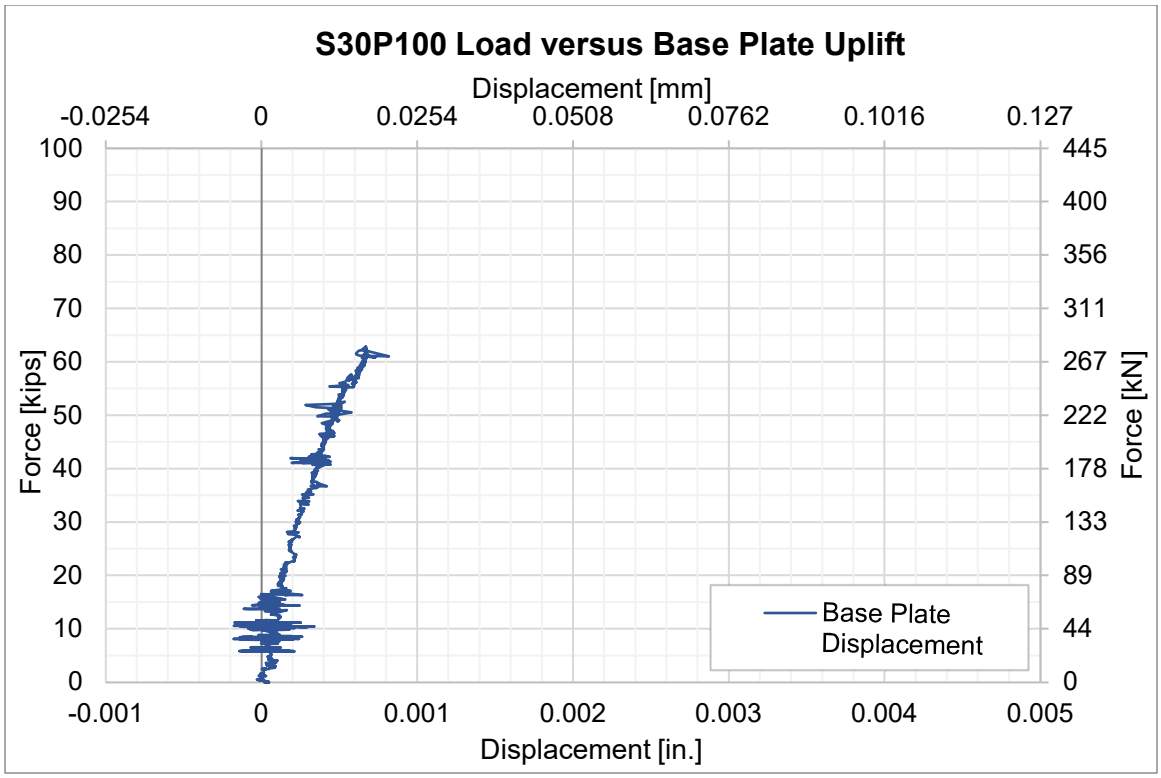

Figure F-1: S30P100 Vertical Displacement Graph.

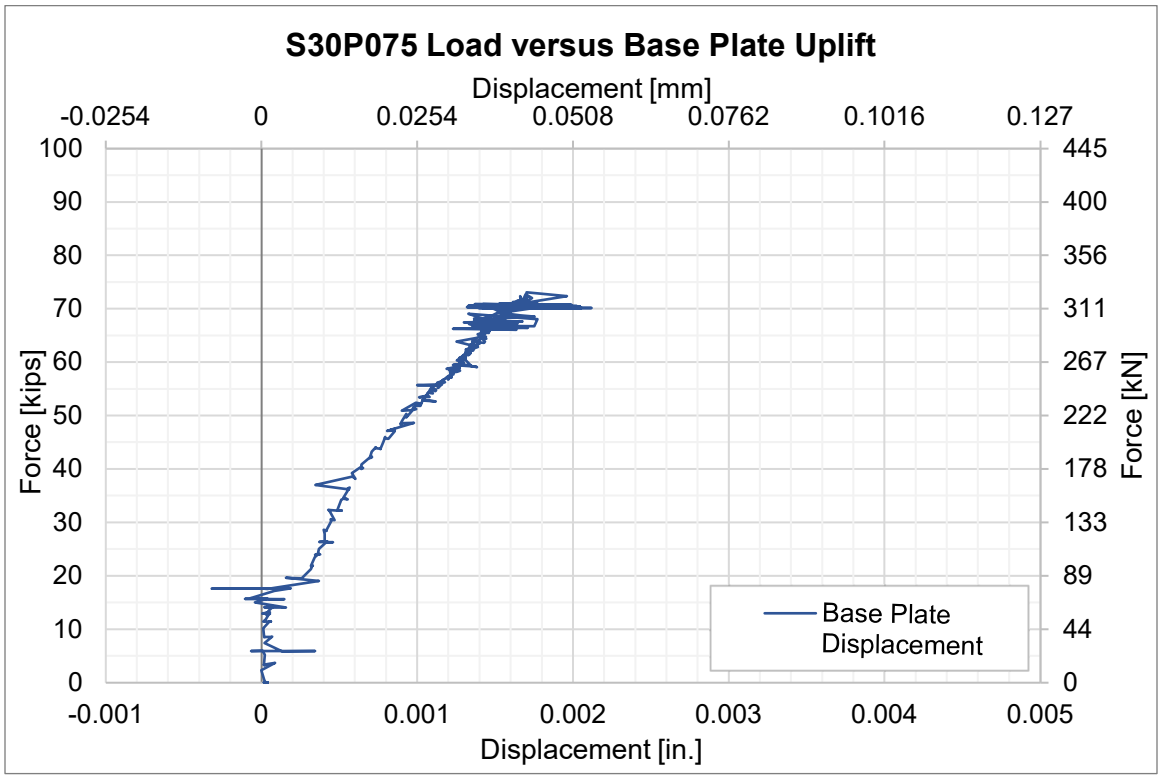

Figure F-2: S30P075 Vertical Displacement Graph.

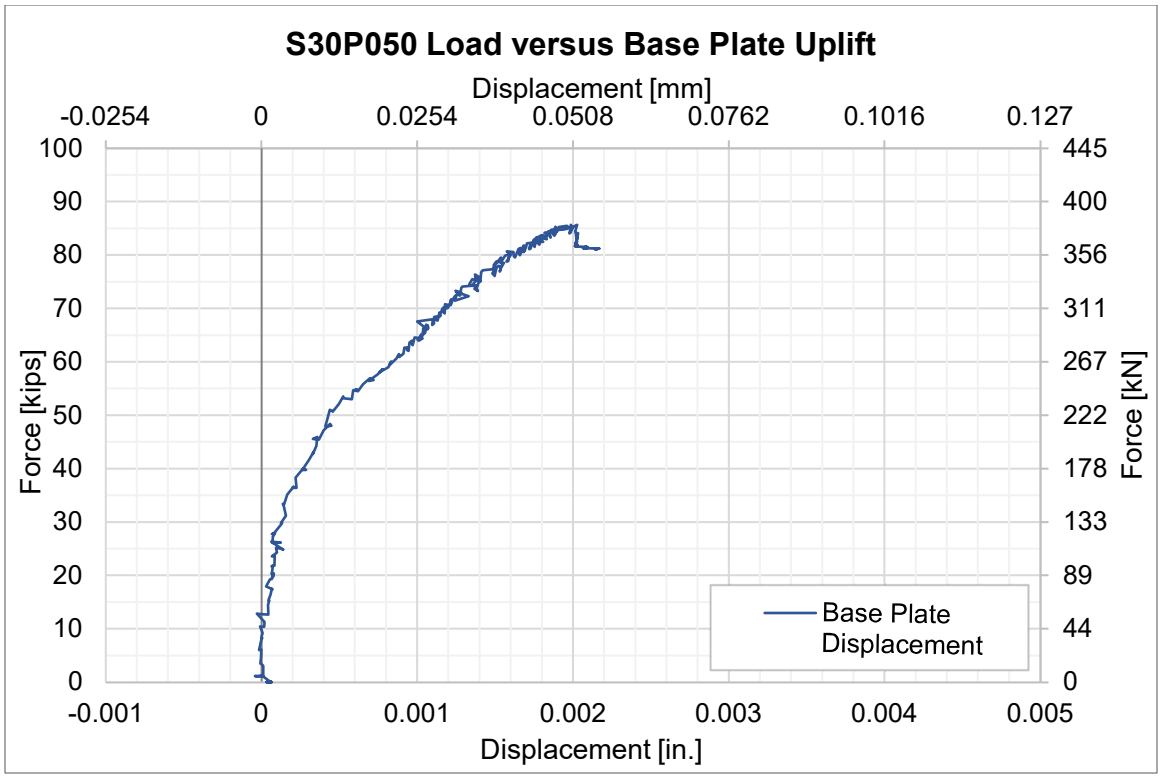

Figure F-3: S30P050 Vertical Displacement Graph.

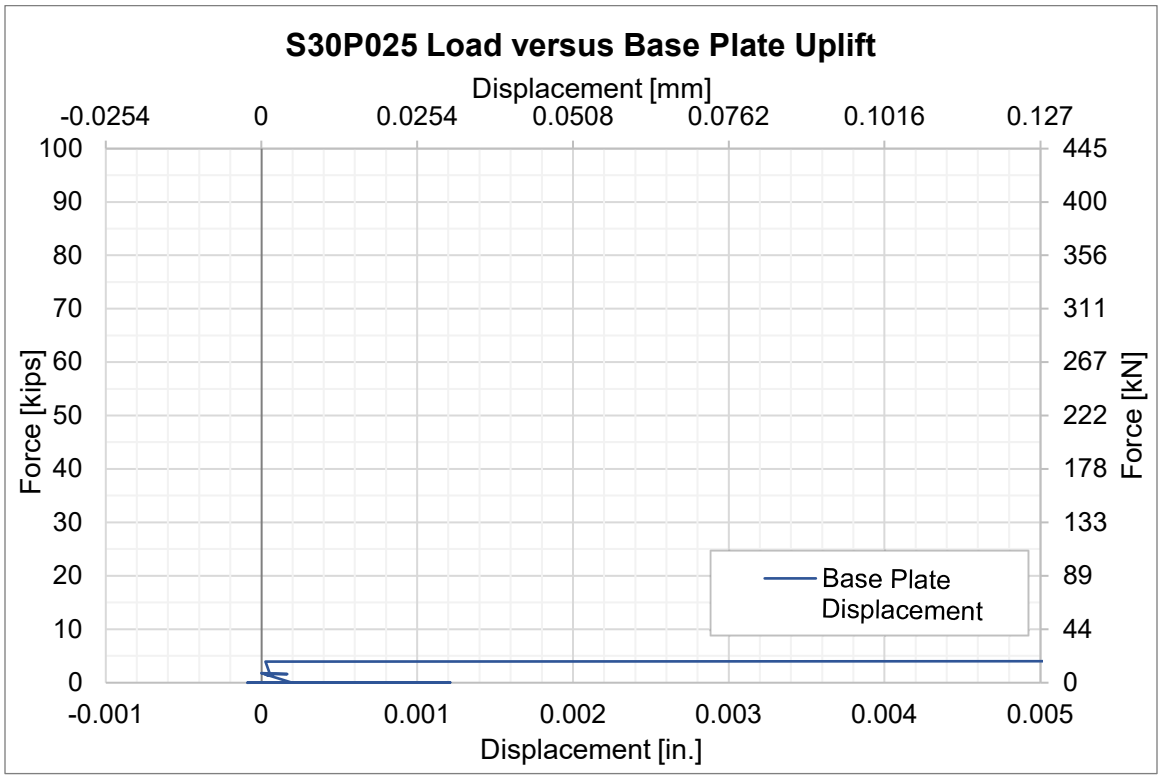

Figure F-4: S30P025 Vertical Displacement Graph.

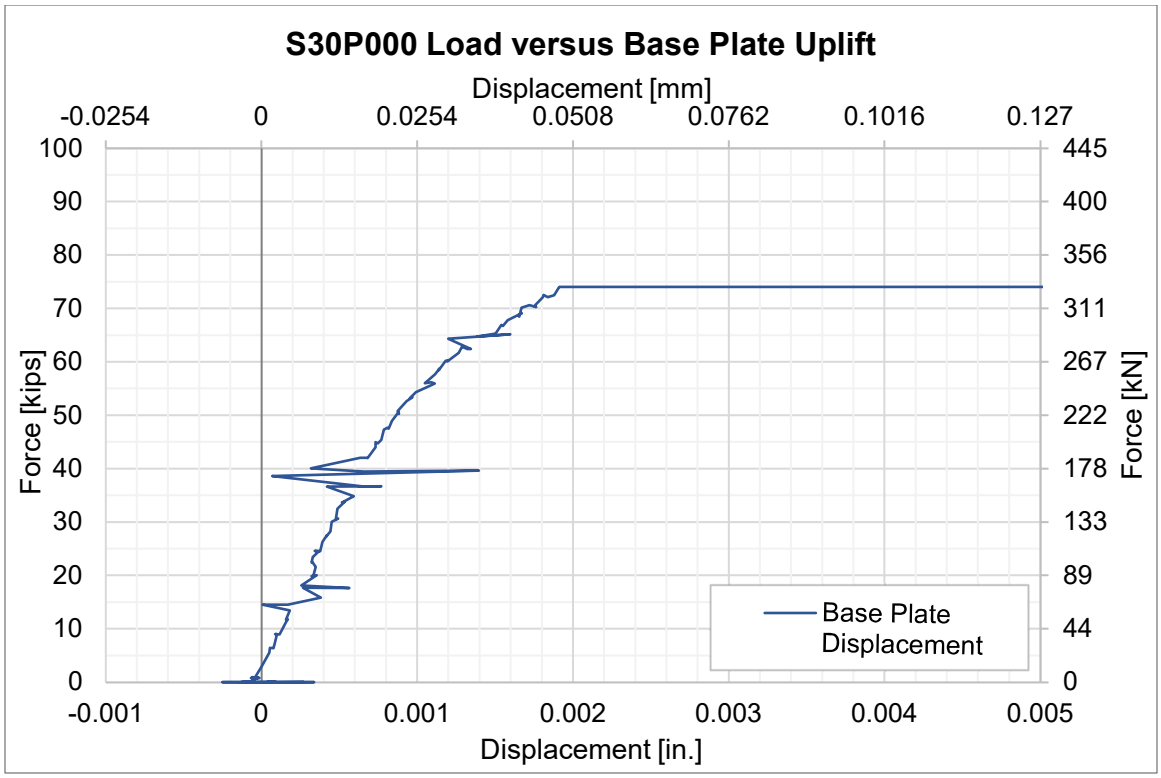

Figure F-5: S30P000 Vertical Displacement Graph.

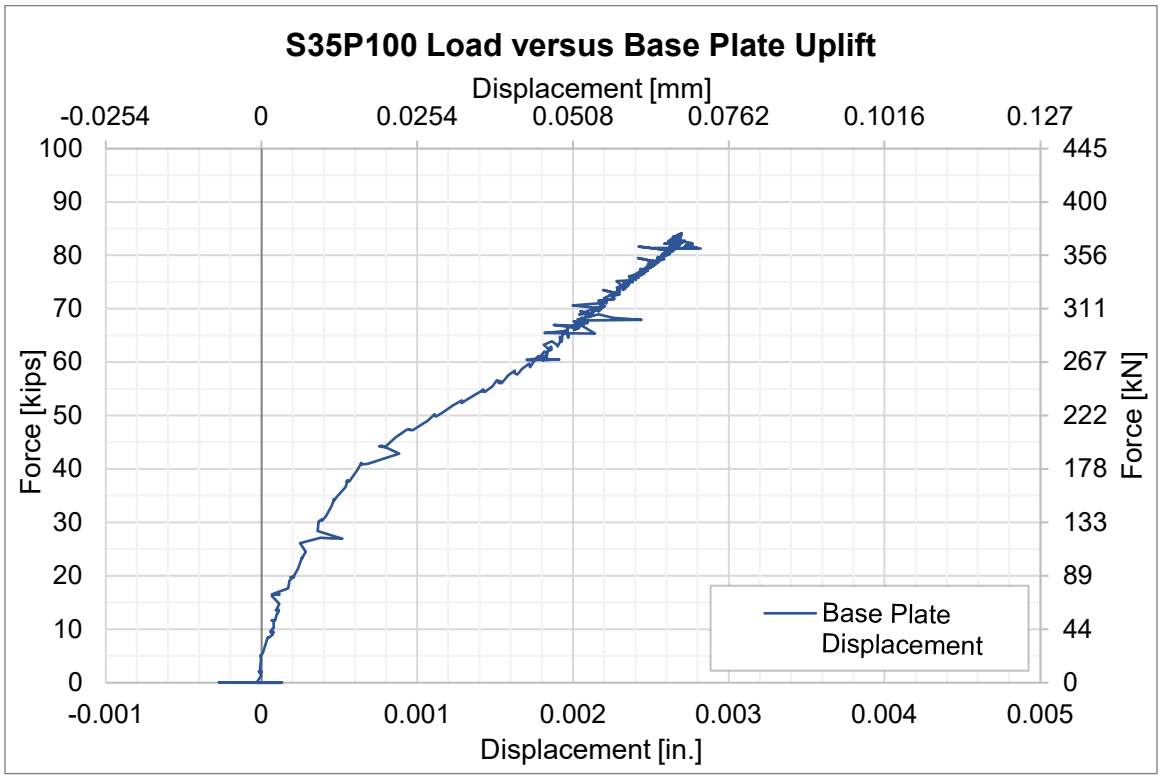

Figure F-6: S35P100 Vertical Displacement Graph.

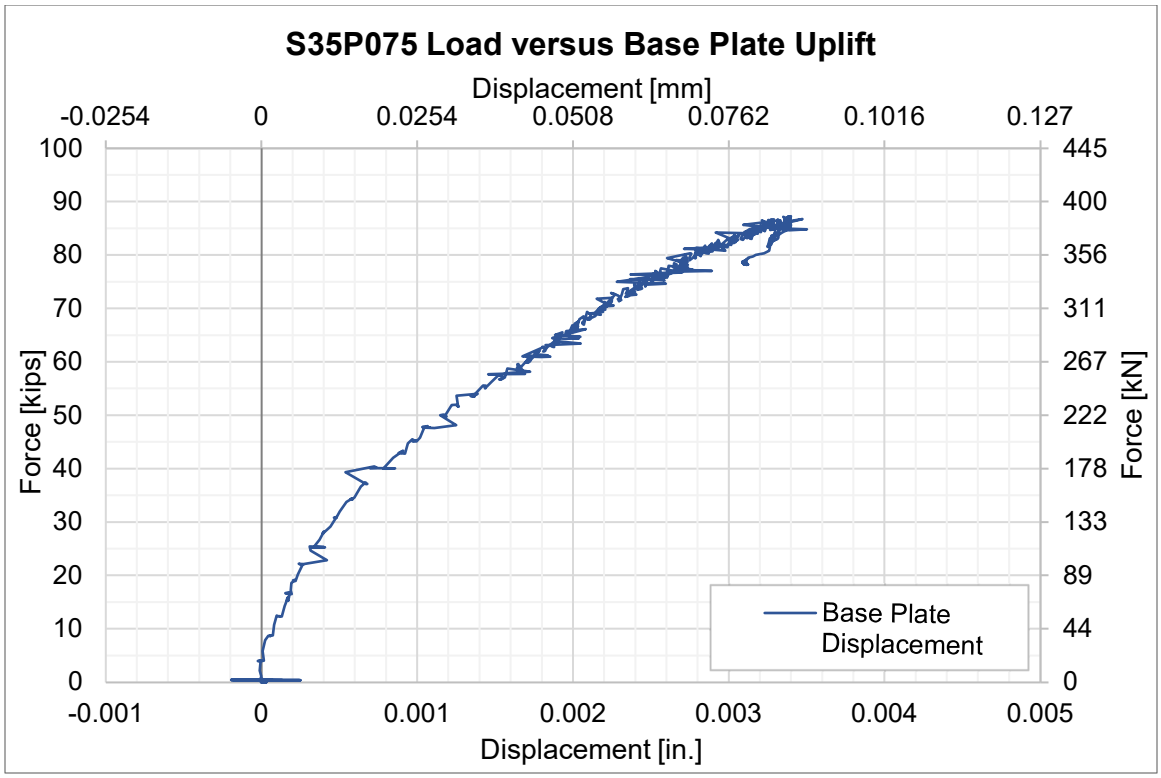

Figure F-7: S35P075 Vertical Displacement Graph.

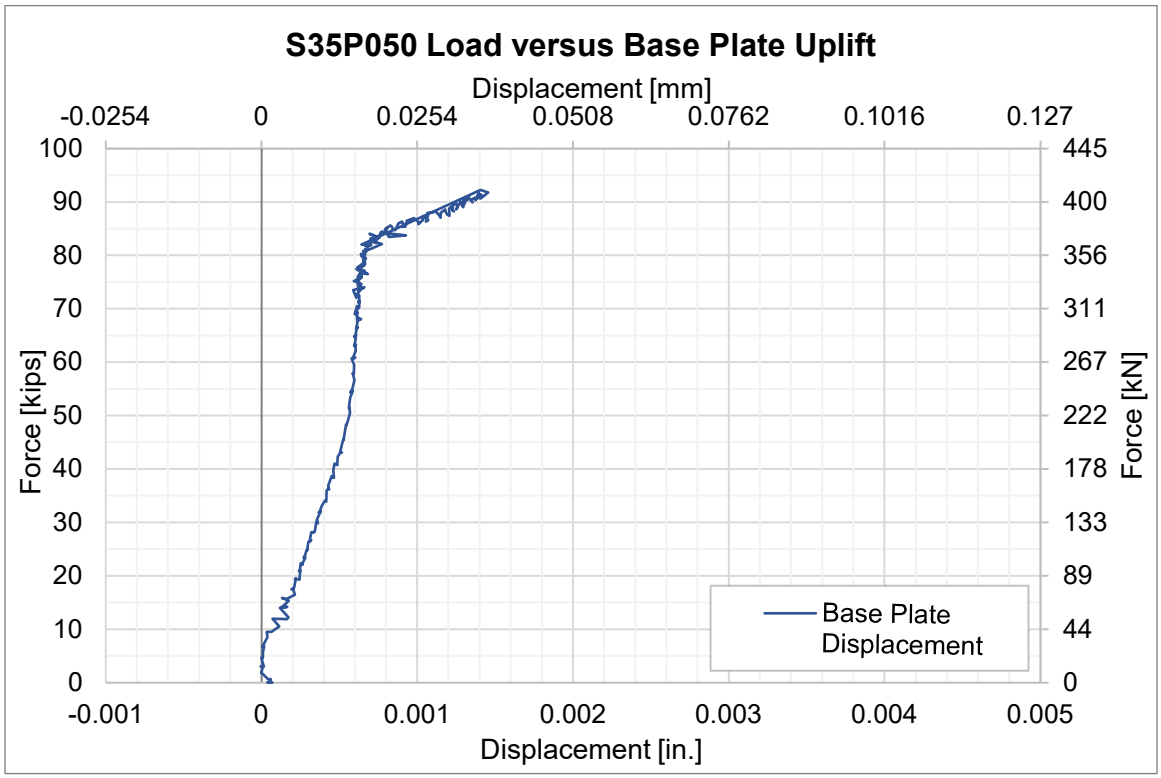

Figure F-8: S35P050 Vertical Displacement Graph.

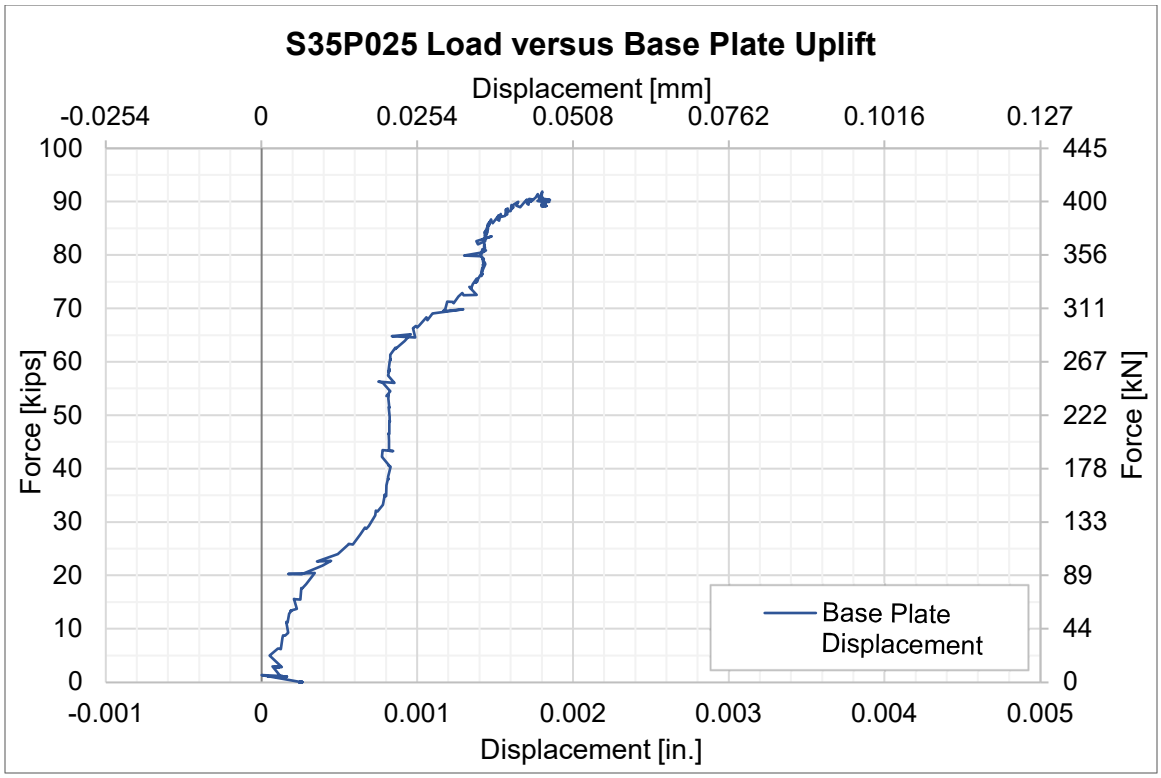

Figure F-9: S35P025 Vertical Displacement Graph.

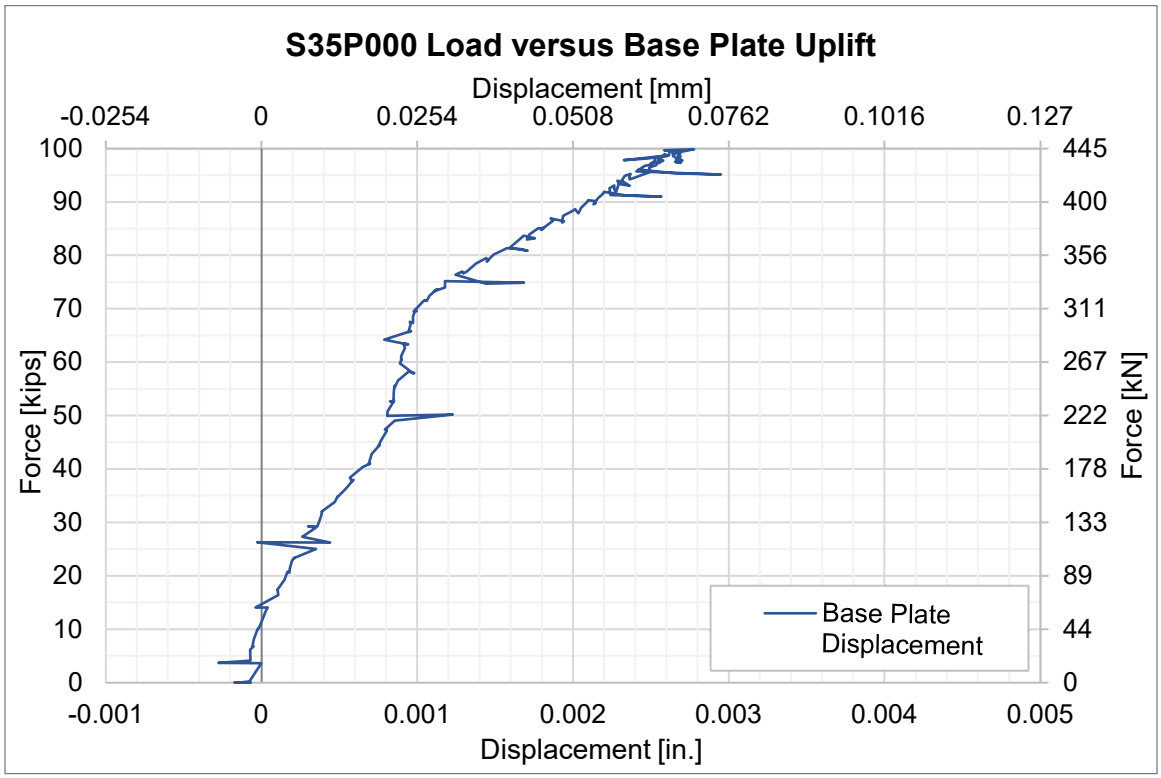

Figure F-10: S35P000 Vertical Displacement Graph.

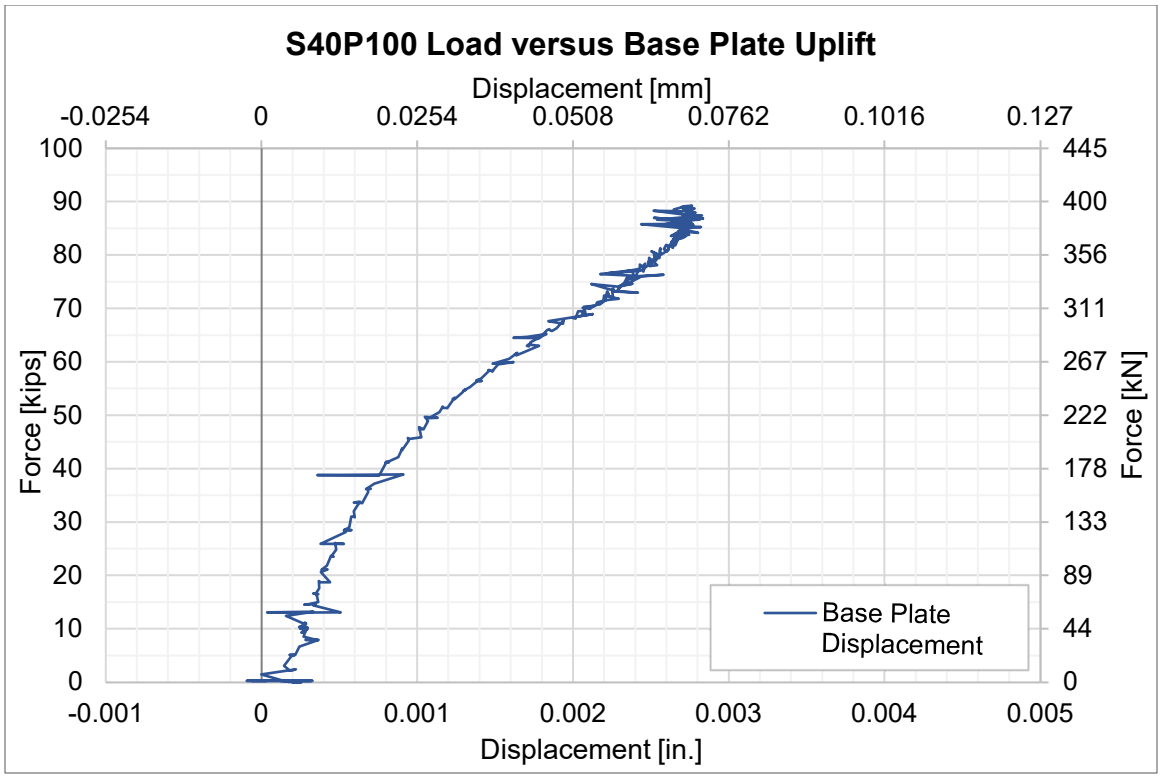

Figure F-11: S40P100 Vertical Displacement Graph.

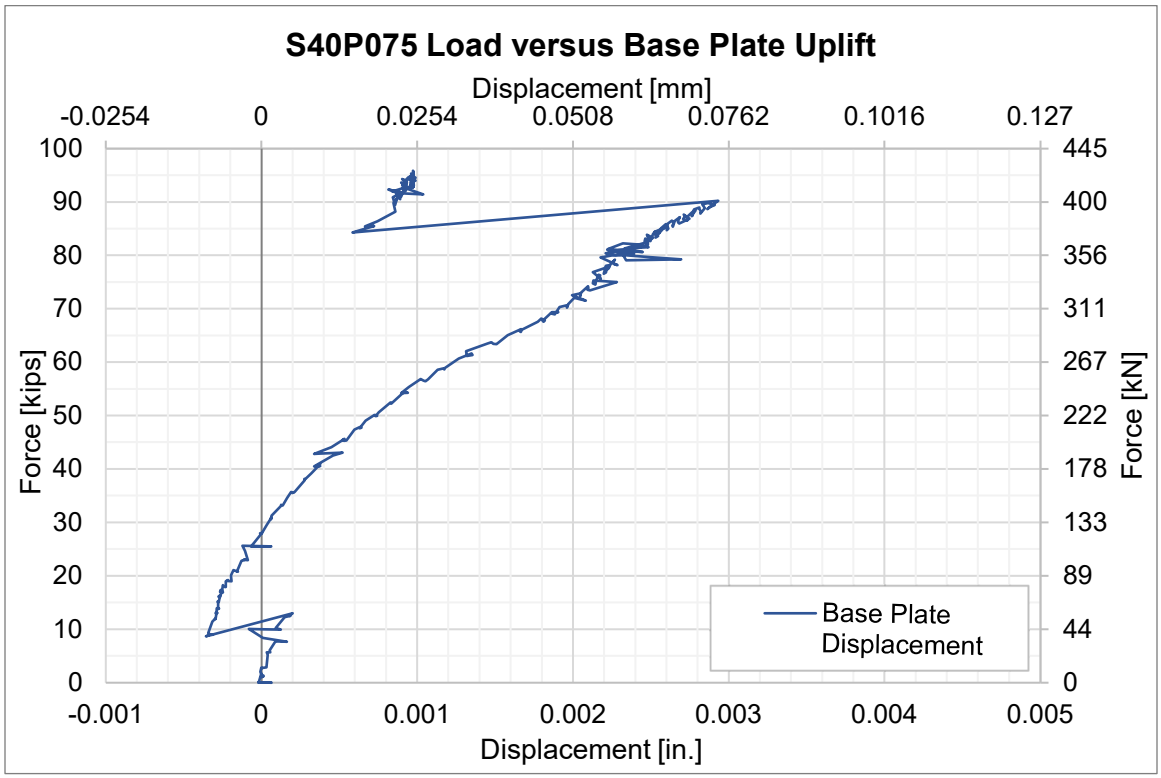

Figure F-12: S40P075 Vertical Displacement Graph.

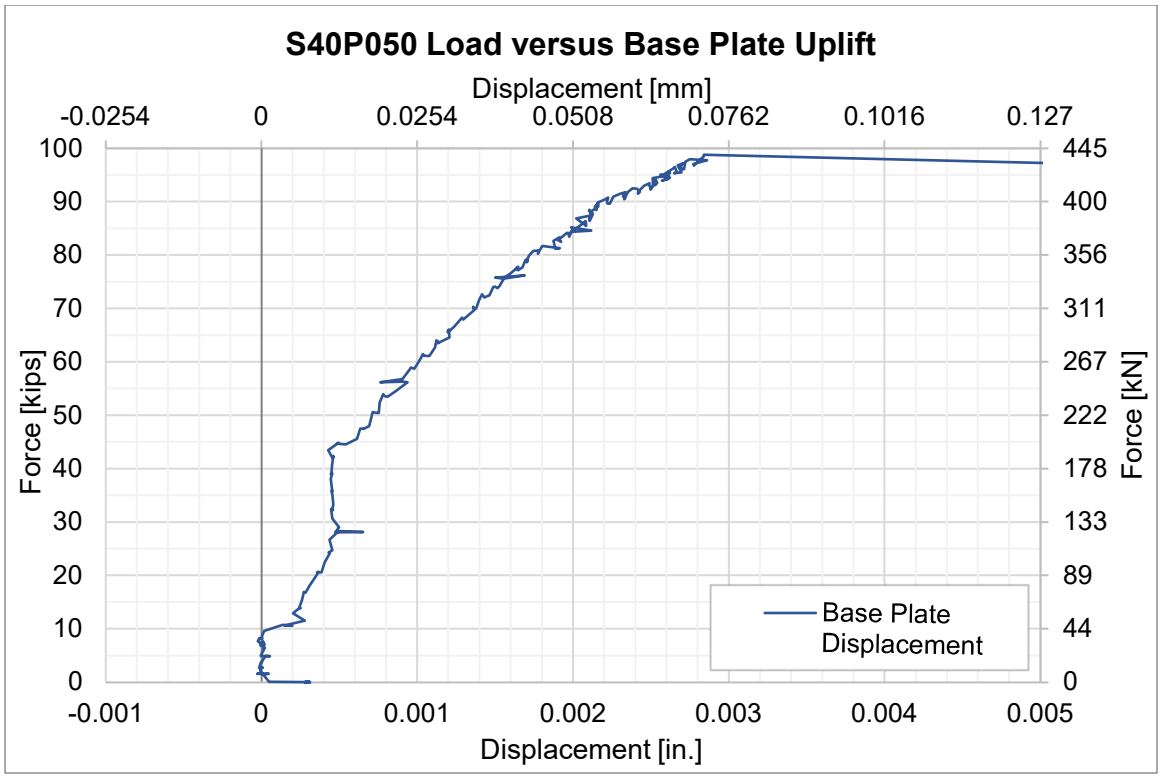

Figure F-13: S40P050 Vertical Displacement Graph.

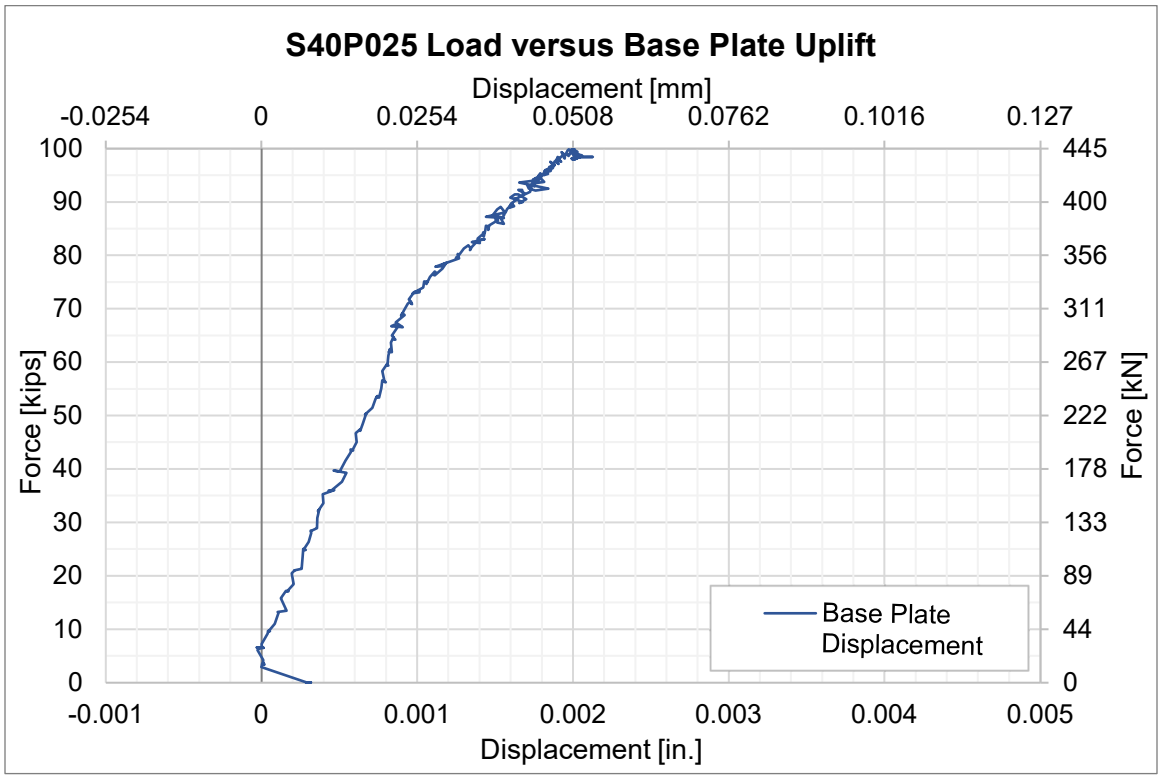

Figure F-14: S40P025 Vertical Displacement Graph.

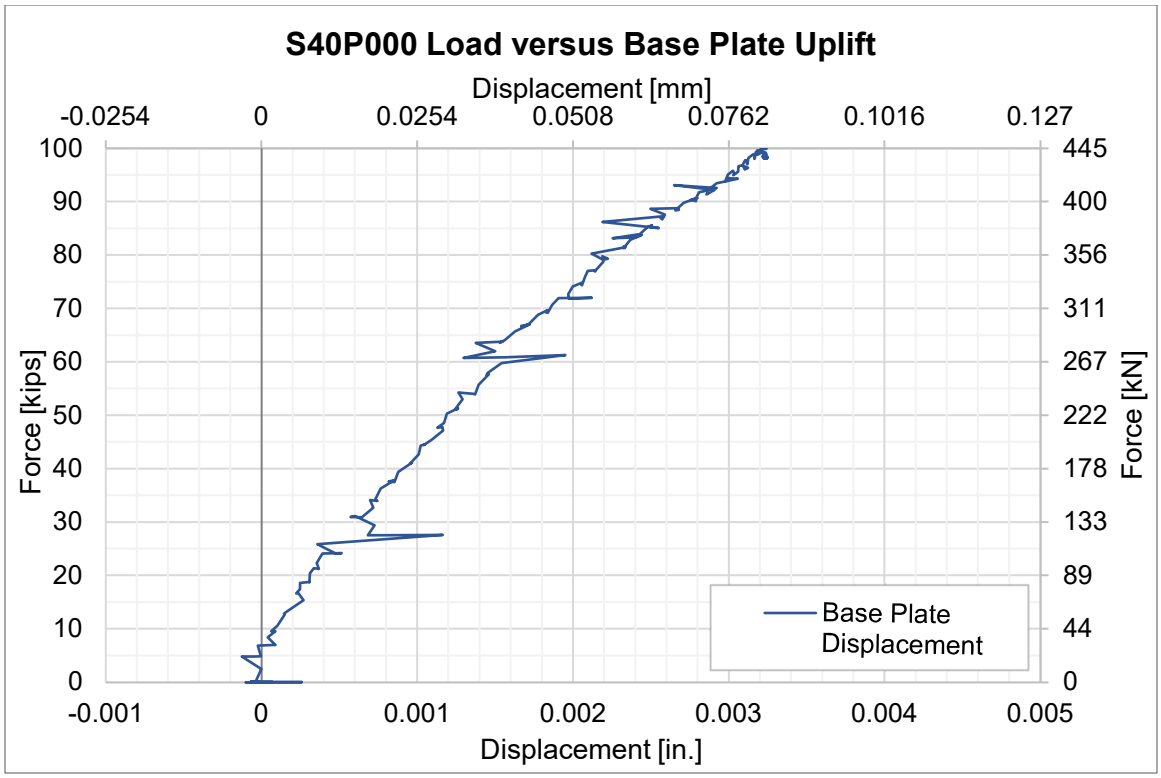

Figure F-15: S40P000 Vertical Displacement Graph.

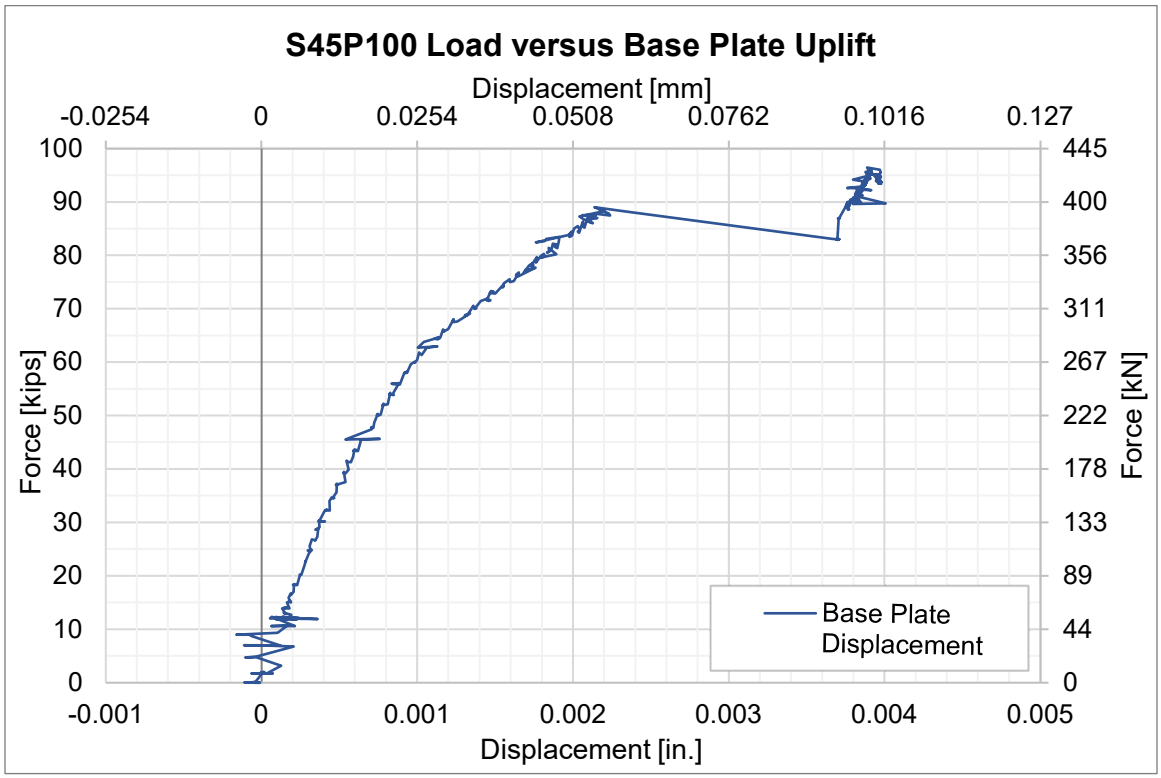

Figure F-16: S45P100 Vertical Displacement Graph.

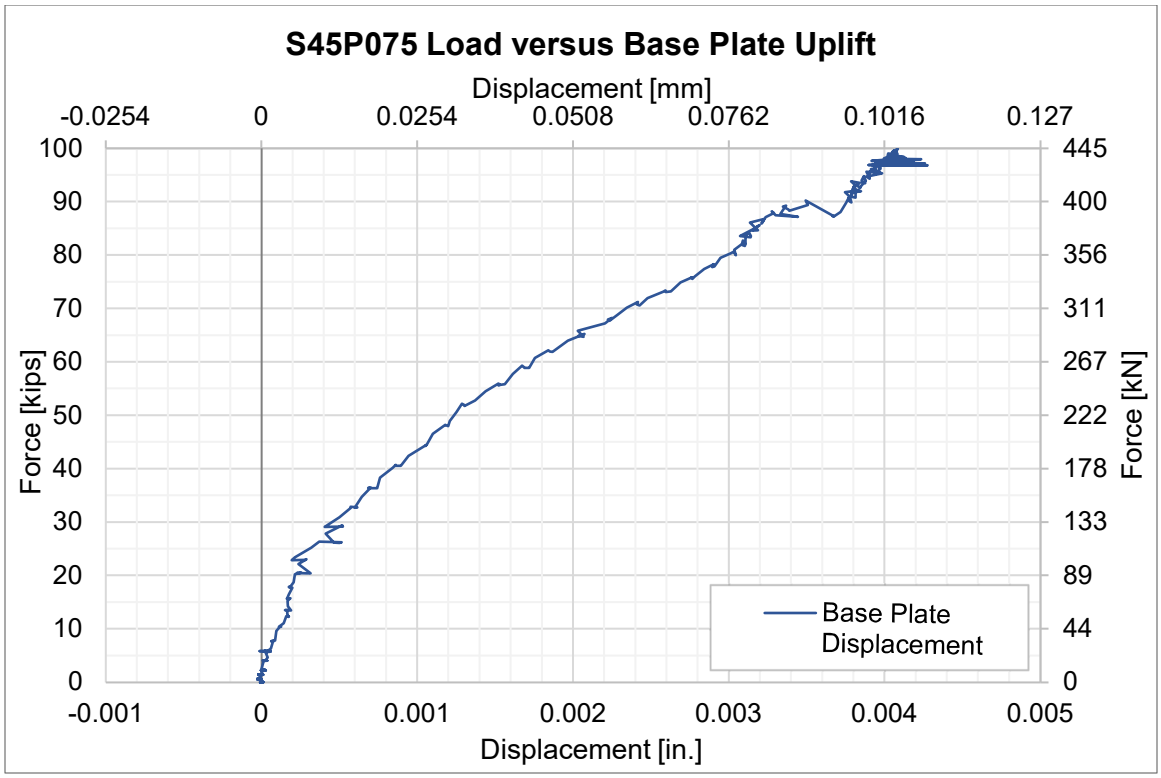

Figure F-17: S45P075 Vertical Displacement Graph.

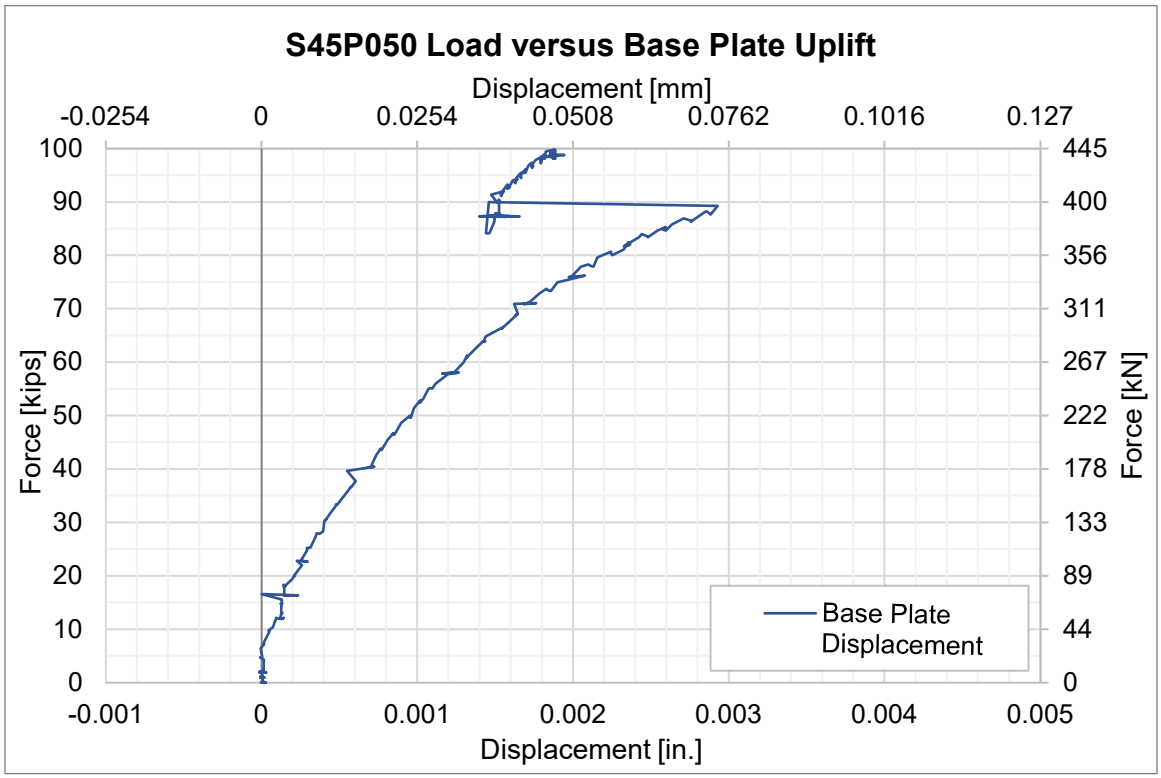

Figure F-18: S45P050 Vertical Displacement Graph.

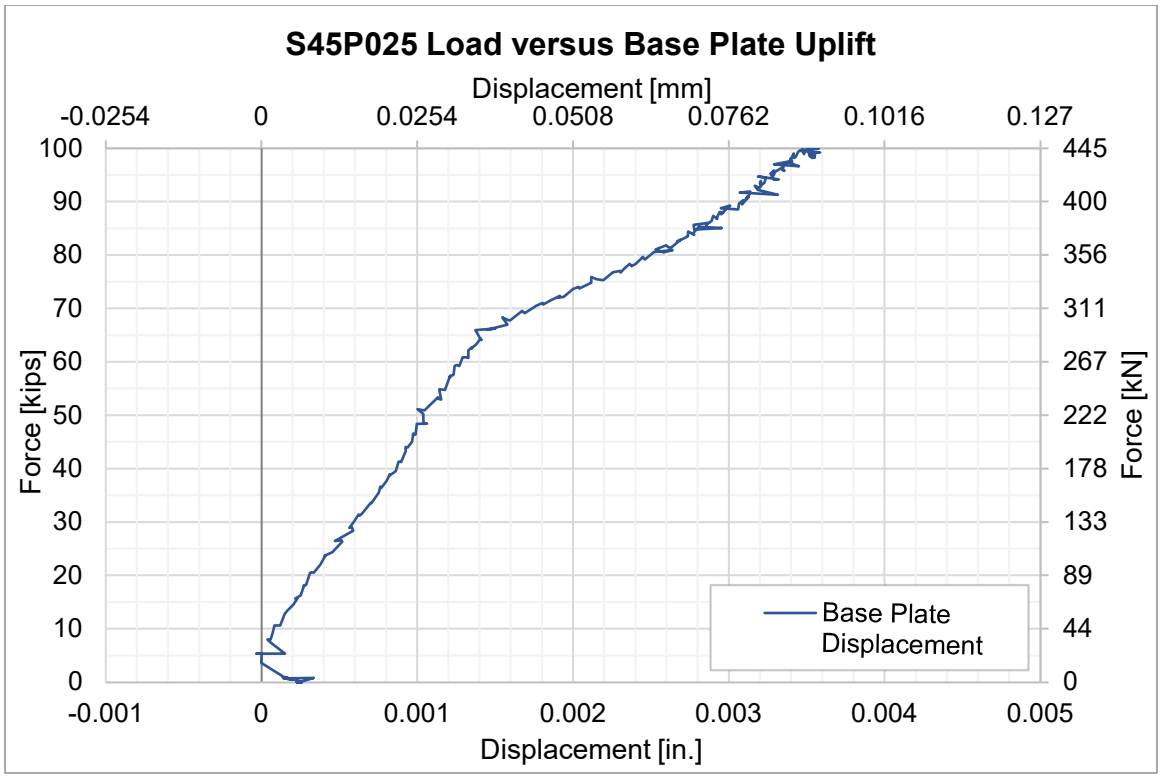

Figure F-19: S45P025 Vertical Displacement Graph.

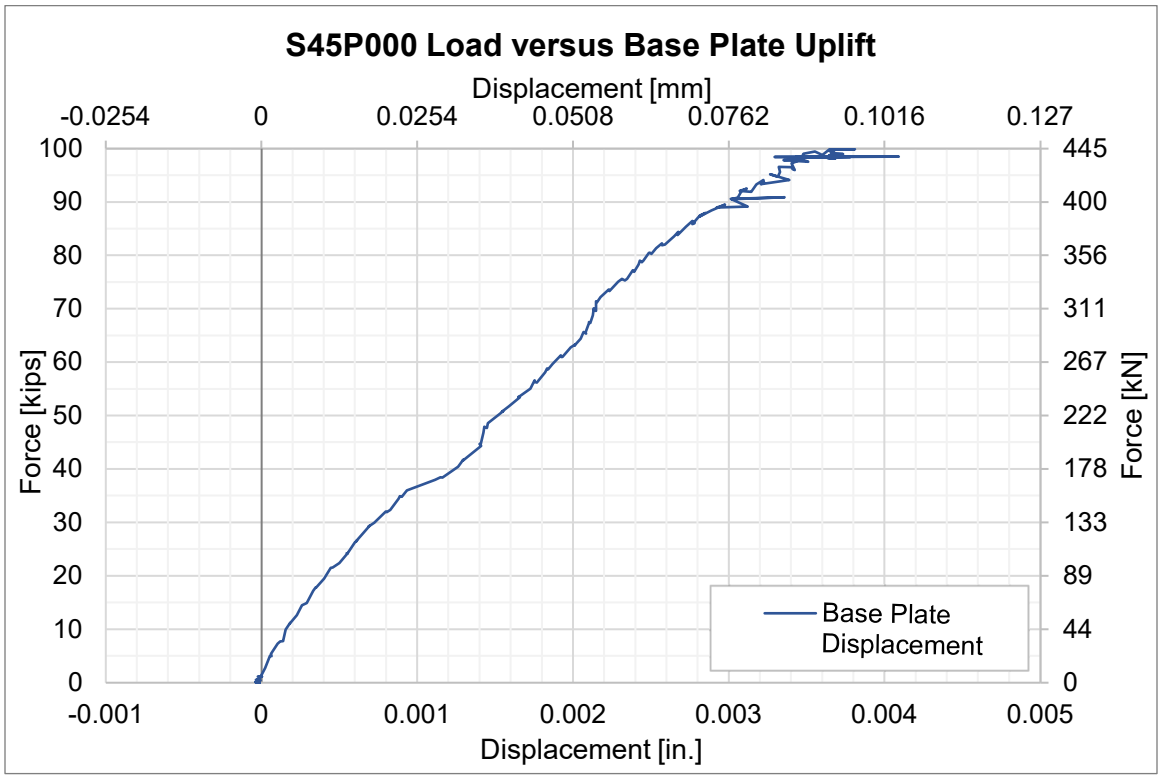

Figure F-20: S45P000 Vertical Displacement Graph.

Appendix G. Load versus Strain Graphs

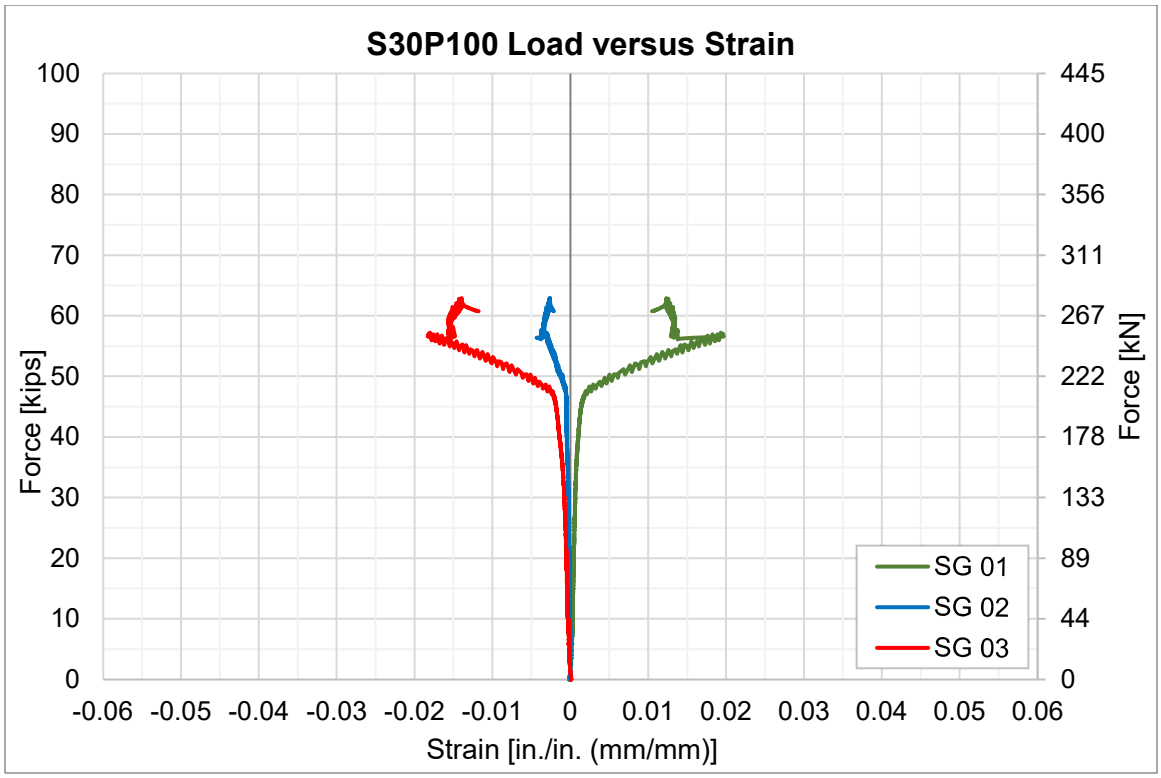

Figure G-1: S30P100 Strain Graph.

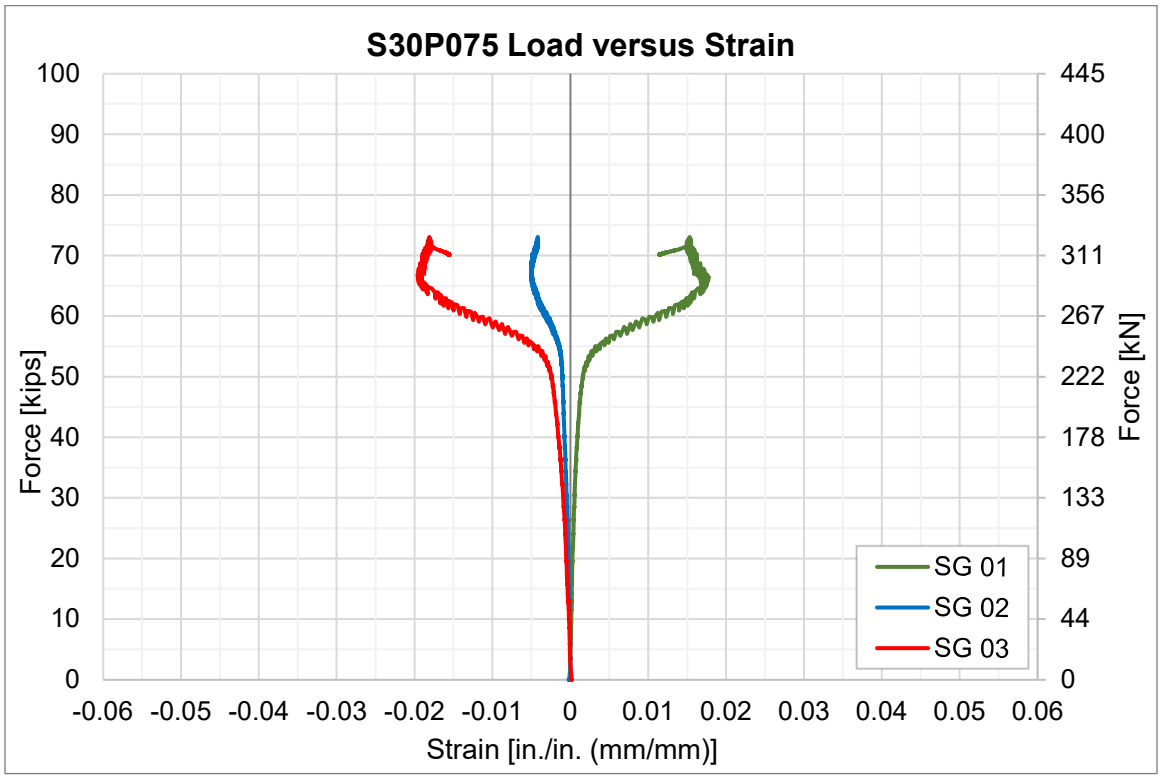

Figure G-2: S30P075 Strain Graph.

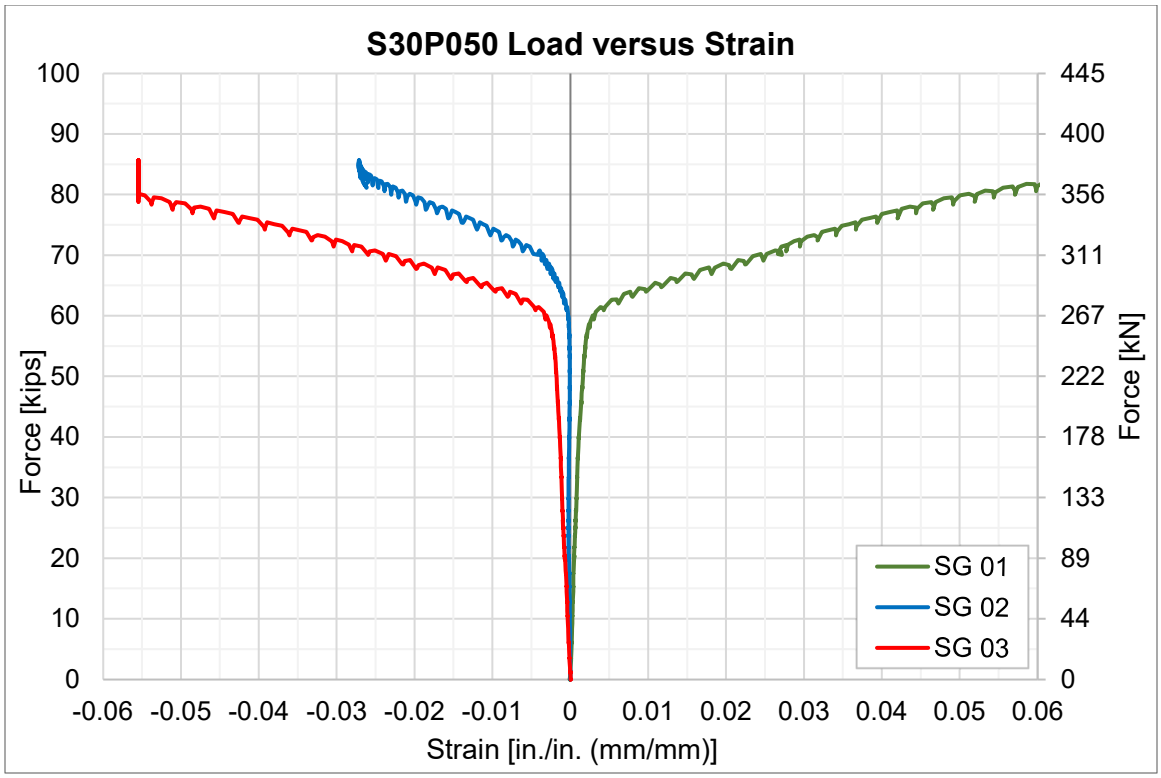

Figure G-3: S30P050 Strain Graph.

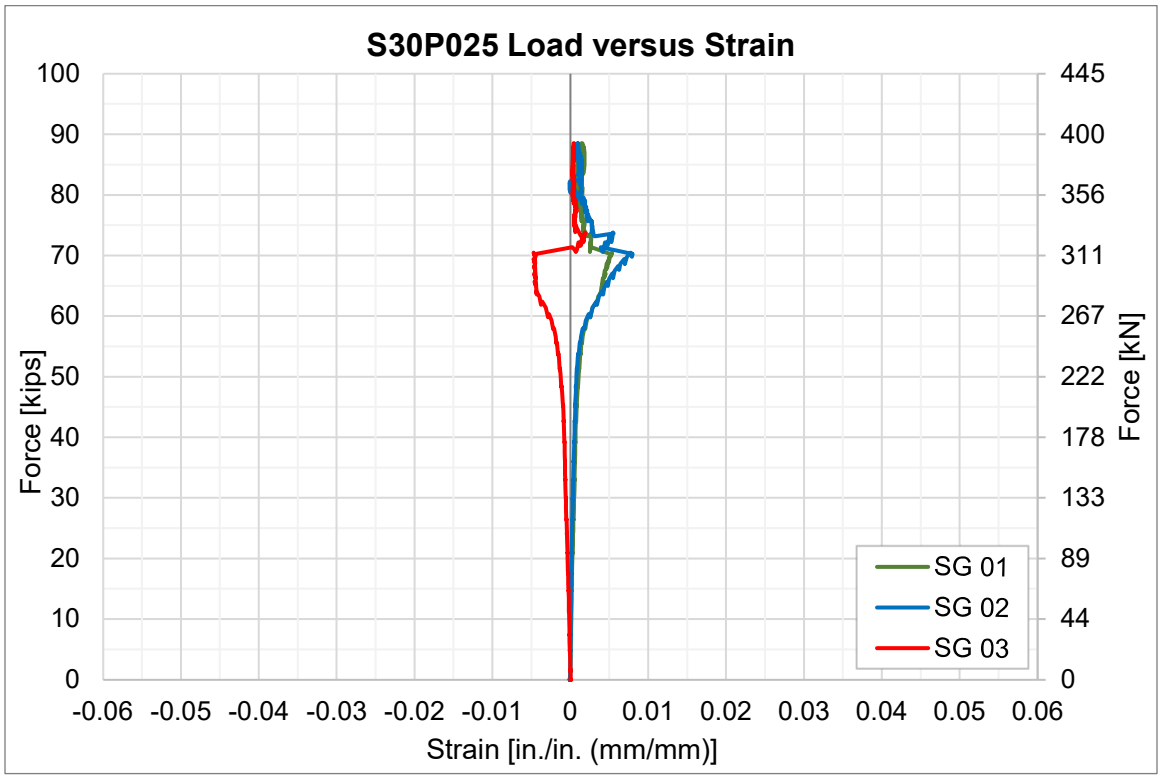

Figure G-4: S30P025 Strain Graph.

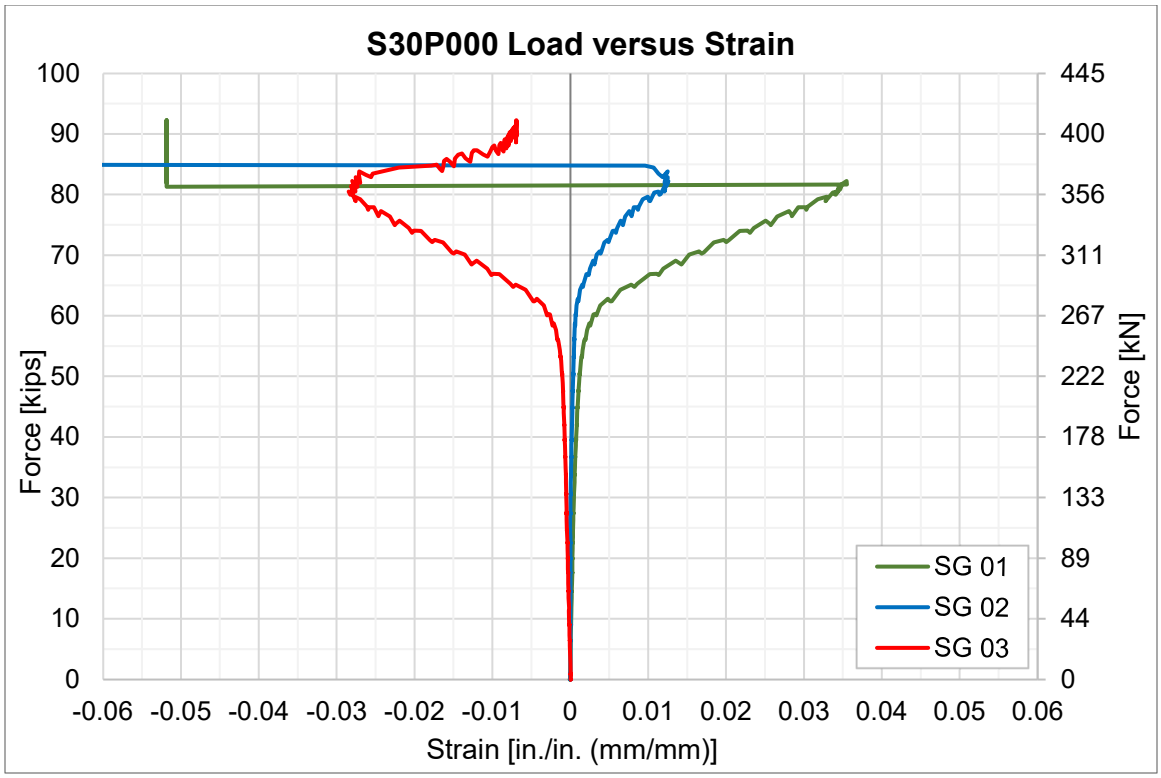

Figure G-5: S30P000 Strain Graph.

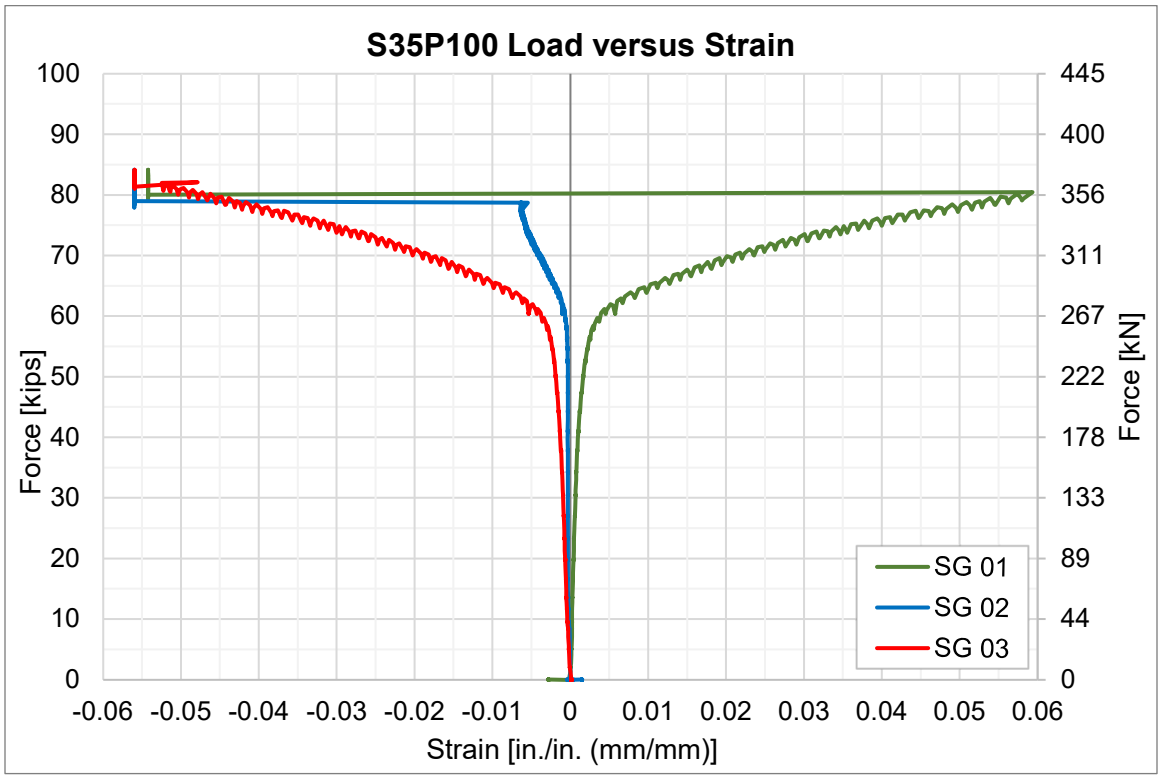

Figure G-6: S35P100 Strain Graph.

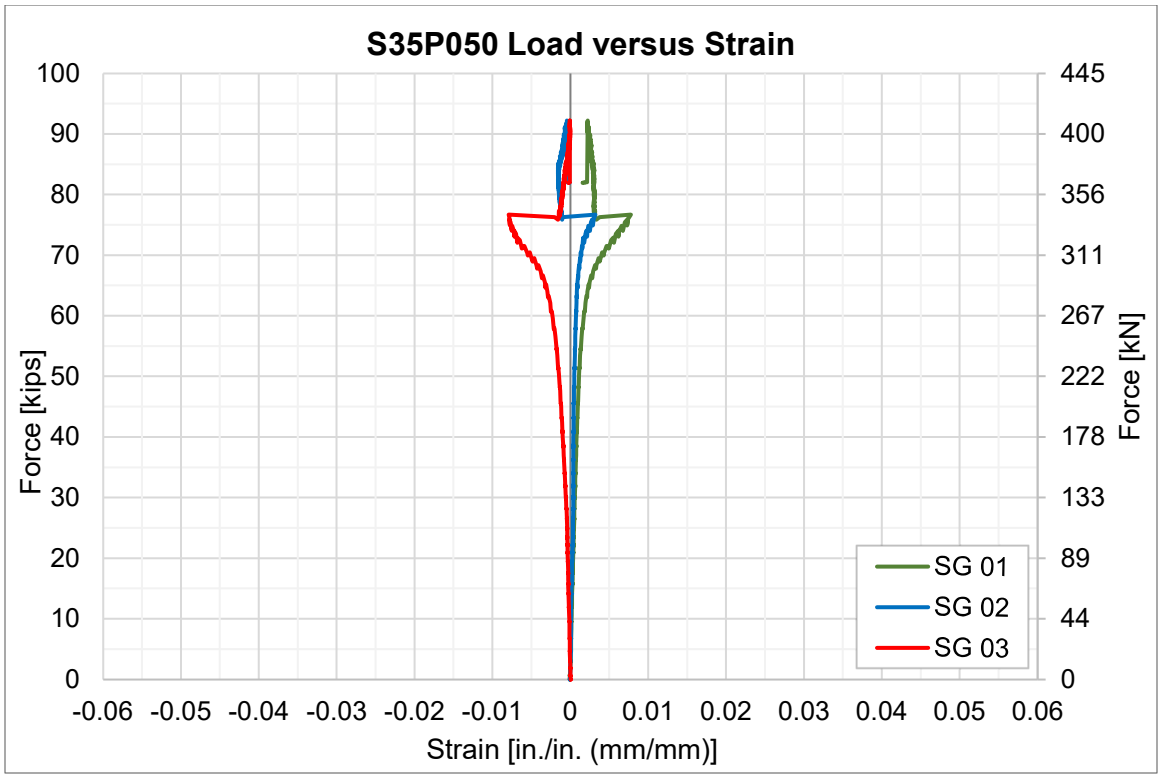

Figure G-7: S35P050 Strain Graph.

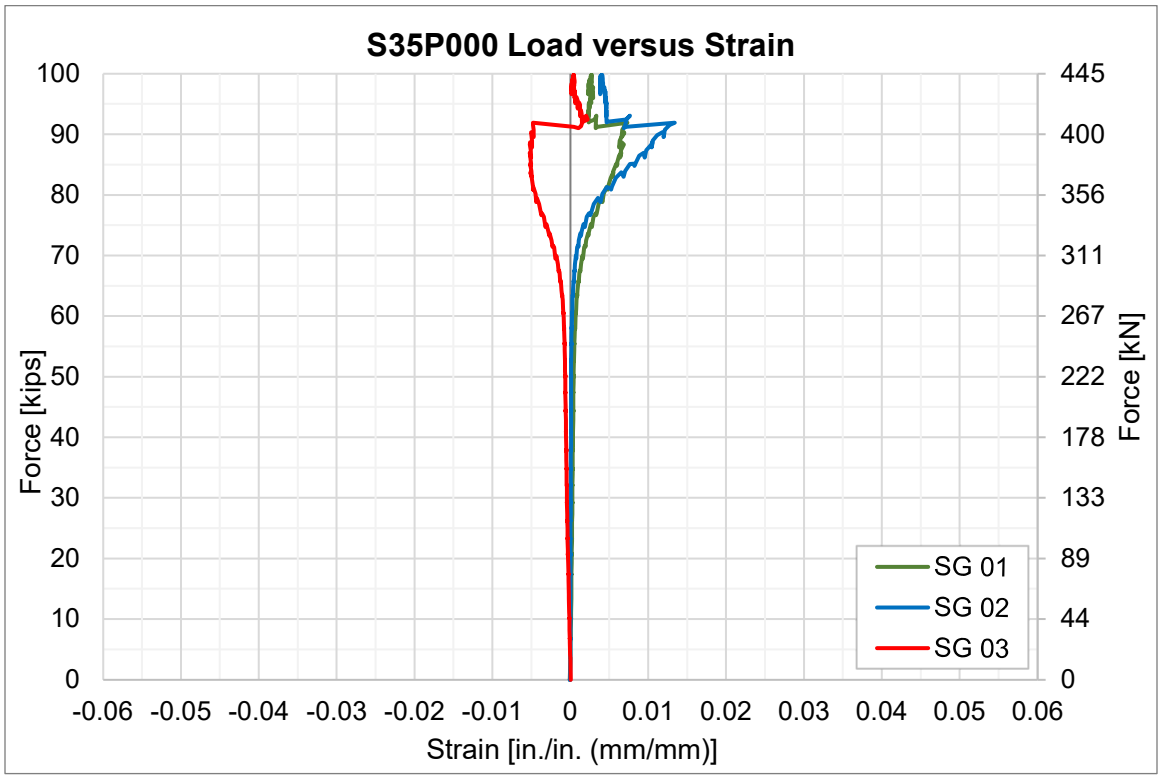

Figure G-8: S35P000 Strain Graph.

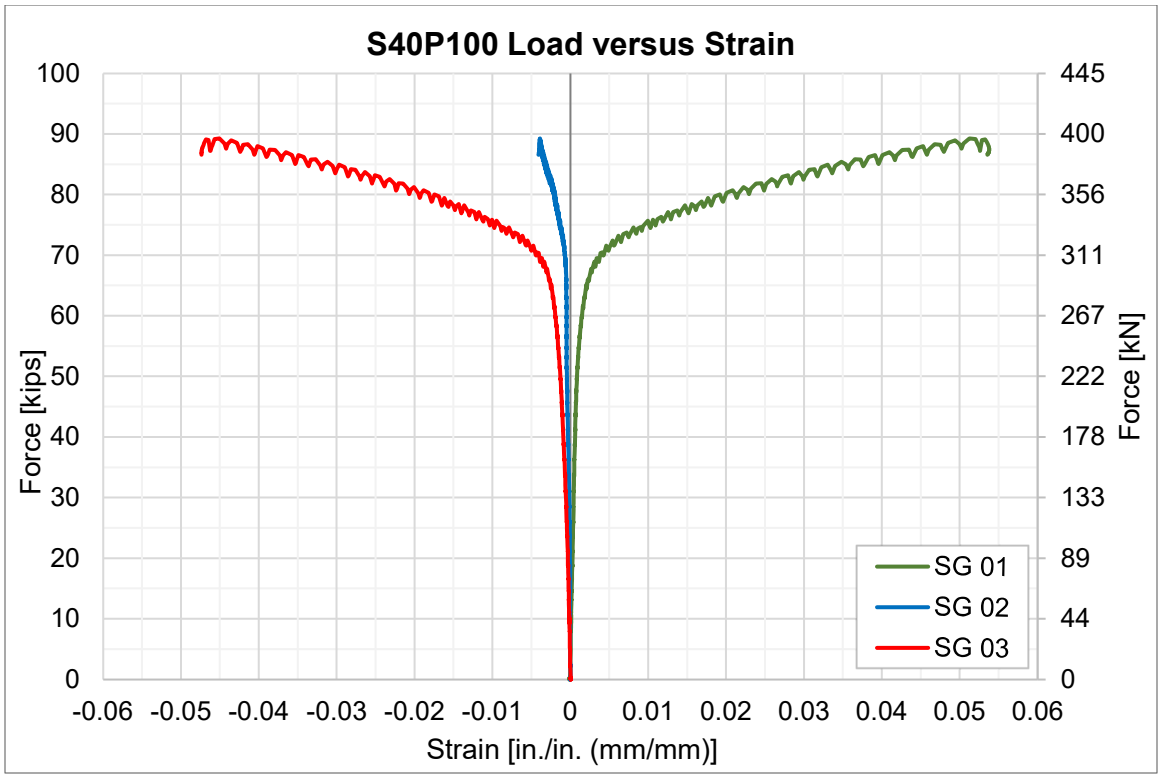

Figure G-9: S40P100 Strain Graph.

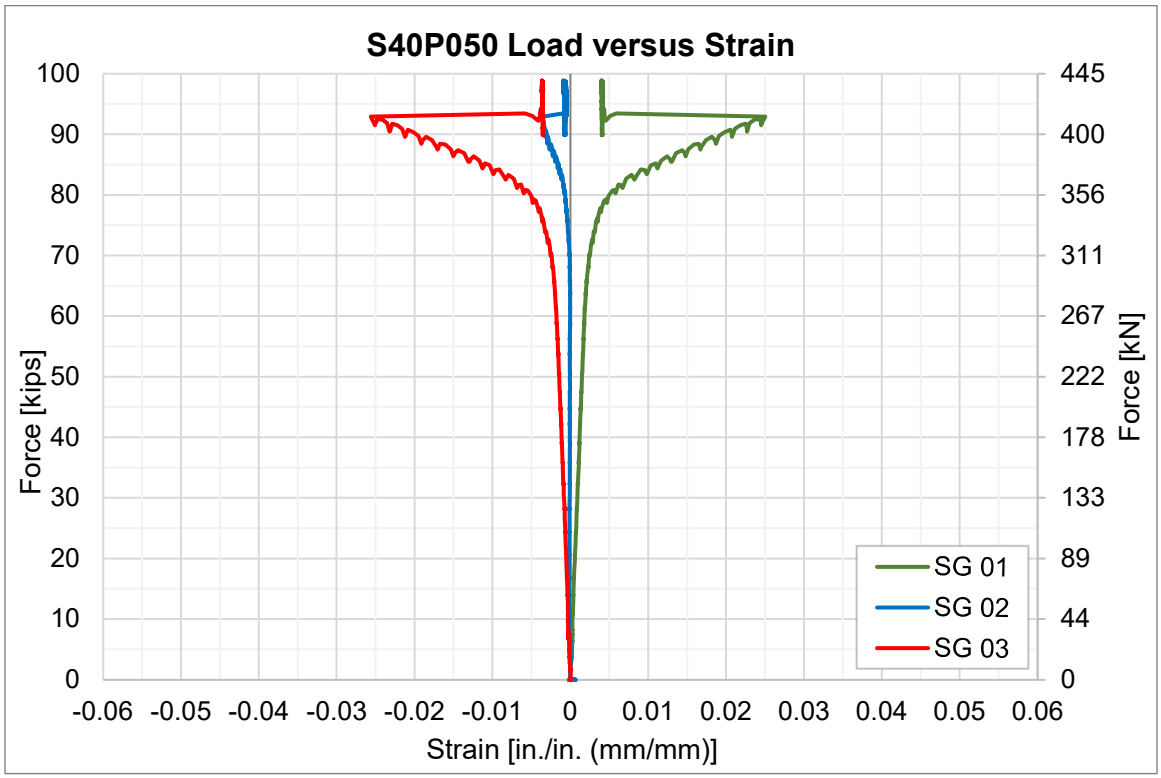

Figure G-10: S40P050 Strain Graph.

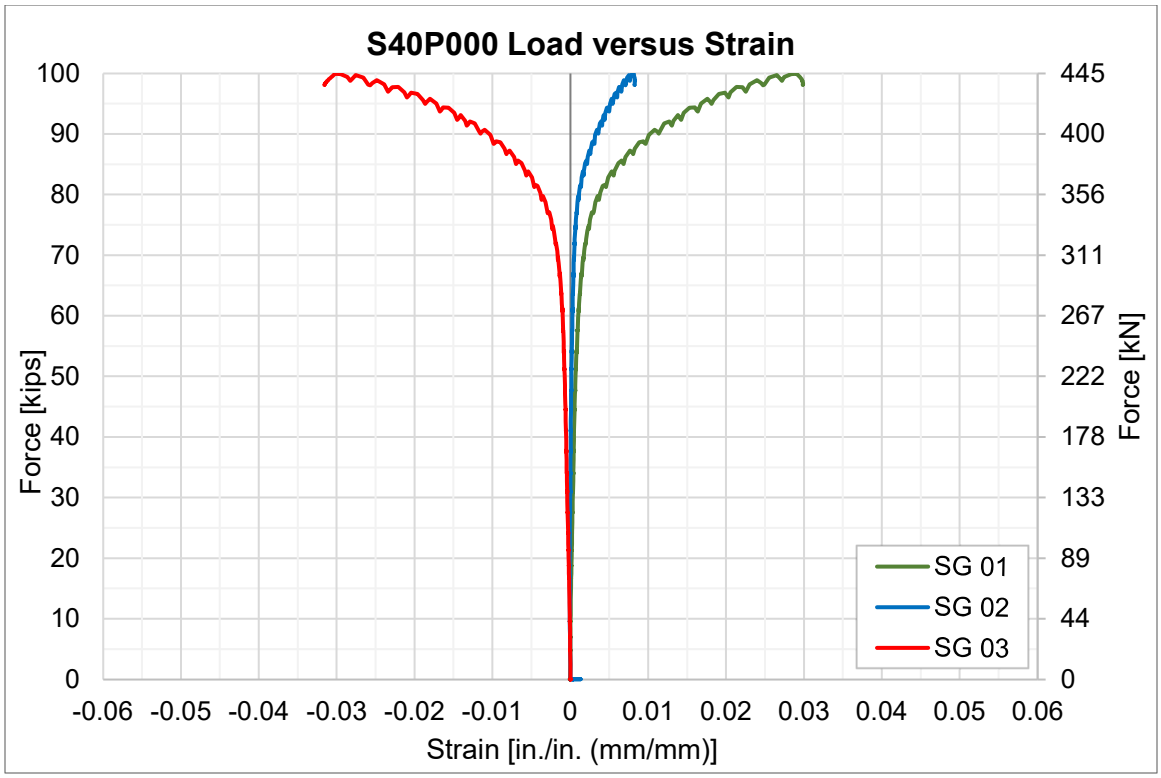

Figure G-11: S40P000 Strain Graph.

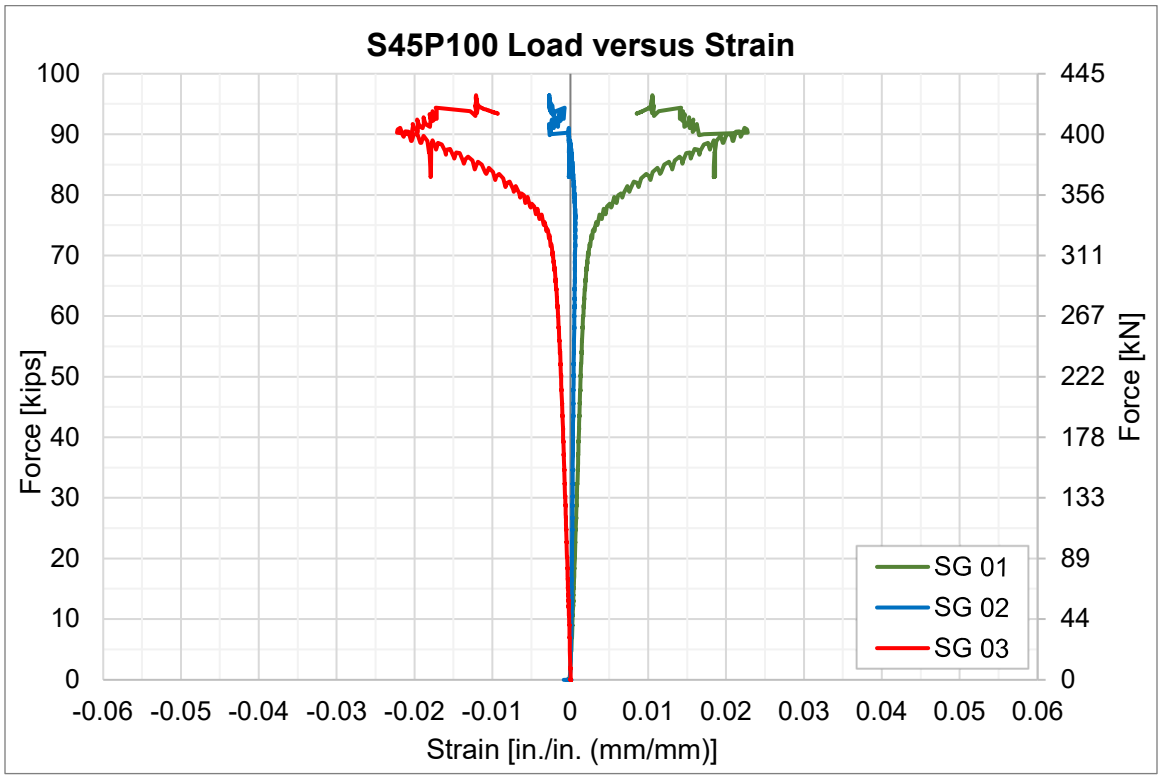

Figure G-12: S45P100 Strain Graph.

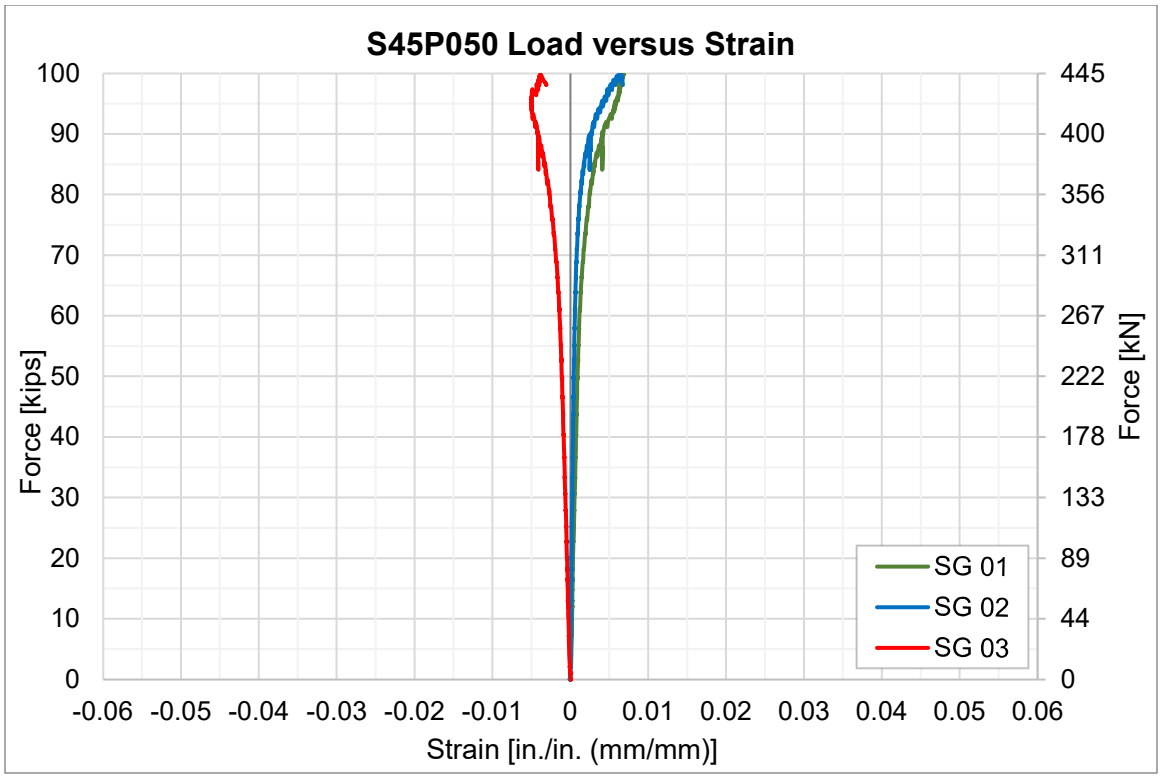

Figure G-13: S45P050 Strain Graph.

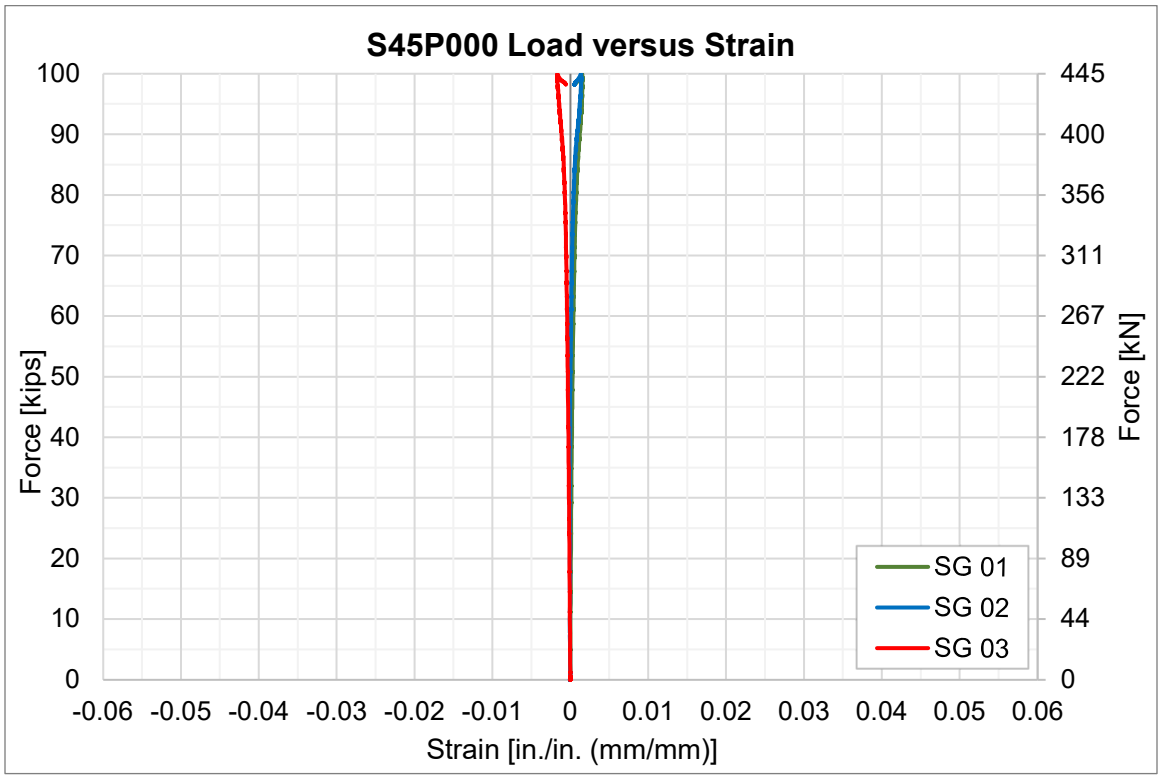

Figure G-14: S45P000 Strain Graph.

Appendix H. S30P100 MATLAB Code

```
% Filtering And Curve-Fitting Operation For Specimen S30P100 %

clc
clear all

drive = "C:\Users\";
user = "taxonds";

% Location Of Data To Be Filtered %
path = "\Box\2020-21 CDKS\DST\12 Experimental Data\Data Analysis\03
Analysis_02_Prefilter";


% Index Of All Test IDs In Order Of Test Number %
TestIDs =
['S30P100';'S35P100';'S40P100';'S45P100';'S30P075';'S35P075';'S40P075';'S45P075';'S30P050
';'S35P050';'S40P050';'S45P050';'S30P025';'S35P025';'S40P025';'S45P025';'S30P000';'S35P00
0';'S40P000';'S45P000'];

for TestNumber = 1

% Convert Test Number To Text String And Add Leading "0" If Needed %
TestNum = string(TestNumber);
if TestNumber <= 9
    TestNum = strcat('0',TestNum);
end

% Set Test ID Based On Test Number %
TestID = TestIDs(TestNumber,:);

% Import Prefiltered Data File %

% String Together Full File Name %
    datafile = strcat(drive, user, path, 'Test', TestNum, '_', TestID,
'_Analysis_Prefilter.xlsm');

    % Read Unmodified Columns %
    RawData = xlsread(datafile,4,'B:G');
    T = RawData(:,1);
    P = RawData(:,2);
    D2 = RawData(:,3);
    SG1 = RawData(:,4);
    SG2 = RawData(:,5);
    SG3 = RawData(:,6);

    % Read Modified Columns %
    Data = xlsread(datafile,4,'H:J');
    TMOD = Data(:,1);
    PMOD = Data(:,2);
    D1MOD = Data(:,3);
```

```
% Put Data That Does Not Need To Be Filtered Into The Output Matrix %
    L = length(P);
    Output(1:L,1)= T(:,1);
    Output(1:L,2) = P(:,1);
    Output(1:L,3) = D2(:,1);
    Output(1:L,4) = SG1(:,1);
    Output(1:L,5) = SG2(:,1);
    Output(1:L,6) = SG3(:,1);
    L = length(TMOD);
    Output(1:L,7) = TMOD(:,1);
    Output(1:L,8) = PMOD(:,1);


% Isolate Data To Be Filtered %
    UnfiltData = D1MOD;

% Begin Filtering Operation %

    count = round(L/15);                    % Sets Window Based On Length Of Vector
                                            % Being Filtered %
    Filter1 = medfilt1(UnfiltData,count);   % Filter 1: Median Filter - Prefilters
                                            % Noisy Data %


    f = 30;                                 % Sampling Frequency -> Leave At 30 %
    f_cutoff = .9;                          % Cut-off Frequency %
    fnorm = f_cutoff/(f/2);
    [b1,a1] = butter(10,fnorm,'low');       % Low Pass Butterworth Filter, 10th Order %
    Filter2 = filtfilt(b1,a1,Filter1);      % Filter 2: Buterworth Filter %

    count = round(L/15);                    % Sets Window Based On Length Of Vector
                                            % Being Filtered %
    Filter3 = medfilt1(Filter2,count);      % Filter 3: Median Filter %


% Curve Fit Filtered Data And Get Table Of Loads %

    % Runs Curve Fit Function For Filtered Data, Value Of 0.9999999 Is Set
    % Such That The Curve Smooths Out Roughness Of Data While Still
    % Following The Trend Of The Data %
        curvefit = fit(Filter3,PMOD,'smoothingspline','SmoothingParam', .9999999);
    % Returns Y Values For Function Based On Displacement Input %
        CurveFitY = curvefit(Filter3);

% Add Filtered And Curve Fit Data To Ouput Table %
    Output(1:L,9) = Filter3;
    Output(1:L,10) = CurveFitY;

% Write Data To File %
   savepath = "\Box\2020-21 CDKS\DST\12 Experimental Data\Data_03_Filtered";
   savefile = strcat(drive, user, savepath);
   cd (savefile)
```

```
    FileName = strcat('Test',TestNum, '_', TestID, '_Filtered.xlsx');
    xlswrite(FileName,Output)

    cd(strcat(drive,user,path))
    clear Output

end

cd(strcat(drive,user,'\Box\2020-21 CDKS\DST\12 Experimental Data\Data Analysis\01 Matlab
Filtering Code'))
```

Appendix I. Typical MATLAB Code

```
%Filtering And Curve-Fitting Operation For All Specimens EXCEPT S30P100

clc
clear all

drive = "C:\Users\";
user = "taxonds";

% Location Of Data To Be Filtered %
path = "\Box\2020-21 CDKS\DST\12 Experimental Data\Data Analysis\03
Analysis_02_Prefilter\";


% Index Of All Test IDs In Order Of Test Number %
TestIDs =
['S30P100';'S35P100';'S40P100';'S45P100';'S30P075';'S35P075';'S40P075';'S45P075';'S30P050
';'S35P050';'S40P050';'S45P050';'S30P025';'S35P025';'S40P025';'S45P025';'S30P000';'S35P00
0';'S40P000';'S45P000'];

for TestNumber = 2:20

% Convert Test Number To Text String And Add Leading "0" If Needed %
TestNum = string(TestNumber);
if TestNumber <= 9
    TestNum = strcat('0',TestNum);
end

% Set Test ID Based On Test Number %
TestID = TestIDs(TestNumber,:);

% Import Prefiltered Data File %

% String Together Full File Name %
    datafile = strcat(drive, user, path, 'Test', TestNum, '_', TestID,
'_Analysis_Prefilter.xlsm');

    % Read Unmodified Columns %
    RawData = xlsread(datafile,4,'B:G');
    T = RawData(:,1);
    P = RawData(:,2);
    D2 = RawData(:,3);
    SG1 = RawData(:,4);
    SG2 = RawData(:,5);
    SG3 = RawData(:,6);

    % Read Modified Columns %
    Data = xlsread(datafile,4,'H:J');
    TMOD = Data(:,1);
    PMOD = Data(:,2);
    D1MOD = Data(:,3);
```

```
% Put Data That Does Not Need To Be Filtered Into The Output Matrix %
    L = length(P);
    Output(1:L,1)= T(:,1);
    Output(1:L,2) = P(:,1);
    Output(1:L,3) = D2(:,1);
    Output(1:L,4) = SG1(:,1);
    Output(1:L,5) = SG2(:,1);
    Output(1:L,6) = SG3(:,1);
    L = length(TMOD);
    Output(1:L,7) = TMOD(:,1);
    Output(1:L,8) = PMOD(:,1);


% Isolate Data To Be Filtered %
    UnfiltData = D1MOD;

% Begin Filtering Operation %

    f = 30;                                 % Sampling Frequency -> Leave At 30 %
    f_cutoff = .9;                          % Cut-off Frequency %
    fnorm = f_cutoff/(f/2);
    [b1,a1] = butter(10,fnorm,'low');       % Low Pass Butterworth Filter, 10th Order %
    Filter1 = filtfilt(b1,a1,UnfiltData);   % Filter 1: Buterworth Filter %

    count = round(L/15);                    % Sets Window Based On Length Of Vector
                                            % Being Filtered %
    Filter2 = medfilt1(Filter1,count);      % Filter 2: Median Filter %


% Curve Fit Filtered Data And Get Table Of Loads %

    % Runs Curve Fit Function For Filtered Data, Value Of 0.9999999 Is Set
    % Such That The Curve Smooths Out Roughness Of Data While Still
    % Following The Trend Of The Data %
        curvefit = fit(Filter2,PMOD,'smoothingspline','SmoothingParam', .9999999);
    % Returns Y Values For Function Based On Displacement Input %
        CurveFitY = curvefit(Filter2);

% Add Filtered And Curve Fit Data To Ouput Table %
    Output(1:L,9) = Filter2;
    Output(1:L,10) = CurveFitY;

% Write Data To File %
   savepath = "\Box\2020-21 CDKS\DST\12 Experimental Data\Data_03_Filtered";
   savefile = strcat(drive, user, savepath);
   cd (savefile)
   FileName = strcat('Test',TestNum, '_', TestID, '_Filtered.xlsx');
   xlswrite(FileName,Output)

   cd(strcat(drive,user,path))
   clear Output
```

```
end

cd(strcat(drive,user,'\Box\2020-21 CDKS\DST\12 Experimental Data\Data Analysis\01 Matlab
Filtering Code'))
```

Architectural Engineering

Capstone Report Approval Form

Master of Science in Architectural Engineering -- MSAE

Milwaukee School of Engineering

This capstone report, entitled "Effects of Bolt Position Within Long Slots on Extended Single Plate Connections" submitted by the student Cassidy N. Jackson, has been approved by the following committee:

Faculty Advisor: _____ Date: _____

Dr. Christopher Raebel, Ph.D.

Faculty Member: _____ Date:_____

Dr. Pouria Bahmani, Ph.D.

Faculty Member: _____ Date: _____

Adam Friedman, M.S.S.T. (Lecturer)